



UNIL | Université de Lausanne

Unicentre

CH-1015 Lausanne

<http://serval.unil.ch>

Year : 2012

SURVIVAL RESPONSE IN THE SKIN

PELTZER Maria de las Nieves

PELTZER Maria de las Nieves, 2012, SURVIVAL RESPONSE IN THE SKIN

Originally published at : Thesis, University of Lausanne

Posted at the University of Lausanne Open Archive.

<http://serval.unil.ch>

Droits d'auteur

L'Université de Lausanne attire expressément l'attention des utilisateurs sur le fait que tous les documents publiés dans l'Archive SERVAL sont protégés par le droit d'auteur, conformément à la loi fédérale sur le droit d'auteur et les droits voisins (LDA). A ce titre, il est indispensable d'obtenir le consentement préalable de l'auteur et/ou de l'éditeur avant toute utilisation d'une oeuvre ou d'une partie d'une oeuvre ne relevant pas d'une utilisation à des fins personnelles au sens de la LDA (art. 19, al. 1 lettre a). A défaut, tout contrevenant s'expose aux sanctions prévues par cette loi. Nous déclinons toute responsabilité en la matière.

Copyright

The University of Lausanne expressly draws the attention of users to the fact that all documents published in the SERVAL Archive are protected by copyright in accordance with federal law on copyright and similar rights (LDA). Accordingly it is indispensable to obtain prior consent from the author and/or publisher before any use of a work or part of a work for purposes other than personal use within the meaning of LDA (art. 19, para. 1 letter a). Failure to do so will expose offenders to the sanctions laid down by this law. We accept no liability in this respect.



UNIL | Université de Lausanne

Faculté de biologie
et de médecine

Département de Physiologie

SURVIVAL RESPONSE IN THE SKIN

Thèse de doctorat ès sciences de la vie (PhD)

présentée à la

Faculté de biologie et de médecine
de l'Université de Lausanne

par

Maria de las Nieves PELTZER

Biotechnologiste de l'Universidad Nacional de Quilmes (UNQUI), Buenos Aires

Jury

Prof. Jean-Pierre Hornung, Président
Prof. Christian Widmann, Directeur de thèse

Prof. Wim Declercq, expert
Prof. Liliane Michalik, expert

Lausanne 2012

Imprimatur

Vu le rapport présenté par le jury d'examen, composé de

<i>Président</i>	Monsieur Prof. Jean-Pierre Hornung
<i>Directeur de thèse</i>	Monsieur Prof. Christian Widmann
<i>Experts</i>	Madame Dr Liliane Michalik
	Monsieur Prof. Wim Declercq

le Conseil de Faculté autorise l'impression de la thèse de

Madame Maria de las Nieves Peltzer

Titulaire d'un diplôme de biologie de l'Université de Quilmes

intitulée

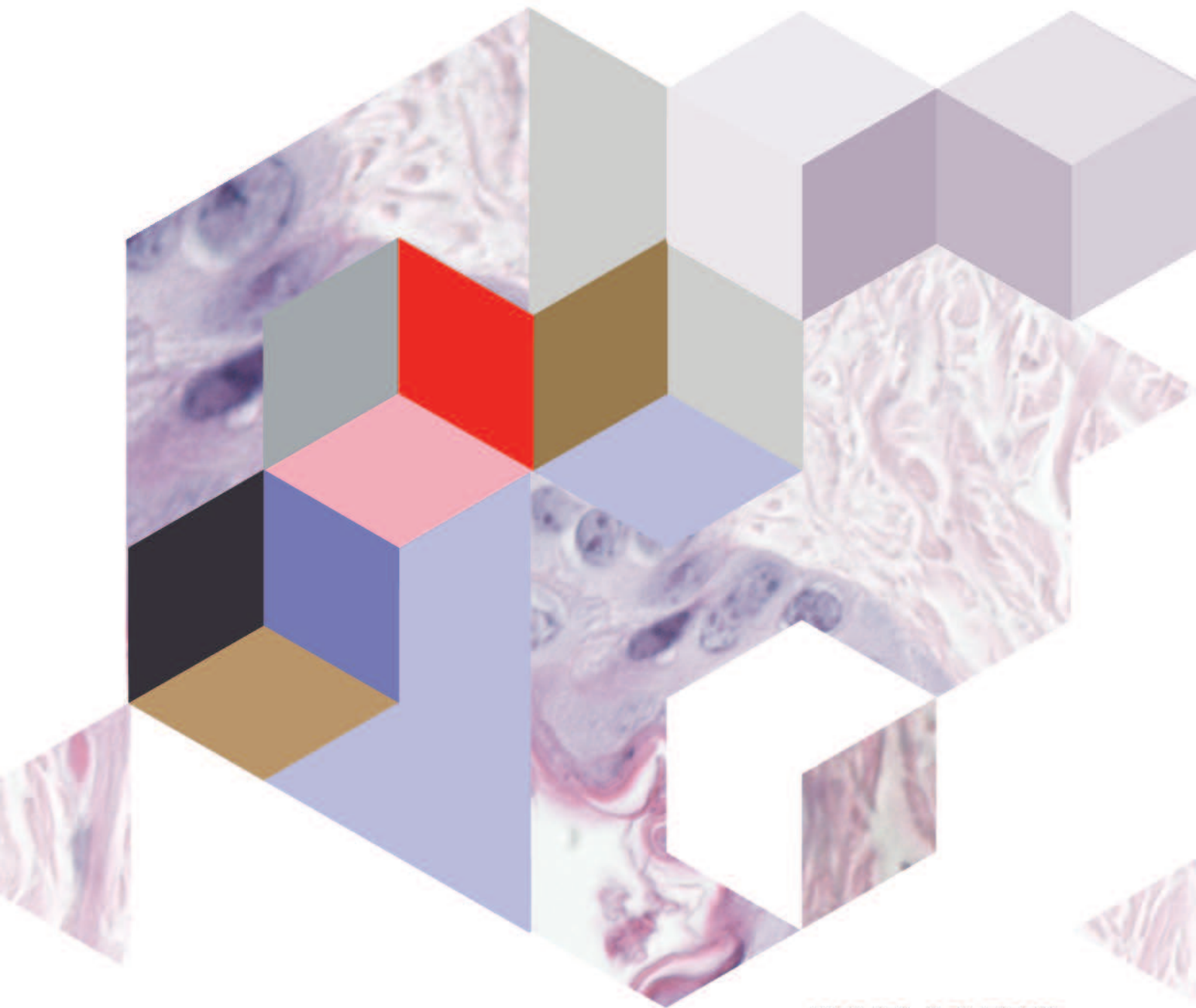
SURVIVAL RESPONSE IN THE SKIN

Lausanne, le 21 septembre 2012

pour Le Doyen
de la Faculté de Biologie et de Médecine

Prof.  Jean-Pierre **Hornung**

SURVIVAL
RESPONSE
IN THE SKIN



NIEVES PELTZER
CHRISTIAN WIDMANN

UNIVERSITÉ DE LAUSANNE

*A mi papa, mi mama y mis hermanas. Por el amor, la confianza y el aguante.
Por todos los sacrificios realizados para que esto se cumpla. Por estar
siempre, en las buenas y en las malas, aca y alla...*

A Alessandro, por darme la fuerza para llegar hasta aca

...y esto es solo el principio

INDEX

SUMMARY / RÉSUMÉ	1
GENERAL INTRODUCTION	5
1. Apoptosis	7
1.1 Mechanisms leading to apoptotic cell death	8
1.2 DNA condensation and fragmentation	12
1.3 Cell shrinkage and plasma membrane bebbing	12
1.4 Nuclear fragmentation	13
1.5 The end of the tunnel	13
2. Inhibitors of apoptosis family (IAPs):the guardians of the cell	14
2.1 Survivin: the ugly duckling	15
3. Caspases: not only inducers of apoptosis	17
4. RasGAP: the on/off button	22
4.1 RasGAP structure	23
4.2 RasGAP as a Ras effector and beyond	24
5. Ras/PI3K/Akt: a signaling cascade important for RasGAP derived-fragment N protection	27
5.1 5.2 The Ras/PI3K/Akt signaling pathway	27
6. Skin: a sophisticated barrier against external insults	31
6.1 The skin triple layer: epidermis, dermis and hypodermis	31
6.2 The sun and the skin: the perfect crime	32
6.3 UV-B light: the prize of a beautiful suntan	34
7. Reference list	37
OBJECTIVES	47
RESULTS Part I	51
Introduction	53
Contribution	54
Reference list	55
Research article	57

INDEX

RESULTS Part II	77
Introduction	79
Contribution	81
Reference list	82
Research article	85
RESULTS Part III	93
Introduction	95
Contribution	97
Reference list	98
Research article	101
Supplementary data	125
DISCUSSION AND PERSPECTIVES	133
Reference list	140
METHODS	141
ACKNOWLEDGEMENTS	185

SUMMARY

Apoptosis is defined as a programmed cell death process operating in multicellular organisms in order to maintain proper homeostasis of tissues. Caspases are among the best characterized proteases to execute apoptosis although lately many studies have associated them with non-apoptotic functions. In the laboratory an anti-apoptotic pathway relying on caspase-3 activation and RasGAP has been described *in vitro*. RasGAP bears two conserved caspase-3 cleavage sites. Under low stress conditions, RasGAP is first cleaved by low caspase-3 activity generating an N terminal fragment (fragment N) that induces a potent anti-apoptotic response mediated by the Ras/PI3K/Akt pathway. High levels of active caspase-3, associated with increased stress conditions, induce further cleavage of fragment N abrogating this anti-apoptotic response. In the present work I studied the functionality of fragment N-mediated protection in physiological conditions as well as the mechanism by which fragment N induces an anti-apoptotic response, with a focus on survivin, an inhibitor of apoptosis.

During my work in the laboratory I found that mice lacking caspase-3 or unable to cleave RasGAP (KI mice) are deficient in Akt activation and more sensitive to apoptosis than wild-type mice in response to stress. This higher sensitivity to stress led to augmented tissue damage, highlighting the importance of this pathway in protection against low stress. In parallel I focused on the study of survivin expression in the skin in response to UV-B light and I found that survivin is induced in the cytoplasm of keratinocytes in response to stress where it may fulfill a cyto-protective role. However fragment N had no effect on survivin expression. In addition, cytoplasmic survivin was increased in keratinocytes exposed to UV-B light, whether RasGAP is cleaved (WT mice) or not (KI mice), indicating that survivin is not involved in fragment N mediated protection.

Altogether these data indicate that fragment N is pivotal for cell protection against pathophysiologic damage and can encourage the development of therapies aimed to strengthen the resistance of cells against aggressive treatments. Importantly, this finding contributes to the characterization of how caspase-3 can be activated without inducing cell death, although further studies need to be conducted in order to completely characterize this pro-survival molecular mechanism.

RÉSUMÉ

L'apoptose est définie comme un processus de mort cellulaire programmée s'exécutant, dans les organismes multicellulaires, afin de maintenir l'homéostasie adéquate des tissus et organes. Les caspases sont des protéases qui déclenchent l'apoptose bien que de récentes découvertes l'impliquent aussi dans des fonctions non-apoptotiques. Il a été démontré dans notre laboratoire que RasGAP était un substrat de la caspase-3 comportant deux sites de clivage conservés. Lors d'un faible stress, RasGAP est clivée par de faibles niveaux de caspase-3 activée, générant un fragment N-terminale qui a des fonctions anti-apoptotique (fragment N) agissant à travers l'activation de la voie Ras/PI3K/Akt. Lors d'un fort stress, quand l'activité de la caspase-3 est élevée, le fragment N est alors lui aussi clivé ce qui abolit sa réponse anti-apoptotique. Dans cette étude, j'ai étudié le rôle du fragment N dans cette signalisation en conditions physiologiques, ainsi que les mécanismes moléculaires par lesquels le fragment N induit une réponse cyto-protectrice, en me concentrant sur la survivine, un inhibiteur de l'apoptose.

Au cours de mon travail dans le laboratoire, j'ai découvert que des souris dépourvues de la caspase-3 ou ne pouvant pas cliver RasGAP sont incapables d'activer Akt et sont, de ce fait, plus sensibles à l'apoptose que des souris de type sauvage en réponse au stress. Cette plus grande sensibilité se manifeste par une augmentation des dommages des tissus, ce qui souligne l'importance de cette voie dans la protection contre de faibles stress.

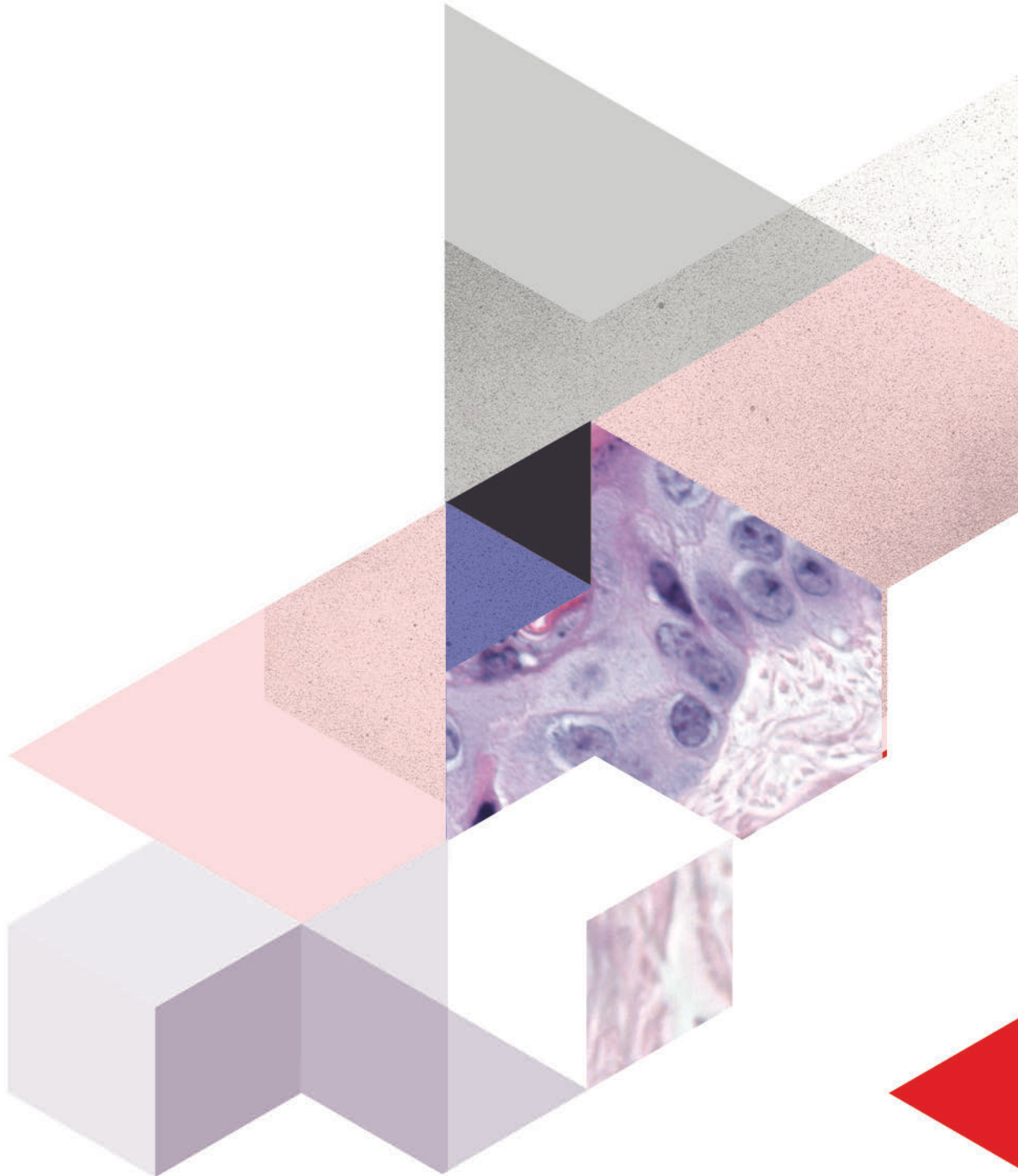
Parallèlement, je me suis concentrée sur l'étude de l'expression de la survivine dans la peau en réponse aux rayons UV-B. J'ai découvert que l'expression de cette protéine était augmentée dans le cytoplasme des kératinocytes en réponse au stress ayant vraisemblablement un rôle cyto-protecteur. Néanmoins, étant donné que l'expression du fragment N n'a aucun effet sur l'expression de la survivine *in vitro*, et que la survivine cytoplasmique est augmentée dans la peau exposée aux rayons UV-B indépendamment du clivage de RasGAP, nous en déduisons que la survivine n'est pas impliquée dans la protection induite par le fragment N.

En conclusion, ces données indiquent que le fragment N est essentiel pour la protection des cellules contre les dommages physiopathologiques et pourraient

mener au développement de thérapies visant à renforcer la résistance des cellules contre des traitements agressifs. Ces résultats sont aussi très importants car ils contribuent à la compréhension du mécanisme d'activation de la caspase-3 n'induisant pas l'apoptose. Toutefois des études complémentaires sont nécessaires afin de décrypter ce signal de survie.

SURVIVAL RESPONSE IN THE SKIN

GENERAL INTRODUCTION



“LIFE IS PLEASANT. DEATH IS PEACEFUL. IT’S THE TRANSITION THAT IS TROUBLESOME”

Isaac Asimov

1. Apoptosis

Apoptosis is a genetically encoded program leading to cell death that is involved in normal development of tissues during embryogenesis, for example removal of superfluous cells for hollowing ducts or deletion of interdigital cells during limb formation, and, in adults, to maintain homeostasis in rapidly renewing tissues, such as the intestine epithelium or hematopoietic cells. Apoptosis plays also an important role in the elimination of old or irreparably damaged cells that could have harmful effects on the health of the organism. Programmed cell death was first described by the German Scientist Carl Vogt in 1842 but it was not until 1972 when John Foxton Ross Kerr (Kerr et al., 1972) was able to distinguish apoptosis from traumatic cell death. He was indeed the first to coin the term “Apoptosis” for this kind of cell death with the help of a Greek Professor at the University of Aberdeen. This is a citation from a footnote in Kerr’s publication. *“We are most grateful to Professor James Cormack of the Department of Greek, University of Aberdeen, for suggesting this term. The word “apoptosis” (ἀπόπτωση) is used in Greek to describe the “dropping off” or “falling off” of petals from flowers, or leaves from trees. To show the derivation clearly, we propose that the stress should be on the penultimate syllable, the second half of the word being pronounced like “ptosis” (with the “p” silent), which comes from the same root “to fall”, and is already used to describe the drooping of the upper eyelid”* (Kerr et al., 1972).

Apoptotic cells are equipped with plasma membrane alterations that allow their rapid removal from tissues before the release of their cytoplasmic content. Because they retain their plasma membrane integrity and are rapidly engulfed by phagocytes, apoptotic cells are not followed by inflammation and promote the recycling of cellular components (Savill and Fadok, 2000). Other sort of cell death, namely “Necrosis”, is accompanied by a rapid loss of membrane integrity and the release of cellular contents into the extracellular space, invariably triggering an immune response (Kerr et al., 1972). In biological terms necrosis plays the role of an alert to danger since

many pathogens and many types of trauma (burns, cuts, etc) facilitate infection (Matzinger, 2002; Chen et al., 2007).

1.1 Mechanisms leading to apoptotic cell death

Apoptosis typically proceeds through one of two signalling cascades termed the intrinsic and the extrinsic pathways (Figure 1), which induce the activation of caspases. **Caspases** are cysteine-dependent aspartate-directed proteases that regulate apoptosis through the cleavage of several proteins ultimately leading to cell death (Taylor et al., 2008). Activation of initiator caspases such as caspase-8, -9 and -10 by either apoptotic pathway mediate the activation of executioner caspase-3, -6 and -7 that finally execute apoptosis.

In the **intrinsic pathway** diverse cytotoxic insults, including growth factor deprivation and DNA damaging agents, initiate apoptosis by activating pro-apoptotic proteins (Figure 1). This phenomenon leads to mitochondrial depolarization that finally commits the cell to die. The pathway is mainly regulated by a balanced interaction between pro and anti-apoptotic members of the B cell lymphoma 2 (Bcl-2) family. Within this family, Bcl-2, Bcl-X_L and Mcl-1 promote cell survival by preventing the apoptosis effectors, Bax and Bak, from damaging the mitochondrial membrane. Upon an apoptotic stimulus, pro-apoptotic Bax and Bak activation, although by a mechanism highly debated, is essentially based on the activity of the apoptosis initiators, the so-called BH3-only proteins. This family comprises Bad, Bik, Bid, Bim, Bmf, Noxa and PUMA, which engage and inactivate their prosurvival relatives (Bcl2, Bcl-X_L and Mcl-1) resulting in Bax/Bak activation. After activation Bax and Bak undergo extensive conformational changes leading to mitochondrial targeting of Bax and homo-oligomerization of Bax and Bak in the mitochondrial membrane (Strasser et al., 2011). These changes initiate the formation of proteinaceous channels (Antonsson et al., 1997) that although not yet well understood, may be formed by Bax and Bak themselves (Martinez-Caballero et al., 2009). Pore formation induces membrane depolarization or **mitochondrial outer membrane depolarization (MOMP)** (Tait and Green, 2010) finally leading to permeabilization and release into the cytoplasm of pro-apoptotic proteins from the mitochondrial intermembrane space.

Cytochrome *c* is one of the main pro-apoptotic proteins to be released from the mitochondria. Once in the cytoplasm, it binds apoptotic protease activating factor 1 (Apaf1), inducing its conformational change and allowing the formation of a heptametrical wheel like structure that functions as a caspase activating platform, termed apoptosome. The apoptosome recruits, dimerizes and activates caspase 9, one of the initiator caspases, which in turn activates the effector caspases -3, -6 and -7. The apoptosome works as a molecular timer since it induces caspase-9 autoprocessing which greatly diminish its affinity for the apoptosome leading to caspase-9 inactivation. Therefore, apoptosome-mediated caspase-9 activation depends on the level of intracellular procaspase-9.

Other pro-apoptotic proteins are released from mitochondria during MOMP such as the second mitochondrial-derived activator of caspase (SMAC, also known as direct IAP-binding protein with low pI, DIABLO), the stress-activated endoprotease OMI (also known as high temperature requirement protein A 2 or HtrA.2) and the apoptosis-inducing factor (AIF), while the latter is released in a slower manner. Although it has been reported that the release of Smac was caspase-dependent (Adrain et al., 2001), later publications sustained that release of the above mentioned pro-apoptotic proteins is caspase independent and that it happens simultaneously with cytochrome *c* release (Goldstein et al., 2000; Goldstein et al., 2005). Once the mitochondria has been depolarized, the release of pro-apoptotic proteins happens in about 5 minutes and the continuous and slow release of AIF suggests that the pore formed during MOMP remains open for a few hours (Munoz-Pinedo et al., 2006). Smac is an inhibitor of the X-linked inhibitor of apoptosis protein (XIAP), a well-known caspase inhibitor (more details in the “inhibitors of apoptosis” section) that upon release from the mitochondria cooperates with cytochrome *c* – mediated caspase-3 activation through XIAP inactivation. OMI belongs to the family of serine proteases that induces apoptosis by inhibiting IAPs in a caspase dependent manner (Suzuki et al. 2001), although it can also function in a caspase-independent fashion directly through its serine protease activity (Garrido and Kroemer, 2004). Finally, AIF once released from the mitochondria, translocates to the nucleus, interacts with DNA and induces chromatin condensation by itself (Ye et al., 2002), triggering apoptosis in a caspase-independent manner.

The **extrinsic pathway** is initiated through the engagement of cell surface death receptors with intracellular death domain (DD) that belong to the tumor necrosis factor (TNF) receptor superfamily, by their specific ligands (Figure 1). Ligation of death receptors such as CD95/Fas or TRAIL receptors TRAIL-R1 and TRAIL-R2 by their cognate ligands, induce aggregation of trimerized receptors leading to the formation of the **death inducing signaling complex (DISC)**. The DISC is composed of the receptor, an adaptor molecule such as Fas- associated death domain (FADD) and the initiator caspase -8 or -10. Oligomerization of caspase-8 upon DISC formation drives its activation, activating in turn its downstream effectors, such as caspase-3. In Type I cells the mere activation of caspase-8 is sufficient to trigger apoptosis independently of MOMP, directly activating effector caspases. In type II cells on the contrary, DISC-induced caspase-8 signaling is amplified through the cross-talk with the mitochondrial pathway by the caspase-8 - mediated cleavage of BH3 - interacting domain death agonist (BID; a BH3 only protein) leading to BID activation and mitochondrial cell permeabilization (Fulda and Debatin, 2006). Signaling by death receptors can be negatively regulated by FLICE-inhibitory protein (FLIP). FLIP is similar in structure to caspase-8 but lacks active site residues. Therefore, FLIP can dimerize with caspases-8 preventing its activation at the DISC (Krueger et al., 2001).

Independently of the pathway leading to cell death, the bottle neck of apoptosis is the activation of effector caspases-3, -6 and -7. These proteases are responsible for the typical morphological changes exhibited by an apoptotic cell, such as chromatin condensation, nuclear fragmentation, cellular shrinkage, and plasma membrane blebbing. These series of events culminate with the formation of apoptotic bodies that present “eat me” signals at the surface to be finally recognized and engulfed by phagocytes.

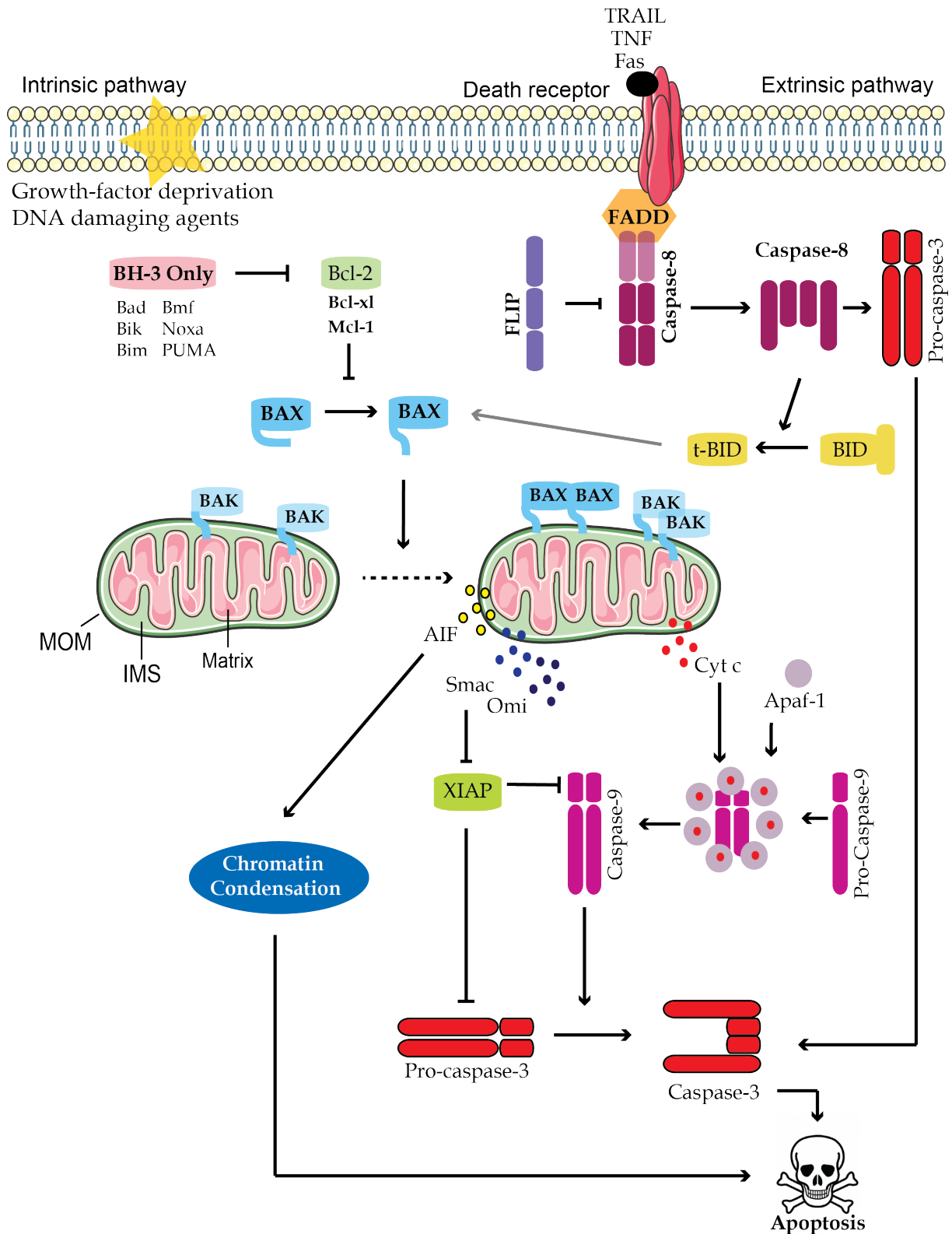


Figure 1: Simplified schematic representation of the intrinsic and extrinsic pathways of apoptosis. Dashed arrows represent the transition between normal and stressed conditions in either pathway. Grey arrow represents the crosstalk between the extrinsic and intrinsic pathways. MOM: mitochondrial outer membrane, IMS: inter-membrane space.

1.2 DNA condensation and fragmentation

DNA condensation and fragmentation are one of the most noticeable features of apoptosis. The pattern of DNA fragmentation is the result of endonuclease-mediated chromatin cleavage at internucleosomal sites and is therefore accompanied by chromatin condensation.

The caspase-activated DNase (CAD) is the best-characterized nuclease that functions exclusively during apoptosis (Widlak and Garrard, 2005). CAD and its inhibitory chaperone the Inhibitor of CAD (ICAD) form an inactive complex. The CAD-ICAD complex can bind DNA but ICAD prevents CAD-mediated DNA digestion by blocking its dimerization. Following caspase-3 activation, ICAD is cleaved and then CAD is released to form homo- or oligomers that become active (Nagata et al., 2003). Although CAD was thought to be involved not only in DNA degradation but also in chromatin condensation, it has been demonstrated that the kinase MST1 is cleaved and activated by caspase-3 (Ura et al., 2001). Once activated, MST1 migrates to the nucleus where it phosphorylates histone 2B (H2B), which is correlated with chromatin condensation (Cheung et al., 2003).

1.3 Cell shrinkage and plasma membrane blebbing

On activation caspases cleave many of the major constituents of the cytoskeleton including actin and actin-binding proteins such as myosin, spectrins, α -actinin, gelsolin and filamin (Taylor et al., 2008). Some components of the microtubular filaments are also caspase-3 substrates comprising tubulins and microtubule-associated proteins such as tau, cytoplasmic dynein intermediate chain and p150^{Glued}. Proteolysis of these structural components of the cytoskeleton contributes to rounding and retraction of the cell observed in the early phases of apoptosis.

Another feature of apoptosis, which is also a consequence of cytoskeleton weakening, is the dynamic membrane blebbing as the cell cytoplasm flows against unsupported regions of the plasma membrane. Rho-associated kinase I (ROCK I), a caspase-3 substrate, plays an important role in this phase of apoptosis. This kinase is a Rho effector and a regulator of actin cytoskeleton dynamics that is activated upon removal of the C-terminal region by caspase-3. This activation leads to myosin

light chain phosphorylation with the consequent contraction of actin bundles. However, in conditions where the cytoskeleton has been disrupted (*i.e.* in the absence of a solid cytoskeleton) the contraction of the actin bundles leads to the formation of blebs (Coleman et al., 2001; Sebbagh et al., 2001).

1.4. Nuclear fragmentation

Nuclear fragmentation relies on the caspase-dependent cleavage of nuclear lamins leading to the disintegration of the nuclear membrane (Rao et al., 1996). However, lamin cleavage alone is not sufficient to cause nuclear disintegration. Because of the attachments between the actin cytoskeleton and the nuclear envelope, this literally tears the nucleus apart during apoptosis and therefore ROCK I also plays a role in nuclear fragmentation (Croft et al., 2005).

1.5. The end of the tunnel

The terminal event of the demolition phase is the ingestion of dead cells by phagocytes. This is achieved by the formation of apoptotic bodies and the release of chemoattractants molecules by the dying cell. The formation of apoptotic bodies is probably a consequence of the actin-myosin mediated process of membrane blebbing, in which membrane-bound extrusions of cytosol become pinched off into independent vesicles (Orlando et al., 2006). Apoptotic cells are not only ready to be eaten but they are capable of attracting phagocytes by the caspase-3 dependent release of chemoattractants lipids such as lysophosphatidylcholine, or by changes in the membrane (Lauber et al., 2003). For instance, phosphatidylserine (PS) is normally confined to the inner plasma membrane leaflet but is translocated to the outer membrane leaflet in a caspase-3 dependent manner (Martin et al., 1995).

2. Inhibitors of Apoptosis Family (IAPs): the guardians of the cell

Inhibitors of apoptosis (IAP), are among the main caspase inhibitors. Eight human IAPs are currently known: XIAP, cIAP1, cIAP2, NAIP, ML-IAP, TS-IAP, BRUCE and the smallest of all, survivin. The feature that defines this family is the presence of the baculovirus IAP repeat (BIR) domain, a zinc binding domain of approximately 70 amino acid residues that mediates protein–protein interactions, and is essential for the anti-apoptotic potential of most IAPs. BIR domains are protein interacting modules and most of them (except BIR1) bind the extreme N-terminus of short peptides of defined sequence named IBM (IAP-binding motif). IBM is found in proteins like caspase-9, -3 and -7 (Scott et al., 2005), Smac/DIABLO and others (Vaux and Silke, 2003). The mammalian IAPs, XIAP, cIAP1 and cIAP2, contain three such domains in their aminoterminal portion (Figure 2). These IAPs also harbor additional domains such as the carboxyterminal RING finger domain that provides them with Ubiquitin ligase (E3) activity (Yang et al., 2000) and a Ub-associated domain (UBA) domain through which they interact with ubiquitylated proteins (Gyrd-Hansen and Meier, 2010). Finally cIAP1 and 2 contain a caspase-recruitment domain (CARD) that, unlike all known CARD domains, it does not interact with CARD-containing proteins. Instead, cIAP 1/2 CARD domain keeps cIAP1/2 into a closed conformation preventing its E3 activity (Lopez et al., 2011).

IAPs counteract apoptosis in different manners. **XIAP** is the only one able to directly inhibit caspases (Figure 1). Inhibition of caspase-9 requires an essential interaction between a groove on its BIR3 domain and a conserved four-residue IBM of the small subunit of caspase-9. Caspase-3 and -7 are inhibited in a different way. The linker region between BIR1 and BIR2 of XIAP interacts with the activated caspase in a revers orientation relative to the substrate, while the BIR2 domain contributes to inhibition by direct interaction with the N-terminus of the small subunits of activated caspase. Binding of XIAP to caspases is antagonized by the mitochondrial protein, Smac (Rumble and Duckett, 2008; Dubrez-Daloz, 2009).

The other well-characterized IAPs are **c-IAP1 and 2**, although they inhibit apoptosis in a more indirect fashion. cIAPs maintain survival through induction of the canonical pathway of NK- κ B activation. Basically the Ub-dependent formation of complex-I, consisting of the adaptor protein TNFRSF1A-associated via death domain (TRADD),

the Ub ligases TRAF2, TRAF5, cIAP1 and cIAP2, and the protein kinase RIPK1, is recruited to the membrane after TNF α binding to its receptor (TNFR1) (Gyrd-Hansen and Meier, 2010). cIAP1/2-mediated K63 ubiquitylation of some components of complex-I, such as RIPK1 and it-self, stimulates Ub-dependent recruitment of trimeric linear ubiquitin chain assembly complex (LUBAC), which promote NK- κ B activation and the induction of pro-survival signals (Haas et al., 2009; Gerlach et al., 2011). Additionally, cIAP1/2 block cell death by preventing the formation of a RIPK1-dependent, caspase-8 activating complex (complex-II) by keeping RIPK1 in complex-I by ubiquitylation (Varfolomeev, 2008). Also cIAP1/2 is able to modulate the non-canonical pathway of NK- κ B, through ubiquitylation and degradation of NIK, a well-known inducer of NK- κ B (Darding and Meier, 2012).

The role of other IAPs, such as **NAIP** or **Survivin** on apoptosis inhibition is not very well understood. NAIP appears to be involved in activation, rather than inhibition, of the pro-inflammatory caspase-1 therefore having a role in inflammation (see section 3). Survivin, bears only one BIR domain and the absence of a structural equivalent to the linker between BIR2 and 3 of XIAP makes survivin not able to bind directly to caspases in the same manner as XIAP (Wheatley and McNeish, 2005). Even though many anti-apoptotic functions have been attributed to this IAP, its role as an antiapoptotic protein is controversial (Yue et al., 2008).

2.1. Survivin: The Ugly Duckling

The exception within the IAP family, Survivin (also called BIR containing protein-5, BIRC5) is a 16.5 kDa protein that functions simultaneously at cell division and apoptosis inhibition. Structurally, Survivin bears only one BIR domain in its N-terminal end that contributes to its function in apoptosis inhibition. In its C-terminal domain, survivin contains an extended carboxy-terminal alpha-helical coiled-coil which is thought to be important for its interaction with microtubules, hence its role in cell division (Li and Altieri, 1999) (Figure 2).

In active proliferating cells, Survivin regulation is cell cycle dependent, being almost undetectable at G1 and S phases and peaking at G2/M (Li et al., 1998). Survivin is a chromosomal passenger (CP) (Uren et al., 2000; Wheatley et al., 2001), and is hence

found in the inner centromere during prophase where they remain until the chromosomes have converged to the metaphase plate. At the metaphase-anaphase transition, survivin relocates to the newly forming microtubules that develop between the separating chromosomes to finally migrate to the cell cortex during anaphase, where it delineates the cleavage plane.

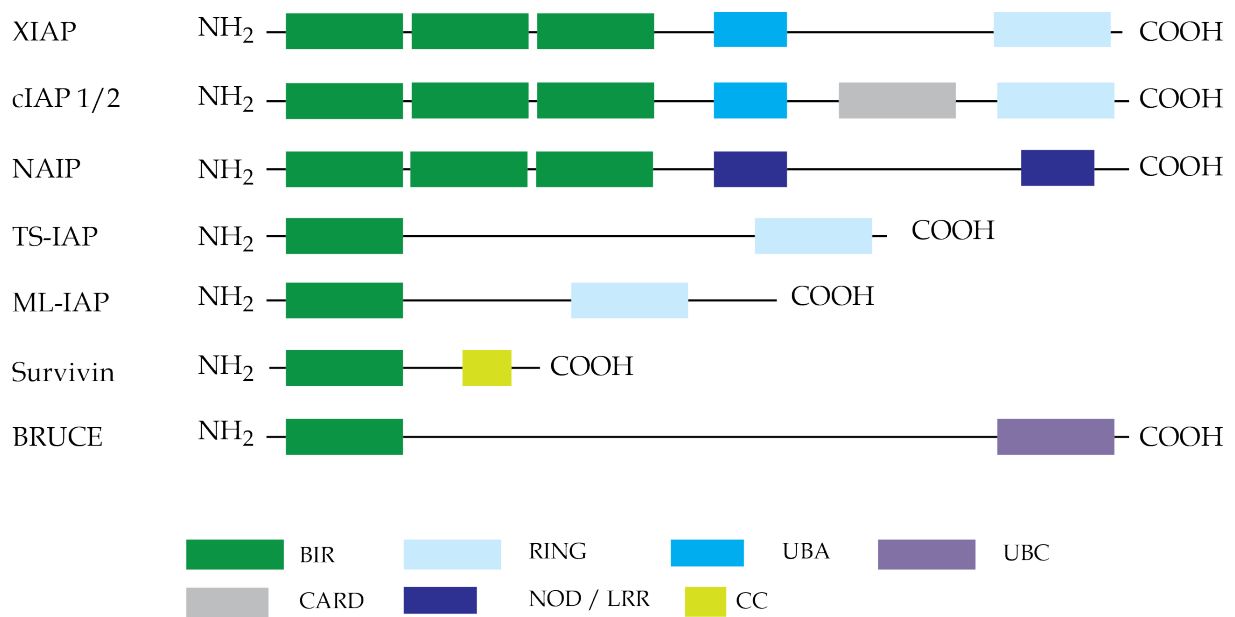


Figure 2: Domain structure of human IAPs. All IAPs are characterized for the presence of at least one BIR domain. BIR: baculovirus IAP repeat. RING: Ub-ligase activity domain. UBA: Ub-associated domain. UBC: Ub-conjugating domain. CARD: caspase recruitment domain. NOD/LRR: nucleotide binding oligomerization domain. LRR: carboxyl-terminal leucine-rich repeat domain. CC: alpha-helical coiled-coil domain.

Endogenous survivin exists in different subcellular pools. Nuclear survivin is only involved in mitosis and has no anti-apoptotic properties. In fact the cytoprotective activity of survivin depends on its active nuclear export through the nuclear export receptor chromosome region maintenance (Crm1) (Rodriguez et al., 2002). Moreover, Dohi and collaborators reported that there is a pool of survivin that

localizes to the mitochondria in tumor cells and that it is translocated into the cytoplasm when cells are subjected to stress (Dohi et al., 2004a; Dohi and Altieri, 2005). Even though survivin is not a direct caspase inhibitor, there are three proposed mechanisms for the survivin anti-apoptotic effect and all of them take place in the cytoplasm (Figure 3). One of the mechanisms relies on survivin direct interaction with Smac/DIABLO (Song et al., 2004; Song et al., 2003), which prevents the neutralizing effects of Smac over XIAP, allowing it to maintain a suppression effect on the effector caspases. The second mechanism proposed is survivin direct binding with XIAP. This interaction leads to the stabilization of XIAP against proteasome degradation. Moreover, the survivin-XIAP complex synergistically inhibits apoptosis induced by Bax expression, whereas survivin has no effect by itself if XIAP is not present in the cell (Dohi et al., 2004b). A third proposed mechanism is the inhibition of caspase-9. This inhibition only takes place when survivin is bound to the hepatitis B – X interacting protein (HBXIP). Once the complex is formed, survivin is able to sequester caspase-9 and thus interfere with the apoptosome assembly (Marusawa et al., 2003).

Survivin anti-apoptotic function is controversial. Yue and collaborators support the idea that cells lacking survivin are more sensitive to apoptosis because of an aberrant mitosis and not because of a role as an IAP (Yue et al., 2008). However, by dissociating survivin mitotic function from anti-apoptotic-survivin it was shown that cells lacking anti-apoptotic survivin are more sensitive to apoptosis, even though mitosis proceed normally (Barret et al., 2010; Colnaghi et al., 2006), suggesting that survivin has indeed anti-apoptotic properties *per se*.

3. Caspases: not only inducers of apoptosis

As described above, caspases are cysteine proteases that cleave many substrates in an aspartate residue to trigger apoptotic cell death or inflammation. A total of 14 caspases have been identified in mammals. They are synthesized as zymogens (inactive proenzymes) and can be classified in 3 groups according to the length and function of their N-terminal prodomain.

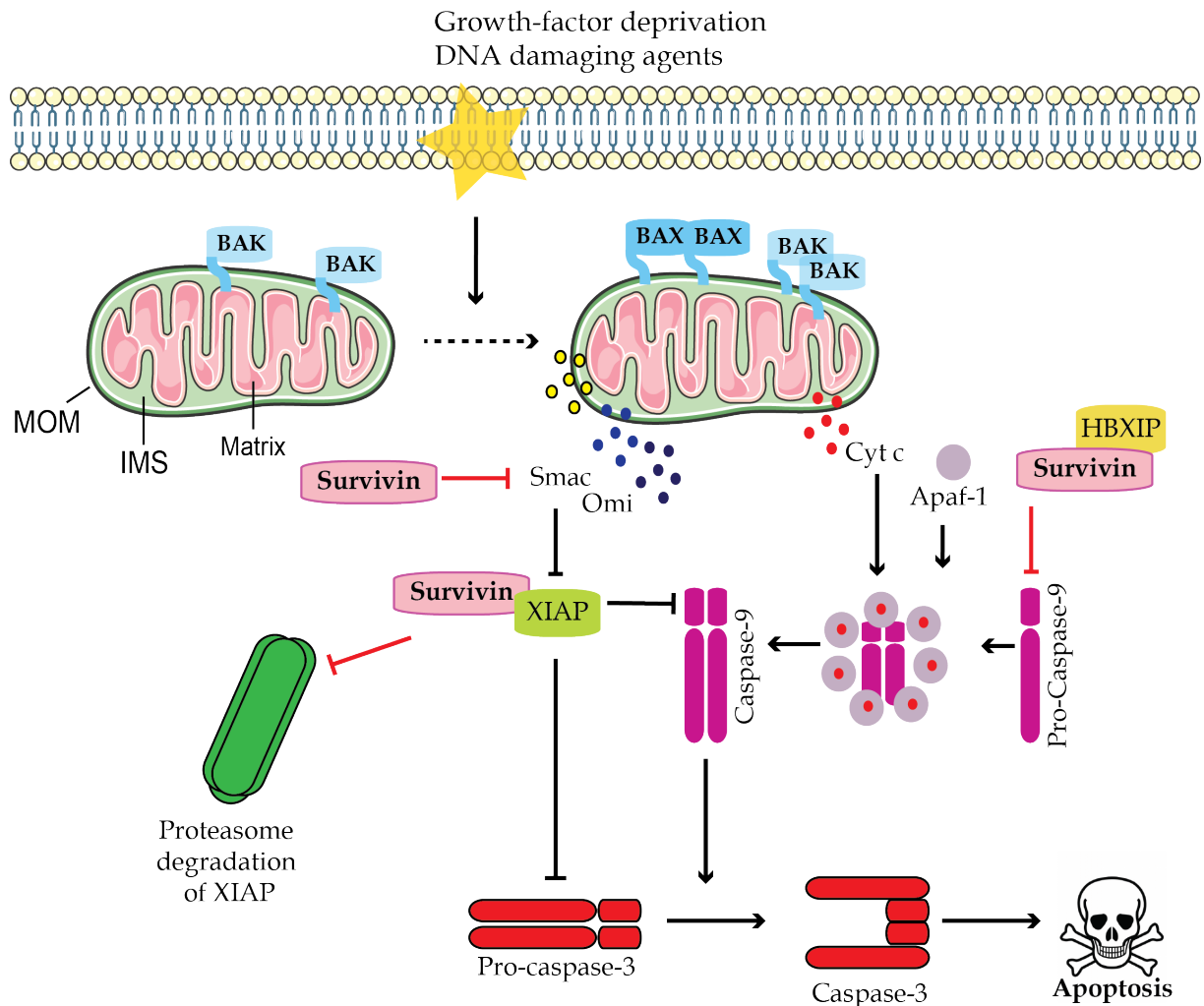


Figure 3: Different anti-apoptotic mechanisms proposed for survivin cytoprotective effect. Dashed arrow represents the transition between normal and stressed condition. MOM: mitochondrial outer membrane, IMS: inter-membrane space.

Caspases with a large prodomain are referred to as inflammatory caspases (group I) and initiator of apoptosis (group II), while those with a short prodomain are called effector caspases (group III) (Figure 4). The large prodomain of procaspases contain a death effector domain (DED), or a caspase recruitment domain (CARD) (Figure 4). These domains are mostly responsible for recruiting initiator caspases into death- or inflammatory- inducing complexes, resulting in proteolytic auto-activation. For

activation, caspases require proteolysis at internal aspartate residues resulting in the formation of a heterotetramer p20₂-p10₂. The activation mechanism of caspases from groups I and II relies on the dimerization and interdomain cleavage, as well as cleavage and release of their prodomains (Figure 4). Executioner caspases are present as dimers in the cell and are activated by cleavage of the interdomain which leads to intramolecular rearrangements and the formation of enzymatically active dimers.

Although caspases have largely been associated with apoptosis induction as described in the previous section, apoptosis can occur independently of caspase activation and *vice versa* the activation of caspases can be involved in non-apoptotic pathways, including inflammatory responses, immune cell proliferation, differentiation of various cell types, and others.

A subfamily of caspases, referred to as **group I** comprises caspases-1, -4, -5, and -13 (a bovine homolog of caspase-4) and mouse caspase-11 (homolog of caspase-4) and -12. These caspases play a role in neuronal cell death. Their main function though is the regulation of inflammatory responses. Indeed caspase-1, the first caspase to be described, is responsible for processing pro-interleukin-1 β into active IL-1 β . Mature IL-1 β is implicated in various immune reactions including the recruitment of inflammatory cells to the site of infection (Launay et al., 2005). Caspase-5 is involved in IL-1 β maturation by interacting with caspase-1 in a multiprotein complex called the inflammasome. Caspase-11, being first described as a caspase-1 activator, triggers caspase-1 independent macrophage death and caspase-1 dependent IL-1 β and IL-18 production in response to a subset of non-canonical inflammatory activators (Kayagaki et al., 2011). Additionally, caspase-11 can interact with actin-interacting protein 1 (Aip1), an activator of cofilin-mediated actin depolymerization, contributing to actin cytoskeleton dynamics (Li et al., 2007) and also to the fusion of phagosomes containing non-pathogenic bacteria with lysosomes (Akhter et al., 2012).

The second group, **group II**, is composed of caspases- 2, -8, -9 and -10 and are known as initiator caspases. Caspase-2 is the most evolutionary conserved caspase although its role in apoptosis remains controversial. It is known, however that this caspase is indeed required in stress-induced apoptosis acting upstream the

mitochondria by inducing cytochrome c release (Lassus et al., 2002). Additionally it has been proposed that caspase-2 is recruited to a platform called PIDD (p53-induced death domain) to form a large multiprotein complex involving the adaptor molecule RAIDD. This platform, called the PIDDosome spontaneously activates caspase-2 and, although it is not sufficient to trigger cell death, it sensitizes cells against genotoxin-induced apoptosis (Tinel and Tschopp, 2004; Jang et al., 2010). On the other hand, the PIDDosome most resembles the inflammasome complex having apoptosis-independent related roles such as activation of the DNA repair machinery (Tinel and Tschopp, 2004). Caspase-8 can have pleiotropic effects since it may promote cell motility mediated by calpain activation (Helfer et al., 2006) and macrophage differentiation by cleavage of the receptor-interacting protein (RIP), resulting in a downregulation of NF κ B required during differentiation (Rebe et al., 2007). Moreover, caspase-8 activation together with cFLIP (the short FLIP isoform) can prevent cells from undergoing programmed necrosis or necroptosis, by cleaving RIP Kinase 1 (RIPK1) (Oberst et al., 2011; Feoktistova et al., 2011).

Caspase-10 is implicated in the activation of NF κ B-dependent prosurvival signaling pathways by a mechanism that is independent of its catalytic domain (Shikama, 1998; Sprick et al., 2002).

The **group III** is composed of caspase-3, -6 and -7 and is the so-called effector caspases. Caspase-3, the well characterized executioner caspase, possesses many apoptosis-independent functions. Cell cycle regulators are substrates for caspase-3. Cleavage of cyclin-dependent kinase inhibitor (CKI) p27 by caspase-3 promotes proliferation of lymphoid cells (Frost, 2001). Another non-apoptotic function of caspase-3 is the cleavage of protein kinase C- δ (PKC- δ) which stimulates keratinocytes differentiation (Okuyama et al., 2004). Active caspase-3 alone or in combination with caspase-9, can induce embryonic stem cells (ESC) differentiation by cleavage and inactivation of Nanog, a transcriptional factor involved in ESC renewal (Fujita et al., 2008). Additionally, caspase-3 activation by pro-inflammatory stimuli can induce microglia activation through the cleavage and activation of the kinase PKC δ dependent pathway, leading to the activation of NF- κ B (Burguillos et al., 2011).

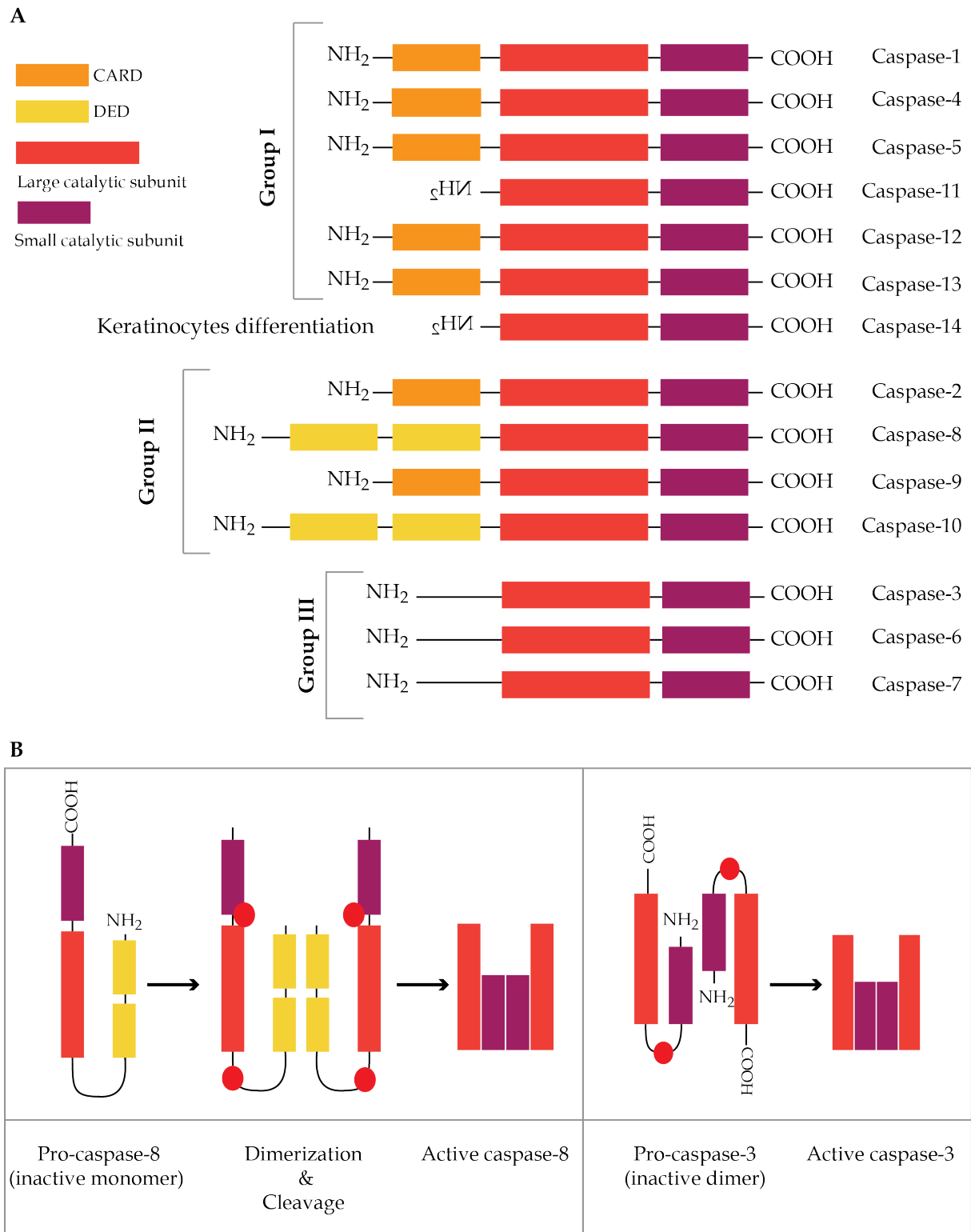


Figure 4: Structure and activations of fourteen characterized caspases. A_ Domain structure of caspases grouped according to their functions. CARD: caspase recruitment domain. DED: death effector domain. B_ Mechanism of proteolytic activation of caspases of group II (left panel) and group I (right panel). Red dots represent the cleavage sites.

Not only this caspase has roles different from apoptosis induction but paradoxically it can induce anti-apoptotic responses in certain conditions. Caspase-3 has been found to activate the B-cell receptor which triggers the cleavage of the kinases Fyn and Lyn generating fragments that inhibit apoptosis (Luciano et al., 2003). In addition, we have demonstrated that RasGAP, a regulator of Ras signaling pathway, when cleaved by caspase-3 generates a potent anti-apoptotic signal *in vitro* in response to diverse stressful stimuli (Yang and Widmann, 2001).

Finally, caspase-14 is an exception within this family of proteases since it is not ubiquitously expressed and it is processed differently presumably in a caspase independent manner (Denecker et al., 2008). Caspase-14 has been associated with the terminal differentiation of human keratinocytes and cornification (Eckhart et al., 2000) and more recently it has been reported to be involved in filaggrin catabolism and maintenance of hydration in the skin (Hoste et al., 2011).

4. RasGAP: the on/off button

Small monomeric G-proteins (guanosine nucleotide - binding proteins) function as molecular switches that control a wide range of cellular processes by coupling cell surface receptors to intracellular effectors at the inner plasma membrane. Monomeric G proteins are a superfamily of GTP binding proteins with intrinsic GTPase activity and based on their sequence homology and function similarity they are classified into five major subfamilies: Ras, Rho, Rab, Ran and Arf (ADP ribosylation factor) (Pamonsinlapatham et al., 2009; Wittinghofer A., 1998). Within these small GTPases, Ras (p21Ras) controls cell proliferation, differentiation, migration and apoptosis. In humans, three RAS genes encode for 3 homologous Ras proteins: HRAS, NRAS, KRAS4A and KRAS4B (alternative splice variants of KRAS). Several members of the Ras superfamily cycles between an active conformation in which they bind GTP and an inactive GDP-bound form (Donovan et al., 2002), resulting in the tracking of internal vesicles, nuclear import, cell cycle progression, cytoskeletal reorganization, and protein translation. Under physiological conditions, the transition between the two states is controlled by **Guanine nucleotide exchange factors** (GEFs), which promote the activation of Ras proteins by stimulating the GDP/GTP exchange, and by **GTPase activating proteins** (GAPs), which accelerate RAS-mediated GTP

hydrolysis (Figure 5A). Inactivation of Ras hydrolysis activity induction by GAPs is indeed the predominant target of most common somatic mutations found in the oncogenic variants of RAS alleles (Pylayeva-Gupta et al., 2011). p120-Ras GTPase activating proteins (p120-RasGAP or RasGAP) has been identified as the essential negative regulator of the Ras-signalling pathway (Bos et al., 2007). RasGAP, is a multi-domain protein and apart from being a regulator of Ras, its N-terminal domain contains a number of signalling modules that mediate interaction with other proteins (see section 4.1 and 4.2) indicating that RasGAP bears functions independent of Ras (Pamonsinlapatham et al., 2009).

4.1. *RasGAP structure*

RasGAP is a 120 kDa cytosolic protein (Figure 5B). In the amino-terminal region it contains a Src Homology 3 (SH3) domain flanked by two SH2 domains. The SH3 domain is essential for Ras downstream signaling since it can bind several effector targets. For instance, RasGAP is able to control Rho-mediated cytoskeletal reorganization through its SH3 domain. Calpain small subunit 1 (Capns 1), a regulator of adhesive complex dynamics, has been reported to be a RasGAP SH3 binding partner. Aurora kinases can similarly interact with RasGAP through this domain. RasGAP SH3 binding protein 1 (G3BP1) is an endoribonuclease that has been characterized as a RasGAP SH3 binding protein (Parker et al., 1996), however a recent study has shown that no interaction exists between these two proteins (Annibaldi et al., 2011). The conserved SH2 domains, on the other hand, have important dynamic roles in specific signals associated with phosphorylated tyrosine kinase receptors such as PDGF and EGF, as well as with the non-receptor tyrosine kinase, v-Scr (Pamonsinlapatham et al., 2009). Both SH2 RasGAP domains are individually capable of binding p190-RhoGAP (a GAP protein specific for the Rho family of small GTPases). Members of the elongation factors family (eEF1A1 and 2), involved in cell proliferation, were also shown to interact with RasGAP SH2 domains (Panasyuk et al., 2008).

The second SH2 domain is followed by a pleckstrin homology (PH) domain that can bind to the GAP domain of RasGAP and interfere with Ras/RasGAP interaction. Furthermore, the expression of isolated RasGAP PH domain specifically inhibits Ras-

mediated signalling and transformation without affecting cellular growth (Drugan et al., 2000).

A calcium-dependent phospholipid-binding domain (CaLB/C2) follows the PH domain which binds Annexin-A6, a Ca^{+2} -regulated protein that forms a complex with RasGAP and induce Ras inactivation (Grewal and Enrich, 2006).

In the carboxy-terminal region of RasGAP is located the catalytic GAP domain. The main mechanisms by which GAPs catalyze GTP hydrolysis comprise the direct chemical contribution of the GAP protein to the active site of Ras; and the immobilization of G-proteins switch regions. RasGAP stabilizes the catalytically important glutamine 61 of Ras and thus the transitional state of the Ras/RasGAP complex, which in turns coordinates the attacking water molecule required for the GTP hydrolysis to take place. Arginine 789 of RasGAP is positioned into the phosphate-binding site neutralizing the emerging negative charge of the α -phosphate during hydrolysis of the GTP to GDP. Oncogenic mutations at positions 12 and 13 of Ras sterically block the proper orientation of the Arg789 of RasGAP and the Glu61 of Ras preventing GTP hydrolysis. Ras^{G12V}, Ras^{G13V} and Ras^{G61V} have therefore oncogenic activity.

4.2. *RasGAP as a Ras effector and beyond*

Ras is activated through the stimulation of tyrosine kinase/growth factor receptors (Lowy and Willumsen, 1993) and regulates diverse cellular responses through distinct signaling pathways such as Raf/MAPK/ERK, PI-3K/Akt and RASSF/MST1/0032, which are mainly involved in cell survival and proliferation. RasGAP binds to activated Ras (Ras-GTP) through its catalytic GAP domain and it is sufficient to favour Ras GTPase activity. Moreover RasGAP has an amino-terminal region similar in structure to “adaptor” proteins, which may indicate that RasGAP can have other functions related or unrelated to its function as a regulator of Ras.

Aurora Kinase has been identified as a binding partner of RasGAP SH3 domain (Gigoux et al., 2002). The human Aurora kinase orthologs (HsAIRK-1 and HsAIRK-2) are proteins involved in proper cell division and are thus cell cycle-dependent. The activation, de-activation and degradation of these proteins are regulated by

phosphorylation (cAMP-dependent protein kinase) and de-phosphorylation (protein phosphatase 1) (Walter et al., 2000). Gigoux and collaborators have proposed a model in which RasGAP regulates Aurora kinase orthologs by facilitating their association with kinases and phosphatases necessary for their regulation, indicating that RasGAP can be implicated in proliferation.

RasGAP and p190-RhoGAP are believed to be implicated in the actin cytoskeleton remodelling (Kulkarni et al., 2000). Constitutive association between these two GTPases has been reported to be required for turnover and reorganization of stress fibers and focal adhesions, independently of Ras activation. In addition RasGAP knock out fibroblasts have dramatically reduced cell migration (Bos et al., 2007), which implies that RasGAP, although by mechanisms not clearly understood, is implicated in cell migration and cytoskeleton remodelling.

RasGAP plays also a pivotal role in the onset of apoptosis. As mentioned in the previous section, p120-RasGAP possesses two conserved caspase-3 cleavage sites (Yang and Widmann, 2001). The sequential cleavage of RasGAP in these two sites by active caspase-3 will determine cell fate (Figure 5C). At low levels of caspase activity, RasGAP is first cleaved at position 455. The N-terminal fragment (fragment N) generated by this cleavage induces a protective response against apoptotic induced cell death. The signaling pathway that mediates this response is the Ras/PI3K/Akt signaling pathway (Yang and Widmann, 2002), which is crucial for cell survival in low stress conditions (Yang et al., 2004). However, when activated caspase-3 level increases due to a stronger stress condition, fragment N is further cleaved at position 157 into fragments N1 and N2, abrogating its anti-apoptotic activity (Yang et al., 2005). The capacity of RasGAP to sense the level of stress within a cell through caspase-3 activity led us to propose this GTPase as cell death *versus* survival molecular switch (Yang et al., 2004).

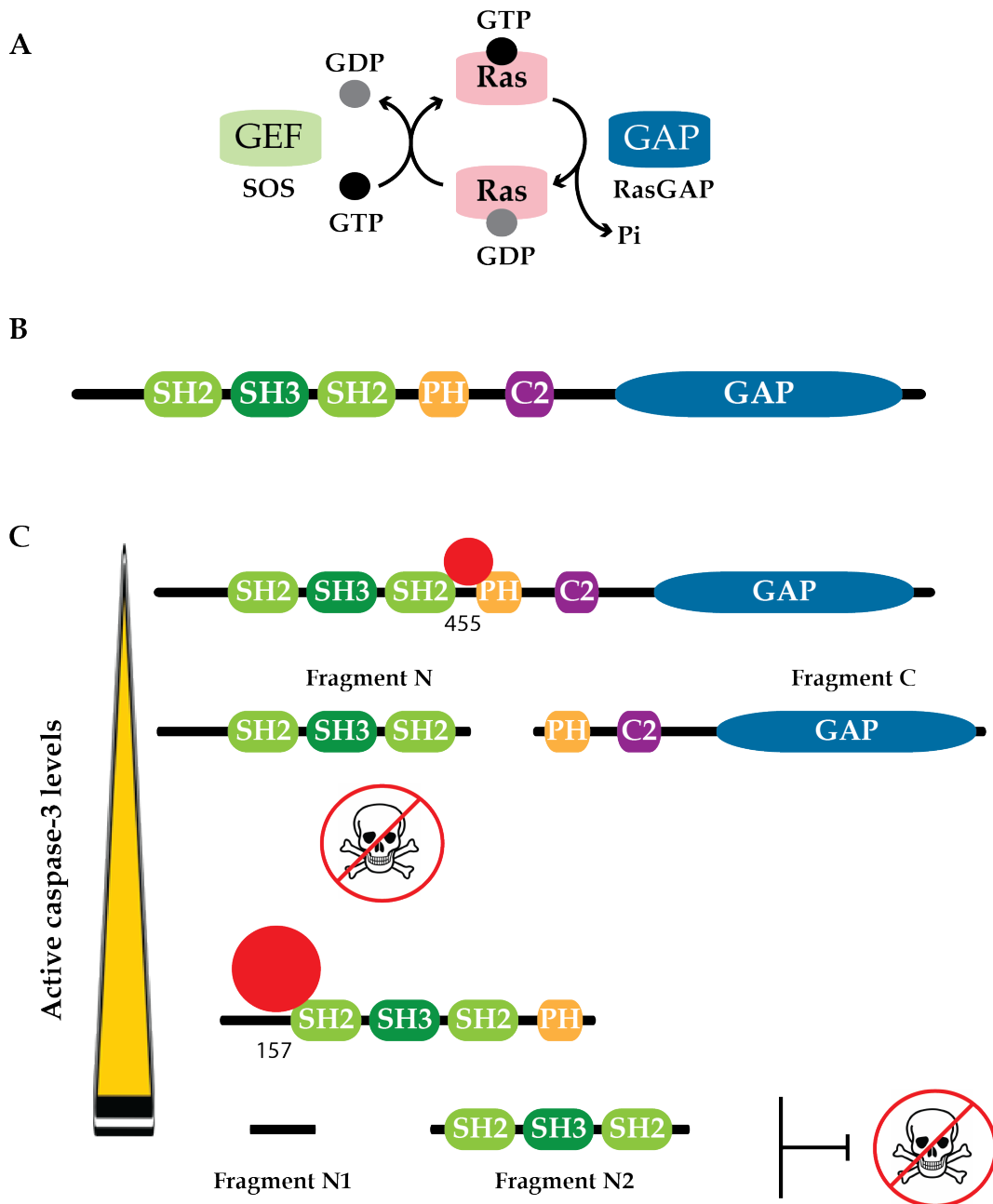


Figure 5: RasGAP function and structure. A_ Ras cycle of activation and inactivation by the Ras-specific Guanine Exchange factor (GEF), SOS, and the Ras GTPase Activating Protein (GAP), RasGAP, respectively. B_ RasGAP domain structure. SH2/3: Scr Homology 2 or 3 domain. PH: pleckstrin homology domain. C2: calcium-dependent phospholipid domain. C_ Caspase-3 - dependent sequential cleavage of RasGAP. The level of stress and of caspase-3 activation is represented by the yellow bar on the left of the figure. Cleavage positions at low or high levels of active caspase-3 are represented by the small and big red dots, respectively. The numbers indicate the cleavage position

5. Ras/PI3K/Akt: a signaling cascade important for RasGAP derived-fragment N induced protection

The cleavage of RasGAP by caspase-3 at position 455 and the resulting N-terminal fragment (hereafter referred to as fragment N) generation are crucial events in the protection of cells against apoptotic cell death *in vitro* (Yang and Widmann, 2001). Several evidences indicate that this protective response requires the activation of Ras, Phosphatidylinositol-3-kinase (PI3K) and Akt since their corresponding dominant negative mutants abrogate completely the inhibitory effect of fragment N on apoptosis. Furthermore, constitutively active forms of Ras, PI3K or Akt mimic fragment N-mediated protective effects. A further indication comes from the overexpression of a caspase-3 insensitive mutant form of fragment N (N-D157A), which is able to induce the activation of the aforementioned proteins (Yang and Widmann, 2002).

5.1. The Ras/PI3K/Akt signaling

The activation of Ras/PI3K/Akt signaling cascade is triggered by the engagement of the tyrosine kinase receptor to their cognate ligands, which induces the dimerization and autophosphorylation at tyrosine residues. Once the receptor has been stimulated, PI3K and Ras are recruited to the membrane where they activate a number of signaling cascades.

PI3K is a heterodimeric protein with an 85-kDa regulatory subunit containing two SH2 domains and a 110-kDa catalytic subunit. Phosphorylated tyrosine residues interact with the SH2 domains of the p85 subunit, recruiting PI3K to the membrane together with the adaptor protein Grb2. Consequently, Grb2 recruits and activates SOS (GEF specific for Ras) inducing the activation of Ras, also recruited to the membrane. Finally Ras determines the activation of p110 of PI3K. Activated p110 transfers phosphate groups to the membrane phospholipid phosphatidylinositol 3,4-bisphosphate (PIP₂) thereby generating the second messenger lipids phosphatidylinositol 3,4,5-triphosphate (PIP₃). These lipids attract a series of kinases bearing PH domains to the plasma membrane such as Akt (or protein kinase B,

PKB), phosphoinositide-dependent kinase 1 (PDK1) (Steelman et al., 2011) and maybe also mTORC2 (Gan et al., 2011), both kinases responsible for Akt activation (Figure 6).

Akt is a 57 kDa enzyme belonging to the ACG protein kinase family. The Akt family includes three isoforms that are highly conserved: Akt1/ α , Akt2/ β , and Akt3/ γ . Whereas Akt1 and 2 are ubiquitously expressed, Akt 3 displays a more restrictive tissue specific pattern of expression, being found abundantly in the nervous tissue (Brazil et al., 2004). All three Akt isoforms share structural homology and contain three domains: an N-terminal pleckstrin (PH) domain, a C-terminal regulatory domain (RD), and a central kinase domain (KD) (Thomas et al., 2002) (Figure 6). At least two residues within Akt are rapidly phosphorylated, including Threonine 308 (T308) which lies within the KD and the Serine 473 within the RD. Akt recruitment to the membrane promotes its phosphorylation by both PDK1 and mTORC2, the latter being a protein complex bearing Rictor, G β L and the mammalian target of rapamycin (mTOR), a conserved Ser / Thr protein kinase (Sarbasov et al., 2005).

Recent data suggests that not only PIP3 can interact with Akt but also phosphatidylserine (PS), another phospholipid highly enriched in the inner leaflet of the plasma membrane. The interaction of the RD with either PIP3 or PS induces an open conformation of the RD that exposes S473 for phosphorylation by mTORC2. Both localization of Akt to the membrane and phosphorylation at S473, promote the ability of PDK1 to phosphorylate T308, leading to full activation of Akt (Huang et al., 2011).

After activation, Akt leaves the membrane to phosphorylate up to 100 substrates thereby modulating a variety of cellular functions. Akt may translocate to the nucleus (Martelli et al., 2006) where it affects either directly or indirectly the activity of various transcriptional factors such as CREB (Du and Montminy, 1998), E2F (Brennan et al., 1997) and NF- κ B (Cheng et al., 2011). Akt stimulates cell proliferation by inactivating p27 (Fujita et al., 2002) and preventing the glycogen synthase kinase-3 β (GSK3 β) - mediated Myc and cyclin D1 inhibition (Vivanco and Sawyers, 2002). Additionally Akt is one of the main regulators of a complex involved in protein translation and ribosome biogenesis; the mTORC1 complex (Guertin et al., 2006). mTORC1 is comprised of mTOR and Raptor and is sensitive to rapamycin (in contrast to the

mTORC2 complex). Akt positively regulates this complex by phosphorylating two different substrates, the GAP TSC2 and PRAS40 (proline-rich Akt substrate of 40 kDa) leading to inactivation of their functions. TSC2 inhibits the small GTPase, Rheb (Ras-homolog enriched in brain), which activates mTORC1. On the other hand PRAS40 negatively regulates mTORC1 through competition with Rheb and thus its phosphorylation leads to inactivation and release of competition. This dual regulation makes Akt the main promoter of the activation of mTORC1 pathway, which turns on the translational machinery to produce ribosomes and increases the protein synthesis rate (Carracedo and Pandolfi, 2008). Conversely, mTORC1 has been shown to inhibit Akt activation by a negative feedback loop mechanism (Carracedo et al., 2008).

Last, but not least, Akt signaling exerts a strong anti-apoptotic effect through the phosphorylation of several targets such as the forkhead transcription factors (FOXO1/3/4) family and BAD. Phosphorylation causes the association of these pro-apoptotic proteins with 14-3-3 proteins in the cytoplasm, which induces the export from the nucleus (van der Horst and Burgering, 2007) or blockage of mitochondrial translocation (del Peso L. et al., 1997), respectively. Another anti-apoptotic Akt target is the murine double minute 2 (MDM2), which antagonizes p53-mediated apoptosis (Steelman et al., 2011).

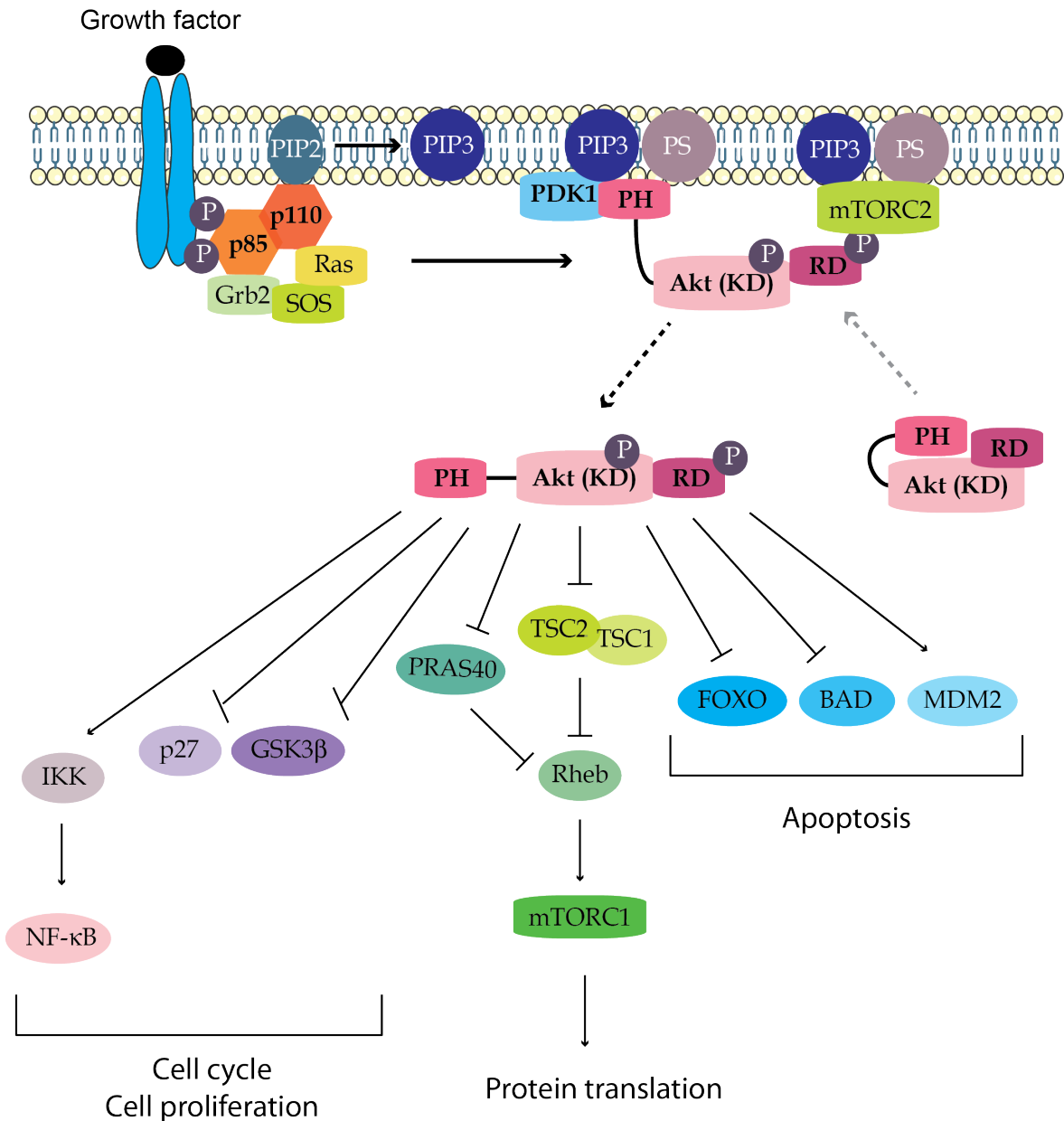


Figure 6: Akt activation mechanism. Akt is activated in the plasma membrane by a series of phosphorylating events. After activation p-Akt detaches from the membrane and activates or inhibits a series of proteins leading to various cellular responses. P: phosphate group. Grey dashed arrow represents the transition between the inactivated and activated state of Akt. Black dashed arrow represents the detachment of already activated Akt from the plasma membrane. Downstream Akt targets are highly simplified and represent an example of the wide downstream signaling cascade triggered by Akt.

6. Skin: a sophisticated barrier against external insults

The skin is a sophisticated and dynamic organ that basically serves as a barrier between the internal environment and the world outside. Yet, the skin plays many important roles in homeostatic and temperature regulation, prevention of loss of fluids, electrolytes and proteins, sensory reception and immune surveillance. In fact without the skin we would literally evaporate.

6.1. The skin triple layer: Epidermis, Dermis and Hypodermis.

The **epidermis** is the most external surface of the skin and contains mostly keratinocytes plus a smaller population of Langerhans cells and melanocytes (Elias, 2007). The epidermis is composed of 4 to 5 layers in humans (2 to 4 layers in mouse), where the outermost one is the *stratum corneum* (Figure 7). This layer is composed of enucleated corneocytes, which are the very last differentiated state of keratinocytes. The following layer is the *stratum lucidum* and, similarly to the *stratum corneum*, is composed of anucleated corneocytes, although this layer is only found in palms and soles. The granular layer (*stratum granulosum*) is just below and is composed of keratinocytes containing keratohyalin granules, which promote hydration and crosslinking of keratin. The middle layer is the spinous layer (*stratum spinosum*) with desmosomal connections between keratinocytes. Langerhans cells, which are immunologically active cells, can be found in this layer. Finally the basal layer (*stratum basale*) is composed mainly of proliferating and non-proliferating keratinocytes attached to the basement layer by hemidesmosomes and integrins. Most cells within the basal layer are the rapidly dividing progeny of stem cells and are referred to as transit amplifying cells which undergo a limited number of divisions before they escape the cell cycle and commit to terminal differentiation, detach by asymmetric cell division from the basement membrane and begin their way towards the surface of the skin (Barrandon and Green, 1987; Jones et al., 2007). Melanocytes, which are the cells that produce melanin and therefore determine the color of the skin, are present in this layer and are connected to keratinocytes through dendrites. Merkel cells are also found and are involved in touch sensation (Farage et al., 2007).

The **dermis**, separated by the epidermis by a basement membrane, is composed mainly of connective tissue and blood vessels (Figure 7). This tissue supports the epidermis and contains elastin and collagen, which give the skin its characteristic elasticity and tensile strength, respectively. The dermis also contains nerve fibers, sensory receptors, hyaluronic acid, responsible for the normal turgor of dermis because of its water-holding capacity, and supportive glycosaminoglycans (GAG).

The **hypodermis** is located below the dermis and is composed of loose connective tissue and subcutaneous fat (Figure 7). It functions as a thermoregulator and provides cushioning and stability to the skin connecting the dermis with internal organs (*Martini F. Fundamentals of Anatomy and Physiology. San Francisco: Benjamin-Cummings, 2004*).

6.2. *The sun and the skin*

The epidermis is a stratified epithelium in which balanced proliferation, differentiation, and cell death are essential for the maintenance of skin organization and function (Fuchs and Raghavan, 2002). The epidermis is constantly exposed to external insults such as ultraviolet radiation (UVR). UV light is electromagnetic radiation with a shorter wavelength than that from visible light (400-780 nm) ranging from 200 nm to 400 nm and is composed of three fractions (Figure 8A).

The shorter one is the UV-C light ranging from 200-290 nm, the longer one is the UV-A light from 320-400 nm and the UV-B that stands midway ranges from 290-320 nm. Even though UV-C photons cause the most striking effects and it is used as germicidal, they are not relevant for human health since they are absorbed by atmospheric layers of oxygen and stratospheric layers of ozone. On the other hand UV-A and B radiations do traverse these layers and can elicit acute and chronic biological effects (Matsumura and Ananthaswamy, 2004). While the longer but less energetic UV-A reaches the basal layer and the deeper dermal compartments (Lavker et al., 2003), UV-B light, being more energetic, is scattered and absorbed faster within the superficial epidermal layers. A biological effect of UVR is established within the skin when chromophores absorb energy that matches their absorption maxima. When UV photons strike the skin part of the energy is reflected, but another

part is transmitted and finally absorbed. Chromophores are molecules that absorb the light energy, resulting in the transition of their electron from the ground state to the excited state. Since the depth of penetration through the epidermis varies with the different wavelengths, the chromophores affected by UV-A and UV-B are different. In this project I was most interested in the keratinocyte response to stress and thus I will focus on UV-B light effects.

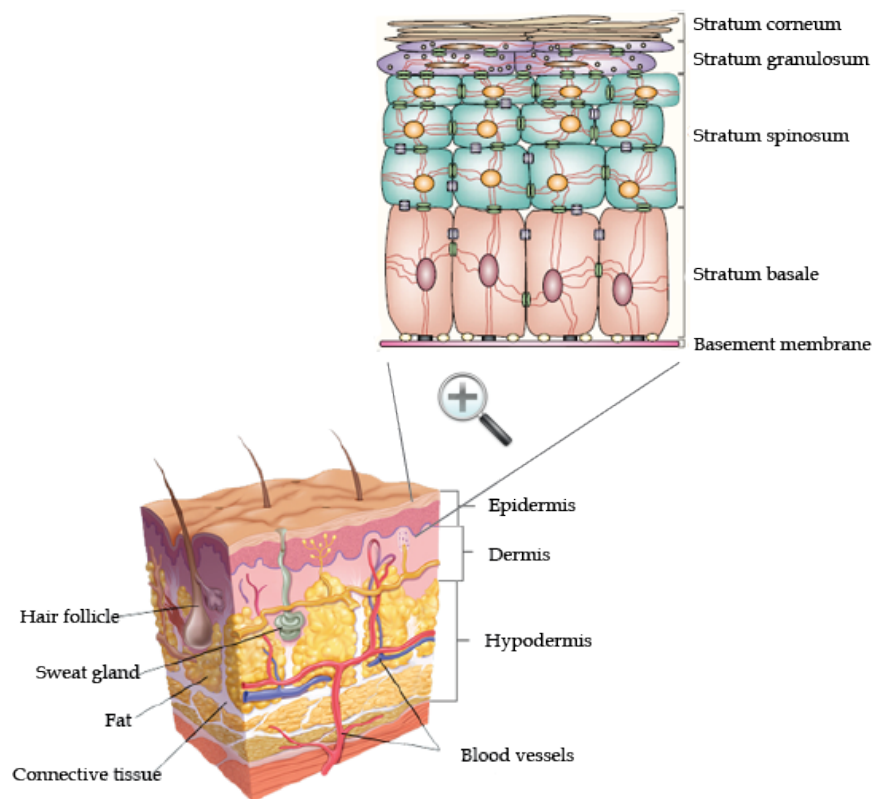


Figure 7: Graphic representation of the skin with a detailed illustration of the epidermis composition. Within the epidermis the cells are well interconnected: green structures are desmosomes, dark gray represents hemidesmosomes, white coloured are focal adhesions and light grey, adherent junctions. *This figure was adapted from (Fuchs and Raghavan, 2002).*

6.3. UV-B light

UV-B is one of the main causes of DNA damage in the skin since its main chromophores include purine and pyrimidine bases in DNA and RNA with an absorption maximum of 200-290 nm. The most common photo-induced reactions in DNA bases, called photoproducts, are the (6-4) pyrimidine-pyrimidone [(6-4)PP] and cyclobutane pyrimidine dimers (CPD) (Figure 8B). CPDs are the result of a covalent linkage between CC or TT bases where UV-B light is absorbed by a double bond in pyrimidine bases (thymidine -T- and cytosine -C- in DNA), opening the bond and allowing it to react with neighboring molecules. If the neighboring molecule is another pyrimidine base they may form a covalent bond resulting in a tight four-membered ring (TT or CC dimer) (Figure 8B). Alternatively, (6-4)PP arise from the formation of a single bond between the C6 position of the 5'-pyrimidine in an adjacent pair, to the C4 position of the 3'-pyrimidine (Friedberg, 2003) (Figure 8B). The presence of these lesions in the DNA double helix drastically alters processes such as replication and transcription, since they not only represent a physical blockage but can also lead to a misspelling of information and apparition of mutations (Batista et al., 2009).

CPDs and (4-6)PPs are mainly repaired by the Nuclear Excision Repair System (NER) machinery that is orchestrated by around 15 proteins. NER first recognizes the damage or distortion in the double-helix and a helicase unwind the strand at the site of damage. This unwinding is followed by an incision at the 3' and 5' ends of the DNA strand and removal of around 25-30 nucleotides. The double strand break is then filled-in by the DNA polymerase δ or ϵ resulting in a repaired damage (Fuss and Cooper, 2006; Nospikel et al., 2009). In order to have adequate time for DNA repair, cells are arrested at G1 or G2 phases of the cell cycle, both events being modulated by the tumor suppressor protein p53 or, the so called "guardian of the genome". If the damage has not been correctly repaired, p53 induces apoptosis or senescence to prevent cells with severely damaged DNA from becoming cancerous (Latonen and Laiho, 2005)

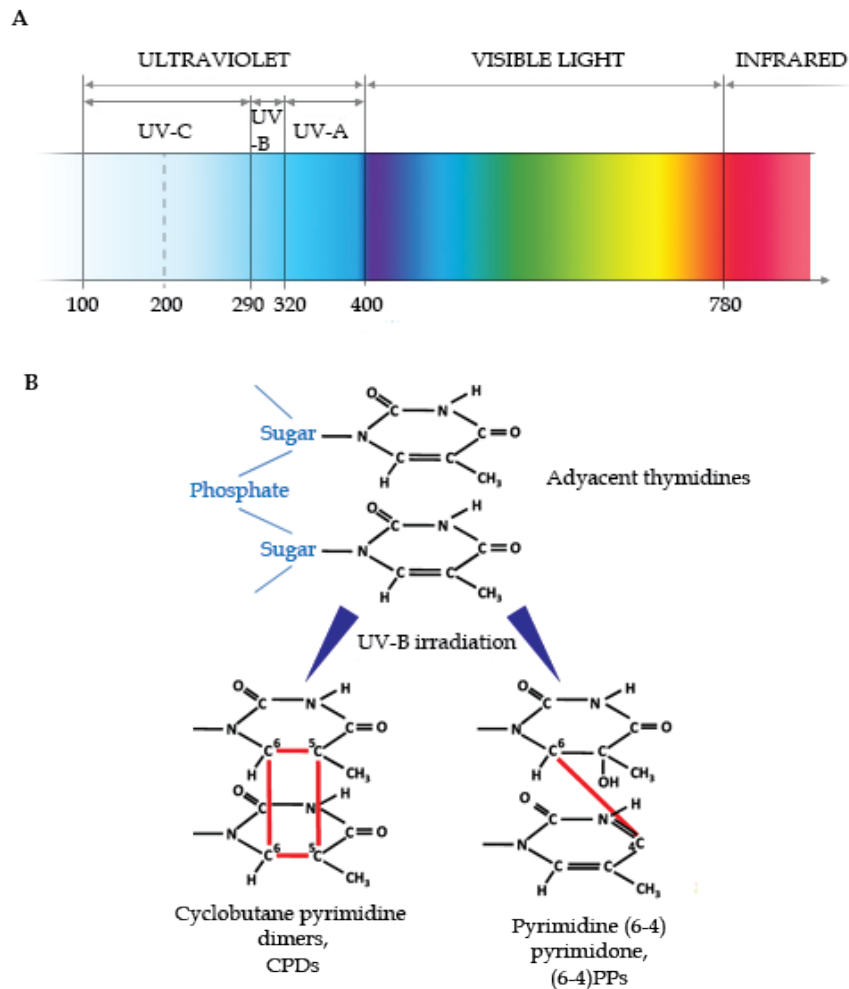


Figure 8: A_ The electromagnetic spectrum. UVR are depicted in light blue. B_ Most common photoproduct lesions in the DNA caused upon exposure to UV-B light. This figure was adapted from (Batista et al., 2009).

Other levels of cellular damage induced by UV-B are the so-called “photosensitizers”, which are proteins targeted by UV-B. Excitation of these chromophores results in their conversion into excited and highly unstable molecules which can transfer the energy of the absorbed photon to adjacent molecules (lipids, proteins and nucleic acids) or and/or to molecular oxygen, leading to the formation of reactive oxygen species (ROS). ROS can then initiate and propagate a complex signal transduction

network dictating the fate of keratinocytes (Batista et. al., 2009; Van Laethem et al., 2005). The skin counteracts with numerous antioxidant defense mechanisms that consist of enzymes, such as catalase and glutathione, and natural antioxidants, like the ascorbic acid and α -tocopherol, that will minimize the deleterious effects of ROS.

Following exposure to UV-B light, if the NER machinery fails to repair excessive DNA damage or the endogenous antioxidant defense systems become overwhelmed by high production of ROS, cells will become sunburn cells (SBC) (Van Laethem et al., 2005). SBC exhibit morphologic characteristics of apoptotic cell death with a pyknotic (condensed) nuclei and eosinophilic cytoplasm and are basically keratinocytes undergoing apoptosis (Saskia Lippens, 2009).

Reference List

- Adrain,C., Creagh,E.M., and Martin,S.J. (2001). Apoptosis-associated release of Smac/DIABLO from mitochondria requires active caspases and is blocked by Bcl-2. *EMBO J* 20, 6627-6636.
- Akhter,A., Caution,K., Abu-áKhweek,A., Tazi,M., Abdulrahman,B., Abdelaziz,D., Voss,O., Doseff,A., Hassan,H., Azad,A., Schlesinger,L., Wewers,M., Gavrilin,M., and Amer,A. (2012). Caspase-11 Promotes the Fusion of Phagosomes Harboring Pathogenic Bacteria with Lysosomes by Modulating Actin Polymerization. *Immunity* 37, 35-47.
- Annibaldi,A., Dousse,A., Martin,S., Tazi,J., and Widmann,C. (2011). Revisiting G3BP1 as a RasGAP binding protein: sensitization of tumor cells to chemotherapy by the RasGAP 317-326 sequence does not involve G3BP1. *PLoS ONE* 6, e29024.
- Antonsson,B., Conti,F., Ciavatta,A., Montessuit,S., Lewis,S., Martinou,I., Bernasconi,L., Bernard,A., Mermod,J.J., Mazzei,G., Maundrell,K., Gambale,F., Sadoul,R., and Martinou,J.C. (1997). Inhibition of Bax channel-forming activity by Bcl-2. *Science* 277, 370-372.
- Barrandon,Y. and Green,H. (1987). Three clonal types of keratinocyte with different capacities for multiplication. *Proc. Natl. Acad. Sci. U. S. A* 84, 2302-2306.
- Barret,R., Osborne,T.P., and Wheatley,S.P. (2010). Phosphorylation of survivin at threonine 34 inhibits its mitotic function and enhances its cytoprotective activity. *Cell Cycle* 8, 278-283.
- Batista,L.s.F.Z., Kaina,B., Meneghini,R.r., and Menck,C.F.M. (2009). How DNA lesions are turned into powerful killing structures: Insights from UV-induced apoptosis. *Mutation Research/Reviews in Mutation Research* 681, 197-208.
- Bos,J.L., Rehmann,H., and Wittinghofer,A. (2007). GEFs and GAPs: critical elements in the control of small G proteins. *Cell* 129, 865-877.
- Brazil,D.P., Yang,Z.Z., and Hemmings,B.A. (2004). Advances in protein kinase B signalling: AKTion on multiple fronts. *Trends Biochem. Sci.* 29, 233-242.
- Brennan,P., Babbage,J.W., Burgering,B.M., Groner,B., Reif,K., and Cantrell,D.A. (1997). Phosphatidylinositol 3-kinase couples the interleukin-2 receptor to the cell cycle regulator E2F. *Immunity* 7, 679-689.
- Burguillos,M.A., Deierborg,T., Kavanagh,E., Persson,A., Hajji,N., Garcia-Quintanilla,A., Cano,J., Brundin,P., Englund,E., Venero,J.L., and Joseph,B. (2011). Caspase signalling controls microglia activation and neurotoxicity. *Nature* 472, 319-324.
- Carracedo,A., Ma,L., Teruya-Feldstein,J., Rojo,F., Salmena,L., Alimonti,A., Egia,A., Sasaki,A.T., Thomas,G., Kozma,S.C., Papa,A., Nardella,C., Cantley,L.C., Baselga,J., and Pandolfi,P.P. (2008). Inhibition of mTORC1 leads to MAPK pathway activation through a PI3K-dependent feedback loop in human cancer. *J Clin. Invest* 118, 3065-3074.
- Carracedo,A. and Pandolfi,P.P. (2008). The PTEN-PI3K pathway: of feedbacks and cross-talks. *Oncogene* 27, 5527-5541.

- Chen,C.J., Kono,H., Golenbock,D., Reed,G., Akira,S., and Rock,K.L. (2007). Identification of a key pathway required for the sterile inflammatory response triggered by dying cells. *Nat Med.* *13*, 851-856.
- Cheng,J., Phong,B., Wilson,D.C., Hirsch,R., and Kane,L.P. (2011). Akt fine-tunes NF-kB-dependent gene expression during T cell activation. *Journal of Biological Chemistry.*
- Cheung,W.L., Ajiro,K., Samejima,K., Kloc,M., Cheung,P., Mizzen,C.A., Beeser,A., Etkin,L.D., Chernoff,J., Earnshaw,W.C., and Allis,C.D. (2003). Apoptotic phosphorylation of histone H2B is mediated by mammalian sterile twenty kinase. *Cell* *113*, 507-517.
- Coleman,M.L., Sahai,E.A., Yeo,M., Bosch,M., Dewar,A., and Olson,M.F. (2001). Membrane blebbing during apoptosis results from caspase-mediated activation of ROCK I. *Nat Cell Biol* *3*, 339-345.
- Colnaghi,R., Connell,C.M., Barrett,R.M.A., and Wheatley,S.P. (2006). Separating the Anti-apoptotic and Mitotic Roles of Survivin. *J. Biol. Chem.* *281*, 33450-33456.
- Croft,D.R., Coleman,M.L., Li,S., Robertson,D., Sullivan,T., Stewart,C.L., and Olson,M.F. (2005). Actin-
- del Peso L., Gonzalez-Garcia,M., Page,C., Herrera,R., and Nunez,G. (1997). Interleukin-3-induced phosphorylation of BAD through the protein kinase Akt. *Science* *278*, 687-689.
- Darding,M. and Meier,P. (2012). IAPs: guardians of RIPK1. *Cell Death Differ* *19*, 58-66.
- Denecker,G., Ovaere,P., Vandenabeele,P., and Declercq,W. (2008). Caspase-14 reveals its secrets. *The Journal of Cell Biology* *180*, 451-458.
- Di-Poi,N., Tan,N.S., Michalik,L., Wahli,W., and Desvergne,B. (2002). Antiapoptotic role of PPARbeta in keratinocytes via transcriptional control of the Akt1 signaling pathway. *Mol Cell* *10*, 721-733.
- Dohi,T. and Altieri,D.C. (2005). Mitochondrial dynamics of survivin and "four dimensional" control of tumor cell apoptosis. *Cell Cycle* *4*, 21-23.
- Dohi,T., Beltrami,E., Wall,N.R., Plescia,J., and Altieri,D.C. (2004a). Mitochondrial survivin inhibits apoptosis and promotes tumorigenesis. *Journal of clinical investigation* *114*, 1117-1127.
- Dohi,T., Okada,K., Xia,F., Wilford,C.E., Samuel,T., Welsh,K., Marusawa,H., Zou,H., Armstrong,R., Matsuzawa,S.i., Salvesen,G.S., Reed,J.C., and Altieri,D.C. (2004b). An IAP-IAP Complex Inhibits Apoptosis. *J. Biol. Chem.* *279*, 34087-34090.
- Donovan,S., Shannon,K.M., and Bollag,G. (2002). GTPase activating proteins: critical regulators of intracellular signaling. *Biochimica et Biophysica Acta (BBA) - Reviews on Cancer* *1602*, 23-45.
- Drugan,J.K., Rogers-Graham,K., Gilmer,T., Campbell,S., and Clark,G.J. (2000). The Ras/p120 GTPase-activating protein (GAP) interaction is regulated by the p120 GAP pleckstrin homology domain. *J Biol Chem.* *275*, 35021-35027.
- Du,K. and Montminy,M. (1998). CREB is a regulatory target for the protein kinase Akt/PKB. *J Biol Chem.* *273*, 32377-32379.

- Dubrez-Daloz,A.D.a.J.C. (2009). IAPS : More than just inhibitors of apoptosis proteins. *Cell Cycle*.
- Eckhart,L., Declercq,W., Ban,J., Rendl,M., Lengauer,B., Mayer,C., Lippens,S., Vandenabeele,P., and Tschachler,E. (2000). Terminal differentiation of human keratinocytes and stratum corneum formation is associated with caspase-14 activation. *J Invest Dermatol* 115, 1148-1151.
- Elias,P. (2007). The skin barrier as an innate immune element. *Seminars in Immunopathology* 29, 3-14.
- Farage,M.A., Miller,K.W., Elsner,P., and Maibach,H.I. (2007). Structural characteristics of the aging skin: a review. *Cutan. Ocul. Toxicol.* 26, 343-357.
- Feoktistova,M., Geserick,P., Kellert,B., Dimitrova,D.P., Langlais,C., Hupe,M., Cain,K., MacFarlane,M., Hacker,G., and Leverkus,M. (2011). cIAPs block Ripoptosome formation, a RIP1/caspase-8 containing intracellular cell death complex differentially regulated by cFLIP isoforms. *Mol Cell* 43, 449-463.
- Friedberg,E.C. (2003). DNA damage and repair. *Nature* 421, 436-440.
- Frost (2001). Exploitation of a non-apoptotic caspase to regulate the abundance of the cdk1 p27KIP1 in transformed lymphoid cells. *Oncogene*.
- Fuchs,E. and Raghavan,S. (2002). Getting under the skin of epidermal morphogenesis. *Nat Rev Genet* 3, 199-209.
- Fujita,N., Sato,S., Katayama,K., and Tsuruo,T. (2002). Akt-dependent Phosphorylation of p27Kip1 Promotes Binding to 14-3-3 and Cytoplasmic Localization. *Journal of Biological Chemistry* 277, 28706-28713.
- Fujita,J., Crane,A.M., Souza,M.K., Dejosez,M., Kyba,M., Flavell,R.A., Thomson,J.A., and Zwaka,T.P. (2008). Caspase Activity Mediates the Differentiation of Embryonic Stem Cells. *Cell Stem Cell* 2, 595-601.
- Fulda,S. and Debatin,K.M. (2006). Extrinsic versus intrinsic apoptosis pathways in anticancer chemotherapy. *oncogene* 25, 4798-4811.
- Fuss,J.O. and Cooper,P.K. (2006). DNA repair: dynamic defenders against cancer and aging. *PLoS Biol* 4, e203.
- Gan,X., Wang,J., Su,B., and Wu,D. (2011). Evidence for Direct Activation of mTORC2 Kinase Activity by Phosphatidylinositol 3,4,5-Trisphosphate. *Journal of Biological Chemistry* 286, 10998-11002.
- Garrido,C. and Kroemer,G. (2004). Life's smile, death's grin: vital functions of apoptosis-executing proteins. *Curr Opin. Cell Biol* 16, 639-646.
- Gigoux,V.+, L'Hoste,S.+, Raynaud,F., Camonis,J., and Garbay,C. (2002). Identification of Aurora Kinases as RasGAP Src Homology 3 Domain-binding Proteins. *J. Biol. Chem.* 277, 23742-23746.
- Goldstein,J.C., Munoz-Pinedo,C., Ricci,J.E., Adams,S.R., Kelekar,A., Schuler,M., Tsien,R.Y., and Green,D.R. (2005). Cytochrome c is released in a single step during apoptosis. *Cell Death Differ* 12, 453-462.

- Goldstein, J.C., Waterhouse, N.J., Juin, P., Evan, G.I., and Green, D.R. (2000). The coordinate release of cytochrome c during apoptosis is rapid, complete and kinetically invariant. *Nat Cell Biol* 2, 156-162.
- Grewal, T. and Enrich, C. (2006). Molecular mechanisms involved in Ras inactivation: the annexin A6-p120GAP complex. *Bioessays* 28, 1211-1220.
- Guertin, D.A., Stevens, D.M., Thoreen, C.C., Burds, A.A., Kalaany, N.Y., Moffat, J., Brown, M., Fitzgerald, K.J., and Sabatini, D.M. (2006). Ablation in mice of the mTORC components raptor, rictor, or mLST8 reveals that mTORC2 is required for signaling to Akt-FOXO and PKCalpha, but not S6K1. *Dev. Cell* 11, 859-871.
- Gyrd-Hansen, M. and Meier, P. (2010). IAPs: from caspase inhibitors to modulators of NF- κ B, inflammation and cancer. *Nat Rev Cancer* 10, 561-574.
- Haas, T.L., Emmerich, C.H., Gerlach, B., Schmukle, A.C., Cordier, S.M., Rieser, E., Feltham, R., Vince, J., Warnken, U., Wenger, T., Koschny, R., Komander, D., Silke, J., and Walczak, H. (2009). Recruitment of the linear ubiquitin chain assembly complex stabilizes the TNF-R1 signaling complex and is required for TNF-mediated gene induction. *Mol Cell* 36, 831-844.
- Helfer, B., Boswell, B.C., Finlay, D., Cipres, A., Vuori, K., Bong, K.T., Wallach, D., Dorfleutner, A., Lahti, J.M., Flynn, D.C., and Frisch, S.M. (2006). Caspase-8 promotes cell motility and calpain activity under nonapoptotic conditions. *Cancer Res.* 66, 4273-4278.
- Hoste, E., Kemperman, P., Devos, M., Denecker, G., Kezic, S., Yau, N., Gilbert, B., Lippens, S., De, G.P., Roelandt, R., Van, D.P., Gevaert, K., Presland, R.B., Takahara, H., Puppels, G., Caspers, P., Vandenabeele, P., and Declercq, W. (2011). Caspase-14 is required for filaggrin degradation to natural moisturizing factors in the skin. *J Invest Dermatol* 131, 2233-2241.
- Huang, B.X., Akbar, M., Kevala, K., and Kim, H.Y. (2011). Phosphatidylserine is a critical modulator for Akt activation. *The Journal of Cell Biology*.
- Jones, P.H., Simons, B.D., and Watt, F.M. (2007). Sic transit gloria: farewell to the epidermal transit amplifying cell? *Cell Stem Cell* 1, 371-381.
- Kayagaki, N., Warming, S., Lamkanfi, M., Walle, L.V., Louie, S., Dong, J., Newton, K., Qu, Y., Liu, J., Heldens, S., Zhang, J., Lee, W.P., Roose-Girma, M., and Dixit, V.M. (2011). Non-canonical inflammasome activation targets caspase-11. *Nature* 479, 117-121.
- Kerr, J.F., Wyllie, A.H., and Currie, A.R. (1972). Apoptosis: a basic biological phenomenon with wide-ranging implications in tissue kinetics. *Br. J Cancer* 26, 239-257.
- Krueger, A., Schmitz, I., Baumann, S., Krammer, P.H., and Kirchhoff, S. (2001). Cellular FLICE-inhibitory protein splice variants inhibit different steps of caspase-8 activation at the CD95 death-inducing signaling complex. *J Biol Chem.* 276, 20633-20640.
- Kulkarni, S.V., Gish, G., van der Geer, P., Henkemeyer, M., and Pawson, T. (2000). Role of p120 Ras-GAP in directed cell movement. *J Cell Biol* 149, 457-470.
- Lassus, P., Opitz-Araya, X., and Lazebnik, Y. (2002). Requirement for caspase-2 in stress-induced apoptosis before mitochondrial permeabilization. *Science* 297, 1352-1354.
- Latonen, L. and Laiho, M. (2005). Cellular UV damage responses--functions of tumor suppressor p53. *Biochim. Biophys. Acta* 1755, 71-89.

- Lauber,K., Bohn,E., Krober,S.M., Xiao,Y.J., Blumenthal,S.G., Lindemann,R.K., Marini,P., Wiedig,C., Zobywalski,A., Baksh,S., Xu,Y., Autenrieth,I.B., Schulze-Osthoff,K., Belka,C., Stuhler,G., and Wesselborg,S. (2003). Apoptotic cells induce migration of phagocytes via caspase-3-mediated release of a lipid attraction signal. *Cell* 113, 717-730.
- Launay,S., Hermine,O., Fontenay,M., Kroemer,G., Solary,E., and Garrido,C. (2005). Vital functions for lethal caspases. *Oncogene* 24, 5137-5148.
- Lavker,R.M., Sun,T.T., Oshima,H., Barrandon,Y., Akiyama,M., Ferraris,C., Chevalier,G., Favier,B., Jahoda,C.A., Dhouailly,D., Panteleyev,A.A., and Christiano,A.M. (2003). Hair follicle stem cells. *J Investig Dermatol Symp. Proc* 8, 28-38.
- Li,F. and Altieri,D.C. (1999). Transcriptional analysis of human survivin gene expression. *Biochem. J.* 344, 305-311.
- Li,F., Ambrosini,G., Chu,E.Y., Plescia,J., Tognin,S., Marchisio,P.C., and Altieri,D. (1998). Control of apoptosis and mitotic spindle checkpoint by survivin. *Nature* 396, 580-583.
- Li,J., Briehner,W.M., Scimone,M.L., Kang,S.J., Zhu,H., Yin,H., von Andrian,U.H., Mitchison,T., and Yuan,J. (2007). Caspase-11 regulates cell migration by promoting Aip1-Cofilin-mediated actin depolymerization. *Nat Cell Biol* 9, 276-286.
- Lopez,J., John,S.W., Tenev,T., Rautureau,G.J., Hinds,M.G., Francalanci,F., Wilson,R., Broemer,M., Santoro,M.M., Day,C.L., and Meier,P. (2011). CARD-mediated autoinhibition of cIAP1's E3 ligase activity suppresses cell proliferation and migration. *Mol Cell* 42, 569-583.
- Lowy,D.R. and Willumsen,B.M. (1993). Function and regulation of ras. *Annu. Rev Biochem.* 62, 851-891.
- Luciano,F., Herrant,M., Jacquelin,A., Ricci,J.E., and Auberger,P. (2003). The P54-cleaved form of the tyrosine kinase Lyn generated by caspases during BCR-induced cell death in B lymphoma acts as a negative regulator of apoptosis. *FASEB J.* 02-0716.
- Martelli,A.M., Faenza,I., Billi,A.M., Manzoli,L., Evangelisti,C., Fal+á,F., and Cocco,L. (2006). Intranuclear 3GÇ₁-phosphoinositide metabolism and Akt signaling: New mechanisms for tumorigenesis and protection against apoptosis? *Cellular Signalling* 18, 1101-1107.
- Martin,S.J., Reutelingsperger,C.P., McGahon,A.J., Rader,J.A., van Schie,R.C., LaFace,D.M., and Green,D.R. (1995). Early redistribution of plasma membrane phosphatidylserine is a general feature of apoptosis regardless of the initiating stimulus: inhibition by overexpression of Bcl-2 and Abl. *J Exp. Med.* 182, 1545-1556.
- Martinez-Caballero,S., Dejean,L.M., Kinnally,M.S., Oh,K.J., Mannella,C.A., and Kinnally,K.W. (2009). Assembly of the mitochondrial apoptosis-induced channel, MAC. *J Biol Chem.* 284, 12235-12245.
- Marusawa,H., MATsuzawa,S., Welsh,K., Zou,H., Armstrong,R., Tamm,I., and Reed,J.C. (2003). HBXIP functions as a cofactor of survivin in apoptosis suppression. *The EMBO Journal* 22, 2729-2740.
- Matsumura,Y. and Ananthaswamy,H.N. (2004). Toxic effects of ultraviolet radiation on the skin. *Toxicol. Appl. Pharmacol.* 195, 298-308.
- Matzinger,P. (2002). The danger model: a renewed sense of self. *Science* 296, 301-305.

- Munoz-Pinedo,C., Guio-Carrion,A., Goldstein,J.C., Fitzgerald,P., Newmeyer,D.D., and Green,D.R. (2006). Different mitochondrial intermembrane space proteins are released during apoptosis in a manner that is coordinately initiated but can vary in duration. *Proc. Natl. Acad. Sci. U. S. A* *103*, 11573-11578.
- Nagata,S., Nagase,H., Kawane,K., Mukae,N., and Fukuyama,H. (2003). Degradation of chromosomal DNA during apoptosis. *Cell Death Differ* *10*, 108-116.
- Nospikel,T. (2009). DNA repair in mammalian cells : Nucleotide excision repair: variations on versatility. *Cell Mol Life Sci.* *66*, 994-1009.
- Oberst,A., Dillon,C.P., Weinlich,R., McCormick,L.L., Fitzgerald,P., Pop,C., Hakem,R., Salvesen,G.S., and Green,D.R. (2011). Catalytic activity of the caspase-8-FLIP(L) complex inhibits RIPK3-dependent necrosis. *Nature* *471*, 363-367.
- Okuyama,R., Nguyen,B.C., Talora,C., Ogawa,E., di Vignano,A.T., Lioumi,M., Chiorino,G., Tagami,H., Woo,M., and Dotto,G.P. (2004). High Commitment of Embryonic Keratinocytes to Terminal Differentiation through a Notch1-caspase 3 Regulatory Mechanism. *Developmental Cell* *6*, 551-562.
- Orlando,K.A., Stone,N.L., and Pittman,R.N. (2006). Rho kinase regulates fragmentation and phagocytosis of apoptotic cells. *Exp. Cell Res.* *312*, 5-15.
- Pamonsinlapatham,P., Hadj-Slimane,R., Lepelletier,Y., Allain,B., Toccafondi,M., Garbay,C., and Raynaud,F. (2009). P120-Ras GTPase activating protein (RasGAP): A multi-interacting protein in downstream signaling. *Biochimie* *91*, 320-328.
- Panasyuk,G., Nemazanyy,I., Filonenko,V., Negrutskii,B., and El'skaya,A.V. (2008). A2 isoform of mammalian translation factor eEF1A displays increased tyrosine phosphorylation and ability to interact with different signalling molecules. *Int J Biochem. Cell Biol* *40*, 63-71.
- Parker,F., Maurier,F., Delumeau,I., Duchesne,M., Faucher,D., Debussche,L., Dugue,A., Schweighoffer,F., and Tocque,B. (1996). A Ras-GTPase-activating protein SH3-domain-binding protein. *Mol Cell Biol* *16*, 2561-2569.
- Pylayeva-Gupta,Y., Grabocka,E., and Bar-Sagi,D. (2011). RAS oncogenes: weaving a tumorigenic web. *Nat Rev Cancer* *11*, 761-774.
- Rao,L., Perez,D., and White,E. (1996). Lamin proteolysis facilitates nuclear events during apoptosis. *J Cell Biol* *135*, 1441-1455.
- Rebe,C., Cathelin,S., Launay,S., Filomenko,R., Prevotat,L., L'Ollivier,C., Gyan,E., Micheau,O., Grant,S., Dubart-Kupperschmitt,A., Fontenay,M., and Solary,E. (2007). Caspase-8 prevents sustained activation of NF-kappaB in monocytes undergoing macrophagic differentiation. *Blood* *109*, 1442-1450.
- Rodriguez,J.A., Span,S.W., Ferreira,C.G., Kruyt,F.A., and Giaccone,G. (2002). CRM1-mediated nuclear export determines the cytoplasmic localization of the anti-apoptotic protein Survivin. *Exp Cell Res* *275*, 44-53.
- Rumble,J.M. and Duckett,C.S. (2008). Diverse functions within the IAP family. *J Cell Sci.* *121*, 3505-3507.
- Samejima,K. and Earnshaw,W.C. (2005). Trashing the genome: the role of nucleases during apoptosis. *Nat Rev Mol Cell Biol* *6*, 677-688.

Sarbassov,D.D., Guertin,D.A., Ali,S.M., and Sabatini,D.M. (2005). Phosphorylation and Regulation of Akt/PKB by the Rictor-mTOR Complex. *Science* 307, 1098-1101.

Saskia Lippens,E.H.P.V.P.A.W.D. (2009). Cell death in the skin. *Apoptosis* 14, 549-569.

Savill,J. and Fadok,V. (2000). Corpse clearance defines the meaning of cell death. *Nature* 407, 784-788.

Sebbagh,M., Renvoize,C., Hamelin,J., Riche,N., Bertoglio,J., and Breard,J. (2001). Caspase-3-mediated cleavage of ROCK I induces MLC phosphorylation and apoptotic membrane blebbing. *Nat Cell Biol* 3, 346-352.

Suzuki,Y., Imai,Y., Nakayama,H., Takahashi,K., Takio,K., and Takahashi,R. (2001). A serine protease, HtrA2, is released from the mitochondria and interacts with XIAP, inducing cell death. *Mol Cell* 8, 613-621.

Scott,F.L., Denault,J.B., Riedl,S.J., Shin,H., Renatus,M., and Salvesen,G.S. (2005). XIAP inhibits caspase-3 and -7 using two binding sites: evolutionarily conserved mechanism of IAPs. *EMBO J* 24, 645-655.

Shikama,K. (1998). The Molecular Mechanism of Autoxidation for Myoglobin and Hemoglobin: A Venerable Puzzle. *Chem. Rev* 98, 1357-1374.

Song,Z., Liu,S., He,H., Hoti,N., Wang,Y., Feng,S., and Wu,M. (2004). A Single Amino Acid Change (Asp 53-> Ala53) Converts Survivin from Anti-apoptotic to Pro-apoptotic. *Mol. Biol. Cell* 15, 1287-1296.

Song,Z., Yao,X., and Wu,M. (2003). Direct Interaction between Survivin and Smac/DIABLO Is Essential for the Anti-apoptotic Activity of Survivin during Taxol-induced Apoptosis. *J. Biol. Chem.* 278, 23130-23140.

Sprick,M.R., Rieser,E., Stahl,H., Grosse-Wilde,A., Weigand,M.A., and Walczak,H. (2002). Caspase-10 is recruited to and activated at the native TRAIL and CD95 death-inducing signalling complexes in a FADD-dependent manner but can not functionally substitute caspase-8. *EMBO J* 21, 4520-4530.

Steelman,L.S., Chappell,W.H., Abrams,S.L., Kempf,R.C., Long,J., Laidler,P., Mijatovic,S., Maksimovic-Ivanic,D., Stivala,F., Mazzarino,M.C., Donia,M., Fagone,P., Malaponte,G., Nicoletti,F., Libra,M., Milella,M., Tafuri,A., Bonati,A., Basecke,J., Cocco,L., Evangelisti,C., Martelli,A.M., Montalto,G., Cervello,M., and McCubrey,J.A. (2011). Roles of the Raf/MEK/ERK and PI3K/PTEN/Akt/mTOR pathways in controlling growth and sensitivity to therapy-implications for cancer and aging. *Aging (Albany, NY)* 3, 192-222.

Strasser,A., Cory,S., and Adams,J.M. (2011). Deciphering the rules of programmed cell death to improve therapy of cancer and other diseases. *EMBO J* 30, 3667-3683.

Tait,S.W.G. and Green,D.R. (2010). Mitochondria and cell death: outer membrane permeabilization and beyond. *Nat Rev Mol Cell Biol* 11, 621-632.

Taylor,R.C., Cullen,S.P., and Martin,S.J. (2008). Apoptosis: controlled demolition at the cellular level. *Nat Rev Mol Cell Biol* 9, 231-241.

Thomas,C.C., Deak,M., Alessi,D.R., and van Aalten,D.M. (2002). High-resolution structure of the pleckstrin homology domain of protein kinase b/akt bound to phosphatidylinositol (3,4,5)-trisphosphate. *Curr Biol* 12, 1256-1262.

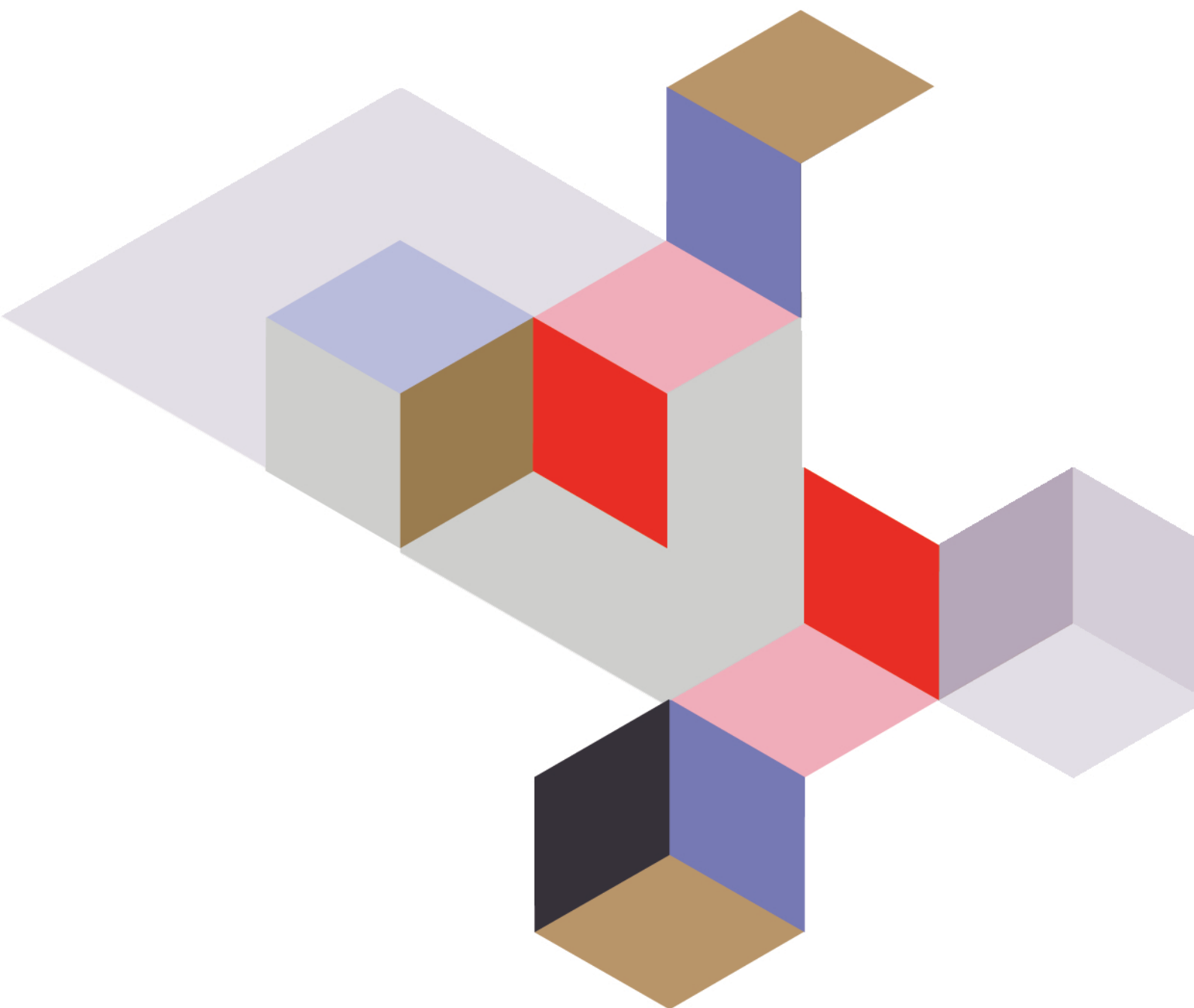
- Tinel,A. and Tschopp,J. (2004). The PIDDosome, a protein complex implicated in activation of caspase-2 in response to genotoxic stress. *Science* 304, 843-846.
- Ura,S., Masuyama,N., Graves,J.D., and Gotoh,Y. (2001). Caspase cleavage of MST1 promotes nuclear translocation and chromatin condensation. *Proc. Natl. Acad. Sci. U. S. A* 98, 10148-10153.
- Uren,A.G., Wong,L., Pakusch,M., Fowler,K.J., Burrows,F.J., Vaux,D.L., and Choo,K.H.A. (2000). Survivin and the inner centromere protein INCENP show similar cell-cycle localization and gene knockout phenotype. *Current Biology* 10, 1319-1328.
- van der Horst,A. and Burgering,B.M.T. (2007). Stressing the role of FoxO proteins in lifespan and disease. *Nat Rev Mol Cell Biol* 8, 440-450.
- Van Laethem,A., Claerhout,S., Garmyn,M., and Agostinis,P. (2005). The sunburn cell: Regulation of death and survival of the keratinocyte. *The International Journal of Biochemistry & Cell Biology* 37, 1547-1553.
- Varfolomeev,E.a.V.D. (2008). (Un)expected roles of c-IAPs in apoptotic and NF κ B signaling pathways. *Cell Cycle*.
- Vaux,D.L. and Silke,J. (2003). Mammalian mitochondrial IAP binding proteins. *Biochemical and Biophysical Research Communications* 304, 499-504.
- Vivanco,I. and Sawyers,C.L. (2002). The phosphatidylinositol 3-Kinase-AKT pathway in human cancer. *Nat Rev Cancer* 2, 489-501.
- Walter,A.O., Seghezzi,W., Korver,W., Sheung,J., and Lees,E. (2000). The mitotic serine/threonine kinase Aurora2/AIK is regulated by phosphorylation and degradation. *Oncogene* 19, 4906-4916.
- Wheatley,S.P., Carvalho,A., Vagnarelli,P., and Earnshaw,W.C. (2001). INCENP is required for proper targeting of Survivin to the centromeres and the anaphase spindle during mitosis. *Current Biology* 11, 886-890.
- Wheatley,S.P. and McNeish,I.A. (2005). Survivin: a protein with dual roles in mitosis and apoptosis. *International review of cytology* 35-88.
- Widlak,P. and Garrard,W.T. (2005). Discovery, regulation, and action of the major apoptotic nucleases DFF40/CAD and endonuclease G. *J Cell Biochem.* 94, 1078-1087.
- Wittinghofer A. (1998). Signal Transduction via Ras. *Biol. Chem* 379, 993-937.
- Yang,J.Y. and Widmann,C. (2001). Anti-apoptotic signaling generated by caspase-induced cleavage of RasGAP. *Mol Cell Biol* 21, 5346-5358.
- Yang,J.Y., Michod,D., Walicki,J., and Widmann,C. (2004). Surviving the kiss of death. *Biochemical Pharmacology* 68, 1027-1031.
- Yang,J.Y., Walicki,J., Michod,D., Dubuis,G., and Widmann,C. (2005). Impaired Akt Activity Down-Modulation, Caspase-3 Activation, and Apoptosis in Cells Expressing a Caspase-resistant Mutant of RasGAP at Position 157. *Mol. Biol. Cell* 16, 3511-3520.
- Yang,J.Y. and Widmann,C. (2002). The RasGAP N-terminal Fragment Generated by Caspase Cleavage Protects Cells in a Ras/PI3K/Akt-dependent Manner That Does Not Rely on NF κ B Activation. *J. Biol. Chem.* 277, 14641-14646.

Yang,Y., Fang,S., Jensen,J.P., Weissman,A.M., and Ashwell,J.D. (2000). Ubiquitin Protein Ligase Activity of IAPs and Their Degradation in Proteasomes in Response to Apoptotic Stimuli. *Science* 288, 874-877.

Ye,H., Cande,C., Stephanou,N.C., Jiang,S., Gurbuxani,S., Larochette,N., Daugas,E., Garrido,C., Kroemer,G., and Wu,H. (2002). DNA binding is required for the apoptogenic action of apoptosis inducing factor. *Nat Struct Biol* 9, 680-684.

Yue,Z., Carvalho,A., Xu,Z., Yuan,X., Cardinale,S., Ribeiro,S., Lai,F., Ogawa,H., Gudmundsdottir,E., Gassmann,R., Morrison,C.G., Ruchaud,S., and Earnshaw,W.C. (2008). Deconstructing Survivin: Comprehensive Genetic Analysis of Survivin Function by Conditional Knockout in a Vertebrate Cell Line. *The Journal of Cell Biology* 183, 279-296.

OBJECTIVES



OBJECTIVES

Professor Widmann's laboratory has been studying the role of RasGAP cleavage by caspases for many years since they discovered that it has a pivotal role in the protection against apoptosis in low stress conditions. In the past few years, they have identified that the N-terminal fragment (fragment N) of RasGAP is responsible to trigger this protective response by inducing the Ras/PI3K/Akt signaling pathway. At present there are two main objectives in the laboratory, which consist of determining whether this anti-apoptotic pathway characterized *in vitro* also plays a role *in vivo* in pathophysiological conditions and to further study the molecular mechanism underlying this protective response by deciphering which of the various Akt downstream targets could be implicated.

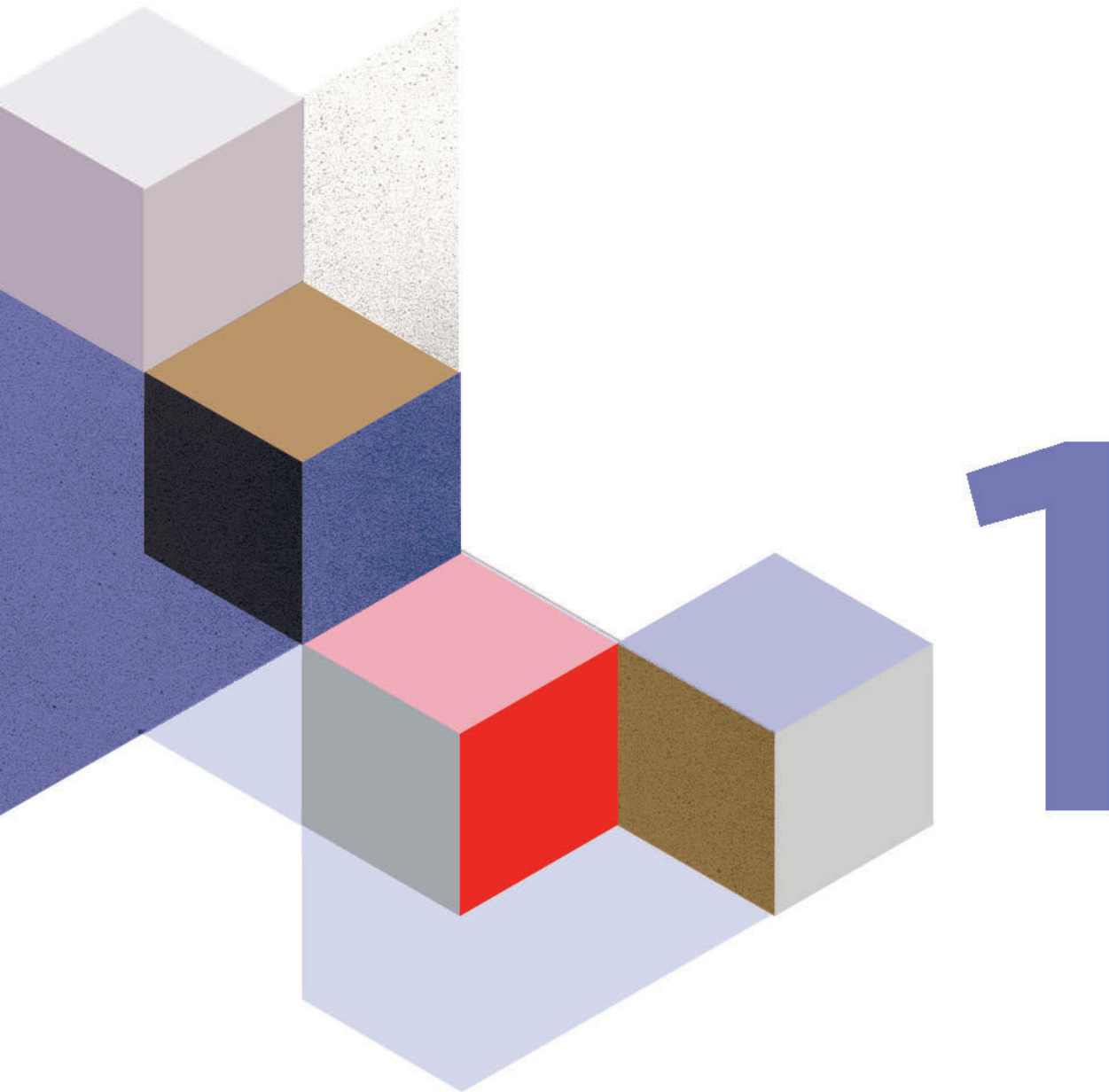
During my thesis I undertook the following research projects:

- I. Using a mouse model unable to generate fragment N (KI mice), together with a caspase-3 knock-out model I have studied the role of the caspase-3 dependent RasGAP cleavage-derived fragment N in mouse skin exposed to UV-B light and contributed to the study of heart and intestine exposed to doxorubicin and DSS, respectively. Understanding the role of fragment N protection *in vivo* may contribute to the discovery of novel anti-apoptotic responses in pathophysiological conditions as well as to the characterization of active caspase-3 in situations where it does not trigger apoptosis.
- II. Survivin is a member of the IAP family of inhibitors of apoptosis and several mechanisms has been proposed for its cyto-protective effect, the majority relying on its cytoplasmic localization. In this work, I have characterized the localization of survivin induction in the skin upon UV-B exposure within cells and within the epidermal layers. Moreover I have studied whether survivin induction in the skin was a mere consequence of cell death or if it was an attempt of the cells to cope with, and prevent apoptosis. These findings contribute to unraveling the role of survivin in cyto-protection in the skin in response to UV-B light.
- III. It has been reported that survivin expression is induced by Akt. Considering this finding together with results obtained during my work (points I and II) I centered

my interest in survivin as a putative Akt target mediating fragment N-dependent anti-apoptotic response. I have therefore studied whether fragment N regulated survivin expression and function as well as its involvement in fragment N-mediated protection in the skin using KI mice exposed to UV-B light. This research contributes to deciphering the downstream targets of Akt that mediate fragment N induced protection.

RESULTS

PART 1



INTRODUCTION

Role of Caspase-3 and RasGAP cleavage *in vivo*.

As detailed in the general introduction, RasGAP acts as a molecular switch within the cells due to its sequential cleavage by active caspase-3 in response to different levels of stress. The N-terminal fragment derived from RasGAP first cleavage by low active caspase-3 induces a potent anti-apoptotic response that relies on the activation of Akt. Further cleavage of the RasGAP N-terminal fragment (fragment N), by high levels of active-caspase-3, abrogates this protective signal and the cell eventually dies by apoptosis (Yang et al., 2004; Yang and Widmann, 2002; Yang and Widmann, 2001).

The overexpression of an uncleavable form of fragment N *in vitro* protects various cell types against different stress stimuli (Yang et al., 2004). Protection induced by fragment N was also demonstrated *in vivo*, using a mouse model in which fragment N was overexpressed specifically in pancreatic β -cell (RIP-N transgenic mice). These cells were protected against apoptosis without affecting their ability to appropriately secrete insulin in physiological conditions and without favoring excessive proliferation (Yang et al., 2009). On the other hand, Akt activation has been reported in response to UV-B irradiation (Ibuki et al., 2010) and therefore it is attractive to postulate that Akt activation in the skin in response to UV-B light depends on fragment N generation.

With the aim of assessing the physiological role of RasGAP cleavage we investigated whether mice lacking caspase-3 or unable to cleave RasGAP exposed to diverse pathophysiological insults, particularly in the skin exposed to UV-B light, were able to activate this potent anti-apoptotic response, relying on Akt activation, described *in vitro*.

CONTRIBUTION

This work has been sent for publication to Molecular and Cellular Biology (MCB) and it is currently under revision. I performed all the experiments concerning the skin and contributed with immunohistochemistry and analysis of phosphorylated Akt in the heart and with immunohistochemistry, analysis and quantification of phosphorylated Akt in the colon. I contributed with the writing of the manuscript

Reference List

- Ibuki,Y., Akaike,M., and Toyooka,T. (2010). PI3-kinase/Akt Pathway Mediates Expression of p53 after UVB Irradiation. *Genes and Environment* 32, 85-91.
- Yang,J.J., Michod,D., Walicki,J., Murphy,B.M., Kasibhatla,S., Martin,S.J., and Widmann,C. (2004). Partial Cleavage of RasGAP by Caspases Is Required for Cell Survival in Mild Stress Conditions. *Molecular and cell Biology* 24, 10425-10436.
- Yang,J.Y., Walicki,J., Jaccard,E., Dubuis,G., Bulat,N., Hornung,J.P., Thorens,B., and Widmann,C. (2009). Expression of the NH(2)-terminal fragment of RasGAP in pancreatic beta-cells increases their resistance to stresses and protects mice from diabetes. *Diabetes* 58, 2596-2606.
- Yang,J.Y. and Widmann,C. (2001). Anti-apoptotic signaling generated by caspase-induced cleavage of RasGAP. *Mol Cell Biol* 21, 5346-5358.
- Yang,J.Y. and Widmann,C. (2002). The RasGAP N-terminal Fragment Generated by Caspase Cleavage Protects Cells in a Ras/PI3K/Akt-dependent Manner That Does Not Rely on NFkappa B Activation. *J. Biol. Chem.* 277, 14641-14646.

Caspase-3 Protects Stressed Organs against Cell Death

AQ: au Hadi Khalil,^a Nieves Peltzer,^a Joël Walicki,^a Jiang-Yan Yang,^a Gilles Dubuis,^a Noémie Gardiol,^b Werner Held,^b Paul Bigliardi,^{c,*} Benjamin Marsland,^d Lucas Liaudet,^e and Christian Widmann^a

Department of Physiology^a and Ludwig Center for Cancer Research of the University of Lausanne,^b Faculty of Biology and Medicine, University of Lausanne, Lausanne, Switzerland, and Department of Dermatology,^c Department of Pneumology,^d and Department of Intensive Care Medicine,^e Centre Hospitalier Universitaire Vaudois and University of Lausanne, Lausanne, Switzerland

The ability to generate appropriate defense responses is crucial for the survival of an organism exposed to pathogenesis-inducing insults. However, the mechanisms that allow tissues and organs to cope with such stresses are poorly understood. Here we show that caspase-3-knockout mice or caspase inhibitor-treated mice were defective in activating the antiapoptotic Akt kinase in response to various chemical and environmental stresses causing sunburns, cardiomyopathy, or colitis. Defective Akt activation in caspase-3-knockout mice was accompanied by increased cell death and impaired survival in some cases. Mice homozygous for a mutation in RasGAP that prevents its cleavage by caspase-3 exhibited a similar defect in Akt activation, leading to increased apoptosis in stressed organs, marked deterioration of their physiological functions, and stronger disease development. Our results provide evidence for the relevance of caspase-3 as a stress intensity sensor that controls cell fate by either initiating a RasGAP cleavage-dependent cell resistance program or a cell suicide response.

Executioner caspases mediate cell death during apoptosis (45). Of these, caspase-3 has the ability to cleave the majority of the caspase substrates (43), and its activity is required for the induction of cell death in response to many apoptotic stimuli (1). While executioner caspases are indispensable for apoptosis, there are situations when their activation does not lead to death. For example, healthy dividing cells can weakly activate caspase-3 in response to mild stresses (47). Caspase-3 also participates, in an apoptosis-independent manner, in T and B cell homeostasis (35, 46), in microglia activation (6), in long-term depression (26), and in muscle (17), monocyte (44), embryonic stem cell (18), and erythroid cell (13) differentiation. However, it remains unclear how activation of caspase-3 under these conditions does not eventually lead to cell death (1, 24). Cells could have an intrinsic ability to tolerate low caspase activity by constitutively expressing antiapoptotic molecules, such as members of the inhibitors of the apoptosis protein family, or may stimulate antiapoptotic pathways in parallel to caspase activation (24). Alternatively, the caspases themselves might activate prosurvival pathways, in particular, when they are mildly stimulated. Indeed, there is evidence in cultured cells that caspase-3 mediates neuroprotection after preconditioning (30) and that caspase-3 activity turns on the antiapoptotic Akt kinase following partial cleavage of the RasGAP protein (47). Other caspase substrates that could potentially induce protective signals once cleaved include p27^{kip1} (14), Lyn (28), synphilin-1 (19), and Rb (42), yet the physiological importance of these cleaved substrates has not been evaluated to date.

In the present study, we have investigated the role played by caspase-3 and its substrate p120 RasGAP in the induction of the antiapoptotic Akt kinase in stressed tissues *in vivo*.

MATERIALS AND METHODS

Caspase-3-KO mice. B6.129S1-*Casp3*^{tm1Flv/J} caspase-3-knockout (KO) mice were purchased from the Jackson Laboratory (Bar Harbor, ME). The mice were genotyped using a mixture of the following three oligonucleotides: wild-type sense (GCG AGT GAG AAT GTG CAT AAA TTC), wild-type antisense (GGG AAA CCA ACA GTA GTC AGT CCT), and caspase-3-knockout antisense (TGC TAA AGC GCA TGC TCC AGA CTG). The

sizes of the amplified fragments are 320 bp for the wild-type allele and 300 bp for the caspase-3-knockout allele.

Generation of RasGAP D455A-knock-in (KI) mice. The strategy and methods used to create the targeting vector are presented in Fig. S1 in the supplemental material.

UV-B exposure and isolation of skin samples. Mice were shaved on both flanks, followed by depilation with depilatory cream (Vee), and 48 h later were anesthetized and illuminated with a Waldmann UV801 KL apparatus equipped with a Philips UV21 UV-B lamp (TL 20W/12RS). The doses of UV-B illumination were 0.05 and 0.3 J/cm² (i.e., 50 mJ/cm² and 300 mJ/cm², respectively), which were measured with a Waldmann Variocontrol dosimeter. In each case, only one side of the mouse was illuminated and the other side was used as a control (i.e., nonexposed skin). Mice were sacrificed 24 h after illumination. The lateral skin biopsy specimens (approximately 2 by 2 cm) were excised from each mouse, fixed in phosphate-buffered saline (PBS) and 4% Formol solution, and embedded in paraffin. The paraffin-embedded skin was cut into 4- μ m sections, deparaffinized, and stained with hematoxylin-eosin for histological observation.

Doxorubicin injection and hemodynamic measurements using left ventricular PV microcatheters. Eight-week-old mice were weighed and injected with a single intraperitoneal doxorubicin dose of 20 mg/kg of body weight using a 2-mg/ml doxorubicin solution (catalog number 733857-01, EBEWE; Pharma) or injected with an equal volume of saline (catalog number 534534; B. Braun Medical AG). At 5 days postinjection, the animals were weighed again (the weight loss at that time was between 10 and 15%). The animals were anesthetized with an intraperitoneal injection of 75 mg/kg ketamine and 10 mg/kg xylazine (the volume of in-

Received 8 June 2012 Returned for modification 9 July 2012

Accepted 29 August 2012

Published ahead of print 4 September 2012

Address correspondence to Christian Widmann, Christian.Widmann@unil.ch.

* Present address: Paul Bigliardi, NUHS/NUS and IMB/A*STAR, Singapore.

H.K. and N.P. contributed equally to this article.

Supplemental material for this article may be found at <http://mcb.asm.org/>.

Copyright © 2012, American Society for Microbiology. All Rights Reserved.

doi:10.1128/MCB.00774-12

jection was 10 μ l per g of mouse). A pressure-volume (PV) SPR-839 catheter (Millar Instruments, Houston, TX) was inserted into the left ventricle (LV) via the right carotid artery. After stabilization for 20 min, heart rate, LV systolic and end-diastolic pressures, and volumes were measured, and stroke volume, ejection fraction, and cardiac output were calculated and corrected according to *in vitro* and *in vivo* volume calibrations with a cardiac PV analysis program (PVAN3.2; Millar Instruments) (38, 39). End-systolic LV PV relationships were assessed by transiently reducing venous return by compressing the inferior vena cava, and LV contractility was assessed from the slope of the LV end-systolic PV relationship (end-systolic elastance), calculated using PVAN3.2, as detailed previously (21, 38). Hearts were isolated, cut into two pieces, and then either snap-frozen or fixed in 4% formalin for histology studies.

DSS-induced colitis and clinical score. Eight-week-old mice were given acidified water supplemented with 5% (wt/vol) dextran sodium sulfate (DSS; molecular weight, 400,000 to 600,000; MP Biomedicals, Illkirch, France) for 72 h and then given normal drinking water for four additional days. Mice were examined daily, and body weight, water consumption, occult blood, and diarrhea were measured. At day 7, mice were sacrificed, the colon length was measured, and a clinical score was estimated according to the procedure described by Ohkawara et al. (36). Percentage of weight loss was calculated by comparing the weight at day 0 and the weight of the mice at sacrifice. Scores were given according to the extent of weight loss: 0, no weight loss; 1, 1 to 5%; 2, 5 to 10%; 3, 10 to 15%; 4, >15%. Diarrhea was scored using a scale with values ranging from 0 to 4: 0, normal; 1, slightly loose feces; 2, loose feces; 3, semi-liquid stool; and 4, liquid stool. Fecal occult blood was detected using guaiac paper (ColoScreen Hemocult kit; Helena Labs, Beaumont, TX), and the associated scores were as follows: 0, none; 2, positive Hemocult result; and 4, gross bleeding. Colons were cut into three equal portions (proximal, middle, and distal), and each portion was further cut into three equal parts, two of which were snap-frozen in liquid N₂ and stored at -80°C for subsequent protein and RNA analysis, and the third portion was fixed in 4% formalin for histology analysis (paraffin sections).

Quantitation of active Akt- and active caspase-3-positive cells in heart, skin, and colon. Sections stained as described in the previous sections were scanned using an automated Nikon Eclipse 90i microscope equipped with Apo Plan \times 20 (0.75 pH 2 PM) and Apo Plan \times 40/1.0 DIC-H objectives and piloted with NIS-Elements Advance Research software (Nikon Instruments Inc., Melville, NY).

Three whole-heart sections were scanned at different levels, and the corresponding whole-section images were generated. The number of pAkt-positive cells was scored manually by counting the number of cells stained with the anti-phospho-Akt antibody (the samples were randomized prior to examination, and the person performing the counting was not aware of the experimental conditions). The total number of cells was determined by automatically scoring the number of nuclei (stained with the Hoechst 33342 dye) using the NIS-Elements AR program (Nikon). In order to minimize errors, all images were acquired with the same contrast (high), size and quality (1280 \times 960), exposure time (4',6-diamidino-2-phenylindole [DAPI], 40 ms; fluorescein isothiocyanate [FITC], 300 ms), and gain (1 \times). The quantification threshold in the automated measurement menu was set at L32 for low and H236 for high, and the area was restricted to 0 to 0.5 μ m² out. In the image menu, the local contrast was set to 30, and in the image-background option, the background was set to 40 for DAPI and to 999 for FITC. Using the binary menu, the holes were filled using the fill holes option. This was performed to avoid multiple counting of the same nucleus. Touching nuclei were separated using the morpho separate objects option. The number of nuclei was displayed under automated measurement results—object data. Skin sections were scanned and analyzed similarly. Fifteen different fields were randomly taken from the proximal, middle, and distal sections of the colon and processed and analyzed as described above.

Apoptosis scoring. Apoptosis on histological slides was assessed by terminal deoxynucleotidyltransferase-mediated dUTP-biotin nick end la-

beling (TUNEL) assay (DeadEnd Fluorometric TUNEL system; catalog number G3250; Promega Switzerland), as per the manufacturer's protocol, and quantitated as described for the Akt staining in the previous section. Apoptosis *in vitro* counting was assessed by scoring the number of cells with pycnotic or fragmented nuclei after Hoechst 33342 staining (48).

Chemicals and antibodies. The Q-VD-OPh caspase inhibitor was from MP Biomedicals (catalog number OPH109). Hexameric FasL (fusion protein between the Fas ligand and the Fc portion of IgG1) (20) was a kind gift from Pascal Schneider (University of Lausanne). The monoclonal and polyclonal anti-phospho-Ser473 Akt antibodies and the cleaved caspase-3-specific antibody were from Cell Signaling Technology (catalog numbers 4051, 9271, and 9664, respectively). The monoclonal anti-phospho-Ser⁴⁷³ Akt antibody was used on skin and colon sections as well as for Western blot assays, while the polyclonal anti-phospho-Ser⁴⁷³ Akt antibody was used on heart sections. The antibody recognizing total Akt was from Santa Cruz (catalog number sc-8312). The anti-RasGAP antibody was from Enzo Life Science (catalog number ALX-210-860-R100). Secondary antibodies (Cy3-coupled donkey anti-rabbit, horseradish peroxidase [HRP]-coupled donkey anti-rabbit, and HRP-coupled donkey anti-mouse antibodies) were from Jackson Immunoresearch (catalog numbers 711-165-152, 715-035-150, and 715-035-150, respectively).

Protein extraction. Snap-frozen skin (0.3-cm² biopsy specimens), heart, and intestine tissue samples were crushed into powder in liquid nitrogen-dipped mortar and pestle and then suspended in 700 μ l lysis buffer (Tris-HCl, 50 mM; EDTA, 1 mM; EGTA, 1 mM; Triton X-100, 1%; dithiothreitol, 1 mM; sodium pyrophosphate, 5 mM; NaF, 50 mM; protease inhibitor cocktail tablet [1 tablet/40 ml buffer; catalog number 04 693 132 001; Roche]; phenylmethylsulfonyl fluoride, 1 mM; glycerol, 10%; pH 7.4). The samples were sonicated (amplitude, 80%; 5 s; twice). Protein concentration was measured by the Bradford assay using bovine serum albumin (BSA) as a standard. Lysates were mixed with an equal volume of sample buffer (62.4 mM Tris-HCl [pH 6.8], 40% glycerol, 5% [vol/vol] β -mercaptoethanol, 2% [wt/vol] sodium dodecyl sulfate [SDS], and 0.04% bromophenol blue) and boiled for 5 min at 95°C before loading on SDS-polyacrylamide gels.

Western blotting. Western blotting was performed and quantitated as described previously (31).

Preparation of tissue section and immunohistochemistry. Mice were euthanized by cervical dislocation. The isolated organs (heart, skin, or intestine) were stored in PBS-4% Formol solution and embedded in paraffin. Four-micrometer sections were deparaffinized in toluene (catalog number 488555; Carlo Erba, Milan, Italy) and rehydrated using graded alcohol and distilled water. Antigen retrieval was performed by immersing sections in sodium citrate buffer (10 mM sodium citrate, pH 6), followed by heating in a microwave oven for 20 min (8 min at 800 W and 12 min at 400 W). Sections were cooled to room temperature and blocked using a 50 mM Tris-HCl, pH 7.6, 0.5% Tween 20, 0.2% BSA solution. The primary antibody was diluted (pAkt, 1/100; cleaved caspase-3, 1/200) in 50 mM Tris-HCl, pH 7.6, 0.5% Tween 20, 0.2% BSA and incubated with the slides for 1 h. Slides were washed 2 times for 10 min each time in 50 mM Tris-HCl, pH 7.6, 0.5% Tween 20. The fluorochrome-conjugated secondary antibody (Jackson Laboratory), diluted 1:300 in 50 mM Tris-HCl, pH 7.6, 0.5% Tween 20, 0.2% BSA, was incubated with the slides for another hour in the dark. Slides were then extensively washed (at least 6 times with one overnight washing step). The nuclei in the sections were then stained with 10 μ g/ml Hoechst 33342. Finally, the slides were mounted in Mowiol (catalogue number 81381; Fluka) at a concentration of 0.1 mg/ml in a solution made of 20% glycerol and 0.1% DABCO (diazobicyclo-octane; catalogue number 33480; Fluka).

Immunohistochemistry with tyramide signal amplification. Tyramide amplification of immunohistochemical signals using phospho-Akt-specific antibodies was performed as described earlier (4). The primary antibody and the secondary HRP antibody were diluted 1/100 and 1/1,000, respectively.

Ethics statement. Experiments on the mice were carried out in strict accordance with the Swiss Animal Protection Ordinance (OPAn). The protocol was approved by the Veterinary Office of the state of Vaud, Switzerland (permit numbers 2055, 2056, and 2361).

MEF preparation. Mouse embryonic fibroblasts (MEFs) from KI and wild-type mice were initially prepared as described earlier by digesting embryonic day 14 embryos for 1.5 h in 0.05% trypsin (5). Using this protocol, MEFs could be generated from wild-type embryos, but none were obtained from the KI embryos (Fig. 5C). Reducing the incubation time in trypsin to 15 min, which presumably lessened a stressful situation on cells, however, allowed production of both wild-type and KI MEFs in more or less similar numbers (Fig. 5C).

Statistics. SAS/STAT (version 9.1) software (SAS Institute Inc., Cary, NC) was used to perform the statistical analyses. Unless otherwise stated, one-way analyses of variance were performed to determine the significance of the observed differences presented in the figures. Asterisks and NS in the figures indicate significant differences ($P < 0.05$) and no significant differences, respectively.

RESULTS

Mice lacking caspase-3 are impaired in their capacity to activate Akt in response to stress. Akt (also called PKB) is a downstream effector of phosphatidylinositol 3-kinase (PI3K) that mediates the survival responses of many cell types and tissues (40) and as such could be involved in stress survival responses across most, if not all, tissues. To determine whether Akt is activated in various tissues and organs in response to pathology-inducing stresses, mice were exposed to three different challenges: exposure of the skin to UV-B, injection of doxorubicin (an anticancer drug inducing cardiomyopathy), and administration of dextran sulfate sodium (DSS) via drinking water to induce colitis. In control skin, very few keratinocytes ($\sim 0.25\%$) expressed the active phosphorylated form of Akt (Fig. 1A). In response to mild UV-B exposure (0.05 J/cm^2), more than 10% of the keratinocytes had active Akt in their cytoplasm (Fig. 1A). In the hearts of untreated mice, cells expressing activated Akt were readily observed. Virtually all of these cells were cardiomyocytes, as determined by their shape and nucleus location (Fig. 1B). Under basal conditions (i.e., no treatment), the percentage of cardiomyocytes with active Akt was much higher ($\sim 6\%$) than that in the epidermis. Doxorubicin increased this percentage in a statistically significant manner to $\sim 10\%$ (Fig. 1B, gray bars). Akin to the situation encountered in the skin, very few cells in the colon epithelium ($\sim 0.7\%$) were found to be positive for active Akt (Fig. 1C). This percentage significantly increased to $\sim 1.2\%$ when colitis was induced by DSS (Fig. 1C, gray bars).

To determine whether Akt activation was dependent on caspase-3, we analyzed caspase-3-KO mice on the C57BL6 background that had reached adulthood and bred (25). When the skin of these mice was exposed to UV-B, the number of keratinocytes with active Akt increased (Fig. 1A, lower right), suggesting that a caspase-3-independent mechanism can participate in the induction of protective signals in the epidermis. However, the UV-B-induced increase in the percentage of active Akt-positive keratinocytes in caspase-3-KO mice was much reduced compared to the situation observed in wild-type mice, and the increase was not statistically significant (Fig. 1A, black bars). This indicates that caspase-3 is required for a maximal Akt response in keratinocytes subjected to UV-B illumination. When caspase-3-KO mice were treated with doxorubicin or DSS, the percentage of cells with active Akt in the targeted organs did not change compared to the nonchallenged situation (compare the gray and black bars in

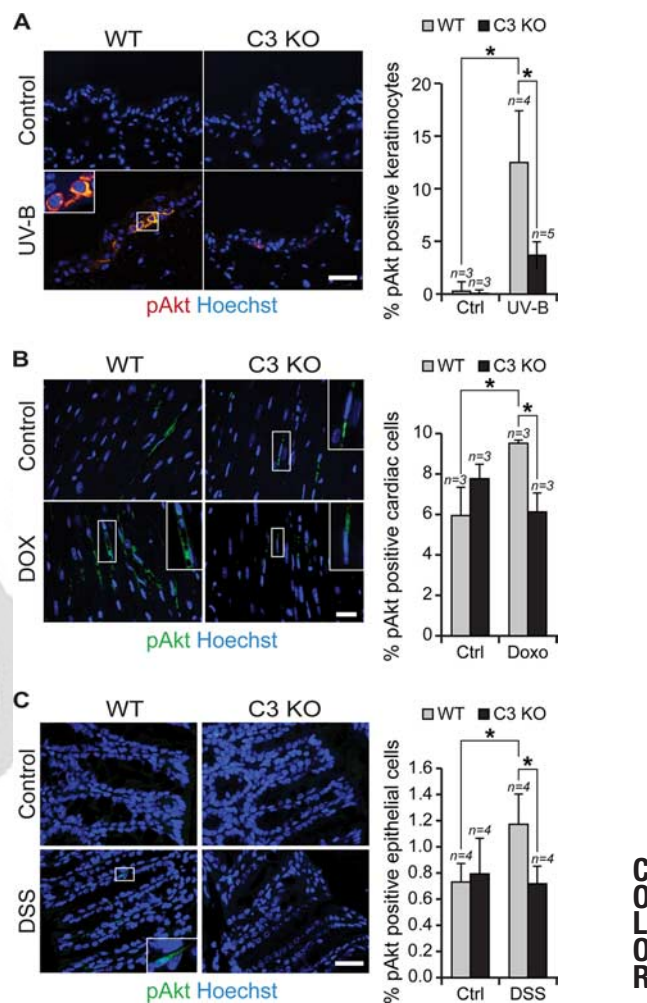


FIG 1 Defective stress-induced Akt activation in mice lacking caspase-3. The indicated numbers of wild-type (WT) and caspase-3-knockout (C3 KO) mice were subjected or not to illumination of their skin with 0.05 J/cm^2 UV-B (A; 2 independent experiments), injection of 20 mg/kg doxorubicin (DOX or Doxo) (B; 2 independent experiments), or exposure to 5% DSS in the drinking water (C; 3 independent experiments) (see Materials and Methods for details). (A to C) Histological sections of the organs and tissues targeted by these stresses were then stained with an antibody recognizing the active phosphorylated form of Akt, and the percentage of phospho-Akt (pAkt)-positive cells was quantitated. Results correspond to the mean \pm 95% CI. The images shown are representative examples of sections labeled with the anti-phospho-Akt antibody (red or green staining) and with Hoechst 33342 (blue staining of the nuclei). Bars, 20 μm .

Fig. 1B and C), indicating that caspase-3 is strictly required for Akt activation in these tissues exposed to stress. To determine if stimulation of caspase-3 activity and not some other noncatalytic functions of the protease is necessary for stress-induced Akt activation, wild-type mice were injected with Q-VD-OPh, a broad-spectrum caspase inhibitor (10). Figures 2A and B show that this compound inhibited UV-B-induced caspase-3 activation in the skin. Q-VD-OPh was found to significantly decrease the ability of epidermal cells to stimulate Akt in response to UV-B (Fig. 2C), indicating that activation of caspases is required for the induction of the antiapoptotic Akt kinase in response to stress.

Increased stress-induced cell death and cell damage in mice lacking caspase-3. Impaired Akt activation in caspase-3-knock-

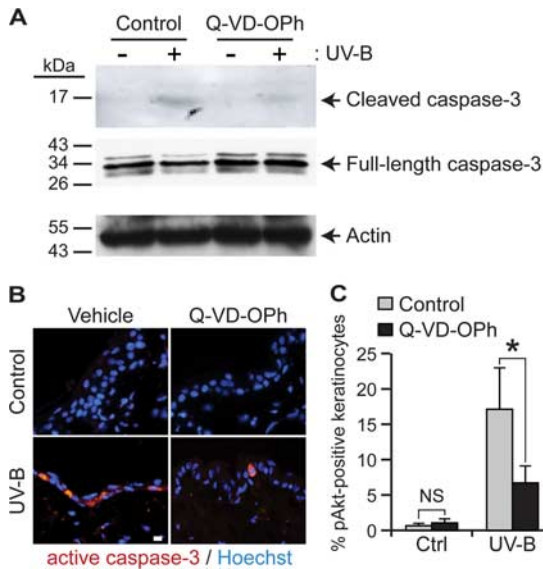


FIG 2 Pharmacological inhibition of caspases hampers UV-B-induced Akt activation in the epidermis. Wild-type mice were injected or not with 50 mg of the Q-VD-OPh caspase inhibitor per kg of mouse 15 min prior to UV-B exposure of the skin (0.3 J/cm^2 [A and B] and 0.05 J/cm^2 [C]). (A) Levels of cleaved active caspase-3, full-length inactive caspase-3, and actin were assessed by Western blotting. This experiment was repeated once with similar results. (B) Levels of active caspase-3 *in situ* were also visualized by immunofluorescence. Bar, $20 \mu\text{m}$. The pictures are representative images of data obtained with three mice per condition. (C) Levels of phosphorylated Akt were assessed as described in Fig. 1. Results correspond to the mean \pm 95% CI of 3 independent experiments ($n = 3$).

out mice may not lead to visible damage of the targeted tissues if the absence of caspase-3 prevents implementation of a cell death response. There are indeed situations where caspase-3 is mandatory for cell death. For example, beta cells from caspase-3-KO mice are fully resistant against streptozotocin-induced death, while beta cells from wild-type mice are not, leading to the development of diabetes (27). In other situations, cell death may still occur in the absence of caspase-3, either as a result of a nonapoptotic type of death or because apoptosis is mediated by other executioner caspases (e.g., caspase-7). In such cases, the absence of a caspase-3-mediated Akt activation might have detrimental consequences. To assess this point, we monitored the extent of stress-induced cell death in the skin and the heart of caspase-3-KO and wild-type mice.

In the skin of wild-type mice, UV-B induced the appearance of keratinocytes with a pycnotic nucleus and densely staining glassy cytoplasm—the so-called sunburn cells (see the inset in the lower left-hand panel in Fig. 3A)—which are apoptotic cells characteristic of those in damaged skin following UV exposure (12). The percentage of sunburn cells generated by UV-B in the skin of caspase-3-KO mice was significantly reduced compared to that in the skin of wild-type mice (Fig. 3A). Similarly, there were fewer TUNEL-positive keratinocytes in the UV-B-illuminated skin of caspase-3 mice than in the skin of wild-type mice (Fig. 3B). This indicates that caspase-3 is a main mediator of UV-B-induced keratinocyte apoptosis. Cells can also die in a necrosis-like, nonapoptotic manner, in particular, when apoptosis pathways are altered (41). Keratinocytes dying in this way are characterized by their irregular shape, an eosinophilic cytoplasm, and hyperchromatic,

condensed, and partly fragmented nuclei (3) (see the inset in the lower right-hand panel in Fig. 3A). UV-B dramatically increased the percentage of keratinocytes undergoing this type of death in the skin of caspase-3-KO mice compared to the skin of wild-type mice (Fig. 3A). When accounting for both apoptosis and necrosis-like deaths, there was more UV-B-mediated death recorded in the skin of caspase-3-KO mice than in the skin of wild-type mice ($8.1 \pm 2.5\%$ versus $4.9 \pm 1.2\%$; mean \pm 95% confidence interval [CI]).

Doxorubicin is a DNA-intercalating drug that induces both caspase-dependent and -independent cell death in various cell types (29), including cardiomyocytes (51). In response to doxorubicin injection, the percentage of cardiomyocytes undergoing apoptosis, as assessed with the TUNEL assay (see a representative example on the left-hand side of Fig. 3C), was significantly higher in caspase-3-KO mice than wild-type mice (Fig. 3C). It therefore appears that apoptosis induced by doxorubicin can be efficiently mediated by executioner caspases other than caspase-3, which is consistent with the observation that doxorubicin efficiently activates caspase-7 (11).

The increased susceptibility of caspase-3-KO mice to doxorubicin-induced cardiomyocyte apoptosis raised the possibility that the lack of caspase-3 affects survival of mice treated with doxorubicin. Figure 3D shows that caspase-3-KO mice survived doxorubicin treatment less efficiently than wild-type mice. This suggests that caspase-3 mediates a protective response in doxorubicin-treated animals that is required to counteract tissue damage induced in a caspase-3-independent manner.

In conclusion, the results presented in Fig. 1 to 3 show that, upon stress exposure, mice lacking caspase-3 are defective in the activation of the prosurvival Akt kinase and that this correlates with increased cell death, tissue damage, and even death of the animals.

Generation of mice expressing a caspase-3-resistant RasGAP mutant. *In vitro*, low caspase-3 activity leads to the cleavage of the RasGAP protein into an amino-terminal fragment, called fragment N, that stimulates Akt in a Ras/PI3K-dependent manner (47, 50), preventing further caspase-3 activation and apoptosis (47). In the presence of high caspase-3 activity, fragment N is further cleaved into two additional fragments (fragments N1 and N2) that are unable to activate Akt (48). Notably, this second cleavage event does not take place if the first cleavage is prevented (49). Further, in the absence of caspase-3 in cells, other executioner caspases, such as caspase-6 and caspase-7, cannot cleave RasGAP (47). RasGAP is therefore a specific caspase-3 substrate. To assess the role of fragment N in Akt stimulation in stressed organs, we generated a KI mouse in which the first RasGAP cleavage site recognized by caspase-3 was destroyed by an aspartate-to-alanine substitution at position 455 (DTVA[455]G) (Fig. 4A and B); the construction of the targeting vector is shown in Fig. S1 in the supplemental material, and genetic analyses of the resulting mice are shown in Fig. 4B and C. This mutation does not affect the function of full-length RasGAP (47). Mice homozygous for the RasGAP^{D455A} allele (KI mice) are viable and fertile, grow normally (Fig. 4D), and show no obvious morphological alterations (Fig. 4E), histologic defects (data not shown), or hematologic abnormalities (see Table S1 in the supplemental material). Expression of RasGAP, caspase-3, Akt, and actin was similar in given tissues and cells derived from wild-type and KI mice (Fig. 4F). The transmission of the mutated alleles occurred with normal Mendelian ratios (among 317 off-

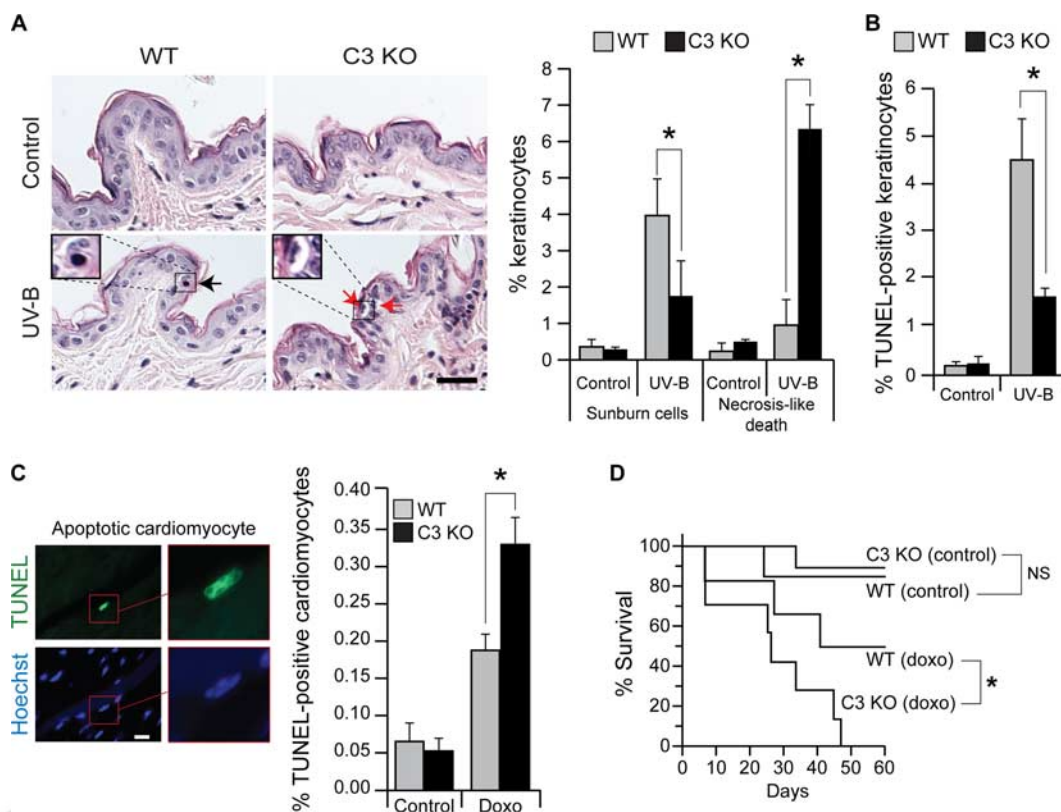


FIG 3 Increased stress-induced cell death and cell damage in mice lacking caspase-3. (A) Histological assessment of sunburn (black arrow) and necrotic-like (red arrows) cells in the epidermis (left and middle) of UV-B (0.05-J/cm²)-irradiated mouse skin. Results correspond to the mean ± 95% CI of measurements performed on 3 and 8 control and irradiated animals, respectively. Bar, 20 μm. (B) Quantitation of TUNEL-positive keratinocytes following UV-B (0.05-J/cm²) irradiation. Results correspond to the mean ± 95% CI (3 animals per condition). (C) Apoptosis assessment by the TUNEL assay in cardiomyocytes from mice injected with 20 mg/kg doxorubicin 5 days earlier. A representative example of an apoptotic cardiomyocyte is shown on the left. Bar, 10 μm. Results correspond to the mean ± 95% CI (3 animals per condition). (D) Survival curves of 6 wild-type and 7 caspase-3-KO mice injected with 20 mg/kg doxorubicin (8 wild-type and 11 caspase-3-KO mice were used in the control noninjected groups). A Wilcoxon test of equality over strata (life-test procedure) was used to assess the significance of the observed difference.

spring obtained from breeding heterozygote +/D455A mice, 22.4% were +/+, 54.3% were +/D455A, and 23.7% were D455A/D455A).

As expected, fibroblasts derived from KI embryos were unable to cleave RasGAP in response to various apoptotic stimuli (Fig. 5A) and were more prone to apoptosis in response to these stimuli than control MEFs (Fig. 5B). Additionally, in contrast to what was observed with wild-type embryos, cells from KI embryos did not survive long-term trypsin digestion (Fig. 5C). MEFs from KI embryos were also impaired in their capacity to activate Akt in response to stress (Fig. 5D). The increased susceptibility of KI cells to death in response to stresses is consistent with the known ability of fragment N to stimulate Akt and inhibit apoptosis in cultured cell lines (47, 49, 50).

Mice that cannot cleave RasGAP at position 455 are unable to activate Akt in response to stress, and they experience increased apoptosis, tissue damage, and organ dysfunction. The KI mice were then used to assess the importance of RasGAP cleavage in Akt activation and in the protection of tissues and organs upon exposure to the pathophysiological challenges described for Fig. 1. In response to low UV-B exposure (0.05 J/cm²), Akt was activated in about 10% of keratinocytes of wild-type mice (Fig. 6A). Akt activation was, however, not observed when the skin was exposed to

higher UV-B doses (0.3 J/cm²) (Fig. 6A) that led to strong caspase-3 activation (Fig. 6B). It is known that low caspase-3 activity leads to fragment N generation, while high caspase-3 activity induces fragment N cleavage into fragments that are no longer able to activate Akt (48). In skin samples, all the RasGAP antibodies that we have tested lit up bands in the 35- to 55-kDa range, precluding visualization of fragment N (52 kDa) (Fig. 6C). These bands may be nonspecifically recognized by the RasGAP antibodies, but it is more likely that they correspond to RasGAP degradation products that are generated in keratinocytes en route to their final differentiation stage in the cornified layer, a process that is known to be associated with massive activation of epidermal proteases (8). Fragment N2, one of the caspase-3-generated products of fragment N (49), was, however, seen in samples derived from skin exposed to 0.3 J/cm² UV-B but not in samples derived from skin exposed to 0.05 J/cm² UV-B (Fig. 6C). These results indicate that Akt is not activated under conditions where fragment N2 is produced, i.e., when fragment N is degraded. In contrast to what was observed in wild-type skin, low doses of UV-B only marginally and nonsignificantly activated Akt in keratinocytes from KI skin (Fig. 6A). This correlated with increased numbers of cells expressing active caspase-3 (Fig. 6B) and cells undergoing apoptosis (Fig. 6D). When the skin was exposed to higher UV-B doses (0.3

Khalil et al.

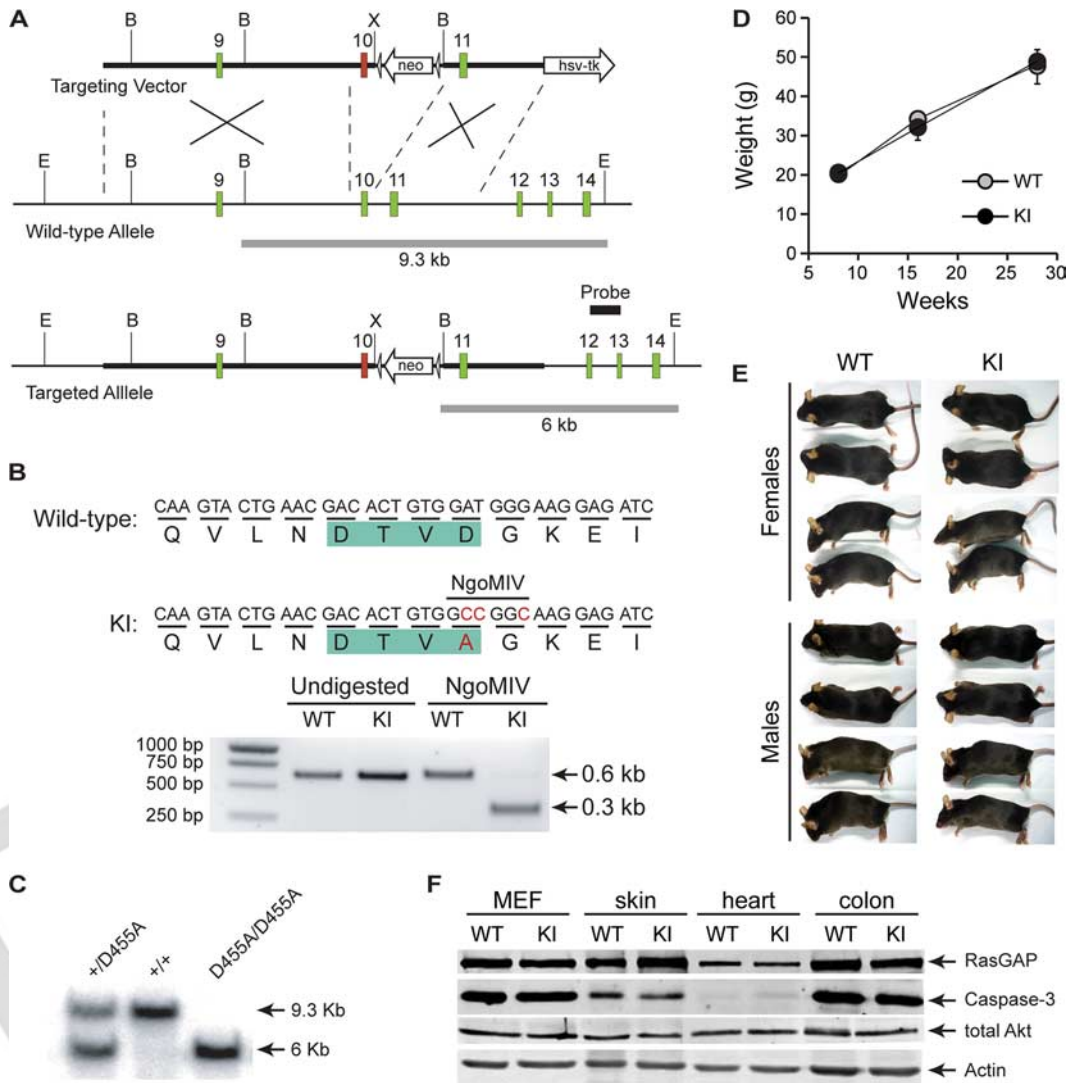


FIG 4 Generation of RasGAP^{D455A/D455A} knock-in mice. (A) The targeting vector consists of mouse RasGAP exons 9, 10, and 11. Exon 10 (indicated in red) bears the RasGAP D455A mutation. E, X, and B₂ EcoRV, XhoI, and BamHI, respectively; gray bars below the alleles, length of the BamHI/EcoRV fragments recognized by the probe (black bar) when genotyping by Southern blot is performed. (B) Detection of the D455A allele by PCR. The D455A allele bears a new NgoMIV restriction site encompassing the aspartate-to-alanine mutation (in red) within the caspase recognition site in RasGAP (in green). Genomic DNA was subjected to PCR amplification using primers flanking exon 10. The amplified fragments, after digestion with NgoMIV or not, were separated on a 1.5% agarose gel. The presence of the D455A mutation results in cleavage of the ~600-bp PCR fragment into two comigrating ~300-bp fragments. (C) Tail-purified genomic DNA was digested with EcoRV and BamHI and tested by Southern blotting using the probe shown in panel A. (D) The body weight of wild-type and RasGAP^{D455A/D455A} knock-in males was monitored at the indicated time points. Results correspond to the mean ± 95% CI of at least 9 determinations per condition. (E) Images from anesthetized 10-week-old mice. (F) The expression of RasGAP, caspase-3, Akt, and actin in the indicated cell type and tissues was assessed by Western blotting.

J/cm²), the extent of apoptosis in the skin of wild-type and KI mice was not significantly different, although there was a trend of a stronger apoptotic response in KI mice (Fig. 6D) that correlated with a tendency of KI mice to activate less Akt (compare the last two bars in Fig. 6A) but more caspase-3 (Fig. 6B) at high UV-B doses. Sunburn cells (see the example in Fig. 6E) were significantly augmented in the epidermis of 0.05-J/cm² UV-B-exposed KI skin compared to wild-type skin (Fig. 6E). The observed difference at higher UV-B doses (0.3 J/cm²) was, however, not statistically significant.

Doxorubicin induced the cleavage of RasGAP into fragment N in the heart of wild-type mice (Fig. 7A). As expected, this was not observed in KI mice (Fig. 7A). Following doxorubicin injection,

the number of cardiomyocytes with activated Akt did not increase in KI mice (Fig. 7B). This was also associated with an increase in the number of apoptotic cells in the heart (Fig. 7C). In response to doxorubicin, KI mice had more impaired cardiac function as measured by hemodynamic parameters (see Table S2 in the supplemental material). Specifically, end-systolic elastance, which is derived from end-systolic pressure volume curves (Fig. 7D) and which is a direct (load-independent) measure of the heart contractile activity, was significantly decreased in KI mice treated with doxorubicin (Fig. 7D and E).

Finally, enterocytes from KI mice were also affected in their capacity to activate Akt in response to DSS (Fig. 8A), and this was accompanied by an increased apoptotic response compared to

ROLOG

F7

F8

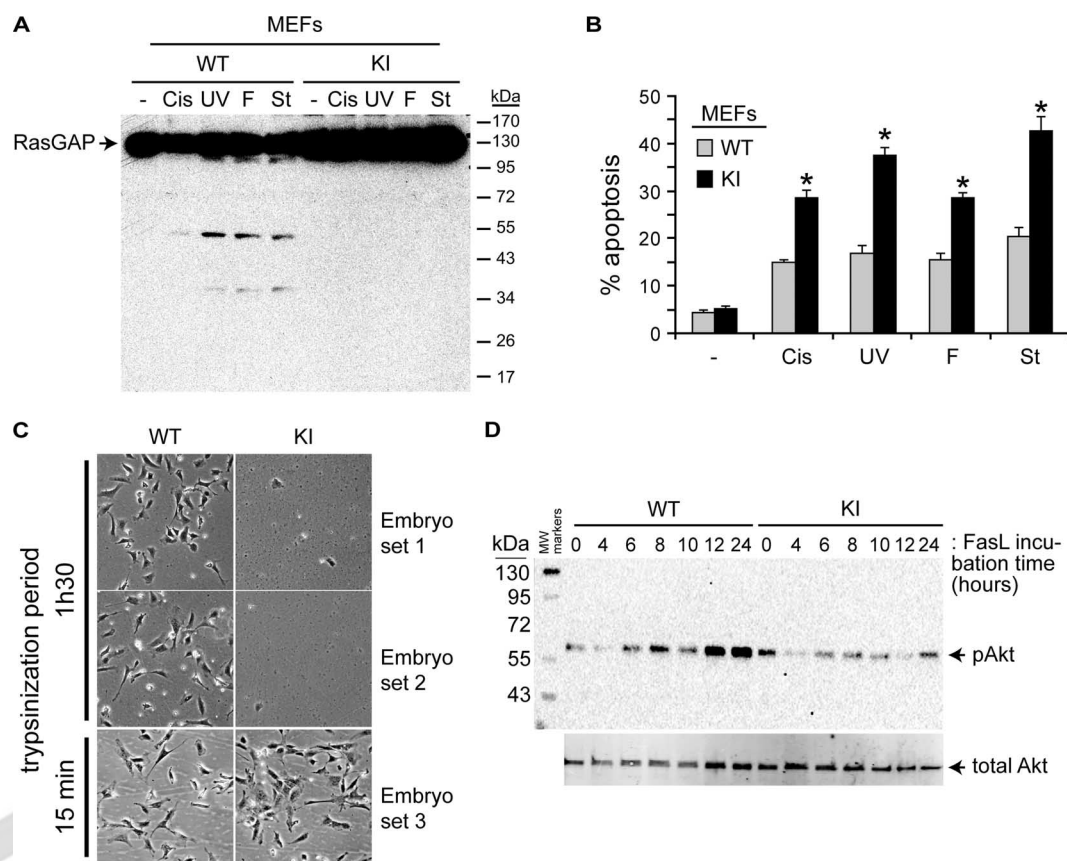


FIG 5 MEFs from RasGAP^{D455A/D455A} knock-in mice do not cleave RasGAP and are more sensitive to apoptosis. (A and B) Wild-type (WT) and KI MEFs were left untreated (–) or treated with 15 μ M cisplatin (Cis), 96 J/m² UV-C (UV), 15 ng/ml FasL (F), and 15 nM staurosporine (St). (A) Cells were lysed 24 h later and analyzed by Western blotting for the presence of RasGAP and its fragments using an anti-RasGAP polyclonal antibody. (B) Alternatively, apoptosis was scored. Results correspond to the mean \pm 95% CI of 3 independent experiments ($n = 3$). (C) Mouse embryonic cells 1 day after their isolation using a trypsinization period of 1 h 30 min or 15 min (see Materials and Methods for details). (D) Wild-type and KI MEFs were treated with 5 ng/ml FasL for the indicated periods of time. Cells were then washed twice with PBS and then incubated for an additional hour in Dulbecco modified Eagle medium at 37°C before lysis. Akt activation and total Akt expression were assessed by Western blotting.

AQ: C

what was seen in wild-type mice (Fig. 8B). At the clinical level, DSS-induced colon damage was more pronounced, as assessed by colon shortening (Fig. 8C) and a more severe DSS-mediated colitis development in KI mice than wild-type mice (Fig. 8D).

DISCUSSION

The role of caspase-3 in the induction of the antiapoptotic Akt kinase was investigated in adult caspase-3-knockout mice in relation to three different pathophysiological conditions: UV-B skin exposure, doxorubicin-induced cardiomyopathy, and DSS-mediated colitis. Each of these stresses led to Akt activation in the tissues affected by the stress. This was, however, blocked or strongly compromised in mice lacking caspase-3. This impaired Akt activation correlated with augmented cell death, tissue damage, and even lethality. A similar defect in Akt activation was observed in KI mice that expressed a caspase-3-resistant form of p120 RasGAP, and this was accompanied by increased apoptosis and stronger adverse effects: increased number of sunburn cells in UV-B-exposed skin, decreased heart function upon doxorubicin injection, and stronger DSS-mediated colitis development. This study therefore identifies a physiological protective mechanism against stress that relies on the activity of an executioner caspase.

Caspase-3 is now known to mediate many nonapoptotic functions in cells (15, 23, 24). It is involved in B cell homeostasis by negatively regulating B cell proliferation following antigen stimulation (46). Caspase-3 is also activated during T cell stimulation (32), and this may participate in T cell proliferation (2, 22). Additionally, caspase-3 is required for erythropoiesis (9). There is thus evidence that caspase-3 plays important functional roles in non-dying hematopoietic cells, but it remains unclear how these cells counteract the apoptotic potential of caspase-3. Cleavage of RasGAP could have been one of the mechanisms allowing these cells to survive following caspase-3 activation. However, T and B cell development occurs normally in the D455A RasGAP KI mice (see Table S1 in the supplemental material). Similarly, the development of mature myeloid and erythroid lineage cells in the bone marrow proceeds normally in the KI mice (see Table S1 in the supplemental material). Therefore, hematopoietic cells use protective mechanisms other than those activated by the cleavage of RasGAP to inhibit apoptosis if caspase-3 is activated during their development.

Caspase-3 is necessary for the development of several tissues. Muscle development and osteoblast differentiation are compromised in the absence of caspase-3 (17, 33, 34). Caspase-3 also plays

Khalil et al.

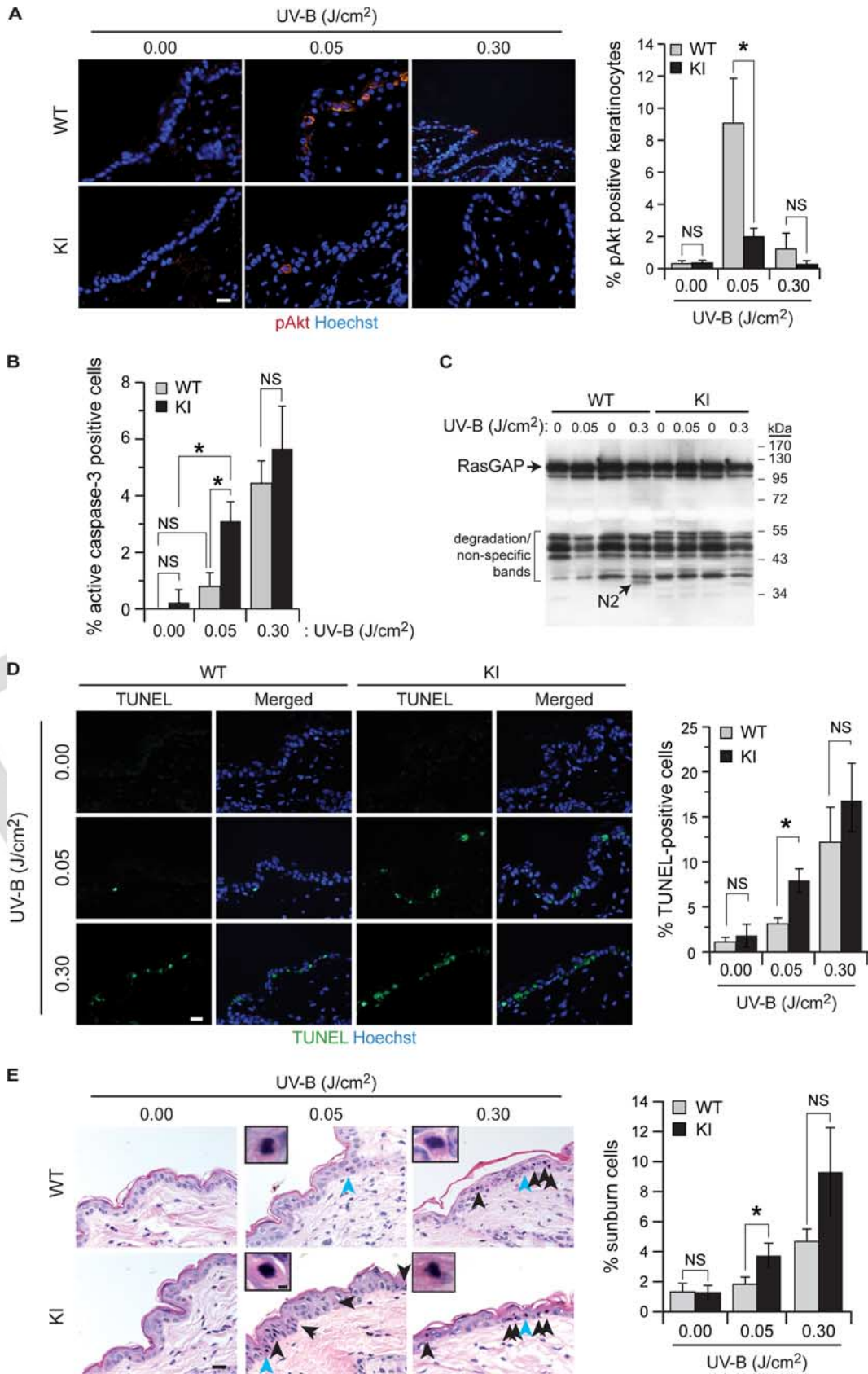


FIGURE 1

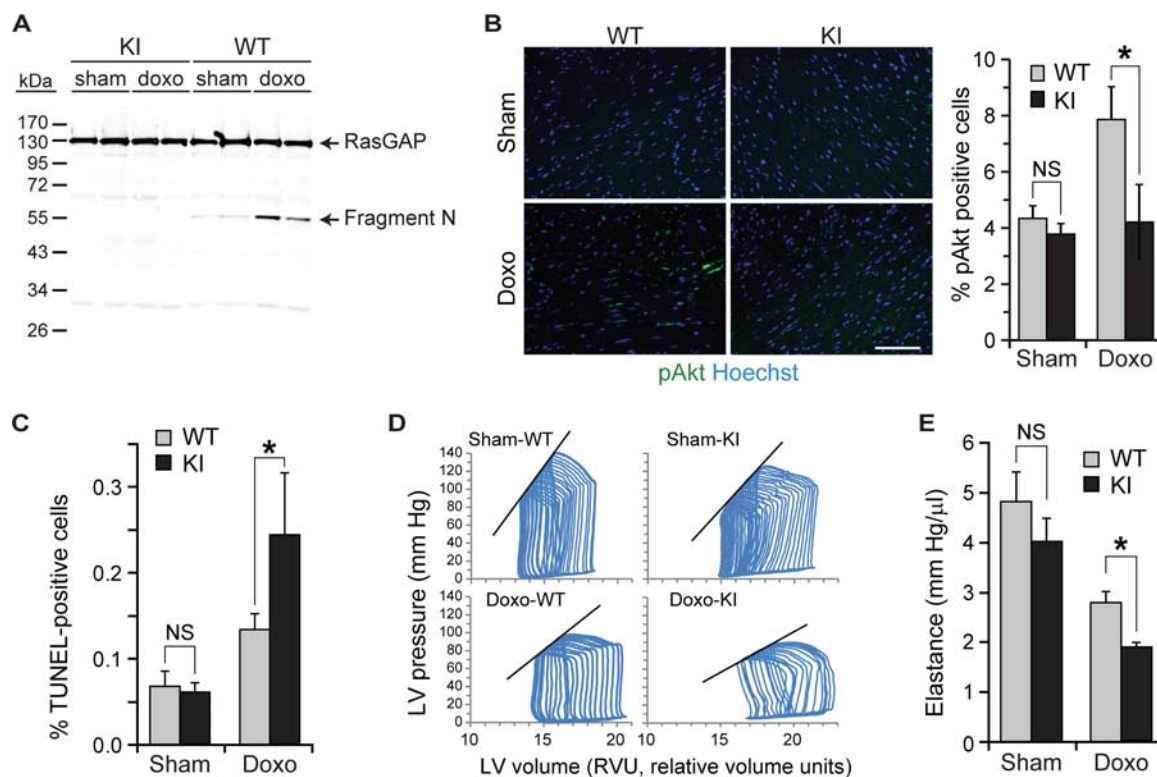


FIG 7 Role of RasGAP cleavage in heart of doxorubicin-treated mice. Wild-type (WT) and RasGAP^{D455A/D455A} (KI) mice were injected with doxorubicin and analyzed 5 days later. (A) Western blot analysis of RasGAP cleavage. This experiment has been repeated once with similar results. (B) Histoimmunofluorescence detection and quantitation of active Akt. Bar, 100 μ m. (C) Assessment of apoptosis by the TUNEL assay. (B and C) Results correspond to the mean \pm 95% CI of measurements performed on 3 animals per condition (three independent experiments). (D) Representative examples of end-systolic left ventricular pressure-volume loops. (E) Heart contractility assessed by end-systolic elastance. Results correspond to the mean \pm 95% CI of measurements performed on 9 to 11 animals per condition (three independent experiments).

important functions in neurogenesis, synaptic activity, neuronal growth cone guidance, and glial development (7, 16, 37). Histological analyses of muscle, bone, and brain tissues did not reveal any defect in the KI mice (data now shown). Moreover, the growth curve and size of wild-type and KI mice were comparable (Fig. 4D and E). Hence, the mechanisms allowing tissues and organs to withstand caspase-3 activation during development do not rely on RasGAP cleavage and remain to be characterized.

In vitro data provided evidence that low caspase-3 activity induced by mild stress generates fragment N, which was responsible for Akt activation and promotion of cell survival. At higher caspase-3 activity induced by stronger insults, fragment N is further processed into fragments that can no longer stimulate Akt, and this favors apoptosis (47). The data obtained *in vivo* in UV-B-exposed skin are consistent with this model. Low doses of UV-B induced no further cleavage of fragment N (i.e., no production of fragment N2) in keratinocytes, and this was accompanied by Akt activation and absence of an apoptotic response. In contrast, high

UV-B doses generated fragment N2 and Akt was no longer activated, and this led to keratinocyte cell death (Fig. 6). *In vivo*, therefore, RasGAP also functions as a caspase-3 activity sensor to determine whether cells within tissues and organs should be spared or die.

The levels of caspase-3 activation that are required to induce partial cleavage of RasGAP into fragment N are at least an order of magnitude lower than those necessary to induce apoptosis (48). *In vitro*, these low caspase activity levels are not easily detected (47). In response to the stress stimuli used in the present study that led to Akt activation, we could not visualize low caspase-3 activation by Western blotting in any of the tissues investigated, although in response to stronger stresses that did not lead to Akt activation (e.g., 0.3 J/cm² of UV-B; Fig. 6), caspase-3 activation could be evidenced (Fig. 2A and B). Nonetheless, blocking caspases with chemical inhibitors or using mice lacking caspase-3 prevented Akt activation induced by low stresses (Fig. 1 and 2). Therefore, caspase-3 exerts an important protective function in tissues and

FIG 6 Role of RasGAP cleavage in UV-B exposed skin. Skin of wild-type (WT) and RasGAP^{D455A/D455A} (KI) mice was exposed to the indicated doses of UV-B. Mice were sacrificed 24 h later, and the exposed skin was isolated for biochemical and histological analyses. (A and B) Histoimmunofluorescence detection and quantitation of active Akt (A) and active caspase-3 (B). Results correspond to the mean \pm 95% CI of measurements performed on 4 to 6 animals (three independent experiments). (C) Western blot analysis of RasGAP cleavage (the blot shown is representative of three independent experiments). (D) Assessment of apoptosis by the TUNEL assay. Results correspond to the mean \pm 95% CI of measurements performed on 5 to 9 animals (three independent experiments). (E) Histological assessment of sunburn cells in the epidermis. Results correspond to the mean \pm 95% CI of measurements performed on 9 to 11 animals (three independent experiments). Cells indicated by light blue arrowheads are enlarged in the insets. Bar, 20 μ m.

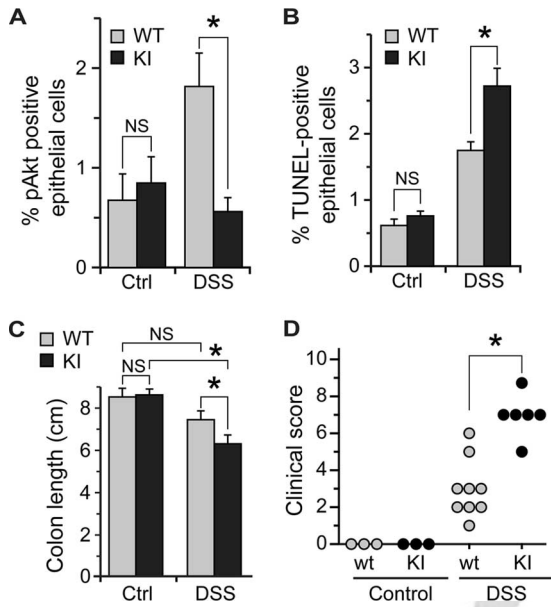


FIG 8 Role of RasGAP cleavage in colon of DSS-treated mice. Wild-type (WT) and RasGAP^{D455A/D455A} (KI) mice were given DSS-containing water for 3 days and normal drinking water for four additional days. The mice were then sacrificed. (A) Quantitation of active Akt on histological sections. Results correspond to the mean \pm 95% CI of measurements performed on 3 to 4 animals per condition (three independent experiments). (B) Assessment of apoptosis by the TUNEL assay. Results correspond to the mean \pm 95% CI of measurements performed on 3 control and 6 to 7 DSS-treated animals per genotype (three independent experiments). (C) Colon damage assessed by variations in colon length. Results correspond to the mean \pm 95% CI of measurements performed on 3 control and 7 to 9 DSS-treated animals per genotype (three independent experiments). (D) Clinical scoring of colitis performed on 7 to 10 animals per condition (three independent experiments). The data were analyzed with a Wilcoxon two-sample two-sided test.

organs in a RasGAP cleavage-dependent manner under conditions where caspase-3 activation may be below the detection threshold of current caspase-3 activation assessment methods.

In conclusion, our study provides the first genetic evidence that in response to various pathology-inducing stresses caspase-3 itself activates the antiapoptotic Akt kinase and that this protective response is mediated through the cleavage of a given caspase-3 substrate, the ubiquitous p120 RasGAP protein. This defense mechanism allows an organism to dampen damage to tissues and organs induced by diverse pathogenic conditions. Hence, procedures aimed at activating the signaling pathways modulated by RasGAP cleavage may represent an attractive strategy to increase the resistance of individuals exposed to environmental or chemical stresses. Additionally, our work has direct implications for therapeutic protocols using caspase inhibitors, as inhibition of caspases could lead to unanticipated adverse effects by decreasing the ability of an organism to cleave RasGAP and defend itself.

ACKNOWLEDGMENTS

This work was supported by Swiss National Science Foundation grants 31003A_119876 and 31003A_141242 1/1 (to C.W.), 310030_135394/1 (to L.L.), and 310030_122012 (to W.H.) and by an Interdisciplinary Research Project subsidiary from the Faculty of Biology and Medicine, University of Lausanne, Lausanne, Switzerland (to C.W. and P.B.).

We thank Andrew Dwyer for critical reading of the manuscript. We thank the Transgenic Animal Facility of the Faculty of Biology and Med-

icine and the University Hospital (University of Lausanne) for generation of the knock-in mice.

H.K., N.P., and C.W. conceived the study. N.P. performed immunofluorescence experiments. H.K. and N.P. performed histology, TUNEL experiments, and the associated quantitation. J.W. generated the KI mice. J.-Y.Y., G.D., N.P., and C.W. performed the experiments on MEFs *in vitro*. N.G. and W.H. analyzed hematopoiesis and lymphopoiesis in mice. N.P. and P.B. performed the UV-B illumination experiments. H.K. and B.M. performed the DSS experiments. H.K. and L.L. analyzed cardiac functions in mice. C.W. wrote the paper. All authors discussed the results.

We declare that we have no conflict of interest.

REFERENCES

- Abraham MC, Shaham S. 2004. Death without caspases, caspases without death. *Trends Cell Biol.* 14:184–193.
- Alam A, Cohen LY, Aouad S, Sekaly RP. 1999. Early activation of caspases during T lymphocyte stimulation results in selective substrate cleavage in nonapoptotic cells. *J. Exp. Med.* 190:1879–1890.
- Bonnet MC, et al. 2011. The adaptor protein FADD protects epidermal keratinocytes from necroptosis *in vivo* and prevents skin inflammation. *Immunity* 35:572–582.
- Bulat N, et al. 2011. RasGAP-derived fragment N increases the resistance of beta cells towards apoptosis in NOD mice and delays the progression from mild to overt diabetes. *PLoS One* 6:e22609. doi:10.1371/journal.pone.0022609.
- Bulat N, Waeber G, Widmann C. 2009. LDLs stimulate p38 MAPKs and wound healing through SR-BI independently of Ras and PI3 kinase. *J. Lipid Res.* 50:81–89.
- Burguillos MA, et al. 2011. Caspase signalling controls microglia activation and neurotoxicity. *Nature* 472:319–324.
- Campbell DS, Holt CE. 2003. Apoptotic pathway and MAPKs differentially regulate chemotropic responses of retinal growth cones. *Neuron* 37:939–952.
- Candi E, Schmidt R, Melino G. 2005. The cornified envelope: a model of cell death in the skin. *Nat. Rev. Mol. Cell Biol.* 6:328–340.
- Carlile GW, Smith DH, Wiedmann M. 2004. Caspase-3 has a nonapoptotic function in erythroid maturation. *Blood* 103:4310–4316.
- Caserta TM, Smith AN, Gultice AD, Reedy MA, Brown TL. 2003. Q-VD-OPH, a broad spectrum caspase inhibitor with potent antiapoptotic properties. *Apoptosis* 8:345–352.
- Cuvillier O, et al. 2001. Sphingosine generation, cytochrome c release, and activation of caspase-7 in doxorubicin-induced apoptosis of MCF7 breast adenocarcinoma cells. *Cell Death Differ.* 8:162–171.
- Daniels F, Jr, Brophy D, Lobitz WC, Jr. 1961. Histochemical responses of human skin following ultraviolet irradiation. *J. Invest. Dermatol.* 37:351–357.
- Droin N, et al. 2008. A role for caspases in the differentiation of erythroid cells and macrophages. *Biochimie* 90:416–422.
- Eymin B, et al. 1999. Caspase-induced proteolysis of the cyclin-dependent kinase inhibitor p27Kip1 mediates its anti-apoptotic activity. *Oncogene* 18:4839–4847.
- Feinstein-Rotkopf Y, Arama E. 2009. Can't live without them, can live with them: roles of caspases during vital cellular processes. *Apoptosis* 14:980–995.
- Fernando P, Brunette S, Megeney LA. 2005. Neural stem cell differentiation is dependent upon endogenous caspase 3 activity. *FASEB J.* 19:1671–1673.
- Fernando P, Kelly JF, Balazsi K, Slack RS, Megeney LA. 2002. Caspase 3 activity is required for skeletal muscle differentiation. *Proc. Natl. Acad. Sci. U. S. A.* 99:11025–11030.
- Fujita J, et al. 2008. Caspase activity mediates the differentiation of embryonic stem cells. *Cell Stem Cell* 2:595–601.
- Giaime E, et al. 2006. Caspase-3-derived C-terminal product of synphilin-1 displays antiapoptotic function via modulation of the p53-dependent cell death pathway. *J. Biol. Chem.* 281:11515–11522.
- Holler N, et al. 2003. Two adjacent trimeric Fas ligands are required for Fas signaling and formation of a death-inducing signaling complex. *Mol. Cell. Biol.* 23:1428–1440.
- Jianhui L, et al. 2010. Endotoxin impairs cardiac hemodynamics by affecting loading conditions but not by reducing cardiac inotropism. *Am. J. Physiol. Heart Circ. Physiol.* 299:H492–H501.

22. Kennedy NJ, Kataoka T, Tschopp J, Budd RC. 1999. Caspase activation is required for T cell proliferation. *J. Exp. Med.* **190**:1891–1896.
23. Kuranaga E, Miura M. 2007. Nonapoptotic functions of caspases: caspases as regulatory molecules for immunity and cell-fate determination. *Trends Cell Biol.* **17**:135–144.
24. Launay S, et al. 2005. Vital functions for lethal caspases. *Oncogene* **24**: 5137–5148.
25. Leonard JR, Klocke BJ, D'Sa C, Flavell RA, Roth KA. 2002. Strain-dependent neurodevelopmental abnormalities in caspase-3-deficient mice. *J. Neuropathol. Exp. Neurol.* **61**:673–677.
26. Li Z, et al. 2010. Caspase-3 activation via mitochondria is required for long-term depression and AMPA receptor internalization. *Cell* **141**:859–871.
27. Liadis N, et al. 2005. Caspase-3-dependent β -cell apoptosis in the initiation of autoimmune diabetes mellitus. *Mol. Cell. Biol.* **25**:3620–3629.
28. Luciano F, Herrant M, Jacquell A, Ricci JE, Auberger P. 2003. The p54 cleaved form of the tyrosine kinase Lyn generated by caspases during BCR-induced cell death in B lymphoma acts as a negative regulator of apoptosis. *FASEB J.* **17**:711–713.
29. Mansilla S, Priebe W, Portugal J. 2006. Mitotic catastrophe results in cell death by caspase-dependent and caspase-independent mechanisms. *Cell Cycle* **5**:53–60.
30. McLaughlin B, et al. 2003. Caspase 3 activation is essential for neuroprotection in preconditioning. *Proc. Natl. Acad. Sci. U. S. A.* **100**:715–720.
31. Michod D, Widmann C. 2007. TAT-RasGAP₃₁₇₋₃₂₆ requires p53 and PUMA to sensitize tumor cells to genotoxins. *Mol. Cancer Res.* **5**:497–507.
32. Miossec C, Dutilleul V, Fassy F, Diu-Hercend A. 1997. Evidence for CPP32 activation in the absence of apoptosis during T lymphocyte stimulation. *J. Biol. Chem.* **272**:13459–13462.
33. Miura M, et al. 2004. A crucial role of caspase-3 in osteogenic differentiation of bone marrow stromal stem cells. *J. Clin. Invest.* **114**:1704–1713.
34. Mogi M, Togari A. 2003. Activation of caspases is required for osteoblastic differentiation. *J. Biol. Chem.* **278**:47477–47482.
35. Newton K, Strasser A. 2003. Caspases signal not only apoptosis but also antigen-induced activation in cells of the immune system. *Genes Dev.* **17**:819–825.
36. Ohkawara T, et al. 2005. Transgenic over-expression of macrophage migration inhibitory factor renders mice markedly more susceptible to experimental colitis. *Clin. Exp. Immunol.* **140**:241–248.
37. Oomman S, Strahlendorf H, Dertien J, Strahlendorf J. 2006. Bergmann glia utilize active caspase-3 for differentiation. *Brain Res.* **1078**:19–34.
38. Pacher P, et al. 2003. Potent metalloporphyrin peroxynitrite decomposition catalyst protects against the development of doxorubicin-induced cardiac dysfunction. *Circulation* **107**:896–904.
39. Pacher P, et al. 2004. Left ventricular pressure-volume relationship in a rat model of advanced aging-associated heart failure. *Am. J. Physiol. Heart Circ. Physiol.* **287**:H2132–H2137.
40. Parcellier A, Tintignac LA, Zhuravleva E, Hemmings BA. 2008. PKB and the mitochondria: AKTing on apoptosis. *Cell. Signal.* **20**:21–30.
41. Peter ME. 2011. Programmed cell death: apoptosis meets necrosis. *Nature* **471**:310–312.
42. Rincheval V, Renaud F, Lemaire C, Mignotte B, Vayssiere JL. 1999. Inhibition of Bcl-2-dependent cell survival by a caspase inhibitor: a possible new pathway for Bcl-2 to regulate cell death. *FEBS Lett.* **460**:203–206.
43. Slee EA, Adrain C, Martin SJ. 2001. Executioner caspase-3, -6, and -7 perform distinct, non-redundant roles during the demolition phase of apoptosis. *J. Biol. Chem.* **276**:7320–7326.
44. Sordet O, et al. 2002. Specific involvement of caspases in the differentiation of monocytes into macrophages. *Blood* **100**:4446–4453.
45. Taylor RC, Cullen SP, Martin SJ. 2008. Apoptosis: controlled demolition at the cellular level. *Nat. Rev. Mol. Cell Biol.* **9**:231–241.
46. Woo M, et al. 2003. Caspase-3 regulates cell cycle in B cells: a consequence of substrate specificity. *Nat. Immunol.* **4**:1016–1022.
47. Yang J-Y, et al. 2004. Partial cleavage of RasGAP by caspases is required for cell survival in mild stress conditions. *Mol. Cell. Biol.* **24**:10425–10436.
48. Yang J-Y, Walicki J, Michod D, Dubuis G, Widmann C. 2005. Impaired Akt activity down-modulation, caspase-3 activation, and apoptosis in cells expressing a caspase-resistant mutant of RasGAP at position 157. *Mol. Biol. Cell* **16**:3511–3520.
49. Yang J-Y, Widmann C. 2001. Antiapoptotic signaling generated by caspase-induced cleavage of RasGAP. *Mol. Cell. Biol.* **21**:5346–5358.
50. Yang J-Y, Widmann C. 2002. The RasGAP N-terminal fragment generated by caspase cleavage protects cells in a Ras/PI3K/Akt-dependent manner that does not rely on NF κ B activation. *J. Biol. Chem.* **277**:14641–14646.
51. Youn HJ, et al. 2005. Induction of caspase-independent apoptosis in H9c2 cardiomyocytes by adriamycin treatment. *Mol. Cell. Biochem.* **270**: 13–19.

AUTHOR QUERIES

AUTHOR PLEASE ANSWER ALL QUERIES

1

AQau—Please confirm the given-names and surnames are identified properly by the colors.
■ = Given-Name, ■ = Surname

AQA—Au: Are units available for “1280 × 960”?

AQB—Au: Please define Q-VD-OPH.

AQC—Au: “MW” was deleted from the label for the first lane in Fig. 5D because molecular weight is a unitless ratio but units of kDa are provided.

Supplemental information

Supplemental Tables

Supplemental table 1: **Hematopoiesis and lymphopoiesis in wild-type and RasGAP^{D455A/D455A} knock-in mice**

Thymocytes, bone marrow (BM) and spleen cells were exposed to a hypotonic buffer to remove erythrocytes. Cells were then incubated with 2.4G2 (anti-CD16/32) hybridoma supernatant to block FC receptors before staining for multi-color flow cytometry (except for the staining of BM precursors). Dead cells were excluded based on 7-AAD uptake. The following antibodies were used CD3 ϵ (17A2), CD4 (RM4-5), CD8 α (53.6.7), CD11b (Mac1, M1/70), CD16/32 (93), CD19 (1D3/6D5), CD25 (PC-61), CD34 (Ram34), CD43 (S7), CD44 (IM781), CD45R/B220 (RA3-6B2), CD45.2 (104.2), CD71 (R17217), CD117 (2B8), CD127 (A7R34), Sca1 (D7), GR-1 (Ly6G, RB68C5), Ter119 (Ter119), BP-1 (6C3), IgM (11/41 or R6-60.2), TCR β (H57), TCR $\gamma\delta$, CD24. The antibodies were conjugated to appropriate fluorochromes (FITC, PE, PE-Texas red, PE-Cy5, PE-Cy5.5, PerCP-Cy5.5, PE-Cy7, APC, Alexa647, Alexa700, APC-Cy7, APC-Alexa780, Pacific blue, efluor450) at the Ludwig Center for Cancer Research of the University of Lausanne (LICR) or purchased from eBiosciences, Becton Dickinson or Biolegend. A cocktail of PE-Cy7-conjugated anti-TCR β , CD3 ϵ , CD4, CD8 α , CD11 β , GR-1, B220, CD19, Ter119, CD161 (PK136) monoclonal antibodies was used to gate out lineage-positive cells. Samples were run on a LSRII flow cytometer (Becton Dickinson) and analyzed with FlowJo software (Tristar).

		WT	KI
Bone Marrow *	x 10 ⁶	29 \pm 3	26 \pm 4
lin ⁻ Sca1 ⁺ c-kit ⁺ (LSK)	x 10 ⁴	7.7 \pm 2.0	7.1 \pm 3.3
lin ⁻ Sca1 ⁻ c-kit ⁺ (LKS ⁻)	x 10 ⁴	57.0 \pm 19.6	53.6 \pm 10.8
lin ⁻ c-kit ⁺ CD127 ⁺ (CLP)	x 10 ⁴	6.0 \pm 2.0	5.1 \pm 2.8
Ter119 ⁺ CD71 ⁺	x 10 ⁶	1.8 \pm 0.2	1.7 \pm 0.3
GR1 ⁺ CD11b ⁺	x 10 ⁶	14.1 \pm 2.6	13.0 \pm 2.5
GR1 ⁻ CD11b ⁺	x 10 ⁶	2.3 \pm 0.2	2.2 \pm 0.5

B220 ⁺ CD43 ⁺	x 10 ⁶	1.3±0.1	1.1±0.2
B220 ⁺ CD43 ⁻	x 10 ⁶	6.2±0.6	5.1±1.0
Thymus	x 10 ⁶	80±20	96±18
CD4 ⁻ 8 ⁻ (DN)	x 10 ⁶	2.3±2.2	2.7±1.6
CD4 ⁺ 8 ⁺ (DP)	x 10 ⁶	68.9±16.4	77.7±21.3
CD4 ⁺ 8 ⁻	x 10 ⁶	5.7±1.8	8.0±3.8
CD4 ⁻ 8 ⁺	x 10 ⁶	2.1±0.8	2.2±0.6
TCR $\gamma\delta$ CD4 ⁻ CD8 ⁻	x 10 ⁶	0.17±0.11	0.26±0.15
Spleen	x 10 ⁶	57±22	70±21
B220 ⁺	x 10 ⁶	21.8±3.2	29.9±2.6
CD3 ⁺ CD4 ⁺	x 10 ⁶	12.3±3.4	13.1±1.5
CD3 ⁺ CD8 ⁺	x 10 ⁶	6.2±2.6	7.7±1.1
CD3 ⁻ CD122 ⁺	x 10 ⁶	0.9±0.6	1.2±0.5

Data are the mean absolute number of cells (\pm SD) from 3-5 different mice.

* Cell counts refer to one hind leg

Interpretation of the results presented in Supplemental Table 2

The bone marrow of D445A and control mice contained a comparable population of Lin⁻ Sca1⁺ c-kit⁺ (LSK) cells that contains haematopoietic stem cells. Further, myeloid/erythroid (Lin⁻ Sca1⁻ c-kit⁺, LKS⁻) and lymphoid committed common lymphoid progenitors (CLP, Lin⁻ c-kit^{lo} CD127⁺) were also present at comparable numbers. Among the LKS⁻ cells there was a normal distribution of CMP (Common myeloid progenitors), GMP (Granulocyte monocyte progenitors) and MEP (Megakaryocyte erythroid progenitors) (not shown)

Further, the development of mature myeloid and erythroid lineage cells in the bone marrow was not perturbed, as judged by the normal numbers of granulocytes (GR1⁺CD11b⁺), monocytes (GR1⁻CD11b⁺) and erythroblasts (CD71⁺TER119⁺). With regard to lymphocyte development, the sizes of the B220⁺CD43⁺ and the B220⁺CD43⁻ populations were comparable. Among immature B220⁺ CD43⁻ cells there were comparable populations of CD19⁻ BP-1⁻, CD19⁺ BP-1⁻ and CD19⁺ BP-1⁺

cells (not shown). Similarly, intrathymic T cell development was also unaffected. This was not only true for TCR $\alpha\beta$ lineage cells but also for CD4⁻CD8⁻ cells expressing TCR $\gamma\delta$.

As expected from the normal presence of immature precursors, the periphery of D445A mice (spleen) contained comparable numbers of B cells (B220), T cells (CD3⁺, both CD4⁺ and CD8⁺ T cells) and NK cells (CD3⁻CD122⁺).

In conclusion, the steady state hematopoiesis and lymphopoiesis was not perturbed in RasGAP^{D455A/D455A} knock-in mice.

Supplemental table 2: Wild-type and RasGAP^{D455A/D455A} knock-in mice hemodynamic parameters injected or not with doxorubicin

Hemodynamic measurements were performed using left ventricular pressure-volume micro-catheters as described in the methods. Doxorubicin induced cardiac dysfunction as shown by reduced left ventricular (LV) systolic pressure, stroke work and dp/dt max, which were related to a depression in contractility, as shown by the significant reduction of end-systolic elastance, an ejection phase measure of contractility. The hearts were not dilated, which is expected in such a short term model of heart failure. Importantly, the reduction of cardiac contractility was significantly more pronounced in RasGAP D455A KI mice, as shown by significantly greater reduction of LV end-systolic pressure, dp/dt max, Ees, as well as significant decrease of dp/dt@edv, an isovolumic phase measure of contractility. Results correspond to the mean \pm 95% CI of measurements performed on 9-11 mice per treatment and genotype.

Variable	Sham-WT	Sham-KI	Doxo-WT	Doxo-KI
HR (bpm)	334 \pm 30	294 \pm 15	245 \pm 14†	255 \pm 22
Esp (mm Hg)	131 \pm 7	115 \pm 7	93 \pm 4†	75 \pm 5†*
Edp (mm Hg)	9.2 \pm 1.5	11.7 \pm 1.5	9.7 \pm 1.3	7.6 \pm 1.0
Esv (μ l)	15.4 \pm 1.1	18.6 \pm 1.4	18.3 \pm 2.2	23.5 \pm 3.2
Edv (μ l)	31.5 \pm 1.6	36.7 \pm 1.8	35.3 \pm 2.3	41.1 \pm 3.9
SV (μ l)	18.5 \pm 1.1	20.5 \pm 2.0	19.5 \pm 1.1	19.8 \pm 1.8
CO (μ l min ⁻¹)	6173 \pm 691	5284 \pm 301	4737 \pm 370	5130 \pm 715
EF (%)	57 \pm 2	55 \pm 2	55 \pm 4	48 \pm 4

SW (mm Hg μ l)	1791 \pm 102	1837 \pm 124	1417 \pm 124†	1188 \pm 123†
dp/dt max (mm Hg sec ⁻¹)	9372 \pm 786	7892 \pm 326	6724 \pm 436†	5173 \pm 495†*
Ese (mm Hg μ l ⁻¹)	4.8 \pm 0.6	4.0 \pm 0.5	2.7 \pm 0.2†	1.8 \pm 0.1†*
dp/dt@edv (mm Hg sec ⁻¹ μ l ⁻¹)	185 \pm 29	143 \pm 11	188 \pm 24	82 \pm 17†*

† p<0.05 vs sham in the same genotype. *p<0.05 WT vs KI

HR, heart rate; Esp, end-systolic pressure; Edp, end-diastolic pressure; Esv, end-systolic volume; Edv, end-diastolic volume; SV, stroke volume; CO, cardiac output; EF, ejection fraction; SW, stroke work; dp/dt max, first derivative of LV systolic pressure increment; Ese, end-systolic elastance (slope of the end-systolic pressure-volume relationship); dp/dt@edv, dp/dt max corrected for end-diastolic volume.

Supplemental Figure

Figure S1: Schematic representation of the D455A targeting vector construction

The 3' and 5' homology arms of the targeting vector were derived from a RasGAP genomic clone (RP22-250D10) obtained by screening the RPCI-22 129S6/SvEvTac mouse BAC library from the BACPAC Resource Center (Children's Hospital Oakland Research Institute, Oakland, California, USA) (2) with a probe corresponding to nucleotides 7137306-7136366 of *Mus musculus* chromosome 13 genomic contig (accession N° NT_039589.2). This led to the identification of three BAC clones (RP22-250D10, #452; RP22-268I2, #453; RP22-257P13 #454). The DNA prepared from these clones was pooled and digested with *Swa*I. The resulting ~10 kb fragment was sub-cloned in the *Eco*RV restriction site of pBluescript II SK + (Stratagene). A plasmid containing RasGAP exons 9, 10, and 11 was identified by PCR and called **RasGAP exons 9-10-11.blu** (plasmid #419). From this plasmid, a blunt-ended ~6.5 kb *Bst*XI fragment [nucleotides 7139579-7145879 from the *Mus musculus* chromosome 13 genomic contig (accession n° NT_039589.2)] was sub-cloned in the *Eco*RV restriction site of pBluescript II SK + to generate the 5' homology arm composed of parts of introns 8 and 9 and exon 9 (the resulting plasmid was called **RasGAP exon 9.blu**; plasmid #427). A ~2.6 kb *Hind*III fragment from RasGAP exons 9-10-11.blu (nucleotides 7138985-7136418 from the chromosome 13 genomic contig) was sub-cloned in the *Hind*III restriction site of pcDNA3 to generate the 3' homology arm composed of parts of introns 10 and 11 and exon 11 (the resulting plasmid was called **RasGAP exon 11.dn3**; plasmid #421). A 590 bp fragment (called the Vital Region [VR] as it encodes amino acid 455 of RasGAP) containing exon 10 and connecting the 5' and 3' homology arms was PCR-amplified from the BAC clones described above using the *Pwo* polymerase (Roche Applied Science, catalogue n° 04 340 868 001), sub-cloned into the *Sma*I and *Not*I sites of pBluescript II SK+, and sequenced twice to confirm that no PCR-generated errors occurred (the resulting plasmid was called **Lox 66-RasGAP Exon 10.blu**; plasmid #427). The mutation of the caspase cleavage site in exon 10 was done using the megaprimer PCR mutagenesis method(1) using the following primers: 1) a sense primer for the first PCR: AA GTA CTG AAC GAC ACT GTG GCC GGC AAG GAG ATC TAT AAC ACA AT. This corresponds to sequence 641-685 of the *Mus musculus* RasGAP

mRNA (gi 21703899) carrying an A to C mutation (underlined) that destroys the first RasGAP caspase cleavage site by substituting an aspartate (D) residue for an alanine (A) (3) and two additional silent mutations (bold) that, together with the D to A mutation, create a new restriction site recognized by the NaeI and NgoMIV endonucleases (see also Figure 4B). 2) an anti-sense primer for the first PCR: TACCTAGCATGAACAGATTG (a random sequence not found in the plasmid) GCGGCCGC (NotI) GTTCTAAAACCCTGGTTATA (3' terminal sequence of the Vital Region; sequence 42026-42007 of the *Mus musculus* BAC clone RP23-222G16 [gi 29367036]). 3) a sense primer for the second PCR: CGTA CCCGGG (SmaI) AGTAGGTGGGTTTCAGGAGCAG (sequence 42007-42026 of the *Mus musculus* BAC clone). 4) an anti-sense primer for the second PCR: TACCTAGCATGAACAGATTG (the same random sequence found in primer 2).

The mutated PCR product was digested with SmaI and NotI and subcloned into the SmaI/NotI sites of pBluescript II SK + [generating plasmid **RasGAP exon 10 (D455A).blu**; plasmid #428].

The LoxP targeting vector plasmid (**Lox-Neo-Lox.Itv**, plasmid #425) is a derivative of the LTV plasmid (a gift from Olivier Staub, Lausanne University, Switzerland) from which the third LoxP site was removed. This Lox-Neo-Lox.Itv plasmid was used as a backbone to construct the targeting vector. It consists of a neomycin-resistance cassette (PGK-Neo) flanked with two LoxP sites and the Herpes Simplex Virus thymidine kinase gene (HSV-TK). RasGAP Exon 11.dn3 was digested with HindIII and the resulting 2.6 kb fragment was ligated into the HindIII site of LTV (generating plasmid **Lox-Neo-Lox-RasGAP Exon 11.Itv**; plasmid #426). The 0.6 kb SmaI/NotI fragment of RasGAP Exon 10 (D455A).blu was ligated into the SmaI/NotI sites of RasGAP Exon 9.blu, creating plasmid RasGAP Exons 9-10 (D455A).blu. Finally, the Sall/NotI 7 kb fragment of RasGAP Exons 9-10 (D455A).blu was inserted into the Sall/NotI sites of LTV-Lox-Neo-Lox-RasGAP Exon 11 plasmid to obtain the final D455A targeting vector [plasmid **RasGAP Exons 9-10 (D455A)-Lox-Neo-Lox-RasGAP Exon 11**; plasmid #441]. This clone was sequenced to verify that the LoxP sites and the D455A mutation were intact.

The targeting vector electroporation, clone selection and injection into C57/BL6 blastocysts was performed at the Transgenic Animal Facility of the University of Lausanne (<http://www.unil.ch/taf>).

Reference List

1. **Nelson, R. M. and G. L. Long.** 1989. A general method of site-specific mutagenesis using a modification of the *Thermus aquaticus* polymerase chain reaction. *Anal.Biochem.* **180**:147-151.
2. **Osoegawa, K., M. Tateno, P. Y. Woon, E. Frengen, A. G. Mammoser, J. J. Catanese, Y. Hayashizaki, and P. J. de Jong.** 2000. Bacterial artificial chromosome libraries for mouse sequencing and functional analysis. *Genome Res.* **10**:116-128.
3. **Yang, J.-Y. and C. Widmann.** 2001. Antiapoptotic signaling generated by caspase-induced cleavage of RasGAP. *Mol.Cell.Biol.* **21**:5346-5358.

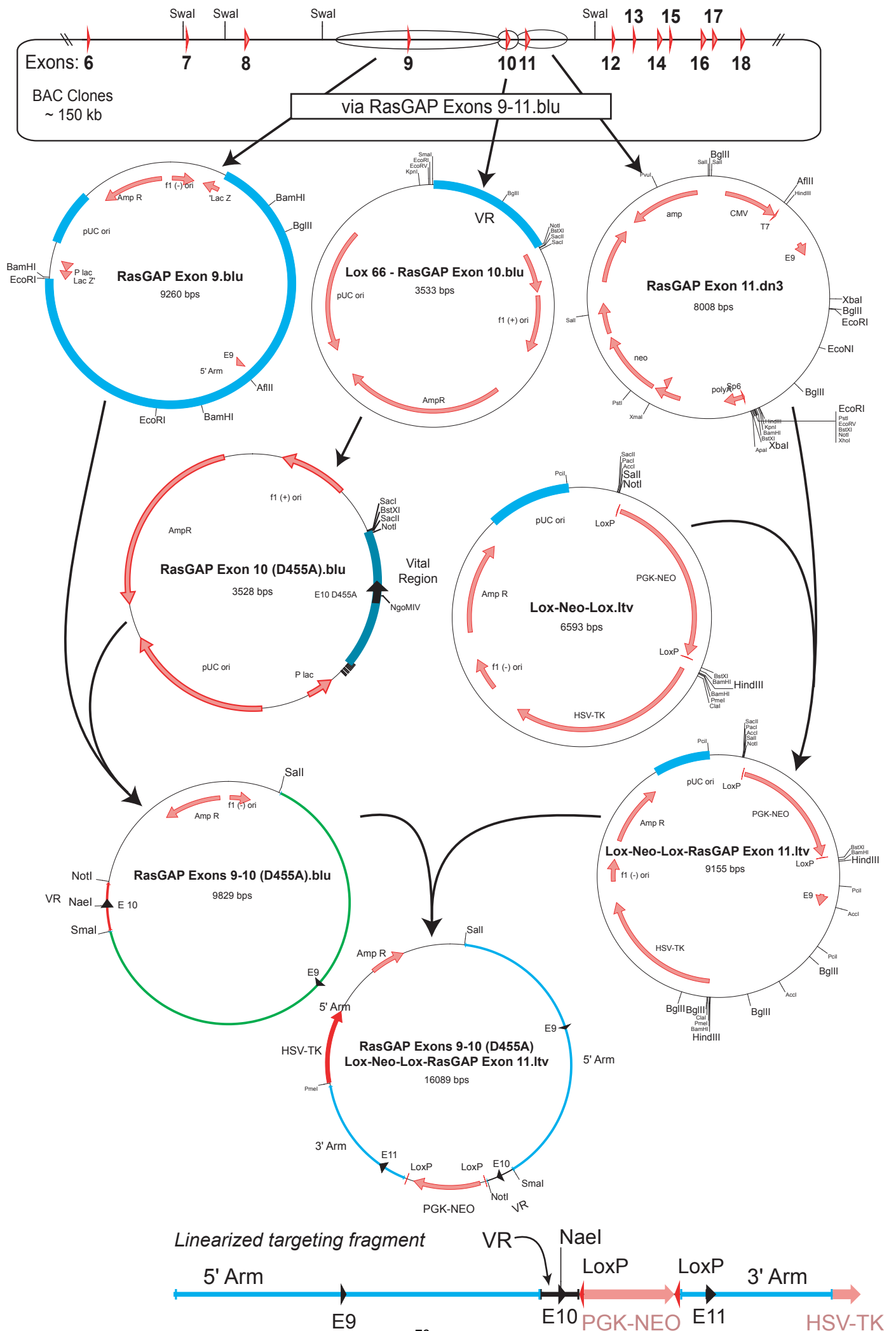
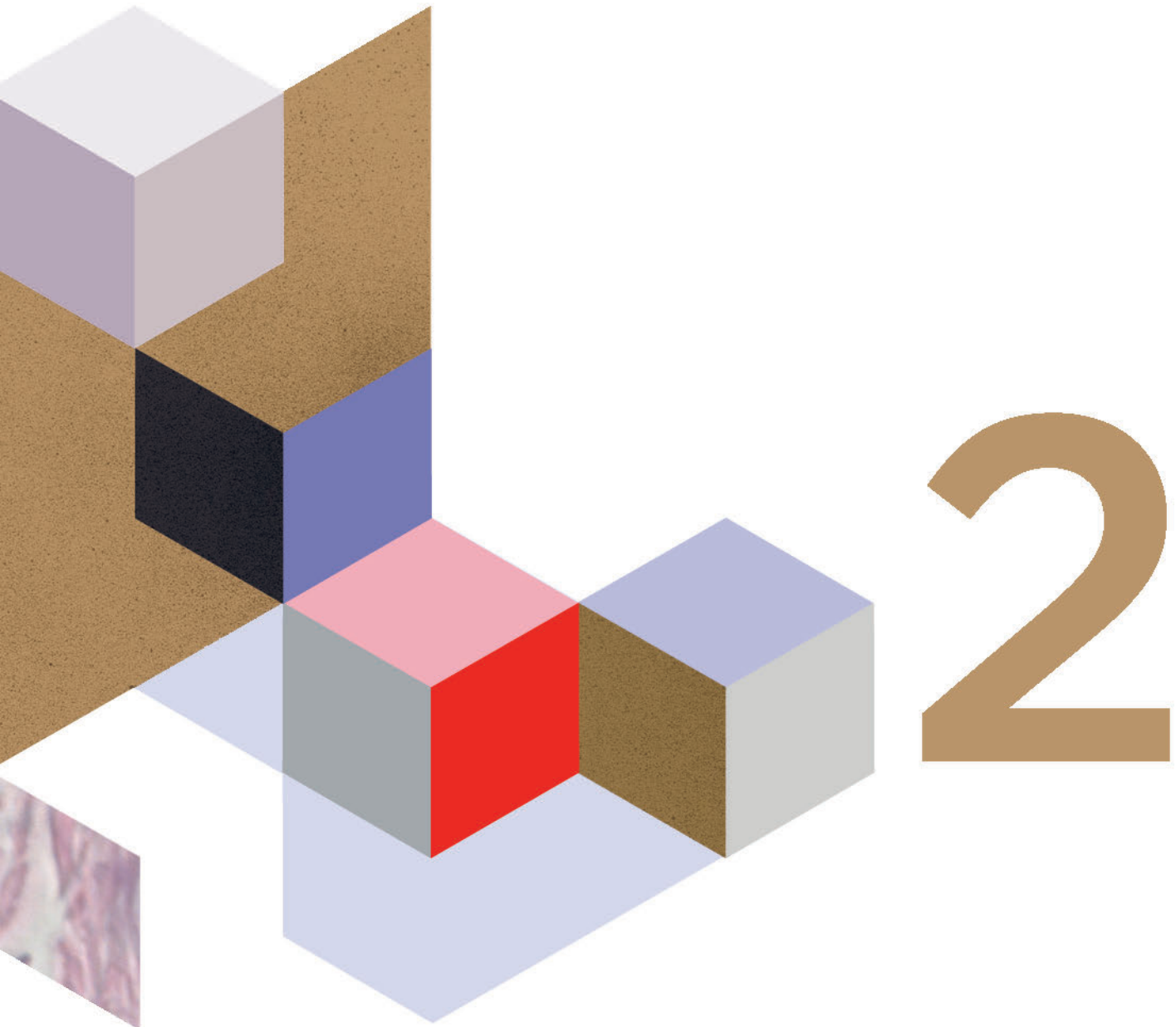


Figure S1

RESULTS

PART 2



INTRODUCTION

UV-B induces cytoplasmic survivin in mouse epidermis

Survivin is an odd member of the “inhibitor of apoptosis (IAP)” protein family. In contrast to the other proteins of this family, such as XIAP or cIAPs, survivin bears only one baculovirus inhibitor of apoptosis protein repeat (BIR) domain although no function as a direct caspase inhibitor. It neither has the really interesting new gene (RING) motif (Wheatley and McNeish, 2005) involved in ubiquitylation of target proteins implicated in proliferation and protection against cell death. Therefore, the effect of survivin in anti-apoptotic responses is highly debated (Banks et al., 2000; Yue et al., 2008; Earnshaw, 2005).

Besides its function as an inhibitor of apoptosis, survivin but not the other members of the family, is a chromosomal passenger that ensures proper chromosome segregation (Vong et al., 2005) and that might protect dividing cells from undergoing apoptosis (Li et al., 1998). One reason that hampers deciphering the apoptosis modulator function of survivin is the involvement of the protein in proper cell division. Indeed, inhibition or absence of survivin has profound detrimental effect on cells by altering mitosis and cytokinesis that ultimately affects cell survival and embryo development (Uren et al., 2000; Speliotes et al., 2000). Nevertheless, there is a consensus that, if survivin does have anti-apoptotic functions, this results from its expression in the cytoplasm or its association to the mitochondria (Connell et al., 2008; Fortugno et al., 2002; Dohi et al., 2004a). For example, the capacity of survivin to protect cells has been attributed to its binding to and stabilization of the anti-apoptotic XIAP protein, to inhibition of caspase-9 via cooperation with HBXIP, and to binding to and inhibition of the pro-apoptotic Smac/Diablo protein (Dohi et al., 2004b; Marusawa et al., 2003; Ceballos-Cancino, 2007). In any case, preventing survivin translocation from the nucleus to the cytoplasm, while not affecting cell division, renders cells more sensitive to irradiation-induced apoptosis (Colnaghi et al., 2006). Therefore, the location of survivin in the cytoplasm seems to be an important factor for its anti-apoptotic function.

Survivin has been reported to be induced in response to UV-B light in mouse skin (Aziz et al., 2004) however a detailed characterization of survivin expression in the various layers of the epidermis and assessment of a potential association of keratinocyte survivin expression *in situ* and cell survival in response to UV-B exposure have not yet been provided. The aim of the present study was thus to define the mode of survivin expression in the skin in response to UV-B and whether there was an association between survivin expression and apoptosis

CONTRIBUTION

This work has been accepted for publication in the Journal of Dermatological Science on June 2012 as is currently on-line. I performed all the experiments and revisions required for the realization of this work and contributed with the writing of the manuscript together with Prof. Widmann.

Reference List

- Aziz, M.H., Ghotra, A.S., Shukla, Y., and Ahmad, N. (2004). Ultraviolet-B Radiation Causes an Upregulation of Survivin in Human Keratinocytes and Mouse Skin. *Photochemistry and Photobiology*, *80*, 602-608.
- Banks, D.P., Plescia, J., Altieri, D.C., Chen, J., Rosenberg, S.H., Zhang, H., and Ng, S.C. (2000). Survivin does not inhibit caspase-3 activity. *Blood* *96*, 4002-4003.
- Ceballos-Cancino, M.E.V.M.a.J.M.-Z. (2007). Regulation of mitochondrial Smac/DIABLO-selective release by survivin. *Oncogene* *26*, 7569-7575.
- Colnaghi, R., Connell, C.M., Barrett, R.M.A., and Wheatley, S.P. (2006). Separating the Anti-apoptotic and Mitotic Roles of Survivin. *J. Biol. Chem.* *281*, 33450-33456.
- Connell, C.M., Colnaghi, R., and Wheatley, S.P. (2008). Nuclear Survivin Has Reduced Stability and Is Not Cytoprotective. *J. Biol. Chem.* *283*, 3289-3296.
- Dohi, T., Beltrami, E., Wall, N.R., Plescia, J., and Altieri, D.C. (2004a). Mitochondrial survivin inhibits apoptosis and promotes tumorigenesis. *Journal of clinical investigation* *114*, 1117-1127.
- Dohi, T., Okada, K., Xia, F., Wilford, C.E., Samuel, T., Welsh, K., Marusawa, H., Zou, H., Armstrong, R., Matsuzawa, S.i., Salvesen, G.S., Reed, J.C., and Altieri, D.C. (2004b). An IAP-IAP Complex Inhibits Apoptosis. *J. Biol. Chem.* *279*, 34087-34090.
- Earnshaw, W.C. (2005). Keeping Survivin Nimble at Centromeres in Mitosis. *Science* *310*, 1443-1444.
- Fortugno, P., Wall, N.R., Giodini, A., O'Connor, D.S., Plescia, J., Padgett, K.M., Tognin, S., Marchisio, P.C., and Altieri, D.C. (2002). Survivin exists in immunochemically distinct subcellular pools and is involved in spindle microtubule function. *J Cell Sci* *115*, 575-585.
- Li, F., Ambrosini, G., Chu, E.Y., Plescia, J., Tognin, S., Marchisio, P.C., and Altieri, D. (1998). Control of apoptosis and mitotic spindle checkpoint by survivin. *Nature* *396*, 580-583.
- Marusawa, H., Matsuzawa, S., Welsh, K., Zou, H., Armstrong, R., Tamm, I., and Reed, J.C. (2003). HBXIP functions as a cofactor of survivin in apoptosis suppression. *The EMBO Journal* *22*, 2729-2740.
- Speliotes, E.K., Uren, A., Vaux, D., and Horvitz, H.R. (2000). The survivin-like *C. elegans* BIR-1 protein acts with the Aurora-like kinase AIR-2 to affect chromosomes and the spindle midzone. *Mol Cell* *6*, 211-223.
- Uren, A.G., Wong, L., Pakusch, M., Fowler, K.J., Burrows, F.J., Vaux, D.L., and Choo, K.H.A. (2000). Survivin and the inner centromere protein INCENP show similar cell-cycle localization and gene knockout phenotype. *Current Biology* *10*, 1319-1328.

Vong,Q.P., Cao,K., Li,H.Y., Iglesias,P.A., and Zheng,Y. (2005). Chromosome Alignment and Segregation Regulated by Ubiquitination of Survivin. *Science* 310, 1499-1504.

Wheatley,S.P. and McNeish,I.A. (2005). Survivin: a protein with dual roles in mitosis and apoptosis. *International review of cytology* 35-88.

Yue,Z., Carvalho,A., Xu,Z., Yuan,X., Cardinale,S., Ribeiro,S., Lai,F., Ogawa,H., Gudmundsdottir,E., Gassmann,R., Morrison,C.G., Ruchaud,S., and Earnshaw,W.C. (2008). Deconstructing Survivin: Comprehensive Genetic Analysis of Survivin Function by Conditional Knockout in a Vertebrate Cell Line. *The Journal of Cell Biology* 183, 279-296.



Contents lists available at [SciVerse ScienceDirect](http://www.sciencedirect.com)

Journal of Dermatological Science

journal homepage: www.elsevier.com/jds



Letter to the Editor

UV-B induces cytoplasmic survivin expression in mouse epidermis

Letter to the Editor

Excessive exposure to ultra-violet (UV) light, the UV-B component (290–230 nm) in particular, represents the most harmful DNA damage-inducing condition that keratinocytes have to face on a regular basis. UV-B exposure induces survivin expression in keratinocytes *in vitro* [1] and *in vivo* [2]. Survivin (BIRC5) is a member of the “inhibitor of apoptosis (IAP)” protein family that can directly or indirectly inhibit caspases, the proteases that mediate apoptosis. Unlike the other members of the family, survivin is also a chromosomal passenger that ensures proper chromosome segregation during cell mitosis. Survivin is often considered as a marker of malignancy, being virtually undetectable in most normal cells and over-expressed in cancer cells [3]. *In vitro* studies indicate that upon stress, survivin may translocate to the cytoplasm [4]. The proposed anti-apoptotic mechanisms allowing survivin to protect cells rely on a cytoplasmic location of the protein where it can either inhibit pro-apoptotic proteins or stabilize anti-apoptotic proteins. However, the implication of survivin in anti-apoptotic responses is highly debated [5]. Nevertheless, there is a consensus that, if survivin does have anti-apoptotic functions, this results from its expression in the cytoplasm or its association to the mitochondria [6]. Indeed, preventing survivin translocation from the nucleus to the cytoplasm, while not affecting cell division, renders cells more sensitive to irradiation-induced apoptosis [7]. However, no publication yet has reported the presence of survivin in the cytoplasm of stressed or damaged cells *in vivo* in non-pathological conditions and hence the physiological role of cytoplasmic survivin is still unclear. The aim of the present study was to define the mode of survivin expression in mouse skin in response to UV-B exposure and determine whether there is an association between survivin expression and apoptosis.

Only a low percentage (about 2–3%) of keratinocytes and follicle cells in non-exposed skin expressed survivin (Fig. 1A, left panel; quantitation shown in Fig. 1C and D; [Supplementary Material](#) including detailed experimental procedures is available online). The majority of these cells displayed a nuclear survivin expression (filled arrowheads in Fig. 1A and B, upper panels; quantitation shown in Fig. 1C and D). The percentage of survivin-positive cells increased in a statistically significant manner starting 24 h post-UV-B irradiation in the epidermis (Fig. 1B; quantitation shown in Fig. 1C) and 48 h post-UV-B irradiation in follicles (Fig. 1D). Virtually no cells in the dermis were found to express survivin, whether the skin was exposed to UV-B or not (Fig. 1A). Upon UV-B

exposure, the location of survivin was mostly nuclear in follicle cells (Fig. 1A, filled arrowhead in right panel), while it was mostly cytoplasmic in keratinocytes (Fig. 1A, open arrowhead in right panel; Fig. 1B, lower panel). Expression of cytoplasmic survivin in follicle cells and nuclear survivin in keratinocytes was not affected by UV-B irradiation (Fig. 1C and D).

To assess which layers of UV-B-exposed epidermis express survivin, co-immuno-staining of survivin with either keratin 5 (a basal cell layer marker) or keratin 10 (a supra-basal layer marker) was performed. Nuclear survivin was exclusively found in the basal cell layer of the epidermis (Fig. 1E). Similarly, cytoplasmic survivin was expressed in keratinocytes of the basal layer of the epidermis, and to a limited extent, in keratinocytes of the supra-basal layer (Fig. 1E). There is evidence that cytoplasmic survivin is present in a few cells of the basal cell layer in normal human epidermis [8]. However, in the present study using mouse epidermis, we did not observe such a cytoplasmic staining for survivin in normal non-exposed conditions. Our results indicate that induction of cytoplasmic survivin upon UV-B irradiation mainly occurs in the proliferative layers of the epidermis, at least in mice.

To assess if there was a correlation between survivin expression in keratinocytes and apoptosis, skin sections of UV-B-irradiated mice were stained with an anti-survivin antibody and labeled with TUNEL to detect apoptotic cells (Fig. 2A). UV-B irradiation increased by about 10 fold the percentage of apoptotic cells (Fig. 2B). Upon UV-B-treatment, about 10% of the keratinocytes expressed survivin in their cytoplasm and about the same percentage of keratinocytes were undergoing apoptosis (Fig. 2C). However, there was limited co-localization of the survivin and TUNEL signals. Indeed, only about 20% of the cytoplasmic survivin-positive cells were apoptotic and conversely, only about 20% of the TUNEL-positive cells expressed cytoplasmic survivin (Fig. 2D). Therefore, the majority of cytoplasmic survivin-positive cells were not undergoing apoptosis, in agreement with data obtained in catagen-phase human hair follicles [9], indicating that translocation of survivin to the cytoplasm is not a consequence of cell death. Rather, UV-B-induced cytoplasmic survivin expression may exert anti-apoptotic functions. On the other hand, the percentage of apoptotic cells within the cytoplasmic survivin-positive keratinocyte population was not decreased (it was in fact higher) compared to survivin-negative keratinocytes (~20% vs ~10%). Possibly, survivin positive keratinocytes are the cells that experienced the highest damage in response to UV-B irradiation and cytoplasmic expression of survivin might represent an attempt to cope with this damage. Further studies would need to be conducted to test this assumption.

In conclusion, this work demonstrates that UV-B irradiation leads to the expression of survivin in the cytoplasmic compartment of keratinocytes located in the basal layer of the mouse epidermis. Earlier work had shown that UV-B can induce

* This work was supported by Swiss National Science Foundation grant 31003A_119876 (to CW).

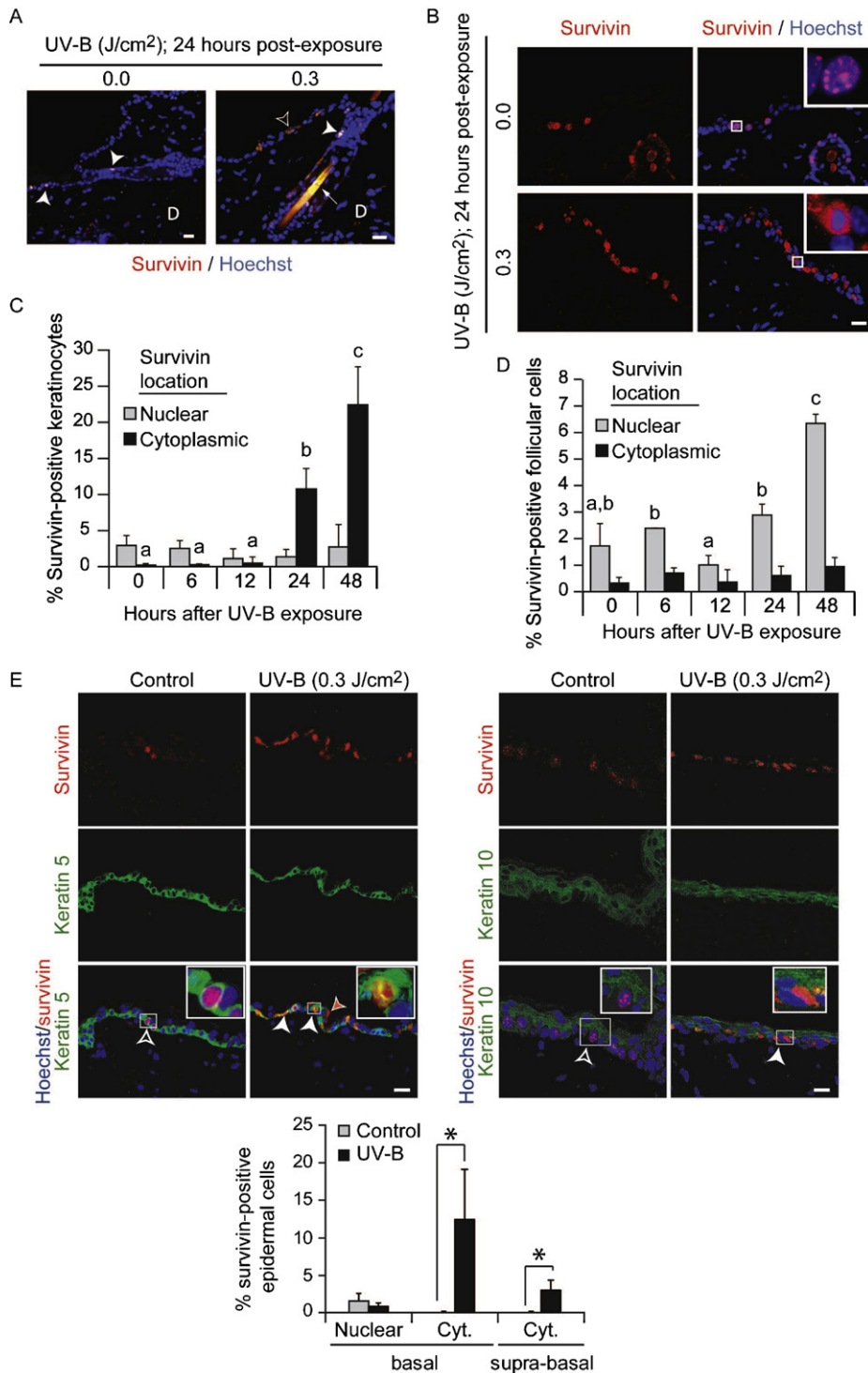


Fig. 1. UV-B induces expression of survivin in the cytoplasm of basal epidermal cells. (A) Representative images of control mouse skins (0.0 J/cm²) and mouse skins 24 h post UV-B (0.3 J/cm²) irradiation. The expression of survivin was visualized by immuno-fluorescence (red staining). Nuclei were stained in blue with the Hoechst 33342 dye. Filled arrowheads, nuclear survivin; open arrowhead, cytoplasmic survivin; D, dermis; arrow, non-specific staining of a hair shaft. (B) Representative images of nuclear versus cytoplasmic survivin expression in epidermal cells 24 h after exposure with the indicated UV-B doses. Insets show enlarged sections with the upper one depicting a cell with nuclear survivin and the lower one depicting a cell with cytoplasmic survivin. (C) Skins of mice were treated as in panel A for the indicated time periods following UV-B (0.3 J/cm²) irradiation. The percentage of epidermal cells expressing survivin in the nucleus or in the cytoplasm was then quantitated. Results correspond to the mean \pm 95% confidence interval (CI) of 3 mice (6, 12, and 48 h-time points) and 8 mice (0 and 24 h-time points). The percentage of keratinocytes expressing cytoplasmic survivin increased significantly over time (conditions with different letters are statistically different), while the percentage of keratinocytes expressing nuclear survivin did not. (D) Alternatively, the percentage of follicle cells expressing survivin in the nucleus or in the cytoplasm was quantitated and analyzed as in panel C. Results correspond to the mean \pm 95% CI of 3 mice (the percentages of follicle cells expressing cytoplasmic survivin did not statistically differ over time after UV-B exposure). (E) Mouse skin were exposed or not to UV-B (0.3 J/cm²) and isolated 24 h later. Survivin (red staining), nuclei (blue staining), keratin 5 (green staining, left panel) and keratin 10 (green staining, right panel) were visualized on skin sections by immunofluorescence. Insets represent enlargement of the indicated areas. Open arrowheads, nuclear survivin; white-filled arrowheads, cytoplasmic survivin in basal layer keratinocytes; orange-filled arrowheads, cytoplasmic survivin in supra-basal layer keratinocytes. The graph represents the quantitation of cells expressing nuclear or cytoplasmic (Cyt.) survivin in the basal and supra-basal layers. The results correspond to the mean \pm 95% CI of 4 mice. Scale bar for all images: 20 μ m.

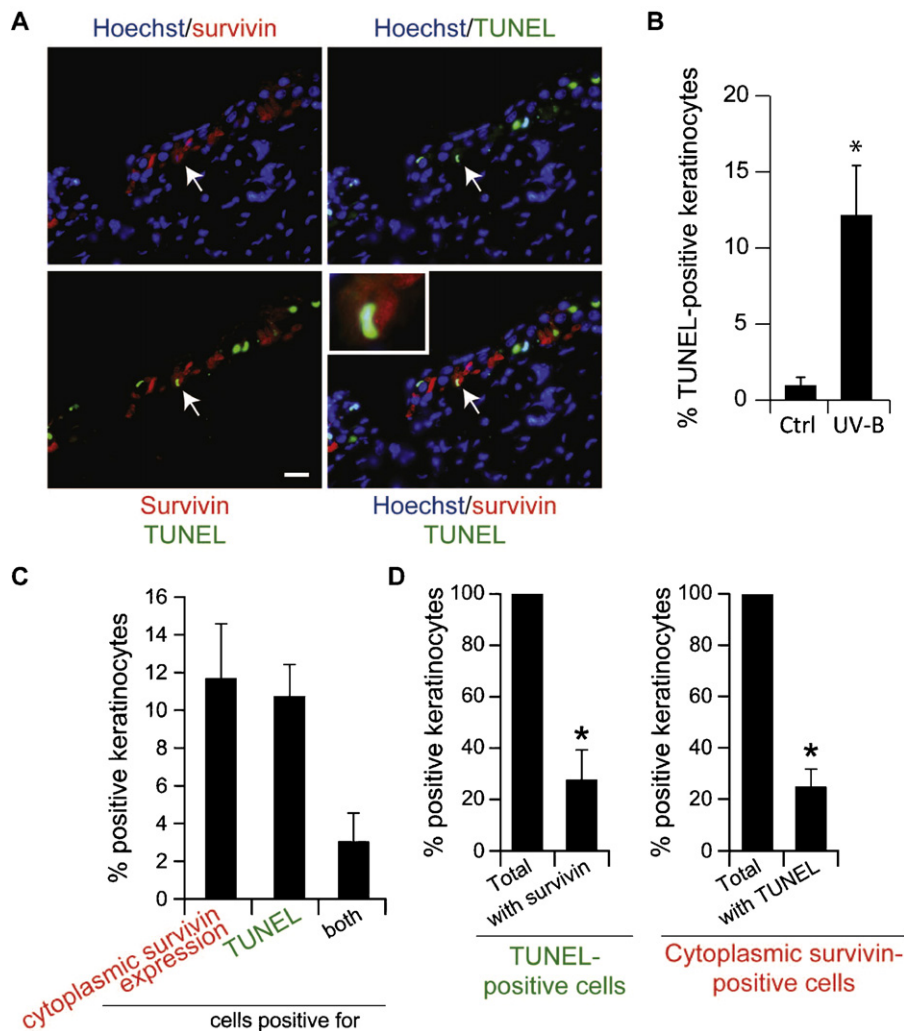


Fig. 2. TUNEL and survivin labeling of UV-B-exposed mouse skin. Mice were treated as in Fig. 1A. (A) Skin sections were labeled with an anti-survivin antibody (red staining), with TUNEL (green staining), and with Hoechst 33342 (blue staining). An example of an apoptotic cell expressing cytoplasmic survivin is indicated with an arrow and enlarged in the inset. Scale bar: 20 μ m. (B) Quantitation of apoptotic keratinocytes 24 h following UV-B (0.3 J/cm²) exposure or not. The results correspond to the mean \pm 95% CI of 7 mice. (C) Quantitation of cells expressing cytoplasmic survivin or positive for TUNEL labeling. (D) The graph on the left hand side only considers TUNEL-positive cells and whether these cells express or not survivin. The right-hand side graph only considers cytoplasmic survivin-positive cells and whether they are apoptotic or not. The results correspond to the mean \pm 95% CI of 4 mice. *statistically different.

survivin expression in mouse skin [10] but in which subcellular compartment this occurred had not been investigated. Data shown here provide the first demonstration that survivin can be induced in the cytoplasm of non-cancer cells in conditions where survivin may exert anti-apoptotic functions (*i.e.* when cells are stressed or damaged). Since cytoplasmic survivin has been shown to counteract apoptosis, this is expected to induce a protective signal in UV-B-exposed keratinocytes. However, no evidence for increased resistance to apoptosis in cytoplasmic survivin expressing keratinocytes could be demonstrated and the exact role played by survivin in the cytoplasm of keratinocytes remains to be defined.

Appendix A. Supplementary data

Supplementary data associated with this article can be found, in the online version, at <http://dx.doi.org/10.1016/j.jdermsci.2012.05.007>.

References

- [1] Dallaglio K, Palazzo E, Marconi A, Dumas M, Truzzi F, Lotti R, et al. Endogenous survivin modulates survival and proliferation in UVB-treated human keratinocytes. *Exp Dermatol* 2009;18:464-71.
- [2] Aziz MH, Ghotra AS, Shukla Y, Ahmad N. Ultraviolet-B radiation causes an upregulation of survivin in human keratinocytes and mouse skin. *Photochem Photobiol* 2004;80:602-8.
- [3] Wheatley SP, McNeish IA. Survivin: a protein with dual roles in mitosis and apoptosis. *Int Rev Cytol* 2005;247:35-88.
- [4] Asumen MG, Ifeacho TV, Cockerham L, Pfandl C, Wall NR. Dynamic changes to survivin subcellular localization are initiated by DNA damage. *Oncol Targets Ther* 2010;3:129-37.
- [5] Yue Z, Carvalho A, Xu Z, Yuan X, Cardinale S, Ribeiro S, et al. Deconstructing survivin: comprehensive genetic analysis of survivin function by conditional knockout in a vertebrate cell line. *J Cell Biol* 2008;183:279-96.
- [6] Connell CM, Colnaghi R, Wheatley SP. Nuclear survivin has reduced stability and is not cytoprotective. *J Biol Chem* 2008;283:3289-96.
- [7] Colnaghi R, Connell CM, Barrett RM, Wheatley SP. Separating the anti-apoptotic and mitotic roles of survivin. *J Biol Chem* 2006;281:33450-56.
- [8] Marconi A, Dallaglio K, Lotti R, Vaschieri C, Truzzi F, Fantini F, et al. Survivin identifies keratinocyte stem cells and is downregulated by anti- β 1 integrin during anoikis. *Stem Cells* 2007;25:149-55.
- [9] Botchkareva NV, Kahn M, Ahluwalia G, Shander D. Survivin in the human hair follicle. *J Invest Dermatol* 2007;127:479-82.

[10] Chun KS, Langenbach R. The prostaglandin E(2) receptor, EP2, regulates survivin expression via an EGFR/STAT3 pathway in UVB-exposed mouse skin. *Mol Carcinog* 2011;50:439-48.

*Corresponding author at: Department of Physiology, Rue du Bugnon 7, 1005 Lausanne, Switzerland. Tel.: +41 21 692 5123; fax: +41 21 692 5505
E-mail address: Christian.Widmann@unil.ch
(C. Widmann)

Nieves Peltzer^a, Paul Bigliardi^{b,1}, Christian Widmann^{a,*}
^aDepartment of Physiology, Biology and Medicine Faculty, University of Lausanne, Switzerland; ^bDepartment of Dermatology, Lausanne University Hospital, Lausanne, Switzerland

¹Current addresses: Institute of Medical Biology (IMB), A*STAR and National University of Singapore (NUS), UMC, Singapore.

30 January 2012

Supplementary material

Materials and methods

Mice

C57/BL6N,129SvEv mice were used in this study. Experiments on mice were carried out in strict accordance with the Swiss Animal Protection Ordinance (OPAn). The protocol was approved by the Veterinary office of the state of Vaud, Switzerland (Permit Number: 2055).

UV-B exposure and skin sample isolation

Anesthetized (100 mg/kg Ketarnorkon [Streuli; catalogue n° 0670940 and 20 mg/kg Rompum [Bayer; catalogue n° 01259402]) 8-week-old mice were shaved and then depilated with Veet depilatory cream on both flanks. Most mice at 8 weeks of age are in the resting phase of the hair cycle (telogen phase). The few mice that were not, as assessed by the presence of dark skin areas (Stenn and Paus, 2001), were not used. Forty-eight hours later, the mice were anaesthetized as described above and irradiated with a Waldmann UV801 KL apparatus equipped with a Philips UV21 UV-B lamp (TL 20W/12RS). The dose of UV-B irradiation was 0.3 J/cm², measured with a Waldmann Variocontrol dosimeter positioned at the same distance from the UV light as the exposed mouse skin. In these conditions, UV-A leakage of this lamp was 1 J/cm² [a dose that should have none or negligible biological effects (Zheng and Kligman, 1993)]. This UV lamp does not generate UV-C. In each case, only one side of the mouse was irradiated and the other side was used as a control (*i.e.* shaved and depilated but non-exposed skin). Mice were laid down on a sterile field with the flank to be irradiated (left flank) facing the lamp so that the control flank (right flank) was facing down and was thus non-exposed. Mice were sacrificed at the indicated times after irradiation. Lateral skin biopsies (approximately 2 x 2 cm) were excised from each mouse, fixed in PBS, 4% formol solution, and embedded in paraffin. The paraffin-embedded skin was cut into 4 µm sections.

Immunofluorescence

Paraffin sections were deparaffinized in two consecutive 5 minute long Xylene 100% baths and rehydrated by successive 2 minute long washes in ethanol 100%, 96%, 75% and 50%. Immunohistochemistry was performed as described (Bulat *et al.*, 2011). Primary antibodies were rabbit monoclonal anti-survivin (Cell Signaling;

catalogue n° 2808), and rabbit polyclonal anti-keratin 5 and anti-keratin 10 (Covance; catalogue n° PRB 159P and PRB 160P, respectively). The secondary antibodies were fluorescein isothiocyanate (FITC)-conjugated AffiniPure donkey anti-rabbit IgG and Cy3-conjugated AffiniPure Fab fragment goat anti-rabbit IgG (Jackson ImmunoResearch Europe; catalogue n° 711-094-152 and 711-165-152, respectively). The Alexa fluor 594 donkey anti-rabbit IgG antibody was from Invitrogen (catalogue n° A21207). All secondary antibodies were used at a 1/300 dilution. Double immuno-fluorescence labeling procedures (including those involving TUNEL staining) were done sequentially over a two-day period. The first day, survivin staining was performed using a primary antibody dilution of 1/300. The subsequent day, keratin staining (using a 1/300 antibody dilution) was performed. Alternatively, after an antigen retrieval step (Bulat *et al.*, 2011), TUNEL (see below) was done first, followed by an overnight wash and survivin staining. In all cases, nuclei were stained with Hoechst 33342 (Molecular Probes; catalogue n° H1399) for 10 minutes before mounting the slides in 0.1 g/ml Mowiol, 0.22% (v/v) glycerol, Tris 0.1 M pH 8.5, 0.1% diazobicyclo-octane. Mowiol was from Calbiochem (catalogue n°475904) and diazobicyclo-octane was from Fluka (catalogue n° 33480).

Apoptosis detection

Apoptosis was detected using the DeadEnd Fluorimetric TUNEL system (Promega; catalogue n° G3250) according to manufacturer's instructions.

Quantitation of fluorescent positive cells

Sections stained as described above were scanned using an automated Nikon Eclipse 90i microscope equipped with an Apo Plan 40x / 1.0 DIC-H objective and piloted with the NIS-Elements Advance Research software (Nikon Instruments Inc. Melville, USA; version 3.10). In order to minimize errors, all images were acquired with the same contrast (high), size and quality (1280 x 960), exposure time (40 ms for Hoechst detection, 50 ms for MK5 detection and TUNEL; 400 ms for MK10 and survivin detection, and 1 s for Alexa fluor detection), and gain (1x for Hoechst detection and 2.8x for the rest). Quantification threshold in the "Automated Measurement" menu was set as "L32" for Low and "H236" for high, and the area was restricted to "0-0.5 μm^2 out ". Using the "Binary" menu, the holes were filled using the

“Fill Holes” option. This was performed to avoid multiple counting of the same nucleus. Touching nuclei were separated using the “Morpho Separate Objects” option. The number of nuclei was displayed under “Automated Measurement Results – Object Data” and the TUNEL- or survivin-positive cells were counted with the “Taxonomy tool”.

Statistics

The data were analyzed using one-way ANOVA (Figure 1C-D) or student t tests with Bonferonni corrections (Figure 1E and Figure 2).

Reference List

- 1 Bulat N, Jaccard E, Peltzer N, Khalil H, Yang JY, Dubuis G, Widmann C: RasGAP-derived fragment N increases the resistance of beta cells towards apoptosis in NOD mice and delays the progression from mild to overt diabetes. PLoS ONE 6:e22609 (2011).
- 2 Stenn KS, Paus R: Controls of hair follicle cycling. Physiol Rev 81:449-494 (2001).
- 3 Zheng P, Kligman LH: UVA-induced ultrastructural changes in hairless mouse skin: a comparison to UVB-induced damage. J Invest Dermatol 100:194-199 (1993).

RESULTS
PART 3



3

INTRODUCTION

Survivin regulation

Survivin is a protein with a dual role in apoptosis and cell division. Its expression and function is hence highly regulated at different levels including transcription, splicing, translation, degradation and intracellular sequestration.

The survivin promoter is conserved between human and mouse. It is a TATA less promoter and contains multiple specificity protein-1 (sp1) - binding sites, two of which are essential for its basal level of transcription. Three cycle-dependent-elements (CDEs) and a cell cycle homology region (CHR) are found within the survivin promoter indicating that it is a protein regulated in a cell cycle dependent manner. The survivin gene is repressed by p53 (Hoffman et al., 2002) and RB and it is activated by the transcription factor E2F1 (Jiang et al., 2004), three proteins known to regulate cell fate either by negatively regulating cell division (p53 and RB) or activating it (E2F1). Additionally transcription of survivin is positively regulated by NF κ B, which is in turn activated by growth factors via Akt-induced activation of IKK α and β (Ozes et al., 1999; Romashkova and Makarov, 1999; Van Antwerp et al., 1998). Other factors known to induce survivin transcription are members of the Ras oncogene family (Sommer et al., 2003), STAT (Gritsko et al., 2006), the anti-apoptotic factor Wnt-2 and the hypoxia-inducible factor-1 alpha (HIF-1 α) (Peng et al., 2006; Chen et al., 2009). Finally, mTOR positively regulates survivin expression via rapid changes in mRNA translation (Vaira et al., 2006).

Post-translational regulation of survivin mainly involves phosphorylation and ubiquitylation. Survivin is phosphorylated by cyclin dependent kinase 1 (CDK1) at Threonine 48 (Yang et al., 2005) at the beginning of the M phase. Although CDK-1 is a kinase that regulates the cell cycle, in the case of survivin it is also believed to regulate cyto-protection since it may mediate survivin interaction with caspase-9 (O'Connor et al., 2000). This phosphorylation site stabilizes survivin against proteasome degradation and increases the binding efficiency with several partners such as Heat shock protein 90 (Hsp90) (Fortugno et al., 2003) and aryl hydrocarbon

receptor-interacting protein (AIP) (Kang and Altieri, 2006). These proteins bind survivin in the cytosol and are important for its cyto-protective function. Aurora B phosphorylates survivin at Threonine 117 and although there is no clear evidence of the role of this phosphorylation site it is most probably involved in cell division rather than in cyto-protection, since Aurora B, together with survivin and others, is responsible for proper completion of mitosis. More recently a novel phosphorylation site was reported at Serine 20 of survivin by Plk1 (Polo-like kinase 1) (Colnaghi and Wheatley, 2010) that is involved in the proper completion of mitosis.

Survivin is ubiquitylated in two different manners. K48 ubiquitylation of survivin by other IAPs targets its proteasomal degradation. K63 ubiquitylation on the contrary, is required for survivin centromere targeting and chromosome alignment (Vong et al., 2005).

Survivin localization within the cell is highly controlled and it is probably the cytoplasmic or even mitochondrial fraction of survivin that dictates the cyto-protective role of this peculiar IAP member (more detailed information on this matter is found in the general introduction).

In the context of our study, it has been reported that the PI3K/Akt signalling pathway is implicated in the upregulation of survivin in vascular endothelial cells and also in tumor cells (Altieri, 2003; Zhao et al., 2010; Papapetropoulos, 2000). These findings together with the results described previously in this work, in which fragment N-dependent Akt activation and cytoplasmic survivin induction were observed in the skin in response to UV-B light, lead us to focus on survivin as a putative Akt downstream target mediating fragment N induced protection. To elucidate the effect of fragment N on survivin, several levels of survivin regulation in the presence of over-expressed fragment N were studied as well as its involvement in fragment N mediated protection.

CONTRIBUTION

This work has been sent to Plos One and is currently under revision. Supplementary information contains other experiments performed in this work concerning survivin regulation although we do not think they are relevant for publication. I performed the experiments concerning survivin and wrote the manuscript with the help of Christian Widmann.

Reference List

- Altieri,D.C. (2003). Survivin, versatile modulation of cell division and apoptosis in cancer. *Oncogene* 22, 8581-8589.
- Chen,Y.Q., Zhao,C.L., and Li,W. (2009). Effect of hypoxia-inducible factor-1alpha on transcription of survivin in non-small cell lung cancer. *Journal of Experimental & Clinical Cancer Research* 28, 29.
- Colnaghi,R. and Wheatley,S.P. (2010). Liaisons between Survivin and Plk1 during Cell Division and Cell Death. *J. Biol. Chem.* 285, 22592-22604.
- Fortugno,P., Beltrami,E., Plescia,J., Fontana,J., Pradhan,D., Marchisio,P.C., Sessa,W.C., and Altieri,D.C. (2003). Regulation of survivin function by Hsp90. *Proceedings of the National Academy of Sciences of the United States of America* 100, 13791-13796.
- Gritsko,T., Williams,A., Turkson,J., Kaneko,S., Bowman,T., Huang,M., Nam,S., Eweis,I., Diaz,N., Sullivan,D., Yoder,S., Enkemann,S., Eschrich,S., Lee,J.H., Beam,C.A., Cheng,J., Minton,S., Muro-Cacho,C.A., and Jove,R. (2006). Persistent Activation of Stat3 Signaling Induces Survivin Gene Expression and Confers Resistance to Apoptosis in Human Breast Cancer Cells. *Clinical Cancer Research* 12, 11-19.
- Hoffman,W.H., Biade,S., Zilfou,J.T., Chen,J., and Murphy,M. (2002). Transcriptional Repression of the Anti-apoptoticsurvivin Gene by Wild Type p53. *J. Biol. Chem.* 277, 3247-3257.
- Jiang,Y., Saavedra,H.I., Holloway,M.P., Leone,G., and Altura,R.A. (2004). Aberrant Regulation of Survivin by the RB/E2F Family of Proteins. *J. Biol. Chem.* 279, 40511-40520.
- Kang,B.H. and Altieri,D.C. (2006). Regulation of Survivin Stability by the Aryl Hydrocarbon Receptor-interacting Protein. *J. Biol. Chem.* 281, 24721-24727.
- O'Connor,D., Grossman,D., Plescia,J., Li,F., Zhang,H., Villa,A., Tognin,S., Marchisio,P.C., and Altieri,D. (2000). Regulation of apoptosis at cell division by p34cdc2 phosphorylation of survivin. *Proc Natl Acad Sci USA.* 97, 13103-13107.
- Ozes,O.N., Mayo,L.D., Gustin,J.A., Pfeffer,S.R., Pfeffer,L.M., and Donner,D.B. (1999). NF-kappaB activation by tumour necrosis factor requires the Akt serine-threonine kinase. *Nature* 401, 82-85.
- Papapetropoulos,A., Fulton,D., Mahboubi,K., Kalb,R.G., O'Connor,D.S., Li,F., Altieri,D.C., and Sessa,W.C. (2000a). Angiopoietin-1 inhibits endothelial cell apoptosis via the Akt/survivin pathway. *J Biol Chem.* 275, 9102-9105.
- Peng,X.H., Karna,P., Cao,Z., Jiang,B.H., Zhou,M., and Yang,L. (2006). Cross-talk between Epidermal Growth Factor Receptor and Hypoxia-inducible Factor-1+ α Signal Pathways Increases Resistance to Apoptosis by Up-regulating Survivin Gene Expression. *J. Biol. Chem.* 281, 25903-25914.

- Romashkova, J.A. and Makarov, S.S. (1999). NF-kappaB is a target of AKT in anti-apoptotic PDGF signalling. *Nature* 401, 86-90.
- Sommer, K.W., Schamberger, C.J., Schmidt, G.E., Sasgary, S., and Cerni, C. (2003). Inhibitor of apoptosis protein (IAP) survivin is upregulated by oncogenic c-H-Ras. *Oncogene* 22, 4266-4280.
- Vaira, V., Lee, C.W., Goel, H.L., Bosari, S., Languino, L.R., and Altieri, D.C. (2006). Regulation of survivin expression by IGF-1/mTOR signaling. *Oncogene* 26, 2678-2684.
- Van Antwerp, D.J., Martin, S.J., Verma, I.M., and Green, D.R. (1998). Inhibition of TNF-induced apoptosis by NF-kappa B. *Trends Cell Biol* 8, 107-111.
- Vong, Q.P., Cao, K., Li, H.Y., Iglesias, P.A., and Zheng, Y. (2005). Chromosome Alignment and Segregation Regulated by Ubiquitination of Survivin. *Science* 310, 1499-1504.
- Yang, J.Y., Walicki, J., Michod, D., Dubuis, G., and Widmann, C. (2005). Impaired Akt Activity Down-Modulation, Caspase-3 Activation, and Apoptosis in Cells Expressing a Caspase-resistant Mutant of RasGAP at Position 157. *Mol. Biol. Cell* 16, 3511-3520.
- Zhao, P., Meng, Q., Liu, L.Z., You, Y.P., Liu, N., and Jiang, B.H. (2010). Regulation of survivin by PI3K/Akt/p70S6K1 pathway. *Biochemical and Biophysical Research Communications* 395, 219-224.

Role of mTOR, Bad, and survivin in RasGAP fragment N-mediated cell protection

Nieves Peltzer, Jiang-Yan Yang, and Christian Widmann

Department of Physiology, University of Lausanne, Switzerland

Short title: Effectors of fragment N-mediated protection

Correspondence to Christian Widmann, Department of Physiology, Bugnon 7, 1005 Lausanne, Switzerland, Phone: +41 21 692 5123, Fax: +41 21 692 5505, E-mail: Christian.Widmann@unil.ch.

Keywords: Survivin, apoptosis, RasGAP, caspases

Abstract

Partial cleavage of p120 RasGAP by caspase-3 in stressed cells generates an N-terminal fragment, called fragment N, which activates an anti-apoptotic Akt-dependent survival response. Akt regulates several effectors, but which of these mediate fragment N-dependent cell protection has not been defined yet. Here we have investigated the role of mTORC1, Bad, and survivin in the capacity of fragment N to protect cells from apoptosis. Rapamycin, an inhibitor of the mTORC1 complex, did not alter the ability of fragment N from inhibiting cisplatin-induced death. Cells lacking Bad, despite displaying a stronger resistance to apoptosis, were still protected by fragment N from cisplatin-induced death. Fragment N expression in cells did neither modulate survivin mRNA nor its protein expression. Additionally, the expression of cytoplasmic survivin, known to exert anti-apoptotic actions in cells, still occurred in UV-B-irradiated epidermis of mouse expressing a caspase-3-resistant RasGAP mutant that cannot produce fragment N. Additionally, survivin function in cell cycle progression was not affected by fragment N. These results indicate that, taken individually, mTOR, Bad, or Survivin are not required for fragment N to protect cells from cell death. We conclude that either other downstream targets of Akt mediate fragment N-induced protection or several Akt effectors can compensate for each other to induce the pro-survival fragment N-dependent response.

Introduction

Activation of executioner caspases was once believed to represent a point of no return in the path to death. However it is now well established that while executioner caspases are indispensable for apoptosis, there are situations when their activation does not lead to death. For example, healthy dividing cells can weakly activate caspase-3 in response to mild stresses [1]. Caspase-3 also participates, in an apoptosis-independent manner, in T and B cell homeostasis [2,3], in microglia activation [4], and in muscle [5], monocyte [6], bone marrow stromal stem cell [7], and erythroid cell differentiation [8].

Low caspase-3 activation in stressed cells induces the partial cleavage of RasGAP into an amino-terminal fragment, called fragment N, that prevents amplification of caspase-3 activation and death in an Akt-dependent manner [9]. Knock-in mice that only express a caspase-3-resistant RasGAP mutant, and therefore cannot generate fragment N in response to stress, are unable to stimulate Akt and are more sensitive to damage induced by various pathophysiological insults (submitted article). Fragment N generation can therefore explain why cells having mildly activated caspase-3 do not necessarily die. On the other hand, when caspase-3 activity is strongly stimulated in cells, fragment N is further processed into smaller fragments, called N1 and N2, that no longer have the capacity to activate Akt [10]. The extent of caspase-3 activity in a cell can therefore be sensed by RasGAP to either mount an efficient Akt-dependent protection when the stress is not too strong [1,11] or to abrogate this protective signal in cells faced with strong insults or apoptotic stimuli [10].

Although Akt can lead to activation of the NF- κ B transcription factor, fragment N-mediated Akt activation does not result in NF- κ B stimulation [12]. In fact, fragment N is able to block NF- κ B activation in response to various stimuli including exposure to inflammatory cytokines [13,14]. Hence fragment N does not rely on NF- κ B activation to protect cells despite that its activation is often promoting cell survival [15,16]. In some cell types, such as pancreatic beta cells, sustained NF- κ B activation leads to apoptosis [17]. In this context at least, the capacity of fragment N to block NF- κ B activation is beneficial and it has indeed been shown that it contributes to fragment N-induced, Akt-dependent anti-apoptotic activity in beta cells [14] [18]. These observations rule out activation of NF- κ B as an Akt-dependent mechanism used by

fragment N to protect cells. Which of the other Akt effectors are required for fragment N to protect cells is not known.

In the present work we investigated whether mTORC1, BAD and Survivin play a role in fragment N-mediated apoptosis inhibition. Mammalian TOR (mTOR) is a protein kinase that exists in two different complexes. The mTORC1 complex contains mTOR and Raptor and is inhibited by rapamycin. Akt indirectly activates mTORC1 by preventing the TSC1/TSC2 GTPase-activating proteins from inhibiting Rheb, the small GTP-binding protein that stimulates mTORC1. The mTORC2 complex contains mTOR and Rictor, is not sensitive to rapamycin, at least in short-term experiments [19], and positively regulates the activation of Akt by phosphorylating it rather than being an Akt effector itself [20,21]. The involvement of mTORC1 in cell survival responses makes it a possible candidate for fragment N mediated protection against apoptosis.

Another putative player in fragment N-induced protective pathway is Bad, a pro-apoptotic member of the Bcl-2 family [22,23]. When phosphorylated by Akt, Bad binds to 14-3-3 proteins and this prevents its capacity to interact with anti-apoptotic Bcl-2 family members. Consequently, phosphorylated Bad loses its pro-apoptotic activity [24].

Survivin (also called BIRC5), an atypical member of the inhibitor of apoptosis (IAP) family of proteins, is also a component of the chromosomal passenger protein complex that ensures proper segregation of sister chromatids and cytokinesis [25,26], and that mediates many other functions during mitosis [27]. The absence of survivin profoundly alters mitosis and cytokinesis and this eventually leads to cell death [25,28]. The exact contribution of survivin in anti-apoptotic responses is controversial and still not well defined. The evidence supporting a caspase-inhibitory function of survivin is consistent with the notion that survivin indirectly affects caspases either by binding and stabilizing XIAP [29], blocking Smac-dependent XIAP inhibition [19, 24, 30, 33] or inhibiting caspase-9 with cooperation with HBXIP [23]. Depending on the cell types and the experimental conditions, activation of Akt can lead to increased survivin expression [30,31].

In the present work, we have investigated whether mTORC1, Bad, and survivin play a role in fragment N-mediated apoptosis inhibition.

Materials and methods

Plasmids

pEGFP-C1 encodes the green fluorescent protein and is from Clontech. The .dn3, .Iti and .cmv extensions indicate that the backbone plasmid is pcDNA3 (Invitrogen, Carlsbad, CA), a lentiviral vector and pCMV5 (Promega), respectively. **HA-hRasGAP(D157A).dn3** encodes an amino-terminal HA (MGYPYDVPDYAS)-tagged human RasGAP mutant that cannot be cleaved by caspase-3 at position 157 (plasmid #125; previously called HA-D157A.dn3 [11]). **HA-hRasGAP[1-455](D157A).dn3** encodes a similarly tagged and caspase-3-resistant version of the 1-455 amino acid fragment of human RasGAP (fragment N) (plasmid #352; previously called N-D157A.dn3 in [11]). **HA-hRasGAP[1-455](D157A).Iti** is the plasmid used for the production of the lentivirus encoding the caspase-resistant form of fragment N (plasmid #353; previously called N-D157A.Iti in [1]). **GFP-HA-hRasGAP[1-157]** (plasmid #231) encodes a fusion protein between GFP and fragment N1 (amino acid 1-157 of human RasGAP). It was generated by subcloning the Apal/HindIII fragment of plasmid HA-hRasGAP[1-158].dn3 (plasmid #147; previously called HA-N1.dn3 in [11]) into pEGFP-C3 (Clontech) opened with the same enzymes. **GFP-HA-hRasGAP[157-455]** (plasmid #213; previously described as GFP-HA-N2 in [32]) encodes a fusion protein between GFP and fragment N2 (amino acid 158-455 of human RasGAP). **E2F1-SPORT6.1** (plasmid # 675) was purchased from Imagenes. Mouse survivin promoter plasmids were obtained by cloning the sequences corresponding to the entire sequence of survivin promoter ([-1296 to +13] or the minimal sequence required for its activation (-283 to +13) (called **mSurvivin promoter [-1296 to +13].gl3**, plasmid number gl3, plasmid number #634, and **mSurvivin promoter [-238 to +13].gl3**, plasmid #633, respectively). The extension .gl3 indicates that the backbone plasmid bears a promoter-less luciferase gene and it was purchased from Promega (name: pGL3 basic, plasmid #95). **pRL-TK** encodes for renilla luciferase and it was used as a efficiency control (plasmid #402).

Cell Culture and chemicals

The RasGAP^{+/+} mouse embryonic fibroblasts (MEFs; clone 12.78), the RasGAP^{-/-} MEFs (clone 12.64), and their derivatives stably expressing wild-type RasGAP or the caspase-resistant D455A mutant [10,33] were maintained in DMEM (Invitrogen

catalogue n°61965) containing 10% newborn calf serum (Invitrogen, catalogue n° 26010-074) at 37°C and 5% CO₂. BAD knock-out MEFs were cultured similarly. Mouse beta cells (Min-6) cells were maintained in modified DMEM complemented with 0.1 mM β-mercaptoethanol and 1 mM sodium pyruvate. HeLa cells were maintained in RPMI 1640 (Invitrogen catalogue n°61870) containing 10% newborn calf serum at 37°C and 5% CO₂. Cisplatin (catalogue n° P4394) and rapamycin (catalogue n° R0395) were purchased from Sigma.

Antibodies

The anti-p70-S6Kianse antibody, the anti-phospho Bad antibody simpler kit and the rabbit anti-survivin 71G4 monoclonal antibody were purchased from Cell Signaling Technology (catalogue n°9205, 9105 and 2808 respectively). Secondary antibodies used for Western blotting were Alexa Fluor 680–conjugated anti-rabbit antibody (Molecular Probes, Eugene, OR; catalogue n°A21109) or IRDye 800–conjugated anti-mouse antibody (Rockland, Gilbertsville, PA; catalogue n°610-132-121). For immunohistochemistry the secondary antibody was Cy3-conjugated AffiniPure Fab fragment goat anti-rabbit IgG (catalogue n°711-165-152) and was purchased from Jackson ImmunoResearch Laboratories.

Lentivirus

Recombinant lentiviruses were produced as described [34]. The minimal amounts of viruses inducing expression of the protein of interest in more than 95% of the cells (as assessed by immunofluorescence) were used.

Transfection and luciferase assay

HeLa cells were transfected with Lipofectamine 2000 (Invitrogen) as described earlier (Yang MCB 2001). Min-6 cells (3×10^5) were co-transfected using Lipofectamine with 0.5 ug of pGL3-survivin promoter – luc, 0.5 ug of a Renilla encoding plasmid and 1 ug of either pcDNA3 plasmid coding for fragment N or pCMV-Sport 6.1 plasmid coding for E2F1. pcDNA3 or SPORT6.1 empty vectors were used as negative controls. Cells were harvested 36 hours after transfection and luciferase activity was measured using Dual-Luciferase® Reporter Assay (Promega). Signals were detected with GLOMAX™ 96 Microplate Luminoteter (Promega) and analyzed with Glomax version 1.7.0 program. Results were normalized with *Renilla* luciferase activity.

RNA extraction and Reverse Transcription

RNA was extracted by lysing cells with 500 µl TRI buffer (1.7 M guanidium thiocyanate, 0.1 M sodium citrate, 0.25% *N*-lauryl-sarcosyl sodium, 0.05 M β-mercaptoethanol, 0.1 M sodium acetate), followed by the addition of 200 µl chloroform. The tubes were then vortexed, kept at room temperature for 5 min, and spun at maximal speed in an Eppendorf centrifuge for 15 min. After the transfer of the aqueous phase in a new tube, 500 µl isopropanol was added and the solution was mixed by inversion approximately five times. The samples were then incubated o/n at –20°C. After spinning 20 min at maximum speed in an Eppendorf centrifuge, the upper phase (isopropanol) was aspirated; the pellet was washed twice with 800 µl 70% ethanol and dried 5–10 min at 50°C. The pellet was finally resuspended in 50 µl of water and RNA was quantitated at 260 nm. Half a microgram of RNA was mixed with 500 ng of random hexamers (Microsynth, Balgach, Switzerland), and water was added to reach a final volume of 11 µl. The samples were incubated 3 min at 70°C and then kept on ice. A mix (14 µl) containing 5 µl of 10nM dinucleotide triphosphates (Promega catalogue number U120D-123D), 0.5 µl of RNasin (Promega catalogue number. N211A), 5 µl of buffer 5x, 2 µl dithiothreitol, 0.5 µl Superscript reverse transcriptase, and 1 µl water (the 5x buffer, the dithiothreitol and the transcriptase coming from the Superscript II reverse Transcriptase Kit; Invitrogen catalog no. 18064–014) was added to the RNA-hexamer mix. After incubation at 39°C for 1 h followed by 15 min at 70°C, the cDNA was diluted 1:3 in water.

Real Time PCR

Quantitative PCR assays were carried out on a real-time PCR detection system (iQ5; Bio-Rad) using iQ SYBR Green Supermix (Bio-Rad catalog no. 170-8862), with 500 nmol/liter primers, 1 µl of template per 20 µl of PCR, and an annealing temperature of 59°C. Melting curve analyses were performed on all PCR to rule out nonspecific amplification. Reactions were carried out in triplicate. The primers used in real-time PCR are: Fw 5'-GCGGAGGCTGGCTTCA-3' and reverse 5'-AGAAAAAACAACACTGGGCCAAATC-3'

Propidium iodide (PI) staining and flow cytometer analysis

HeLa (3×10^5) cells were seeded in 3.5 cm dishes and infected with either an empty virus or an HA-N encoding virus. 72 hours after infection, cells were synchronized in G1-S boundary with 400 μ M of mimosine for 18 hours. Cells were released from mimosine blockage by changing the medium, and harvested at different time points. Cells were washed twice with 1x PBS and fixed with ethanol 100% for 15 minutes at -20°C . After fixation cells were spun down at 2000 rpm at 4°C and washed once with 1x PBS. Cells were resuspended in 1 ml of PI staining buffer (100 mM Tris pH7, 150 mM NaCl, 1 mM CaCl_2 , 0.5 mM MgCl_2 , 0.1% NP-40, 20 μ g/ml RNase A, 1mg/ml propidium iodide diluted 1/500) and put into sorter tubes. After 15 minutes incubation at room temperature in the dark, the cells were ready for analysis. Cells were scanned in a Flow Cytometer Beckman Coulter FC500 with the following parameters: FSC 95 Volts-1 Gain, SSC 519 Volts-1Gain, FL3 lin 313 Volts-1 Gain. The population of cells to analyze was gated according to their size (FSC forward scatter) and granularity (SSC side scatter) to exclude dead cells and clumps. Within this cell population cells were gated according to the peak of intensity versus the integrated signals to exclude debris and doublets. The number of cells considered to be representative of the total cell population for DNA content analysis was 10.000 cells.

Western blot analysis

Cells were lysed in monoQ-c buffer [11] and protein quantification was performed by Bradford technique. Equal amounts of protein were migrated in a polyacrylamide gel and transferred onto a Trans-Blot nitrocellulose membrane (Bio-Rad reference n°10484060). Membranes were blocked with 0.5% non-fat milk and incubated for 1 hour at 4°C with specific primary antibodies. Blots were washed with TBS/Tween 0.1%, incubated with specific secondary antibodies and visualized with the Odyssey infrared imaging system (LICOR Biosciences, Bad Homburg, Germany). Quantification was performed using the Odyssey infrared imaging software.

Apoptosis measurements

Apoptosis in HeLa cells was determined by scoring the number of transfected cells (i.e. cells expressing GFP) displaying pycnotic or fragmented nucleus [32]. Apoptosis in infected MEFs was similarly assessed but in all cells.

Immunocytochemistry

HeLa cells were seeded in coverslips. 24 hours later coverslips were transferred to a clean dish and the immunocytochemistry was performed. Cells were fixed with 2% paraformaldehyde diluted in 1x PBS for 15 minutes at room temperature. After washing thrice with PBS cells were permeabilized with 0.2 % Triton X diluted in 1x PBS for 10 minutes at room temperature. After washing with PBS unspecific binding sites were blocked using DMEM culture medium complemented with 15% newborn calf serum. After 20 minutes at room temperature, primary antibody anti-HA (1/100) was added and incubated for 1 hour at room temperature in a dark and humid chamber. Secondary antibody was added after three washes in PBS for 1 hour at room temperature in a dark and humid chamber. After extensive washes in PBS nuclei were stained with Hoechst 33342 (Molecular Probes; catalogue n° H1399) for 10 minutes before mounting the slides in 0.1 g/ml Mowiol, 0.22% (v/v) glycerol, Tris 0.1 M pH 8.5, 0.1% diazobicyclo-octane. Mowiol was from Calbiochem (catalogue n°475904) and diazobicyclo-octane was from Fluka (catalogue n° 33480)

Mice and UV-B irradiation

C57 BL6/sv129 *wild type* (WT) and Ras^{D455A/D455A} *knock in* (KI) mice were described in [Khalil, Peltzer et al., 2012; MCB (accepted)] and were treated as described in [35].

Immunofluorescence in skin sections

Paraffin sections were deparaffinized in two consecutive 5 minute long Xylene 100% baths and rehydrated by successive 2 minute long washes in ethanol 100%, 96%, 75% and 50%. Immunohistochemistry was performed as described [21]. Nuclei were stained with Hoechst 33342 (Molecular Probes; catalogue n° H1399) for 10 minutes before mounting the slides in 0.1 g/ml Mowiol, 0.22% (v/v) glycerol, Tris 0.1 M pH 8.5, 0.1% diazobicyclo-octane. Mowiol was from Calbiochem (catalogue n°475904) and diazobicyclo-octane was from Fluka (catalogue n° 33480). Quantitation of fluorescent positive cells was performed as previously described [35].

Data presentation and statistics

Results are expressed as the mean \pm 95% confidence intervals (CI). The statistical tests used were one way ANOVAs unless otherwise stated. Normality of the data was verified with the Shapiro-Wilk test.

Results and discussion

To prevent cleavage of fragment N into the smaller N1 and N2 fragments, which can potentially generate confounding results, the experiments described below were performed with a form of fragment N that has its caspase-3 cleavage site destroyed [1,11].

mTOR does not mediate fragment N-induced protection

S6 kinase, an mTORC1 substrate, was phosphorylated in HeLa cells cultured in the presence of serum (Figure 1A, first lane). This phosphorylation was fully blocked by rapamycin (Figure 1A, second lane) indicating that mTORC1 is the sole kinase mediating S6K phosphorylation in serum-cultured HeLa cells. In starved conditions (Figure 1A, third lane), mTORC1 was no longer activated as indicated by the absence of S6K phosphorylation. As expected from its ability to stimulate Akt, fragment N activated mTORC1-dependent S6K phosphorylation (Figure 1A, last two lanes). However, the ability of fragment N to protect cells from cisplatin induced apoptosis was unaffected by rapamycin (Figure 1B), suggesting that mTORC1 activation is redundant or plays no role in fragment N-mediated protection.

Phosphorylation of Bad does not play a major role in fragment N-mediated protection

Bad is a pro-apoptotic protein that is blocked from triggering apoptosis by Akt-mediated phosphorylation on serine 136 [24]. Bad can be phosphorylated by other kinases, such as PKA, on serine 112 [36]. As expected from its ability to stimulate Akt, fragment N expressed in HeLa cells induced Bad phosphorylation on serine 136 but not on serine 112 (Figure 2A). Fragments N1 and N2, the fragment N cleavage products generated by high caspase-3 activity that are unable to stimulate Akt [10], did not induce Bad phosphorylation (Figure 2A).

The potential contribution of Bad in fragment N-mediated cell protection was assessed in MEFs derived from wild-type and Bad knock-out mice. Figure 2B displays the possible outcome of experiments using these cells expressing or not fragment N and stimulated with increasing concentrations of cisplatin. As Bad mediates part of the apoptotic response to cisplatin [37], reduced cisplatin-induced death is expected in Bad KO MEFs (orange lines). If Akt-induced Bad

phosphorylation does not play any role in the protection mediated by fragment N, the latter should decrease the extent of apoptosis to similar extent in wild-type and Bad KO MEFs (Figure 2B, left graph). In other words, the maximal percent decrease in apoptosis induced by fragment N should be similar in both MEF types as shown in the inset above the left graph in Figure 2B. In contrast, if Bad phosphorylation is the sole mechanisms by which fragment N protects cells, the sensitivity of Bad KO MEFs to cisplatin should be unaffected by the presence of fragment N (Figure 2B, right graph). In this case, for Bad KO cells, the difference between the apoptosis curves in the presence or in the absence of fragment N should be minimal (orange lines in the inset above the right graph in Figure 2B). The middle graphs in Figure 2B display a situation where Bad phosphorylation is partially contributing to fragment N-mediated cell protection. The actual experiment (Figure 2C) generated a pattern that corresponded to the scenario presented on the left of Figure 2B. Therefore, Bad phosphorylation plays no or only minimal role in fragment N-induced cell protection, or if it does contribute, then this can be fully compensated by other Akt effectors.

Fragment N does not regulate survivin

There is evidence that Akt can induce survivin expression [31,38,39]. As survivin may display anti-apoptotic activity in some conditions [29–31,40,41], it could be one of the main targets of fragment N that mediates its survival effects. We therefore assessed whether fragment N can regulate survivin by determining if it modulated its expression *in vitro* and *in vivo* and whether it affected survivin capacity to regulate cell division.

The effect of fragment N on survivin transcription was assessed by luciferase assay in which either the minimal or the entire sequence of the mouse survivin promoter were used. Fragment N expression in cells had no significant effect on either promoter activities (Figure 3A). As a positive control for this experiment, cells were transfected with an E2F1-expressing vector that is known to mediate survivin transcription [42] and this resulted, as expected, in an increase in survivin promoter activity (Figure 3A). To further confirm these results, real time PCR was performed to measure survivin mRNA in cells expressing or not fragment N. Figure 3B shows that fragment N did not induce an increase in the mRNA coding for survivin. Furthermore, survivin protein levels were not affected by fragment N (Figure 3C).

We have recently demonstrated that UV-B exposure of the epidermis leads to Akt phosphorylation in a caspase-3 and RasGAP cleavage-dependent manner (submitted article). Moreover it has also been shown that survivin expression and relocalization to the cytoplasm, where it is supposed to induce its anti-apoptotic response [43], is induced in mouse skin in response to UV-B light [35]. Given that fragment N induces Akt in the epidermis of UV-B-irradiated mice (submitted article) and that cytoplasmic survivin expression is augmented in this same tissue [35], we tested whether survivin expression in the skin is affected in knock-in (KI) mice that cannot generate fragment N because of a mutation in the first caspase-3 cleavage site of RasGAP. Control and KI mice were exposed to UV-B light 24 hours prior to biopsy and survivin levels were monitored in the skin by immunofluorescence. The percentage of keratinocytes expressing cytoplasmic survivin was increased by UV-B in a dose-dependent manner. This increase was similar in wild-type and KI mice (Figure 3D). This indicates that even though mice unable to generate fragment N are more sensitive to apoptosis (submitted article), they are still able to induce cytoplasmic survivin expression to levels that are observed in wild-type mice (Figure 3D). These results suggest that cytoplasmic-survivin is not involved in fragment N-mediated protection, at least in mouse skin. Of note, the percentage of keratinocytes expressing nuclear survivin was not affected by UV-B light (Figure 3D).

Survivin is a protein with an important role in mitosis, with a peak of expression at G2/M phase and is therefore highly regulated in a cell cycle dependent manner [42,44]. Even though fragment N does not appear to affect survivin levels, it may regulate its well-described function during mitosis. In order to study whether fragment N affects cell cycle, cells expressing or not fragment N were synchronized in G1 using a mimosine block and then released from this block to resume cell cycling. Figure 4 shows that ectopic expression of fragment N did not alter the cell cycle of HeLa cells. There is thus no evidence that fragment N regulates survivin *in vitro* or *in vivo*.

In conclusion, the results presented in this work did not point to a crucial role of a given Akt effector in fragment N-mediated cell protection. Fragment N-mediated protection was not affected by mTOR inhibition or in BAD KO cells. Furthermore, survivin expression was neither modulated by fragment N nor was its function impaired in cells unable to generate fragment N upon stress. Possibly, fragment N relies on several Akt downstream targets to mount an efficient cell survival response.

Alternatively, Akt effectors that we have not tested in the present work may fulfill most of the anti-apoptotic response induced by fragment N. Further studies need to be conducted to determine the exact contribution of Akt targets that mediate the capacity of fragment N to protect cells.

Acknowledgements

We thank the late Dr. Stanley Korsmeyer for the gift of the Bad knock-out MEFs. This work was supported by Swiss National Science Foundation grant 31003A_141242 / 1 (to CW).

Reference List

1. Yang J-Y, Michod D, Walicki J, Murphy BM, Kasibhatla S, Martin S, Widmann C (2004) Partial cleavage of RasGAP by caspases is required for cell survival in mild stress conditions. *Mol Cell Biol* 24: 10425-10436.
2. Newton K, Strasser A (2003) Caspases signal not only apoptosis but also antigen-induced activation in cells of the immune system. *Genes Dev* 17: 819-825.
3. Woo M, Hakem R, Furlonger C, Hakem A, Duncan GS, Sasaki T, Bouchard D, Lu L, Wu GE, Paige CJ, Mak TW (2003) Caspase-3 regulates cell cycle in B cells: a consequence of substrate specificity. *Nat Immunol* 4: 1016-1022.
4. Burguillos MA, Deierborg T, Kavanagh E, Persson A, Hajji N, Garcia-Quintanilla A, Cano J, Brundin P, Englund E, Venero JL, Joseph B (2011) Caspase signalling controls microglia activation and neurotoxicity. *Nature* 472: 319-324.
5. Fernando P, Kelly JF, Balazsi K, Slack RS, Megeney LA (2002) Caspase 3 activity is required for skeletal muscle differentiation. *Proc Natl Acad Sci USA* 99: 11025-11030.
6. Sordet O, Rebe C, Plenchette S, Zermati Y, Hermine O, Vainchenker W, Garrido C, Solary E, Dubrez-Daloz L (2002) Specific involvement of caspases in the differentiation of monocytes into macrophages. *Blood* 100: 4446-4453.
7. Miura M, Chen XD, Allen MR, Bi Y, Gronthos S, Seo BM, Lakhani S, Flavell RA, Feng XH, Robey PG, Young M, Shi S (2004) A crucial role of caspase-3 in osteogenic differentiation of bone marrow stromal stem cells. *J Clin Invest* 114: 1704-1713.
8. Droin N, Cathelin S, Jacquelin A, Guery L, Garrido C, Fontenay M, Hermine O, Solary E (2008) A role for caspases in the differentiation of erythroid cells and macrophages. *Biochimie* 90: 416-422.
9. Yang J-Y, Michod D, Walicki J, Widmann C (2004) Surviving the kiss of death. *Biochem Pharmacol* 68: 1027-1031.
10. Yang J-Y, Walicki J, Michod D, Dubuis G, Widmann C (2005) Impaired Akt activity down-modulation, caspase-3 activation, and apoptosis in cells expressing a caspase-resistant mutant of RasGAP at position 157. *Mol Biol Cell* 16: 3511-3520.
11. Yang J-Y, Widmann C (2001) Antiapoptotic signaling generated by caspase-induced cleavage of RasGAP. *Mol Cell Biol* 21: 5346-5358.
12. Yang J-Y, Widmann C (2002) The RasGAP N-terminal fragment generated by caspase cleavage protects cells in a Ras/PI3K/Akt-dependent manner that does not rely on NF- κ B activation. *J Biol Chem* 277: 14641-14646.
13. Yang JY, Walicki J, Jaccard E, Dubuis G, Bulat N, Hornung JP, Thorens B, Widmann C (2009) Expression of the NH₂-terminal fragment of RasGAP in pancreatic β -

cells increases their resistance to stresses and protects mice from diabetes. *Diabetes* 58: 2596-2606.

14. Bulat N, Jaccard E, Peltzer N, Khalil H, Yang JY, Dubuis G, Widmann C (2011) RasGAP-derived fragment N increases the resistance of beta cells towards apoptosis in NOD mice and delays the progression from mild to overt diabetes. *PLoS ONE* 6: e22609.
15. Beg AA, Baltimore D (1996) An essential role for NF- κ B in preventing TNF- α -induced cell death. *Science* 274: 782-784.
16. Romashkova JA, Makarov SS (1999) NF- κ B is a target of AKT in anti-apoptotic PDGF signalling. *Nature* 401: 86-90.
17. Eldor R, Yeffet A, Baum K, Doviner V, Amar D, Ben Neriah Y, Christofori G, Peled A, Carel JC, Boitard C, Klein T, Serup P, Eizirik DL, Melloul D (2006) Conditional and specific NF- κ B blockade protects pancreatic β cells from diabetogenic agents. *Proc Natl Acad Sci U S A* 103: 5072-5077.
18. Yang J-Y, Walicki J, Abderrahmani A, Cornu M, Waeber G, Thorens B, Widmann C (2005) Expression of an uncleavable N-terminal RasGAP fragment in insulin-secreting cells increases their resistance toward apoptotic stimuli without affecting their glucose-induced insulin secretion. *J Biol Chem* 280: 32835-32842.
19. Sarbassov DD, Ali SM, Sengupta S, Sheen JH, Hsu PP, Bagley AF, Markhard AL, Sabatini DM (2006) Prolonged rapamycin treatment inhibits mTORC2 assembly and Akt/PKB. *Mol Cell* 22: 159-168.
20. Hay N, Sonenberg N (2004) Upstream and downstream of mTOR. *Genes Dev* 18: 1926-1945.
21. Hay N (2005) The Akt-mTOR tango and its relevance to cancer. *Cancer Cell* 8: 179-183.
22. Youle RJ, Strasser A (2008) The BCL-2 protein family: opposing activities that mediate cell death. *Nat Rev Mol Cell Biol* 9: 47-59.
23. Strasser A, Cory S, Adams JM (2011) Deciphering the rules of programmed cell death to improve therapy of cancer and other diseases. *EMBO J* 30: 3667-3683.
24. Datta SR, Brunet A, Greenberg ME (1999) Cellular survival: a play in three Akts. *Genes Dev* 13: 2905-2927.
25. Yue Z, Carvalho A, Xu Z, Yuan X, Cardinale S, Ribeiro S, Lai F, Ogawa H, Gudmundsdottir E, Gassmann R, Morrison CG, Ruchaud S, Earnshaw WC (2008) Deconstructing Survivin: comprehensive genetic analysis of Survivin function by conditional knockout in a vertebrate cell line. *J Cell Biol* 183: 279-296.

26. Stauber RH, Mann W, Knauer SK (2007) Nuclear and cytoplasmic survivin: molecular mechanism, prognostic, and therapeutic potential. *Cancer Res* 67: 5999-6002.
27. Ruchaud S, Carmena M, Earnshaw WC (2007) Chromosomal passengers: conducting cell division. *Nat Rev Mol Cell Biol* 8: 798-812.
28. Castedo M, Perfettini JL, Roumier T, Andreau K, Medema R, Kroemer G (2004) Cell death by mitotic catastrophe: a molecular definition. *Oncogene* 23: 2825-2837.
29. Dohi T, Okada K, Xia F, Wilford CE, Samuel T, Welsh K, Marusawa H, Zou H, Armstrong R, Matsuzawa S, Salvesen GS, Reed JC, Altieri DC (2004) An IAP-IAP complex inhibits apoptosis. *J Biol Chem* 279: 34087-34090.
30. Dan HC, Jiang K, Coppola D, Hamilton A, Nicosia SV, Sebt SM, Cheng JQ (2004) Phosphatidylinositol-3-OH kinase/AKT and survivin pathways as critical targets for geranylgeranyltransferase I inhibitor-induced apoptosis. *Oncogene* 23: 706-715.
31. Zhao P, Meng Q, Liu LZ, You YP, Liu N, Jiang BH (2010) Regulation of survivin by PI3K/Akt/p70S6K1 pathway. *Biochem Biophys Res Commun* 395: 219-224.
32. Annibaldi A, Michod D, Vanetta L, Cruchet S, Nicod P, Dubuis G, Bonvin C, Widmann C (2009) Role of the sub-cellular localization of RasGAP fragment N2 for its ability to sensitize cancer cells to genotoxin-induced apoptosis. *Exp Cell Res* 315: 2081-2091.
33. Lakhani SA, Masud A, Kuida K, Porter GA, Jr., Booth CJ, Mehal WZ, Inayat I, Flavell RA (2006) Caspases 3 and 7: key mediators of mitochondrial events of apoptosis. *Science* 311: 847-851.
34. Annibaldi A, Dousse A, Martin S, Tazi J, Widmann C (2011) Revisiting G3BP1 as a RasGAP binding protein: sensitization of tumor cells to chemotherapy by the RasGAP 3127-326 sequence does not involve G3BP1. *PLoS One* 6: e29024.
35. Peltzer N, Bigliardi P, Widmann C (2012) UV-B induces cytoplasmic survivin expression in mouse epidermis. *J Dermatol Sci* .
36. Downward J (1999) How BAD phosphorylation is good for survival. *Nat Cell Biol* 1: E33-E35.
37. Hayakawa J, Ohmichi M, Kurachi H, Kanda Y, Hisamoto K, Nishio Y, Adachi K, Tasaka K, Kanzaki T, Murata Y (2000) Inhibition of BAD phosphorylation either at serine 112 via extracellular signal-regulated protein kinase cascade or at serine 136 via Akt cascade sensitizes human ovarian cancer cells to cisplatin. *Cancer Res* 60: 5988-5994.
38. Belyanskaya LL, Hopkins-Donaldson S, Kurtz S, Simoes-Wust AP, Yousefi S, Simon HU, Stahel R, Zangemeister-Wittke U (2005) Cisplatin activates Akt in small cell lung cancer cells and attenuates apoptosis by survivin upregulation. *Int J Cancer* 117: 755-763.

39. Hu H, Li Z, Chen J, Wang D, Ma J, Wang W, Li J, Wu H, Li L, Wu M, Qian Q, Chen J, Su C (2010) P16 reactivation induces anoikis and exhibits antitumour potency by downregulating Akt/survivin signalling in hepatocellular carcinoma cells. *Gut* .
40. Arora V, Cheung HH, Plenchette S, Micali OC, Liston P, Korneluk RG (2007) Degradation of Survivin by the X-linked Inhibitor of Apoptosis (XIAP)-XAF1 Complex. *J Biol Chem* 282: 26202-26209.
41. Marusawa H, Matsuzawa S, Welsh K, Zou H, Armstrong R, Tamm I, Reed JC (2003) HBXIP functions as a cofactor of survivin in apoptosis suppression. *EMBO J* 22: 2729-2740.
42. Jiang Y, Saavedra HI, Holloway MP, Leone G, Altura RA (2004) Aberrant regulation of survivin by the RB/E2F family of proteins. *J Biol Chem* 279: 40511-40520.
43. Connell CM, Colnaghi R, Wheatley SP (2008) Nuclear survivin has reduced stability and is not cytoprotective. *J Biol Chem* 283: 3289-3296.
44. Li F, Altieri DC (1999) Transcriptional analysis of human survivin gene expression. *Biochem J* 344 Pt 2: 305-311.

Figure legends

Figure 1: **mTORC1 is not involved in fragment N-induced cell survival**

HeLa cells were transfected with a GFP-expressing plasmid together with empty pcDNA3 or with pcDNA3 encoding the D157A caspase-resistant form of fragment N. Twenty-four hours later, the cells were incubated or not 90 min with 20 ng/ml rapamycin. **A.** The cells were lysed after an additional 24-hour period and the extent of S6K phosphorylation was assessed by Western blot. **B.** Alternatively, after the rapamycin pre-incubation period, the cells were treated or not with 10 μ M cisplatin for 24 hours and, apoptosis was scored (mean \pm 95% CI of 5 independent experiments performed in triplicate). Means with different symbol (# or &) are significantly different.

Figure 2: **Bad modulation plays little role in fragment N-induced cell survival**

A. MEFs were infected with an empty lentivirus or with lentiviruses encoding fragments N, N1, and N2, as indicated. Alternatively, HeLa cells were transfected with empty pcDNA3 or with pcDNA3 encoding the fragments N. The cells were lysed 24 hours later. The extent of Bad phosphorylation was assessed by Western blot using antibodies specific for Bad phosphorylated on serine 112 or serine 136. Triangles indicate non-specific bands. **B.** Predicted apoptotic response in cells lacking or not Bad in the presence or in the absence of fragment N. See text for details. **C.** MEFs expressing or not Bad were infected with an empty lentivirus or with a fragment N-encoding lentivirus. Forty-eight hours later, the cells were incubated with the indicated concentrations of cisplatin. Apoptosis was assessed after an additional 24 hour-period. The inset depicts the reduction in the percentage of apoptosis induced by the expression of fragment N in wild-type or Bad KO cells at the indicated doses (using the values of the main figure). The results correspond to the mean \pm 95% CI of sextuplets derived from 4 independent experiments. Statistics were done by repeated measures ANOVA tests.

Figure 3: **Fragment N does not regulate survivin expression**

A. Min6 cells were co-transfected with a luciferase expressing vector under the control of either a minimal promoter sequence required for survivin activity (left graph) or the entire survivin promoter sequence (right graph) with increasing amounts

of fragment N- (closed circles) or E2F1- (open circles) encoding plasmids. The results correspond to the mean \pm 95% CI of 6 (left panel) and 3 (right panel) independent experiments performed in triplicate. Repeated measures ANOVA tests were performed to determine if there was significant increase in luciferase activity induced by the E2F1- or fragment N-encoding plasmids (normality was verified with the Shapiro-Wilk test). **B-C.** MEFs were infected with an empty virus or with a lentivirus encoding the HA-tagged version of the D157A fragment N mutant. Survivin mRNA levels were analyzed 24 hours later by quantitative RT-PCR (panel B). The location of the 672FW and 672RV primers (red arrows), used for the amplification of the survivin mRNA, is depicted on top of the graph. Alternatively, cells were lysed and the protein expression of HA-fragment N and survivin was assessed by Western blotting (panel C). The results correspond to the mean \pm 95% CI of 3 independent experiments. **D.** Skins of mice were irradiated with low (0.05 J/cm^2) and high (0.3 J/cm^2) doses of UV-B light. Expression of nuclear and cytoplasmic survivin was assessed by immunofluorescence *in situ* (left panel). The quantitation shown on the right-hand side corresponds to percentages of keratinocytes displaying nuclear or cytoplasmic survivin (mean \pm 95% CI of 6 and 10 mice for the low and high UV-B dose exposure, respectively). No cells were found to display both cytoplasmic and nuclear survivin expression.

Figure 4: **Fragment N does not affect cell cycling**

HeLa cells, infected with an empty virus or with a lentivirus encoding the HA-tagged version of the D157A fragment N mutant, were synchronized at G1 by treatment with mimosine for 18 hours. The cells were then washed and cultured in fresh medium for the indicated periods of time. **A.** Representative histograms obtained at different time points after release from the mimosine block (NT, not synchronized cells). **B.** Immunocytochemistry-based detection (gold staining) of fragment N in the infected cells. The nuclei are colored in blue (Hoechst staining). **C.** Percentage of cells in each phase of the cell cycle as determined by PI staining (DNA content). Results represent the mean \pm 95 % CI of 4 independent experiments.

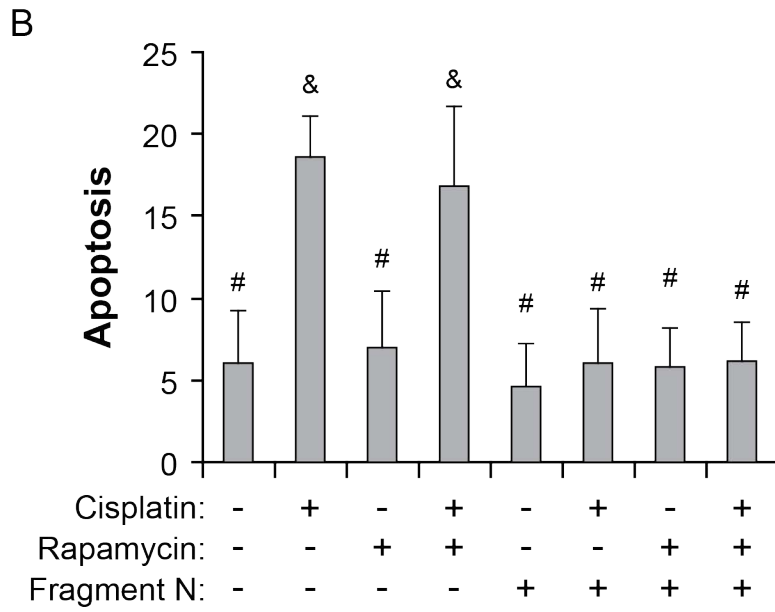
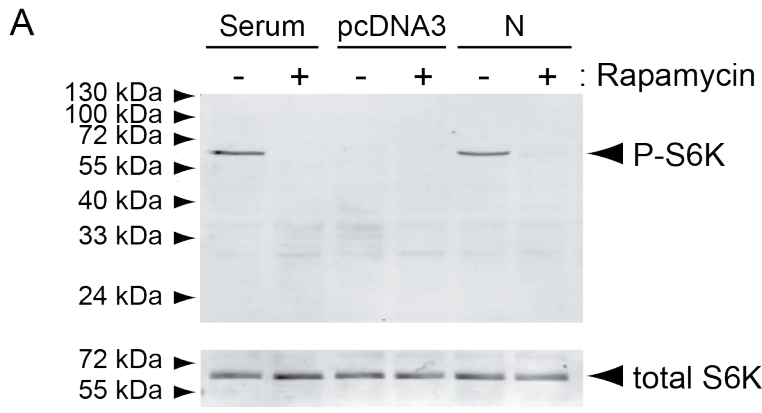


Fig. 1

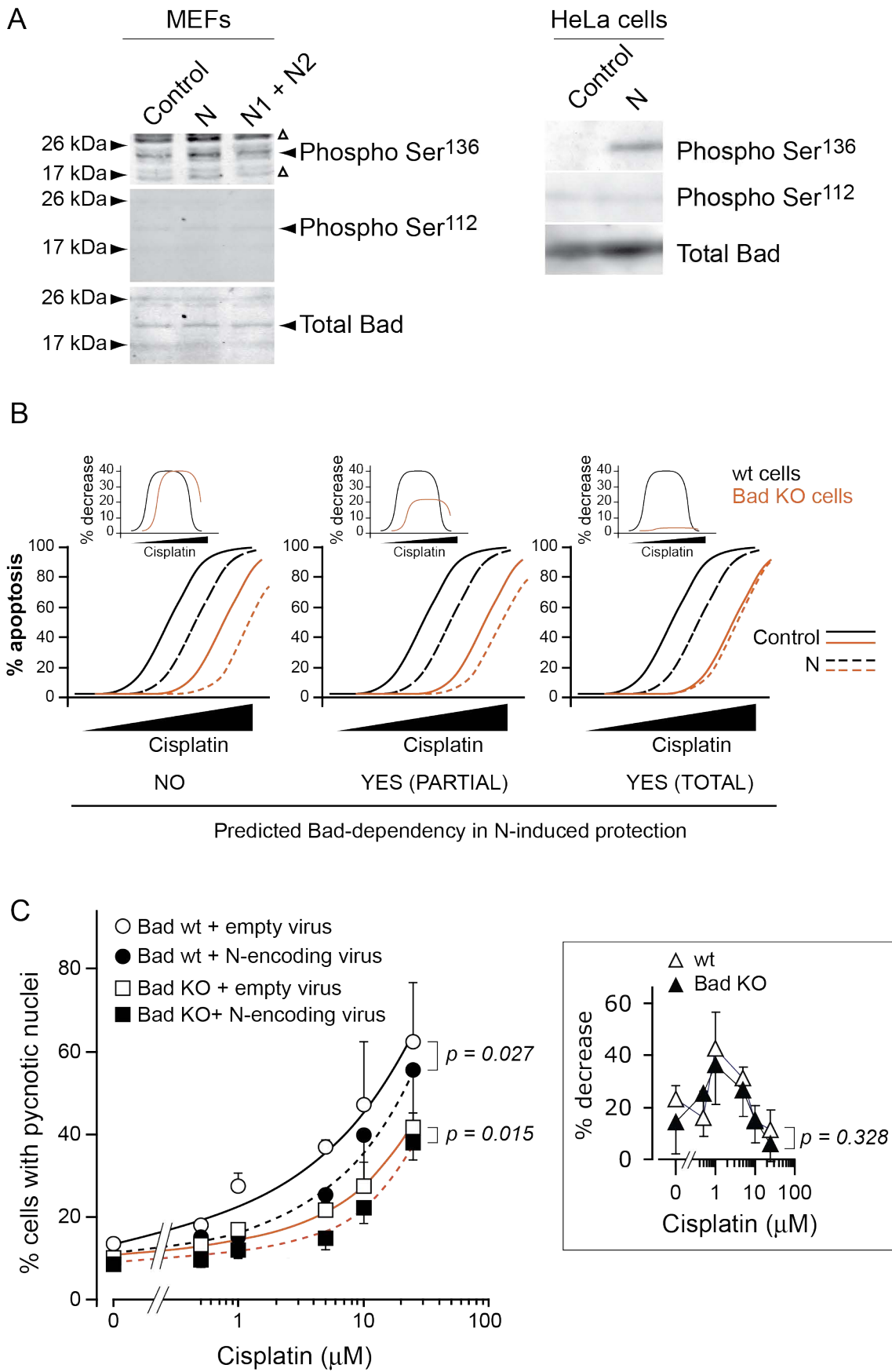


Fig. 2

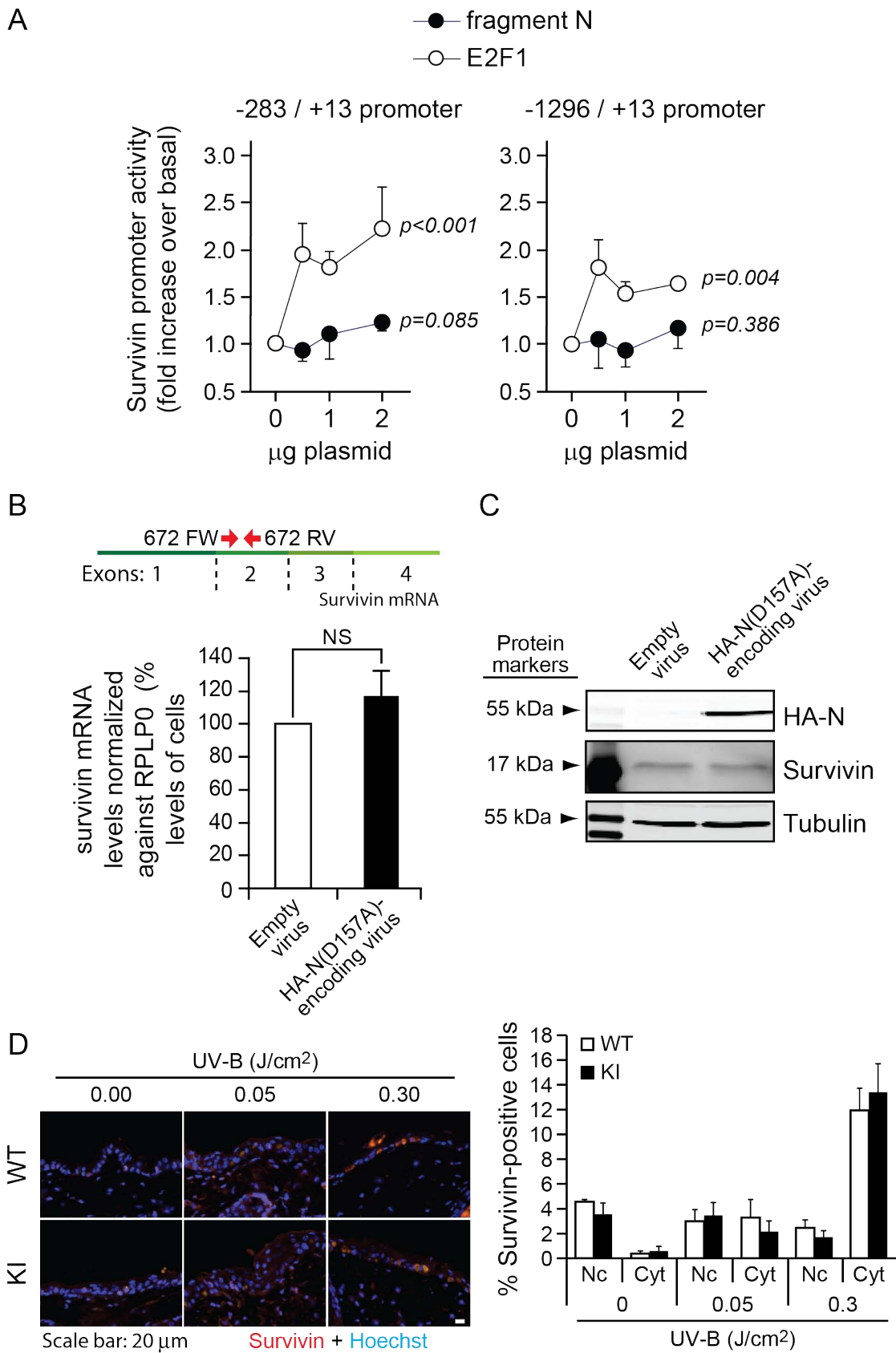


Fig. 3

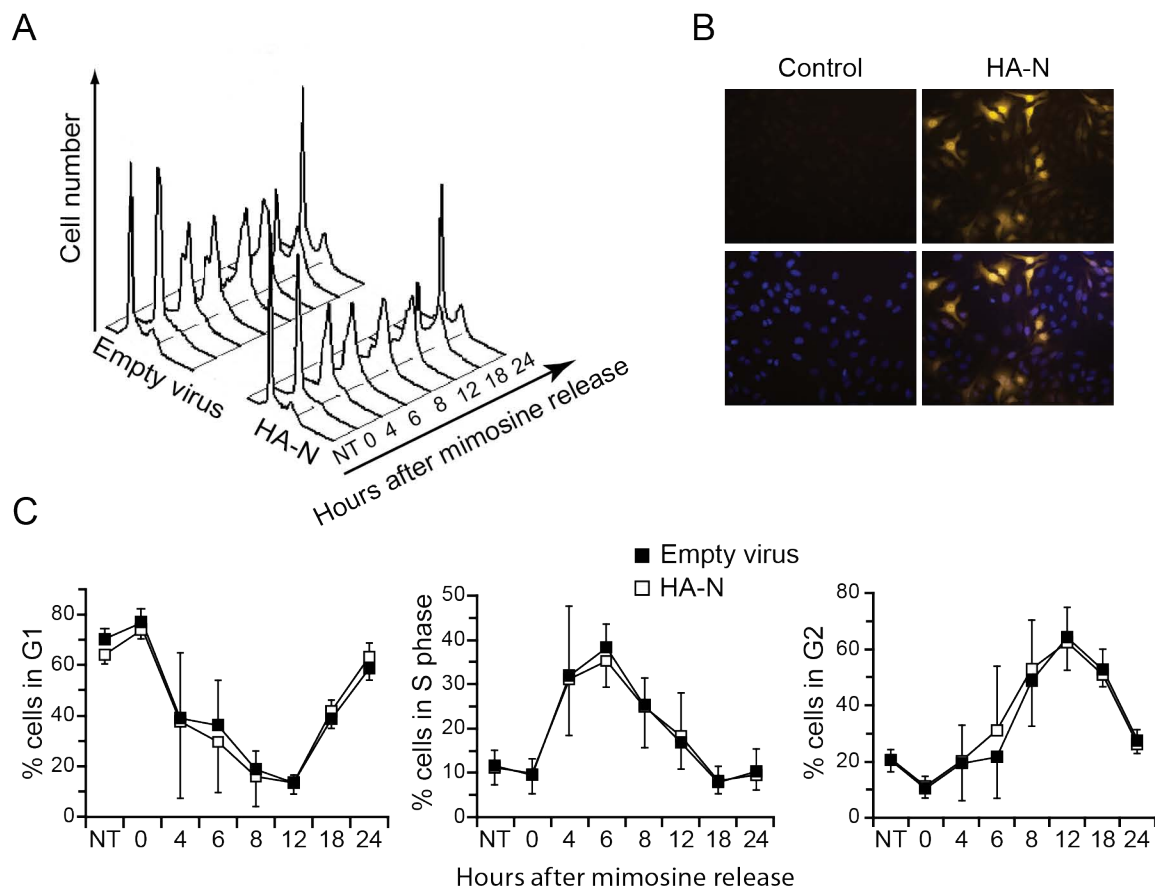


Fig. 4

SUPPLEMENTARY DATA

Supplemental materials and methods

Cell fractioning

At least 1×10^6 cells were harvested with hypotonic lysis buffer (HEPES pH 7.4 10 mM, MgCl₂ 10 mM, KCl 42 mM) and incubated at 4°C for 20 minutes. Cells were homogenized using a dounce and spinned down at 300 x g for 5 minutes at 4°C. After two washing steps with hypotonic buffer cells were resuspended with hypotonic buffer complemented with 1% Triton X100. The lysate was sonicated 4 times 15 seconds followed by a centrifugation at 10.000 g for 10 minutes at 4°C. The obtained pellet was resuspended in lysis buffer (0.5% Triton X-100, 500 mM Tris-HCl pH 7.5, 137 mM NaCl, 10% glycerol, 0.5% Triton X-100) complemented with 0.5% SDS and the nuclear fraction was recuperated. The supernatant was centrifugated at 10.000 x g for 10 minutes at 4°C. The supernatant represented the the cytoplasmic fraction.

Mitochondria purification

MEF cells were harvested in PBS and centrifuged 10 minutes at 1000 x g. After resuspending the cells in isotonic mitochondrial buffer (10mM HEPES pH 7.4, 210 mM mannitol, 70 mM sucrose, 1 mM EDTA, 1 tablet/50ml EDTA-free protease inhibitor (Roche)), cells were broken by twenty passages through a 25G1 0.5- by 25-mm needle fitted on a 2 ml syringe and centrifuged at 1500 x g for 5 minutes. This procedure was repeated twice and supernatants from each step were pooled and centrifuged 5 minutes at 1500 x g. Supernatant was collected, centrifuged 5 minutes at 2000 x g and further centrifuged 10 minutes at 9000 x g. Supernatant was conserved and represented the cytoplasmic content. Pellet was then resuspended in mitochondrial buffer (MB), centrifuged 10 minutes at 7000 x g and the pellet (mitochondrial fraction) was finally resuspended in MB. Protein content was quantitated by Bradford.

SUPPLEMENTARY RESULTS

Posttranscriptional regulation of Survivin

As previously mentioned, survivin is targeted to proteasomal degradation by ubiquitylation. Moreover, phosphorylation of survivin plays a role in its subcellular localization but also in its stability. Connell and collaborators have shown that the cytoplasmic fraction of survivin has an increased half-life as compared to the nuclear pool (Connell et al., 2008). In order to assess whether fragment N has an effect on survivin protein stability, either MEFs or HeLa cells were treated with cycloheximide to block translation and harvested at different time points after blockage (Figure 1). This allowed us to follow the degradation of Survivin in a time dependent manner and to decipher if fragment N could extend the half-life of the protein in two different cell types. Surprisingly even if the presence of fragment N slightly induced survivin protein levels, its turnover was accelerated as compared to control conditions independently of the cell type used (Figure 1A and B). We exclude the possibility that the fragment N is degraded during the experiment since its half-life is of 10.5 hours (Bulat et al., 2011) and as observed by western blot fragment N protein levels did not decrease upon translation blockage (Figure 1A). These results suggest that fragment N does not induce survivin stabilization.

Fragment N does not affect survivin subcellular localization

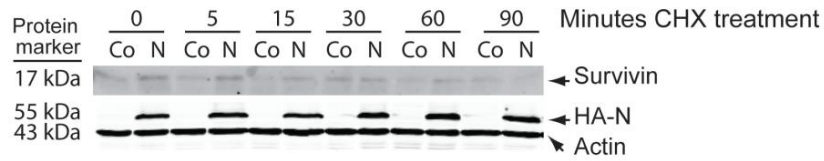
Survivin exists in different subcellular compartments and nuclear or cytoplasmic fractions of survivin bear different functions. Survivin is translocated to the cytoplasm of keratinocytes of mouse skin in response to stress and apparently this relocation is related to cytoprotection (Peltzer et al., 2012). Furthermore cytoplasmic fraction of survivin has an increased half-life as compared to the nuclear pool of survivin and sending survivin to the nucleus abolishes its antiapoptotic effect (Connell et al., 2008). So far we did not observed an effect on survivin expression by fragment N but since its localization is essential for protection *in vitro* we tested the effect of fragment N on survivin translocation to the cytoplasm in response to stress. To answer this question we treated MEFs from either WT or KI mice with a low concentration of

cisplatin (10 μ M) that induce a mild stress and analyzed the induction of survivin in different cellular compartments (Figure 2A). Low concentration of cisplatin resulted in an increase in the levels of survivin expression both in the nucleus and cytoplasm, although a more pronounced effect was observed in the nuclear pool of survivin (Figure 2A and B). However there was a slight or no difference in the levels of cytoplasmic survivin expression in response to cisplatin in WT and KI cells, suggesting that survivin translocation does not need a functional RasGAP cleavage, and fragment N generation, *in vitro*, in agreement with data obtained in keratinocytes.

Mitochondrial pool of survivin

Dohi and collaborators have reported the existence of a mitochondrial pool of survivin that is rapidly discharged in the cytosol in response to a cell death stimulus (Dohi et al., 2004). In order to assess if fragment N is able to increase the levels of this particular pool of survivin we purified mitochondria from cells overexpressing or not fragment N and assessed the levels of survivin. As shown in Figure 3, fragment N did not affect the mitochondrial levels of survivin in MEFs and thus this pool of survivin is not regulated by fragment N. The survivin non-mitochondrial content (cytoplasm plus nuclei), was not affected by fragment N, confirming the results presented earlier in this section (Figure 5_Results)

A



B

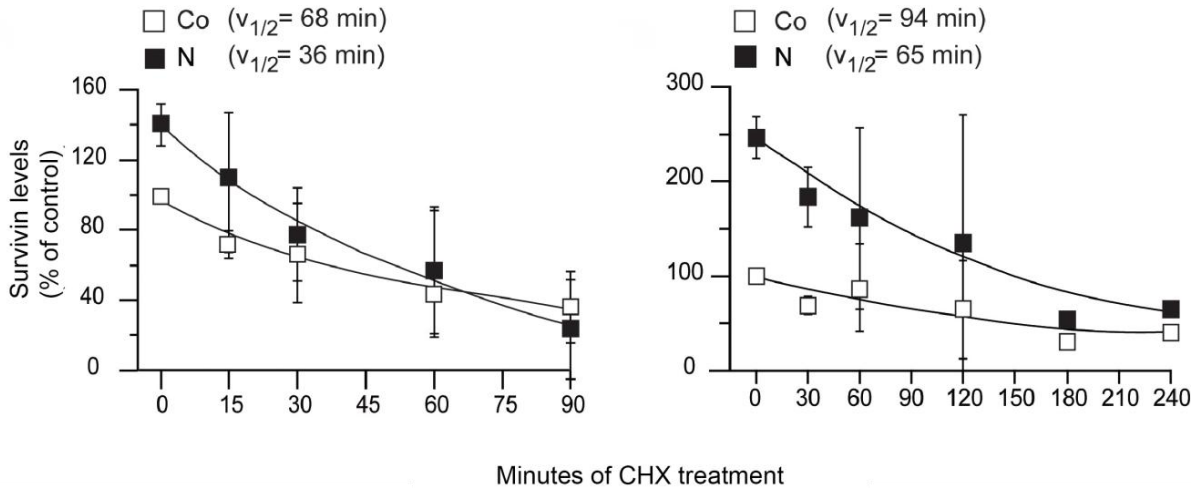


Figure 1: Survivin stability in the presence of fragment N. A_B_ MEFs were infected with an empty virus (Co), or an HA-N encoding virus (N) and treated for 0, 30, 60 and 90 minutes with cycloheximide (CHX 50 µg/ml). Representative image of protein lysates analysed by Western blot (A) and quantification of survivin band intensities normalized to actin (B, left panel). B (right panel)_ HeLa cells were transfected with pcDNA 3 (Co) or with an HA-N encoding plasmid (N) and treated for 0, 30, 60, 120, 180 and 240 minutes with cycloheximide. Only quantifications are shown. Values correspond to 3 independent experiments ± 95 % CI except for points 180, 210 and 240 that were performed just once

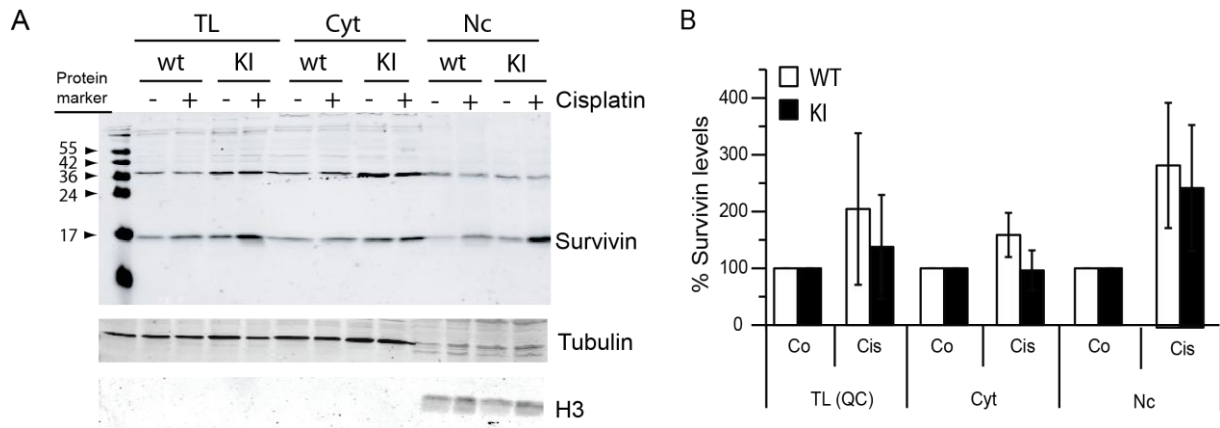


Figure 2: Survivin localization in response to mild stress. Both wild type (WT) and RasGAPD455A/D455A (KI) MEFs were treated with a low concentration of cisplatin (15 μ M) and 16hs later cell fractionation was performed. **A_** Representative western blot depicting survivin protein levels in different cell compartments in control or cisplatin treated cells. Purity of the fractions was confirmed by tubulin (for cytoplasmic fraction) and Histone 3 (for nuclear fraction). **B_** Quantitation of band intensities shown in A. The results represent the average of 4 independent experiments \pm 95% CI. TL: total lysate, Cyt: cytoplasmic fraction, Nc: nuclear fraction.

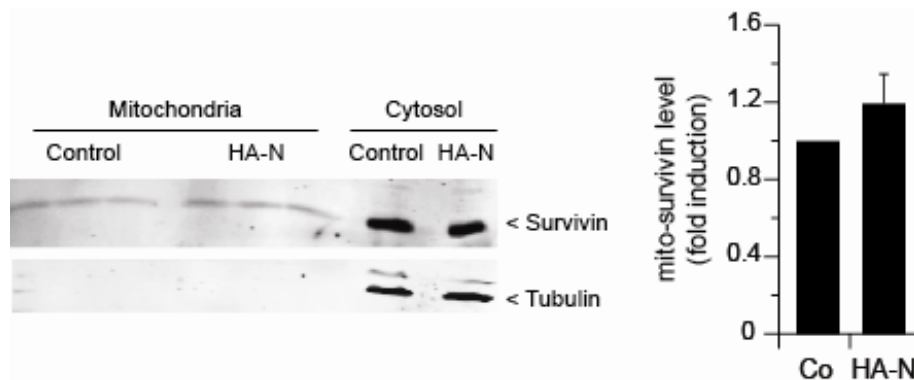
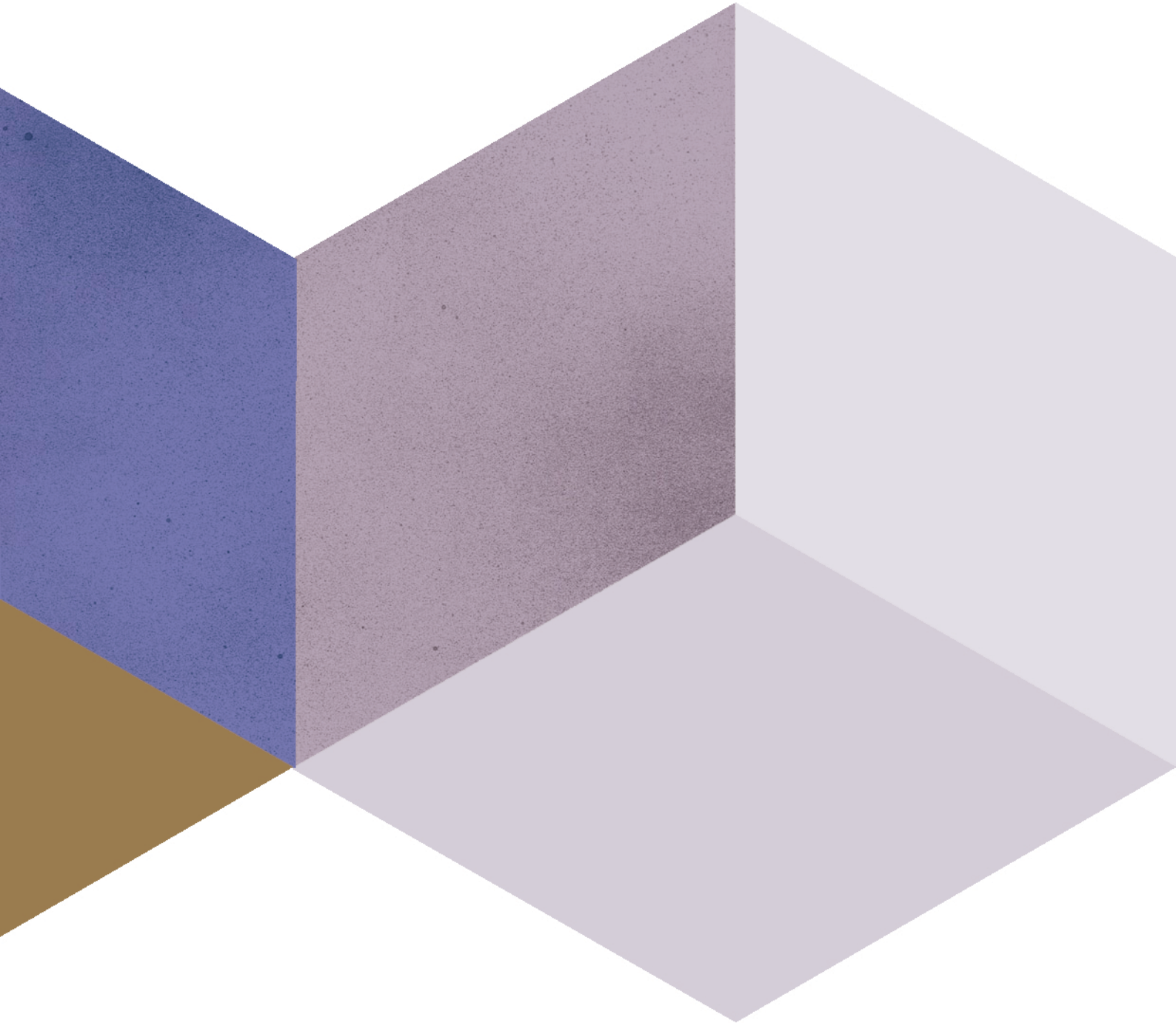


Figure 3: Mitochondrial survivin levels in the presence of fragment N. MEFs were infected with an empty virus (Control), or an HA-N encoding virus (HA-N). Mitochondrial protein content was isolated and survivin levels were detected by western blot. Mitochondria-free protein content is shown as control (left panel). Quantitation of band intensities are shown (right panel). The results represent the average of 3 independent experiments \pm 95% CI.

Reference List

- Bulat,N., Jaccard,E., Peltzer,N., Khalil,H., Yang,J.Y., Dubuis,G., and Widmann,C. (2011). RasGAP-Derived Fragment N Increases the Resistance of Beta Cells towards Apoptosis in NOD Mice and Delays the Progression from Mild to Overt Diabetes. *PLoS ONE* 6, e22609.
- Connell,C.M., Colnaghi,R., and Wheatley,S.P. (2008). Nuclear Survivin Has Reduced Stability and Is Not Cytoprotective. *J. Biol. Chem.* 283, 3289-3296.
- Dohi,T., Beltrami,E., Wall,N.R., Plescia,J., and Altieri,D.C. (2004). Mitochondrial survivin inhibits apoptosis and promotes tumorigenesis. *Journal of clinical investigation* 114, 1117-1127.
- Peltzer,N., Bigliardi,P., and Widmann,C. UV-B induces cytoplasmic survivin expression in mouse epidermis. *Journal of Dermatological Science.*
- Yang,J.-Y., Michod,D., Walicki,J., Murphy,B.M., Kasibhatla,S., Martin,S., and Widmann,C. (2004a). Partial cleavage of RasGAP by caspases is required for cell survival in mild stress conditions. *Mol. Cell Biol.* 24, 10425-10436.
- Yang,J.-Y., Michod,D., Walicki,J., and Widmann,C. (2004b). Surviving the kiss of death. *Biochem. Pharmacol.* 68, 1027-1031.
- Yang,J.-Y. and Widmann,C. (2002). A subset of caspase substrates functions as the Jekyll and Hyde of apoptosis. *Eur. Cytokine Netw.* 13, 387.
- Yang,J.Y., Walicki,J., Michod,D., Dubuis,G., and Widmann,C. (2005). Impaired Akt Activity Down-Modulation, Caspase-3 Activation, and Apoptosis in Cells Expressing a Caspase-resistant Mutant of RasGAP at Position 157. *Mol. Biol. Cell* 16, 3511-3520.

**DISCUSSION
PERSPECTIVES**



DISCUSSION AND PERSPECTIVES

Caspase-3 being one of the major proteases involved in cell death is usually linked to induction of apoptosis. In the last few years though, many functions different from execution of apoptosis have been proposed for this protease. In our laboratory, we have previously shown that low levels of caspase-3 induce an anti-apoptotic response *in vitro* through the cleavage of RasGAP and the consequent activation of the Ras/PI3K/Akt signaling pathway. This finding explains how cells undergoing a mild stress do not die despite the activation of caspases.

In the present work I have shown that the protective pathway initiated by caspase-3 activation and fragment N generation is important for the protection of keratinocytes of mouse skin exposed to UV-B light, cardiomyocytes of mouse heart injected with doxorubicin, and enterocytes in mouse colon treated with DSS. In all the experimental conditions studied, I have found that abrogation of the anti-apoptotic pathway induced by fragment N either by blocking caspases (caspase-3 KO mouse model and caspase inhibitor injection in WT mice), or preventing RasGAP cleavage (RasGAP KI mouse model where the first caspase-3 cleavage site of RasGAP has been destroyed), resulted in a deficiency of Akt activation which was translated in a higher sensitivity to apoptosis. This data suggests that RasGAP cleavage- induced anti-apoptotic response is essential to prevent cell death in low stress conditions *in vivo*. Most interestingly, blocking RasGAP cleavage and therefore fragment N generation rendered mice prone to an overall dysfunction of the organs where the stress stimulus was applied. The relevance of fragment N generation in this response was highlighted when WT mice were challenged with a high UV-B dose. Interestingly in this condition, there is a reduction of Akt activation and an increase in apoptosis as compared to the low UV-B exposed skin. Remarkably, phosphorylated Akt levels and percentage of apoptotic cells in WT mice exposed to a high dose of UV-B were comparable to those observed in KI mice exposed to the same dose. These observations indicate that not only RasGAP cleavage is important for protection, but it is specifically the presence of fragment N, since if not generated or destroyed (KI mice or WT mice in response to high stress) the protective response is turned off. In these conditions, active caspases-3 levels in the skin are almost undetectable. This is not the first evidence of the importance of the levels of caspases in the decision of

cell fate. Caspase-8 has anti-necroptosis functions, favoring apoptosis by cleaving RIPK1 (Darding et al 2012), however low activation of caspases-8 allows RIPK1 activation and association with RIPK3, triggering necroptosis and inflammation (Bonnet et al. 2011; Declercq et al., 2011).

Other systems in the cell function as molecular switch determining cell fate in response to the level of stress present in the cell. The well-known tumor suppressor, p53 has different functions according to the type and level of stress suffered by the cell. A wide variety of stressful conditions (DNA damage, hypoxia, heat shock, nutrient deprivation and oncogene activation) result in the accumulation and activation of p53 and, despite all these stresses converge in the activation of p53, the expression pattern of downstream genes appears to be specific for each stress and therefore the physiological output is different (apoptosis, senescence or survival). p53 can either block cell division and induce DNA repair, sparing the cell from death when damage is mild or transient. However, when damage is extensive or stress continues persistently, p53 switches to drive the elimination of affected cells (Gottlieb and Vousden, 2010; Hunziker et al., 2010). RasGAP, as p53, regulate cell fate according to the level of stress in the cell, indicating that indeed cells can use the same proteins to protect or sacrifice themselves. Furthermore, a recent work has demonstrated that the ability of p53 to behave differently according to the stress is not due to the level of p53 itself, but to the dynamics of p53 expression (Purvis et al., 2012). Whether RasGAP cleavage also behaves in pulses or in a sustained manner, or whether a chronic or an acute stress would affect RasGAP cleavage or fragment N mediated response remains to be determined.

The targeting of the signaling pathway relying on RasGAP cleavage can potentially be developed into therapies, aimed to increase resistance of sensitive cells exposed to environmental or chemical stresses, or to prevent death in pathological conditions such as Parkinson disease (Lev et al., 2003), heart failure (Gill et al., 2002) and diabetes (Mathis et al., 2001; Thomas et al., 2009) that are characterized by excessive apoptosis in the brain, heart and pancreatic beta cells, respectively. On the contrary, it would be stimulating to assess whether mice unable to cleave RasGAP into fragment N are more resistant to tumor incidence, postulating RasGAP cleavage, and particularly fragment N, as a new target for the study of cancer development.

In parallel with this work, I have studied another survival response in the skin relying on the previously reported induction of survivin in keratinocytes exposed to UV-B light. By studying the expression of survivin *in vivo*, in mouse skin exposed to UV-B light, I have observed an induction of survivin takes place specifically in the cytoplasm of keratinocytes of the basal cell layer, which are actively proliferating cells. This induction and redistribution of survivin to the cytoplasm is not a consequence of cell death but rather of cellular damage. However, our data indicate that survivin function as an anti-apoptotic protein is not very potent since the percentage of apoptotic cells in the cytoplasmic survivin positive population was greater than in the population of cytoplasmic survivin negative population. Further studies would need to be conducted in order to assess for instance, if the population of cytoplasmic survivin positive cells received the highest damage in response to UV-B and the expression of cytoplasmic survivin is an attempt to cope with this stress. DNA photoproducts generation would be an interesting approach to study the level of damage in each individual cell within the epidermis and it would help us determine whether there is a correlation between cellular damage and survivin expression in the cytoplasm.

Altogether, this is the first time that survivin has been reported to translocate to the cytoplasm in response to an apoptogenic stress *in vivo* in a non-pathological condition and in normal mouse skin. This finding is important in the context of cancer biology since cytoplasmic survivin is usually associated with cancer with little or no expression in normal cells. Here, I demonstrate that non-tumor cells are able to activate cytoplasmic survivin with no effect on nuclear survivin that is linked with proliferation. The presence of survivin in damaged keratinocytes and also in cancer or disease, may indicate that survivin is expressed when cells are undergoing a stressful condition.

The discovery that cytoplasmic survivin is induced in the skin together with the observation that Akt is also activated in skin in response to UV-B light in a caspase-3 and fragment N dependent manner, lead me to investigate whether the induction of cytoplasmic survivin was a consequence of fragment N-dependent Akt activation. However, cytoplasmic survivin was induced in UV-B exposed keratinocytes independently on RasGAP cleavage. Moreover, the maximal cytoplasmic survivin expression was observed at a high UV-B dose, which does not correlate with

fragment N generation and Akt activation. These results indicate that survivin is not an important player in fragment N mediated protection at least in keratinocytes exposed to UV-B light. Further, this observation suggests that survivin is not regulated by Akt in high stress conditions and the effect of Akt on survivin expression should be re-evaluated, at least in keratinocytes.

Other Akt targets were studied for their involvement in this protective pathway such as mTOR and BAD but none of them play major roles in fragment N-mediated protection, even though induction of mTOR activity and phosphorylation of BAD were observed in response to fragment N overexpression. Albeit the existence of many other Akt targets that could be involved in this pathway, it is also possible that fragment N elicits a pleiotropic effect, initiating a cooperative network to prevent cell death through the activation of Akt. Hence one of the main issue that remains to be established in the future is whether fragment N affects directly Akt post-translational modifications leading to its final activation, such as phosphorylation or ubiquitylation, or if it is an indirect mechanism relying upstream of Akt.

For instance, fragment N could prevent RasGAP from inhibiting Ras- induced signaling, by physical interaction with the GAP domain of RasGAP or by stabilizing Ras-GTP and therefore recruitment to the membrane and activation of PI3K and Akt. The effect of fragment N on the Akt activators mTORC2 and PDK1 activity as well as their recruitment to the membrane should also be clarified. Similarly, the importance of the different isoforms of Akt implicated in this protective response could contribute to elucidate the molecular mechanism underlying RasGAP cleavage.

Preliminary data performed in HCT116 cells suggests that Akt1, but not Akt2 is important for fragment N-mediated protection given that only Akt1 Knock out (KO) cells are not protected by overexpressed fragment N in response to FasL-induced apoptosis. Akt2 KO cells, on the contrary are still protected by fragment N, suggesting that specifically Akt1 plays an essential role in this pathway. Interestingly, it has been reported that the absence of Akt2, but not of Akt1, impaired NF- κ B activation in prostate cancer cells (Dan et al., 2008) indicating that indeed different isoforms of Akt can have different effects on downstream targets. Notably, fragment N was shown to block NF- κ B activation despite the fact that it activates Akt (Bulat et al., 2011), (Yang et al., 2009). The fact that specifically Akt2, but not Akt1, blocks NF-

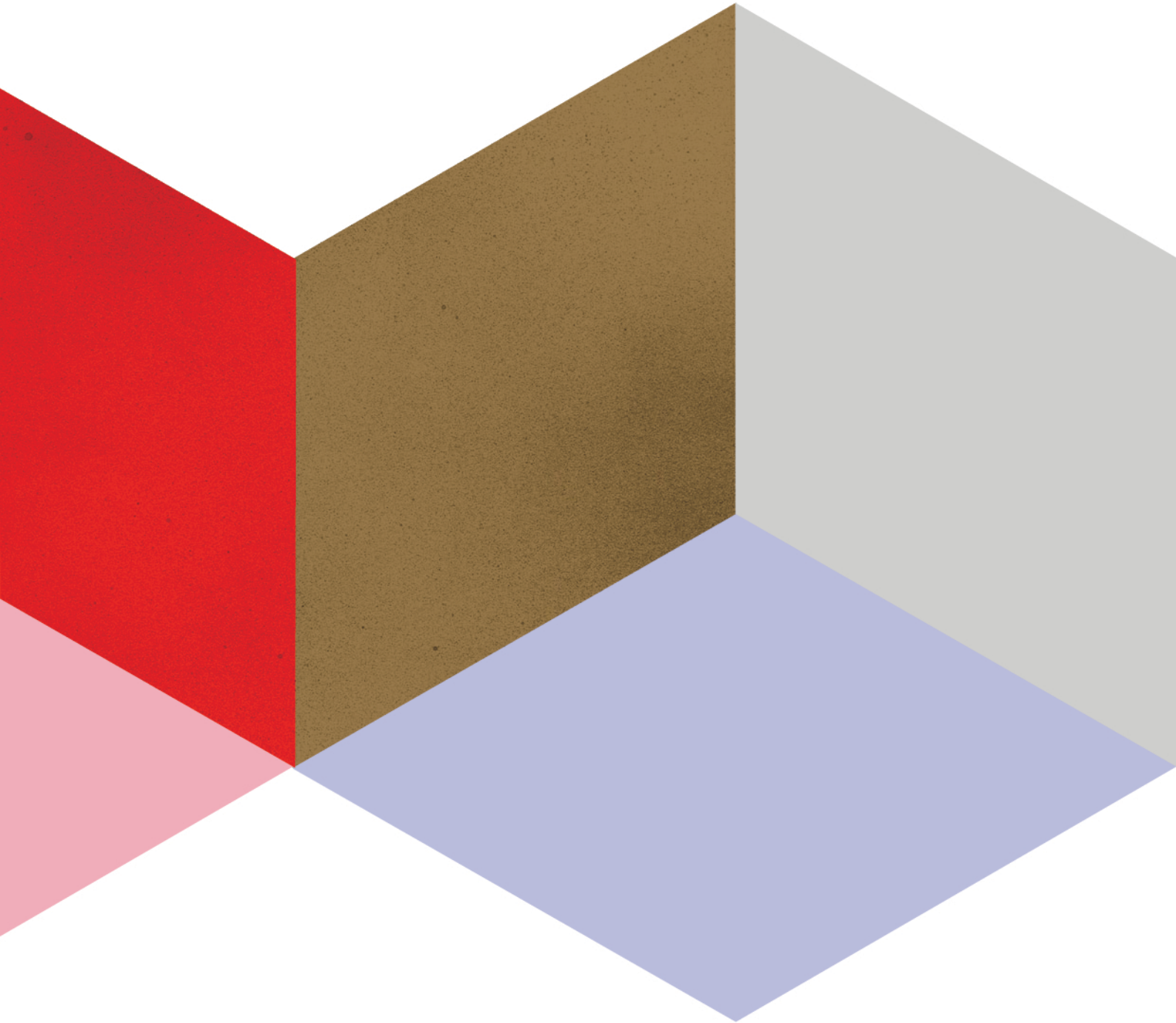
kB, correlates with our preliminary results suggesting that Akt1, but not Akt2, may be specifically involved in this protective response, and may explain how fragment N can block NF-kB even though it activates Akt (*i.e* in an Akt1 independent manner). These preliminary results also correlate with the activation of Akt in the skin observed in this work, since it has been reported that Akt1 is the predominant isoform expressed and activated in the skin in wound healing experiments (Di-Poi et al., 2002). The specific role of Akt1 in fragment N-mediated protection and how does fragment N selectively activates Akt1 is still a matter of future research. The importance of the different Akt isoforms implicated in this response need to be deeply studied and can contribute to elucidate the molecular mechanism underlying RasGAP cleavage.

Taken together, in this work I have discovered a new anti-apoptotic pathway operating *in vivo* in response to different pathophysiological stresses which encourages a new line of research in the development of therapies aimed to prevent massive cell death, as well as contributing to our basic knowledge of how caspase-3 can be activated without inducing apoptosis. A more profound research on the mechanism of fragment N induced protection is required for the understanding of this paradoxical but potent anti-apoptotic response.

Reference List

- Bonnet,M.C., Preukschat,D., Welz,P.S., van Loo,G., Ermolaeva,M.A., Bloch,W., Haase,I., and Pasparakis, M. (2011). The Adaptor Protein FADD Protects Epidermal Keratinocytes from Necroptosis In Vivo and Prevents Skin Inflammation. *Cell* 35, 572-582.
- Bulat,N., Jaccard,E., Peltzer,N., Khalil,H., Yang,J.Y., Dubuis,G., and Widmann,C. (2011). RasGAP-Derived Fragment N Increases the Resistance of Beta Cells towards Apoptosis in NOD Mice and Delays the Progression from Mild to Overt Diabetes. *PLoS ONE* 6, e22609.
- Dan,H.C., Cooper,M.J., Cogswell,P.C., Duncan,J.A., Ting,J.P.Y., and Baldwin,A.S. (2008). Akt-dependent regulation of NF- κ B is controlled by mTOR and Raptor in association with IKK. *Genes & Development* 22, 1490-1500.
- Darding,M and Meier,P. (2012). IAPs: Guardians of RIPK1. *Cell death and Differentiation* 19, 58-66
- Declercq,W., Takahashi,N., Vandenabeele,P (2011). Dual Face Apoptotic Machinery: From Initiator of Apoptosis to Guardian of Necroptosis. *Cell* 35, 493-495
- Gill,C., Mestril,R., and Samali,A. (2002). Losing heart: the role of apoptosis in heart disease-- a novel therapeutic target? *FASEB J* 16, 135-146.
- Gottlieb,E. and Vousden,K.H. (2010). p53 Regulation of Metabolic Pathways. *Cold Spring Harbor Perspectives in Biology* 2.
- Hunziker,A., Jensen,M.H., and Krishna,S. (2010). Stress-specific response of the p53-Mdm2 feedback loop. *BMC. Syst. Biol* 4, 94.
- Lev,N., Melamed,E., and Offen,D. (2003). Apoptosis and Parkinson's disease. *Prog. Neuropsychopharmacol. Biol Psychiatry* 27, 245-250.
- Mathis,D., Vence,L., and Benoist,C. (2001). beta-Cell death during progression to diabetes. *Nature* 414, 792-798.
- Purvis,J.E., Karhohs,K.W., Mock,C., Batchelor,E., Loewer,A., and Lahav,G. (2012). p53 dynamics control cell fate. *Science* 336, 1440-1444.
- Thomas,H.E., McKenzie,M.D., Angstetra,E., Campbell,P.D., and Kay,T.W. (2009). Beta cell apoptosis in diabetes. *Apoptosis*. 14, 1389-1404.
- Yang,J.Y., Walicki,J., Jaccard,E., Dubuis,G., Bulat,N., Hornung,J.P., Thorens,B., and Widmann,C. (2009). Expression of the NH(2)-terminal fragment of RasGAP in pancreatic beta-cells increases their resistance to stresses and protects mice from diabetes. *Diabetes* 58, 2596-2606.

METHODS



Reagents

1. HEPES buffer (2X) pH 7.05 (23°C):

1.1. Important note: always calibrate the pH meter before starting preparing the Hepes buffer.

1.2. Composition.

Chemicals	Final concentration	Source/Company	Code/quantities
NaCl	280 mM	Fluka	71380 (1 kg)
KCl	10 mM	Fluka	60130 (1 kg)
Na ₂ HPO ₄	1.5 mM	Merck	1.06586.0500 (500 g)
D-glucose•H ₂ O	12 mM	Merck	1.08342.1000 (1 kg)
HEPES	50 mM	Fluka	54461 (250 g)

1.3. Recipe.

Chemicals	For 500 ml
NaCl	8 g
KCl	0.38 g
Na ₂ HPO ₄	0.1 g
D-glucose•H ₂ O	1.1 g
HEPES	5 g
Adjust pH with NaOH (1 N, then 0.1 N) to 7.05 (23°C)	See 1.4

1.4. Add ddH₂O to about 450 ml, then adjust to pH 6.8-6.9 with 1 N NaOH, and finally to pH 7.05 with 0.1 N NaOH. Complete to 500 ml with ddH₂O. Control that the pH is still at 7.05.

1.5. Sterilize through a 0.22 µm 500 ml Stericups (Millipore #SCGPU05RE). Under a sterile hood, aliquot in 50 ml tubes (40 ml per tube). Write the lot number and the date on the tubes (**the lot number should be indicated in your laboratory book**). Store at -20°C.

2. Others

Chemicals	Source/Company	Code/quantities	Solvent	[stock]	Storage	Sterile
NaOH	Fluka	#71690 (500 g)	ddH ₂ O	10 N	Room temp.	no
Chloroquine	Sigma	C6628 (25g)	PBS	25 mM	-20°C	yes
CaCl ₂ •2H ₂ O (MW 147.02)	Acros	207780010 (1 kg)	ddH ₂ O	2.5 M	4°C	yes
Gelatin	Fluka	48722 (500 g)	PBS	0.1%	4°C	yes
DMEM, glutamax I, 4.5 g/l glucose, sans sodium pyruvate	Gibco	61965026 (500 ml)				
Newborn calf serum (NBCS), heat inactivated	Gibco	26010041 (500 ml)				

2.1. Preparation of NaOH solutions.

NaOH can cause irreversible damage to the eyes. It is thus mandatory to wear glasses when preparing or using NaOH solutions. The preparation of 10 N NaOH involves a highly exothermic reaction, which can cause breakage of glass container. Prepare this solution with extreme care in plastic beakers. To 80 ml of H₂O, slowly add 40 g of NaOH pellets, stirring continuously. As an added precaution, place the beaker on ice. When the pellets have

Transfection (calcium-phosphate)

dissolved completely, adjust the volume to 100 ml with H₂O. Store the solution in a plastic container at room temperature (plastic containers are to be used because NaOH slowly dissolves glassware). Sterilization is not necessary.

2.2. Preparation of a 25 mM chloroquine solution.

In a 50 ml Falcon tube, add 0,645 gr of chloroquine and complete to 50 ml with ddH₂O. Transfer to a 50 ml syringe and sterilize through a 0.22 µm filter (Millex – GV filters [Millipore #SLGV025LS]). Under a sterile hood, aliquote in 15 ml tubes (10 per tube). Write the lot number and the date on the tubes (**the lot number should be indicated in your laboratory book**).

2.3. Preparation of a 2.5 M CaCl₂ solution.

In a 50 ml Falcon tube, add 18.4 g of CaCl₂•2H₂O and complete to 50 ml with ddH₂O. Transfer to a 50 ml syringe and sterilize through a 0.22 µm filter (Millex – GV filters [Millipore #SLGV025LS]). Under a sterile hood, aliquote in 15 ml tubes (10 per tube). Write the lot number and the date on the tubes (**the lot number should be indicated in your laboratory book**).

2.4. Preparation of a PBS/0.1% gelatin solution (500 ml).

Add 0.5 g gelatin and 50 ml PBS 10X to 450 ml ddH₂O in a glass bottle. Autoclave and store at 4°C.

Procedure

Day 0.

1. Plate cells in appropriate medium (use gelatinized dishes if required).

Cells	Number per 10 cm dish	Number per well (6 well-plates)	medium	Gelatinized dish
HEK 293 and derived cell lines	2·10 ⁶	350'000	DMEM; 10% NBCS	yes

1.1. Gelatinization of the dishes.

Place the indicated volume of PBS/0.1% gelatin in the dish (tilt the plate to cover the entire surface with the solution). Wait at least 10 min. Just before adding the cells to the plates, aspirate the PBS/0.1% gelatin (do not allow the plates to dry).

1.2.

Dish size	Volume of PBS/01% gelatin
10 cm	2-5 ml
6 well plates	0.5 ml

Transfection (calcium-phosphate)

Day 1.

2. Prewarm the HEPES 2X buffer in a 37°C water bath (at least 20 min). In case the buffer is thawed, mix very well before using.
3. Add the DNA in the indicated volume of H₂O. Add the corresponding volume of 2.5 M calcium solution. Mix **10 times** by pipetting the solution up and down. Allow 20-30 min the solution to equilibrate.
- 4.

Cells	Dish size	Volume of medium in the dish	DNA amount	Volume of water in which the DNA is added	Volume of 2.5 M calcium to be added
HEK293	10 cm	10 ml	5-20 µg	450 µl	50 µl
	6 well plate	2 ml	2 µg	90 µl	10 µl

5. Add 25 µM chloroquine to the cell culture medium (not necessary to change the medium).
Note: if the cells are grown in RPMI medium (e.g. HeLa cells), you have to replace it with DMEM because RPMI medium is not compatible with the present transfection technique.
- 6.

Dish size	Volume of medium	Volume of stock
10 cm	10 ml	10 µl
6 well plates	2 ml	2 µl

7. Place the plates back in the incubator for at least 10 min.
8. Add the indicated volume of prewarmed (37°C) 2X HEPES buffer to the DNA/calcium solution, mix 5 times by pipetting the solution up and down. Incubate for 1 minute exactly (starting from the moment the HEPES has been added to the DNA; not from the time when the mixing is finished). Put the DNA-HEPES mix in the culture medium (rock the plate left to right and up and down 2 times).

Dish size	Volume of HEPES 2X to be added
10 cm	500 µl
6 well plate	100 µl

9. Incubate the cells at 37°C for 8-16 hours (**always mention this time of incubation in your laboratory book**). Replace the transfection medium with normal culture medium containing penicillin and streptomycin [use a 1:100 dilution of a Penicillin-Streptomycin Glutamine 100X solution (10'000 units/ml penicillin G; 10 mg/ml streptomycin sulfate; 29,2 mg/ml L-glutamine; 10 mM sodium citrate; 0.14% NaCl {GibcoBRL #10378-016})] to avoid contamination (the DNA used for the transfection is generally not sterile!).
10. Expected transfection efficiencies (count at least 500 cells).

Cells	Transfection efficiency
HEK293	30-80%
COS	30-40%

11. **In your laboratory book, always mention how long after step 7 were the cells analyzed.**

References

1. Jordan et al. - Nucl. Acid Res. (1996) **24**:596 (#3461)

Reagents

Chemicals	Source/Company	Code/quantities
Lipofectamine 2000 (1 mg/ml)	Gibco/Invitrogen	11668-019 (1.5 ml)
RPMI1640 Medium	SIGMA	R8758 (500 ml)
DMEM	SIGMA	D5796 (500 ml)
Newborn calf serum, heat inactivated	SIGMA	N4637 (500 ml)
15 ml polystyrene round-bottom tube	Becton Dickinson	352057

Procedure

Day 0.

1. Plate cells in appropriate medium according to Table I.

Table I

Cells	Number per 10 cm dish	Number per well of 6 well-plates	medium
HeLa cells	0.5-2·10 ⁶ (use 0.5·10 ⁶ cells for P-Akt assay)	4 10 ⁵	RPMI, 10% NBCS

Day 1.

- a. Add the required DNA amounts at the bottom of sterile Eppendorf tubes (see column 3 of Table II). Using a 2 ml plastic pipette, add the serum-free medium (for the volume of medium to be used, please refer to column 3 of Table II). Using the same plastic pipette, transfer the required volume of serum-free medium to the 15 ml polystyrene round-bottom tubes (for the volume of medium to be used, please refer to column 4 of Table II).
- b. Mix the Lipofectamine 2000 stock solution gently before use, centrifuge quickly to pellet the drops to the bottom of the tube, and then add the Lipofectamine 2000 to the serum-free medium that has been placed in the 15 ml tubes (for the volume of Lipofectamine 2000 to be used, please refer to the column 4 of table II). Mix gently and incubate 5 minutes at room temperature.
- c. Using 1 ml tips, add the diluted DNA drop by drop to the diluted lipofectamine2000. Mix gently and incubate 20 min at room temperature.
- d. Just before the next step, wash the plates twice with serum-free culture medium (see column 5 of Table II for the volumes to be used).

Transfection (lipofectamine)

-
- e. Add serum-free culture medium to the DNA + lipofectamine mix with a 5 ml plastic pipette and, using the same plastic pipette, add this mixture to the cells (refer to column 6 of Table II for the volumes to be used).
 - f. Incubate 5 hours at 37°C in a CO₂ incubator
 - g. After 5 hours replace the medium with serum-containing medium (use twice as much as the volumes indicated in column 5 of Table II). The cells can then be processed according to the experimental design.

Table II

1	2	3	4	5	6
Cells	Dish size	Total DNA amount (µg) and Dilution Volume (µl)	Lipofectamine 2000 (µl) and Dilution Volume (µl)	Washing steps (volume to be used)	Volumes of serum-free medium to be added to the Lipofectamine-DNA mix
HeLa	10 cm dish	7 µg in 600 µl	8-10 µl in 600µl	5 ml	3.8 ml
HeLa	6 well-plate	4 µg in 250 µl	4 µl in 250 µl	2 ml	1.5 ml

Western blot**Apparatus**

Transfer tank located in the drawers next to Christian's office door. It is the transparent tank containing red-black electrode module inside. Gel cassettes and sponges are either in the drawer above the one containing the tanks or above the sink in the middle of the lab.

Materials and reagents1. *Plastic sheets, commercial Enhanced chemiluminescence (ECL) solution and other reagents.*

1.1. Materials and reagents.

Materials and reagents	Source/Company	Code/quantities
Plastic sheets Kapak Tubular Roll Stock [9.5''x250' #5 Scotchpak (2 Mil)].	Kapak Parkdale Drivewe, Minneapolis, Minnesota 55416 • 1681	
Tris	Sigma	T1503 5Kg
Tween	Acros	p7949 100ml
Milk		
ECL reagent Supersignal West Femto Substrate	Pierce	#34095
Ponceau S	Acros	161470250 (25 g)

1.2. **Ponceau S Staining Solution [0.1%(w/v) Ponceau S in 5% (v/v) acetic acid]**

- 1g Ponceau S
 - 50ml acetic acid
 - Make up to 1 liter with ddH₂O
- Store at 4°C. Do not freeze.

Alternative recipe:0.2% (w/v) Ponceau S in 3% (v/v) acetic acid.

1.3. **Tris-buffer saline (TBS; 18 mM HCl, 130 mM NaCl, 20 mM Tris pH 7.2)**

- 30ml HCl
- 152g NaCl
- 48g Tris base
- Up to 1L dH₂O

1.4. **TBS/tween**

- 19L dH₂O
- 1L 20X TBS
- 0.1% Tween (final concentration)

1.5. **TBS/milk**

- 5% powdered milk (25g for 500ml of TBS/tween)
- TBS/tween
- Alternatively some primary antibodies work better if they are diluted in 5% BSA (5%BSA in TBS/tween)

2. *Home-made ECL solution.*

2.1. Composition of the stocks.

Western blot

Chemicals	Stock concentration	Final concentration	Source/Company	Code/quantities
Luminol (3-aminophthalhydrazide)	250 mM (1 g in 22.7 ml DMSO). Make 1.5 ml aliquotes	1.25 mM	Sigma	A-8511 (1 g)
P-coumaric acid	90 mM (0.5 g in 33.3 ml DMSO). Make 660 µl aliquotes.	0.2 mM	Acros	12109-0250 (25 g)
Tris	1 M pH 8.5	100 mM	Boehringer Mannheim	708976 (1 kg); IBCM stock
H ₂ O ₂ 30%	30%	0.01%	Merck	1.07210.0250 (250 ml)

Solution 1: 2.5 mM luminol and 0.4 mM coumaric acid in 100 mM Tris pH 8.5.

Solution 2: 0.02% H₂O₂ in 100 mM Tris pH 8.5.

3. *Home-made enhanced ECL solution Note: for the moment this is not working (use the above recipe instead).*

3.1. Composition of the stocks.

Chemicals	Stock concentration	Final concentration	Source/Company	Code/quantities
Luminol (3-aminophthalhydrazide)	250 mM	1.25 mM	Sigma	A-8511 (1 g)
p-iodophenol	(in DMSO)	50 µM		
Tris	1 M pH 8.5	100 mM	Boehringer Mannheim	708976 (1 kg); IBCM stock
H ₂ O ₂ 30% (8.82 M)	30%	2 mM	Merck	1.07210.0250 (250 ml)

Procedure

1. General remarks.

- 1.1. The conditions of incubation of the blots have to be adapted for each antigen and each antibody used. Therefore, the procedures presented in the following sections have to be considered as general guidelines and should not be assumed to work in all cases. Indications of possible improvements when the conditions are not found optimal will be mentioned.
- 1.2. Always centrifuge the tubes containing the antibodies before usage.
- 1.3. In principle, do not incubate two blots in the same bag.
- 1.4. Never touch the blot with bare hands. Use gloves and move the blots with tweezers.
- 1.5. The following procedure should be considered only for the small gels (see SOP12.1).

Western blot

2. Migration on gels.

Percentage of acrylamide	Separation
8%	40-200 kDa
10%	30-200 kDa
12%	20-200 kDa
4-20%	7-250 kDa
8-16%	15-250 kDa

3. Transfer to membranes.

3.1. After migration, proteins are transferred to nitrocellulose filters (Schleicher and Schuell, BA83 0.2, μ m, no. 401380) or PVDF membranes. Instruction on how to do this can be found in the same drawer as the material used for the transfer and for the SDS-PAGE (see SOP 12.1).

3.2. Transfer buffers.

David has recently tested the two following buffers. According to him, transfer buffer II works better.

Composition of transfer buffer I.

Chemicals	Stock solution	Final concentration	Source/Company	Code/quantities
CAPS	1M pH11	10 mM	Acros	172621000 (100 g)
Methanol		10%	Fluka	65543 (5 l)

CAPS 1M stock solution (500 ml): 110 g CAPS (MW 221.3) and 20 g NaOH in water. The pH should be 11. Store in the dark at 4°C.

Prepare the transfer buffer (5 liters) directly in the transfer tank (50 ml CAPS 1M, 500 ml methanol, and water up to 5 liters).

Methanol evaporation ensures that the buffer does not heat too much. Therefore the transfer buffers cannot be used too many times. Without methanol, the buffer would boil during the transfer!

Transfer o/n at 600 mA.

Composition of the transfer buffer II.

Chemicals	10X stock (1 liter)	Final concentration (1X transfer buffer)	Source/Company	Code [quantities]
Tris	30.2 g	1 mM	Biosolve ltd	20092388 [4 kg]
Glycine	144 g	8 mM	ACROS	120070050 [5 kg]
SDS	10 ml of a 10% solution in water	0.001%	Biosolve ltd	19822359 [0.5 kg]

Prepare the transfer buffer 1X (5 liters) directly in the transfer tank.

Add 500 ml of the 10X buffer, 1 liter of methanol and water up to 5 liters.

Transfer 5 hours at 660 mA.

Currently the situation with the transfer buffers is like this: they are located above the sink were other materials for the transfer can also be found (sponges, etc.), There are several bottles of 10x transfer buffer. In order to make 1x transfer buffer, mix 100 ml of the 10X preparation with 700ml of water and 200ml of some alcohol (methanol or ethanol).

3.3 After preparing the transfer tank, place the top on and plug it into a power supply machine (make sure that the plus and minus plugs are connected right: you do not want your proteins to be released on the wrong side directly into the transfer buffer). Transfer is usually preformed at 250 mA (constant amperage) for one hour or one hour and twenty minutes.

Western blot

- 3.4 Check if the protein markers have been transferred (one should see the markers on the membrane and not on the gel).
4. This protocol should be used when there are no particular problems to get a strong signal
 - 4.1. Ponceau S Stain for Western blots.

Background. *This is a rapid and reversible staining method for locating protein bands on Western blots. Sensitivity is somewhat less than Coomassie blue and produces reddish pink stained bands; minor components may be difficult to resolve. The stain is useful because it does not appear to have a deleterious effect on the sequencing of blotted polypeptides and is therefore one method of choice for locating polypeptides on Western blots for blot-sequencing. The stain binds strongly to nylon-based filter media but is fine for nitrocellulose and PVDF membranes. Incubate the membrane for up to an hour in staining solution with gentle agitation. Rinse the membrane in distilled water until the background is clean. The stain can be completely removed from the protein bands by continued washing. Stain solution can be re-used up to 10 times.*

How we use it in the laboratory. Incubate the blot in Ponceau for 2-3 min to visualize the proteins and to determine whether the transfer was homogeneous. With a pen, mark the position of the molecular weight markers. The blots are then subjected to the following incubations.
 - 4.2. wash 3x 20 min at room temperature with TBS/0.1% Tween 20 (TBS/Tween; found in the big tank next to the sink near the entrance of the laboratory).
 - 4.3. 45-60 min at room temperature with TBS/5% powdered milk (TBS/milk).
 - 4.4. overnight with the primary antibody (in TBS/milk) at 4°(in a cold room).
 - 4.5. 3x 20 min at room temperature with TBS/Tween.
 - 4.6. 45 min at room temperature with TBS/milk.
 - 4.7. 45 min with the secondary antibody (in TBS/milk) at room temperature (if the secondary antibody bears a fluorochrome sensitive to light [e.g. antibodies required for the odyssey detection; see SOP 17], make sure that incubation is performed in a black box).
 - 4.8. 3x 20 min at room temperature with TBS/tween (in the dark).
5. Detection of the secondary antibodies on films.
 - 5.1. This method should be used only for antibodies and antigens that do not generate strong signals. If this is not the case, detect the secondary antibodies with the BioRad Fluor-S imager (refer to SOP 2.0) or even better with the Odyssey apparatus (see SOP 17).
 - 5.2. Check that the developer has been turned on and is ready to be used.
 - 5.3. Prepare a cassette that should contain a fluorescent ladder (to position your film on the blot later on).
 - 5.4. Wash a glass plate thoroughly (first with soap, rinse with water and finally with ethanol).
 - 5.5. Prepare the ECL reagent by mixing equal volumes of solutions I and II. You need about 1 ml for each 10 cm² of your blot.
 - 5.6. Cut some Kappak plastic sheet that will be used to contain your blot during the exposure to films. Seal it but leave one side open.
 - 5.7. Take the blot with tweezers and touch some absorbing paper with one of its corner to remove the liquid in excess. Place the blot on the glass plate with the transferred proteins up. Pour the ECL reagent on the blot. Check that the whole surface is covered and wait one minute.
 - 5.8. With tweezers, transfer the blot in the Kappak bag. Remove the bubbles and seal the bag. Using absorbing paper, remove the liquid on the exterior of the bag. Place the bag in the cassette as close as possible to the fluorescent ladder. Tape the bag on one side.
 - 5.9. Immediately, go to the dark room with the sealed blot, the films and a cassette. Place a film on the blot. Close the cassette. Wait one minute. Remove the first film that you insert in the developer. While the first film develops, place a second one on the blot and close the cassette. When the first film comes out, check the intensity of the signal. If it is weak, expose the second film for 5-15 min. If it is too strong, develop the second film immediately (it will of course be too dark too) and expose a third film to 5-15 seconds. If the film has to be exposed for 1-2 seconds, tape it on the other side of the cassette. This will ensure that when you close the lids, the film will not move. Note again that if the signal is strong, you should not use this technique (see point 3.1).
 - 5.10. Keep all the films (the overexposed ones are often used to position the molecular weight markers). All the films should be labeled (**do it immediately**) with the date, the experiment number, the exposure time, the type of ECL used, and the experimental conditions for each lane. Also try (when possible) to identify the bands on your blots.
6. Detection of the secondary antibodies with the BioRad Fluor-S imager.

Western blot

- 6.1. Refer to SOP 2.0.
 - 6.2. In this case also, the images obtained should be labeled: date, the experiment number, the exposure time, the type of ECL used, and the experimental conditions for each lane. Also try (when possible) to identify the bands on your blots.
 7. Quantitation of the ECL signal.
 - 7.1. In principle, quantitation should not be performed using films because the signal on films is not linear (you need more than one photon to activate the silver grains) and saturates rapidly.
 - 7.2. If possible, quantitation should be performed using the BioRas Fluor-S imager. Please refer to SOP 2.0.
 8. Detection of the secondary antibodies using the Odyssey system (Licor).
 - 8.1. Refer to SOP 17.
 9. No signal
 - 9.1. Increase the incubation with the antibodies: o/n incubation with the first antibody and 2-4 hours with the secondary antibody. Perform the incubations at 4°C.
 - 9.2. Reduce the “stringency” of the incubation buffer. Milk containing buffer can possibly quench a fraction of the antibody. The following buffers are ranked from highest to lowest stringency: milk-containing buffer, BSA containing-buffer, tween-containing buffer, PBS or Tris buffer.
 10. How to store antibodies.
 - 10.1. It is possible to reuse antibodies many times and this should be done whenever the antibody is rare and not available commercially. The solution containing the antibody needs to contain 0.05% azide (NaN₃) and 10 mM EDTA.
 11. Very important: after completion of the Western blot procedure, always store the nitrocellulose membranes in Kappak bags at -20°C for further potential use.
-

References

1. Widmann et al. *Biochem. J.* (1995) **310**:203 (#3461)
2. Yang et al. *Mol. Cell Biol.* (2001) **21**:5346 (#3666)

Western blot

Reagents

Chemicals/medium	Source/Company	Code/quantities
JETstar maxi	Genomed	20 prep (#220020)
Isopropanol		
Glycerol		
Tris		
EDTA		

TE: Tris 10 mM pH 7.4, EDTA 1 mM.

Bacteria culture

- For most plasmids, inoculate 250 ml of LB with the appropriate antibiotic (see SOP 8.0) with:
 - a tip that has touched a colony on an Agar plate
 - a few ml of a mini-prep culture
 - a chunk of a glycerol stock taken with a yellow tip
- Incubate o/n at 37°C in a shaker.
- If required, take 1 ml of the culture to prepare a glycerol stock (put this one ml in an Eppendorf tube, centrifuge in an Eppendorf centrifuge at 4'000 rpm for 5 min, discard the supernatant and resuspend the pellet in 300-500 µl of a sterile 10% glycerol solution; store at -70°C).

Maxi prep

- Principle.
 The procedure employs a modified alkaline/SDS method to prepare the cleared lysate. After neutralization, the lysate is applied onto a JETstar column and the plasmid DNA is bound to the anion exchange resin. Washing the resin removes RNA and all other impurities. Afterwards, the purified plasmid is eluted from the column and finally concentrated by alcohol precipitation.
 The supplier says that the JETstar purified plasmid DNA is of a higher quality than 2 x CsCl purified plasmid DNA.
 The expected yield for a maxi column is between 300-500 µg of DNA.
- Centrifuge the cultures in 250 ml bottles at 5'000 rpm for 5-10 min at 4°C using the GSA rotor in the Sorvall RC-5B centrifuge. Check that the rotor is clean before and after use. Clean if necessary and always remove any liquid present.
- Place the column on the "blue cow". Add 30 ml of solution E4 in the column and let flow by gravity.
- Note: RNase must be added to solution E1 prior to its first use. Just poor the lyophilized RNase powder into bottle E1 and mix. Add the sticker indicating that the RNase has been added, the date and your name.
 Discard the supernatant. Resuspend the pellet in 10 ml of solution E1.
- Add 10ml of solution E2 and mix gently. Incubate 5min at room temp on a rocker (Rocker Inotech; shake 9, timer 5, frequency 17).
- Add 10 ml of solution E3 and mix immediately by inverting the bottle 5 times. Transfer to a 50 ml blue Falcon tube (do not use yellow Falcon tube since they are more fragile and may break during the centrifugation). Centrifuge at 9'000 rpm for 10 min at 20°C using the SLA 600TC rotor in the Sorvall RC-5B centrifuge.
- Poor the supernatant on the column and let flow by gravity. Wash the resin with 60 ml of solution E5.
- Place the column on a 50 ml blue Falcon tube and secure the column on the tube with tape. Add 15 of solution E6 and let flow by gravity.

9. Add 10.5 of isopropanol. Mix and incubate on ice for at least 1 hour (alternatively, the tube can be stored o/n at -20°C).
 10. Centrifuge at 10'000 rpm for 30 min at 4°C using the SLA 600TC rotor in the Sorvall RC-5B centrifuge. Discard the supernatant being very careful not to loose the pellet that is not always firmly adherent (sometimes not at all).
 11. Add about 20 ml of 70% ethanol. Centrifuge at 10'000 rpm for 10 min at 4°C using the SLA 600TC rotor in the Sorvall RC-5B centrifuge. Discard the supernatant as above. Aspirate all the residual drops with a long white tip.
 12. Resuspend the pellet in 500 μl of TE.
 13. Measure the concentration with the spectrophotometer using a 1/100 dilution in a quartz cuvette. One OD at 260 nm corresponds to 50 $\mu\text{g}/\text{ml}$ of DNA. The ratio between the OD at 260 nm and the OD at 280 nm should be between 1.8 and 2.0.
 14. Write down the concentration of the maxi prep in the plasmid files as well as on the tube.
-

Day 1

Put two coverslips per well in a 6 well plate and incubate 30 minutes with gelatine 0.1%. After this time remove the gelatine and put the cells over them. Make sure the coverslip is well attached to the surface of the well (push it down softly with a tip).

Day 2

1. Put 1 coverslip / well in a new 6 well plate and wash with 2 ml of PBS 1x
2. Fix the cells to the coverslip surface by treating with PAF 2% (paraformaldehyde diluted in PBS) for 15 minutes
3. Wash once with PBS
4. In order to permeabilize the membranes, incubate the coverslips with triton 0.2% (diluted in PBS) for 10 minutes
5. Wash once with PBS
6. To block unspecific binding sites of the antibody incubate 15 minutes with DMEM + 10% FCS
7. Dilute the antibody in DMEM + 10% FCS (see dilution in the datasheet of each antibody). Put a drop of 60 ul in a parafilm very well straightened over the bench and place the coverslip upside down over the drop (the cells have to be in contact with the antibody solution). Incubate 1 hour at room temperature in a humid environment. We usually use a polystyrene box with a wet absorbing paper stick inside and cover the coverslips with this box.
8. Remove the excess of the antibody solution by touching an absorbing paper with the border of the coverslip and place it with the cells facing up in a new well. Wash with PBS 1x.

Sometimes the antibody solution can be recycled, add 0.05% azide to avoid contamination and store it at 4°C

9. Dilute the secondary antibody in DMEM + 10% FCS, according to experimental experience, usually it's between 1/300-1/500

If we use an antibody coupled to a fluorophore, from now on everything has to be done in low light conditions

10. Proceed as in step 7
11. Proceed as in step 8. Wash extensively, around 4 washes of 20 minutes each.
12. Incubate the coverslips with Hoechst diluted in PBS 1x (1/1000) for 10 minutes
13. Mounting of the slides: More than one coverslip per slide can be placed. Put 2 ul of per coverslip Vectashield (mounting medium) and place the coverslip very carefully upside down (cells facing towards the vectashield) over it.
14. Seal the coverslips with nail polishing. Store at 4°C and away from the light.

Apparatus

Spectrophotometer Beckmann Life Science DU®530

Materials and reagents

Chemicals	Source/Company	Code/quantities
Bovine serum albumin (BSA)	Sigma	A-7906
Orthophosphoric acid	Acros	201140010
Coomassie blue	Acros	191480250
Ethanol	Biosolve	20655
Whatman paper	Whatman	3030917
Plastic microcuvettes 1.5ml	Brand	7590.15
NaOH	Fluka	71690

BSA standard

Concentration (mg/ml)	µl of stock (10 mg/ml)	µl of water
0.0	0	1000
0.5	50	950
1.0	100	900
1.5	150	850
2	200	800

Standards are kept at -20°C. Each person makes her/his own standards.

Bradford reagent

Reagents	Quantity
Orthophosphoric acid	400 ml
Coomassie blue	0.4 g
Ethanol 95%	200 ml
Water	Up to 4 l

Important: Add the Coomassie Brilliant Blue powder only at the end, after preparing the whole solution!!!!

Filter through WHATMAN

Cuvettes:

Disposable cuvettes

1.5 semimicro

Dimensions 12.5 x 12.5 x 45mm

Brand cat : 7590.15

Measure of the concentration of proteins:

	Standard (duplicate)	Samples (duplicate)	Blank
NaOH 0.2N	200ul	200ul	
Lysate		3.3ul	
Standard	10ul		
Bradford's reagent	1.8ml	1.8ml	1.8ml

Bradford' reagent has a dispenser ready with 1.8ml

- Keep in dark before to measure min. 15 minutes (not necessary)
- Standards and samples must be measured twice.
- Read the absorption at 590-600nm:
- `Main menu` `fixed λ` `Blank`
- Make an average of standards
- Read the samples
- Put the paper, online, print
- Make an average of your samples and the difference between of them should be less as 5%
- Use the excel program to calculate yours concentrations

Another way to measure the protein concentrations is as follow:

Introduce the values into the spectrophotometer twice:

`Main menu` `Protein assay` `bradford` `enter` `STD curve` `enter` `more` `enter` `create table` `enter` `0` `enter` `0`
`enter` `0.5` `enter` `0.5` `enter` `1.0` `enter` `1.0` `enter` `1.5` `enter` `1.5` `enter` `entry done.`

Zero with Bradford's reagent

Lecture of standards, when we have the curve: `entry done`

`Dil 1.00` Changer and put factor 3.00 `enter`

Read yours samples and you have directly the protein's concentration then is the same thing as the possibility number one.

IMPORTANT NOTE

The viral supernatants produced by these methods might, depending upon your retroviral insert, contain potentially hazardous recombinant virus. The user of these systems must exercise due caution in the production, use and storage of recombinant retroviral virions, especially those with amphotropic and polytropic host ranges. This consideration should be applied to all genes expressed as amphotropic and polytropic pseudotyped retroviral vectors. Appropriate guidelines should be followed in the use of these recombinant retrovirus production systems.

The user is strongly advised NOT to create retroviruses capable of expressing known oncogenes in amphotropic or polytropic host range viruses.

According to the Swiss Legislation all the manipulations done using lentiviruses, must be performed in a P2 security Laboratory.

For details and authorization for using the P2 Lab, contact Sylvain Lengacher at the Institute of Physiology (tel. 021 692 55 46, email: Sylvain.Lengacher@unil.ch)

For some additional information concerning the Lentiviral Systems you can check the following websites.

Garry Nolan's Lab website at Stanford University: <http://www.stanford.edu/group/nolan/>

Didier Trono's Lab website at Geneva University: <http://www.tronolab.com/>

Reagents.

Hexadimethrine bromide (Polybrene), Fluka (Sigma Cat. N° 52495)

Sucrose, Fluka (Sigma Cat. N° 84100)

Paraformaldehyde 95 %, (Sigma Cat. N° 441244)

Penicillin-Streptomycin Glutamine 100x solution, (GibcoBRL Cat N° 10378-016)

0.45 µm filters, Millex-HN, 0.45µm, 25mm, stérile, 50/PK (Milian Cat N° SLHN025NS)

0.22 µm filters, Millex-GN, 0.22µm, 25mm, stérile, 50/PK (Milian Cat N° SLGN025NS)

Chloroquine (Sigma Cat. N°C6628).

Laminin, mouse (1 mg) (BD Bioscience Cat. N° 354232)

Poly-D-Lysine (20 mg) (BD Bioscience Cat. N° 354210)

Biocidal ZF (1 l) (WAK Chemie Cat N° WAK-ZF-1)

Solutions.

1X Phosphate Buffered Saline (PBS)

NaCl, 8 g

KCl, 0.2 g

Na₂PO₄, 1.44 g

KH₂PO₄ 0.24 g

H₂Odd 800ml

Adjust pH to 7.4 with HCl.

Adjust volume to 1 liter with additional distilled H₂O. Sterilize by autoclaving.

Tris-EDTA (TE) buffer. (10 mM Tris; 1 mM EDTA; pH 8.0)

1 M Tris pH 8.0 1 ml

0.5 M EDTA pH 8.0 0.2 ml

H₂Odd 98.8 ml

Autoclave

Polybrene 5 mg/ml (10 ml).

Dissolve 5 mg of Polybrene in 10 ml of PBS. Filter through a 0.22 µM filter, aliquot in eppendorf tubes (1 ml per tube) and store either at 4°C or at -20°C.

Chloroquine 25 mM (50 ml).

Dissolve 399.8 mg of Chloroquine in 50 ml of PBS. Filter through a 0.22 µM filter, aliquot in 15 ml falcon tubes (10 ml per tube) and store at -20°C.

Sodium Acetate 3 M pH 5.2 (100 ml).

To 24.6 gr of sodium acetate (Sigma Cat. N° S-2889), add 90 ml of nanopure water. Adjust the pH to 5.2 (with glacial acetic acid) and complete to 100 ml.

Fixation Solution (2% Paraformaldehyde 3% Sucrose).

- a. Weigh 0.2 gr paraformaldehyde in a 15 ml tube.
- b. Add 6 ml PBS.
- c. Warm up to 60°C and vortex.
- d. Add drops of 0.5 M NaOH, warm up to 60° C and vortex until it dissolves.
- e. Add 0.3 gr of Sucrose and make up the volume to 10 ml with PBS.
- f. Make sure the final solution is neutral.

Procedure

Note: for details on the transfection protocol, refer to SOP001 *Transfection (calcium-phosphate)*.

Day 0.

1. Prepare five 10 cm gelatinized Petri dishes containing 2 - 2.5x10⁶ HEK293T cells in 10 ml medium.

Gelatinization of the dishes.

Place between 2 to 5 ml of PBS/0.1% gelatin in the dish [See SOP001] (tilt the plate to cover the entire surface with the solution). Wait at least 10 min. Just before adding the cells to the plates, aspirate the PBS/0.1% gelatin (do not allow the plates to dry).

Day 1.

2. Prewarm all the solutions in a 37°C water bath (at least 20 min). In case the buffer is thawed, mix very well before using.
3. Add 25 µM chloroquine (10 µl of the 25 mM solution) to the cell culture medium (not necessary to change the medium). Place the plates back in the incubator for at least 10 min.

The addition of chloroquine to the medium appears to increase retroviral titer by approximately two fold. This effect is presumably due to the lysosomal neutralizing activity of the chloroquine (3). It is extremely important that the length of chloroquine treatment does not exceed 12 hours. Longer periods of chloroquine treatment have a toxic effect on the cells causing a decrease in retroviral titers.

4. In a 15 ml Falcon tube prepare the following master mix:

	Volume or quantities
H ₂ O	Variable
pCMV delta R8.91	37,5 µg
pMD.G	12,5 µg
Lentiviral vector (e.g. Prom.lti) encoding the gene of interest	50 µg
CaCl ₂	250 µl
2xHepes	2500 µl
FINAL VOLUME	5 ml

All the plasmid should be prepared using Qiagen or Genomed Maxiprep kits and ethanol precipitated. In case the yield of the plasmid is not very high it should be purified using the CsCl purification method.

- Ethanol Precipitation:
 - a- Carefully calculate the volume of your DNA solution.
 - b- Add 1/10 volume of 3 M Sodium Acetate pH 5.2, mix well.
 - c- Add 2 volumes of cold absolute ethanol.
 - d- Keep at -20° C for at least 1 hour.
 - e- Centrifuge 10' at maximum speed.
 - f- Discard supernatant and wash pellet with ethanol 70 % three times.
 - g- Air dry and resuspend in TE.
 - h- Measure DNA concentration.
5. Mix well, by passing 5 times the solution through a 5 ml pipette.
 6. Exactly 60 seconds after mixing the 2xHepes with the CaCl₂-DNA mixture, add 1 ml precipitate per plate.
 7. Incubate for 6-8 hours in an incubator (37°C - 5% CO₂).
 8. Remove medium, wash once with PBS and put fresh medium containing penicillin and streptomycin to avoid contamination (the DNA used for the transfection is generally not sterile!).
 9. 48 hours after the transfection, collect the supernatant of the plates in a 50 ml Falcon Tube.
 10. Centrifuge for 5' at 1500 rpm (~400 g) at 4°C to pellet the detached cells (ALC PK 130 centrifuge, rotor N° T535).
 11. Filter the cleared virus-containing supernatant through a 0.45 µm filter, wrapping everything in a towel humidified with biocidal to avoid aerosols.
 12. Once the virus is filtered, aliquot in 15 ml falcon tubes.

Note: The size of the aliquots may change according the use you will give to your virus.

13. Keep the virus at -80°C.

Freezing does not appear to cause more than a 2-fold drop in titer, as long as the cells do not undergo more than one freeze/thaw cycle. If the cells undergo more than one freeze/thaw cycle, there is a significant drop in retroviral titer.

14. If the virus encodes for a protein that can be detected, calculate functional titer by immunocytochemistry (See SOP011 *Immunocytochemistry*), as detailed below [for siRNA encoding lentiviruses you may calculate your functional titer by monitoring by western blot the conditions that lead to the best decrease of the targeted proteins, (See SOP006.1 *Western Blot*)].

1. Laminin-Polylysine coating

PolyLysine.

Comes as 20 mg/vial. Add sterile H₂O to the vial to a final volume of 1 ml to make a 1 mg/ml stock solution (in a 50 ml falcon tube). Make 1 ml (=1 mg) aliquots. Store at -20 C.

Laminin.

Comes as 1 mg/vial. Add sterile H₂O to the vial to a final volume of 1 ml to make a 1 mg/ml stock solution. Make 100 µl (=100 µg) aliquots. Store at -70 C.

Coating Coverslips.

1. Thaw 1 tube of polylysine and laminin solution.
2. Add laminin, poly-lysine to 25 ml of sterile H₂O.
3. Use 50 µl solution for each coverslips. Place at 37° C for 2 hrs.
4. Rinse 3x with PBS, and use to plate cells.

2. Plate the appropriate number of cells (according to your cells type) in six-well dishes, with two laminin-coated coverslips in each well.

Cells	Number per well (6 well-plates)	Medium	Coating
GAP ^{+/+} and derived cell lines	3-5 · 10 ⁴	DMEM; 10% NBCS	Polylysine /Laminin
HEK 293 and derived cell lines	35 · 10 ⁴	DMEM; 10% NBCS	Polylysine /Laminin
β-Tc-Tet and derived cell lines	10 ⁵	DMEM (without L-Glu); 15% Horse Serum (Heat decomplexed); 2,5% FCS; 2 mM L-Glu; 10 mM HEPES pH 8; 1 mM Na-Pyruvate	Polylysine /Laminin

3. Incubate cells at 37°C, for 12-18 hours.

Important: infect cells when they are not more than 50% confluent.

- The following day, thaw the frozen virus at 37°C (shake often) and once nearly completely thawed, keep on ice. The virus should stay at 0°C all the time.
- Add various amounts of viruses according to the table below, add 2 µl of a 5 mg/ml polybrene stock solution and complete with fresh medium to 3 ml.

Cell #	0 ml	0.25 ml
0.5 ml	1 ml	2 ml

- Immediately thereafter, seal the plates with parafilm and centrifuge them 45' at 2'500 rpm (~800 g) (ALC PK 130 centrifuge, rotor N° T537).
- Incubate overnight in incubator (37°C - 5% CO₂).
- Change medium after 24 hours.
- Remove medium 72 hs after infection and rinse once with 2 ml of PBS.
- Fix cells by adding 1 ml of PBS-2% paraformaldehyde-3% Sucrose, for 15 minutes.
- The following immunocytochemistry steps can be performed on the bench (*See SOP011*).
- Knowing the number of cells at the moment of infection and the smallest volume that leads to expression of the gene of interest in ~100% of the cells, you can estimate the number of infective particles per ml.

References

- Jordan et al. - Nucl. Acid Res. (1996) **24**:596. For transfection.
- Dull, T. et al. - *J.Virol.* 72.11 (1998): 8463-71. For 3rd generation lentiviral vectors.
- Mulligan, R.C. and Berg, P. - PNAS 78, 2072-2076 (1981)

Author: Alessandro Annibaldi

Introduction.

In molecular biology, reverse transcription polymerase chain reaction (RT-PCR) is a laboratory technique for amplifying a defined piece of a ribonucleic acid (RNA) molecule. The RNA strand is first reverse transcribed into its DNA complement or complementary DNA, followed by amplification of the resulting DNA using polymerase chain reaction. This can either be a 1 or 2 step process.

Polymerase chain reaction itself is the process used to amplify specific parts of a DNA molecule, via the temperature-mediated enzyme DNA polymerase.

Reverse transcription PCR is not to be confused with real-time polymerase chain reaction which is also marketed as RT-PCR.

The present SOP only describes the reverse transcription part of the procedure.

RNA isolation.

Day 0

1. Add 500 µl of TRI reagent (for 10^5 to 3×10^7 cells) to the cells and scrape them. Incubate at room temperature for 5 minutes.
2. Add 200 µl of Chloroform, vortex and incubate 5 minutes at room temperature.
3. Spin 15 minutes at maximum speed (13'000 rpm in the Eppendorf centrifuge 5415R; $16'100 \times g$).
4. Transfer the aqueous phase into a new tube, add 500 µl of isopropanol, mix by inverting the tube a few times and put at -20°C o/n.

Day 1

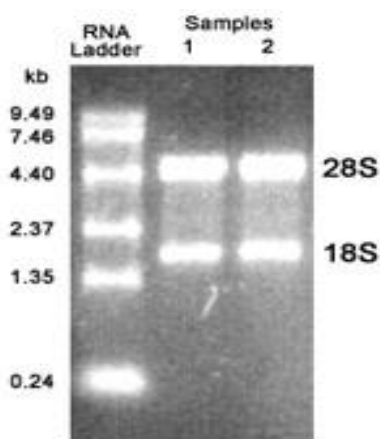
1. Spin 20 minutes at high speed (13'000 rpm in the Eppendorf centrifuge 5415R; $16'100 \times g$). At this stage if you do not see the pellet, add 40 µl of NaCl 5 M, mix by inverting the tube a few times and spin down again 15 minutes.
2. Aspirate the isopropanol.
3. Wash with 800 µl of ethanol 70%.
4. Place the tubes in the thermomixer (Eppendorf Thermomixer Comfort, it is located in the lab) at 60°C for 10 minutes without shaking to let them dry.
5. Resuspend the pellet in 50 µl of high quality water.
6. Quantitate the RNA using the Eppendorf Biophotometer located in the lab. Push button n°9 to select the program to quantitate RNA, take the quartz cuvette QS 1.000 (usually located next to the Biophotometer), fill the cuvette with 200 µl of TE pH 8.0 and add 2 µl of your RNA. Mix. Click on the button labelled "Dilution" and enter the dilution (2:200). Proceed with the quantitation. Do not forget to do first the blank by filling the same cuvette with 200 µl of TE and subsequently clicking on the button labelled 'Blank'. You will get 260 nm values. An A260 reading of 1.0 is equivalent to $\sim 40 \mu\text{g/ml}$ single-stranded RNA.

Note that measuring the 260 nm/280 nm absorbance ratio of your samples is not a very informative method to monitor the purity of your preparation (despite what is written in some protocols) (Glasel, 1995). Note also that this ratio is influenced by the pH and ionic strength of the solution. As pH increases, the A280 decreases while the A260 is unaffected. This results in an increasing A260/A280 ratio (Wilfinger *et al.*, 1997). Because water often has an acidic pH, it can lower the A260/A280 ratio. It is recommended to use a buffered solution with a slightly alkaline pH, such

as TE (pH 8.0), as a diluent (and as a blank) to assure accurate and reproducible readings. An example of the variation in A260/A280 ratio at different pH values is shown below

BLANK/DILUENT	A260/A280 ratio
DEPC-treated water (pH 5-6)	1.60
Nuclease-free water (pH 6-7)	1.85
TE (pH 8.0)	2.14

7. To have a better idea of the quality of your RNA, run it on an agarose-formaldehyde gel as follows:
 - a. Melt 0.5 g of agarose in 37 ml of H₂O, cool down a little bit, add 5 ml of 10x MOPS buffer and 8.75 ml of formaldehyde 36.5 %.
 - b. RNA loading: prepare a mix composed of a few micro litres of your RNA (corresponding more or less to 500 ng), one fifth of the final volume with 5X RNA denaturing buffer, and water (usually up to a final volume of 10 µl).
 - c. Perform electrophoresis in 1x MOPS.
 - d. If your RNA preparation is good, you should see 2 bands, the highest one corresponds to the 28S RNA, the lowest one to the 18S RNA.



Reverse Transcription

0.5-1.0 µg total RNA

1.0 µl of a 500 ng/µl oligo dT solution in water.

The Oligo dT primer is purchased from Microsynth; you have to send an e-mail to the following address:

administration@microsynth.ch asking for Random Hexamer D(N)6. Once you receive the tube (the quantity received is indicated on the datasheet), dissolve the oligo dT in water to get a concentration of 500 ng/µl. The oligo dT solution can be stored at -80 °C (alternatively, if you use them quite often, you can store some aliquots at -20 °C). For the delivery you can write in the e-mail your customer number, like that they automatically know your delivery address).

Add water to 11 µl.

3 minutes at 70°C and then keep on ice

Reverse transcription

Prepare the mix according to the table below. The buffer 5x, the DTT, the dNTPs, the RNAsin, and the reverse transcriptase come from the Superscript II Reverse Transcriptase Kit.

Reagent	μ l
dNTPs 10 mM each	5
RNAsin	0.5
Buffer 5x	5
DTT	2
Superscript reverse transcriptase	0.5
H2O	1
Total	14

Add the RNA to the mix and perform an incubation at 39°C for 1 hour followed by 15 minutes at 70°C. Your cDNA is now ready to be amplified by PCR.

Materials and reagents	Source/Company	Code
Agarose	Eurogenetec	EP-0010-10
β -mercaptoethanol	Sigma	M6250
Bromophenol blue	Fluka	18030
EDTA	Fluka	03620
Ethidium Bromide	Acros	170960010
Formamide (25 M)	Fluka	47670
Formaldehyde 36.5% (13.2 M)	Fluka	47629
Ficoll	Pharmacia Biotech	17-0400-01
Guanidinium Thiocyanate	AppliChem	593-84-0
MOPS (morpholinopropanesulphonic acid)	Sigma	M3183
N-Lauryl Sarcosil sodium	Sigma	L9150
NaOH	Fluka	71690
Phenol (water saturated)	EUROBIO	GEXPHE01-0U
RNA sin	Promega	N211A
SDS	Sigma	L4390
Sodium Acetate	Sigma	S288
Sodium Citrate	Sigma	C8532
dATP	Promega	U120D
dGTP	Promega	U121D
dCTP	Promega	U122D
dTTP	Promega	U123D
Superscript II Reverse Transcriptase Kit (Buffer 5x, DTT and Superscript reverse transcriptase)	Invitrogen	18064-014

TRI solution (1.7 M guanidinium thiocyanate, 0.1 M sodium citrate, 0.25% sarcosyl, 0.05 M β -mercaptoethanol, 0.1M sodium acetate)

Reference List

Glasel, J.A. (1995). Validity of nucleic acid purities monitored by 260nm/280nm absorbance ratios. *BioTechniques* 18, 62-63.

Wilfinger, W.W., Mackey, K., and Chomczynski, P. (1997). Effect of pH and ionic strength on the spectrophotometric assessment of nucleic acid purity. *BioTechniques* 22, 474-481.

Author : Alessandro Annibaldi

Introduction.

In molecular biology Cell Fractioning is a laboratory technique used to break cells and separate their molecular and structural components. Cell Fractioning can be divided in two steps: Homogenization and Fractionation. The Homogenization phase, whose purpose is to break the cell, is obtained either by the osmotic alteration of the media where cells are broken open through the utilization of an hypotonic buffer or by mechanical disruption. The Fractionation phase relies on the utilization of centrifugations at different speeds and times to separate cellular components on the basis of their size.

Cell Fractioning (Nuclei/Cytoplasm).

Day 0

Spread at least $2 \cdot 10^6$ in a 10 cm plate. If you want to look at the localization of one or more exogenous protein transfect your cells according to either SOP 1.0 or SOP 3.0, depending on the cell type with which you are working.

Day 1

1. Wash your 10 cm plate with PBS.
2. Add 400 μ l of lysis buffer 0.5% Triton X-100.
3. Scrape cells and incubate on ice for 20 minutes.
4. Centrifugate at 13.000 rpm (16'100 x g) in the Eppendorf centrifuge 5415R located in the lab.
5. Transfer the supernatant (membrane/cytoplasm fraction) into a new Eppendorf tube and keep the pellet.
6. Quantitate the protein concentrations of your samples using the Eppendorf Biophotometer located in the lab (see SOP 13.0 [Bradford]).
7. After completing the quantitation, add the loading buffer according to the amount of protein you want to load. At this point your **Cytoplasmic fraction** is ready to be loaded or alternatively you can store it at -20 °C.
8. Rinse the pellet representing the nuclear/mitochondrial fraction with the lysis buffer once and resuspend in the lysis buffer containing 0.5% SDS. Shear the released genomic DNA by sonication. The sonicator (Heischer DmbH) is now located downstairs, in a room that is in front of Peter Clark's group cell culture room. The settings you have to use are the followings:
Cycle (representing the number of cycles per second): 0.8-0.9.
Amplitude: 80%
9. Once there you have to insert the metallic tip of the sonicator inside your Eppendorf tube and press the black button located on the top of the sonicator for 10 seconds. Two sonications are enough to completely break the DNA. After each sonication place the sample back on ice for a few seconds. Before processing the next sample, wash the metallic tip of the sonicator first with ethanol 70% and then with water. Dry the tip with a clean tissue.
10. After sonication, centrifuge at 13.000 rpm (16'100 x g) in the Eppendorf centrifuge 5415R and transfer the supernatant in a new Eppendorf.

11. Quantitate the protein concentrations of your samples using the Eppendorf Biophotometer located in the lab (see SOP 13.0 [Bradford]).
12. After completing the quantitation, add the loading buffer according to the amount of protein you want to load. At this point your **Nuclear fraction** is ready to be loaded or alternatively you can store it at -20 °C.

Cell Fractioning (Nuclei, Mitochondria, Cytoplasm and Membrane)

Day 0

Start from at least $10 \cdot 10^6$ using 10 cm plates. If you want to look at the localization of one or more exogenous protein transfect your cells according to either SOP 1.0 or SOP 3.0, depending on the cell type with which you are working.

Day 1

1. Wash your 10 cm plate with PBS.
2. Add 300 µl of hypotonic lysis buffer.
3. Scrape cells and incubate on ice for 20 minutes.
4. Centrifugate at 300 x g 5 minutes at 4 °C in the Eppendorf centrifuge 5415R to pellet nuclei.
5. Transfer the supernatant in a new eppendorf and wash the pellet twice with the lysis buffer. For each wash add 250 µl of lysis buffer, centrifugate at 300 x g and discard the supernatant.
6. Resuspend the pellet in 200 µl of lysis buffer + Triton X100 1%.
7. Quantitate the protein concentrations of your samples using the Eppendorf Biophotometer located in the lab (see SOP 13.0 [Bradford]).
8. After completing the quantitation, add the loading buffer according to the amount of protein you want to load. At this point your **Nuclear fraction** is ready to be loaded or alternatively you can store it at -20 °C.
9. For the mitochondrial fraction start from point number 5. After transferring the supernatant in a new Eppendorf tube, centrifugate at 10'000 x g in the Eppendorf centrifuge 5415R located in the lab for 10 minutes at 4 °C to pellet mitochondria.
10. Transfer the supernatant in a new Eppendorf tube and resuspend the pellet in 200 µl of lysis buffer + Triton X100 1%.
11. Sonicate as described above.
12. Quantitate the protein concentrations of your samples using the Eppendorf Biophotometer located in the lab (see SOP 13.0 [Bradford]).
13. After completing the quantitation, add the loading buffer according to the amount of protein you want to load. At this point your **Mitochondrial fraction** is ready to be loaded or alternatively you can store it at -20 °C.
14. Take the supernatant you transferred in a new Eppendorf tube (point number 10) and centrifugate at 100'000 x g 1.5 hours at 4 °C. For this centrifugation, you have to use the ultra-centrifuge named Centrikon T-108 located in the P2 lab. The rotor, 'Kontron 18425', is

located in the fridge in front of Romano Regazzi's lab. Tubes that suit the rotor are provided from Beckman and the maximum volume you can put in the tubes is 1 ml. After the centrifugation (as well as before using it) clean it with ethanol 70% and water. Do not forget to put the rotor back to its storage place.

15. Transfer the supernatant in a new Eppendorf tube.
16. Quantitate the protein concentrations of your samples using the Eppendorf Biophotometer located in the lab (see SOP 13.0 [Bradford]).
17. After completing the quantitation, add the loading buffer according to the amount of protein you want to load. At this point your **Cytoplasmic fraction** is ready to be loaded or alternatively you can store it at -20 °C.
18. Resuspend the pellet in 150 µl of lysis buffer + Triton X100 1%.
19. Sonicate as described above.
20. Quantitate the protein concentrations of your samples using the Eppendorf Biophotometer located in the lab (see SOP 13.0 [Bradford]).
21. After completing the quantitation, add the loading buffer according to the amount of protein you want to load. At this point your **Membrane fraction** is ready to be loaded or alternatively you can store it at -20 °C.

Materials and reagents	Source/Company	Code
TRIS (Trizma base)	Sigma	T1503
Triton X-100	Fluka	93426
NaCl	Acros	207790050
Glycerol	Fluka	49780
MgCl ₂	MERCK	TA 808932
KCl	Fluka	60130
SDS (sodium dodecyl sulphate)	Sigma	L4390
HEPES	AppliChem	A3724
Centrifuge tubes 11 x 34 mm	Beckman	343778

Lysis buffer (0.5% Triton X-100, 500 mM Tris-HCl pH 7.5, 137 mM NaCl, 10% glycerol, 0.5% Triton X-100)

For 10 ml

5 ml of Tris-HCl pH 7.5 1M

274 µl of NaCl 5M

1 ml of glycerol 100%

50 µl of Triton X-100

Up to 10 ml with water

Hypotonic lysis buffer (10 mM HEPES pH 7.4, 10 mM MgCl₂, 42 mM KCl)

For 10 ml

200 µl of HEPES pH 7.4 500 mM

100 µl of MgCl₂ 1 M

420 µl of KCl 1 M

Up to 10 ml with water

Immunohistochemistry (IHC) in fluorescence on paraffin sections**Author: Nieves Peltzer****Materials and reagents**

Materials and reagents	Source/Company	Code
Coplin Jar (Figure 1)		
Ethanol	Merck	K38929083
Xilene		
Tris 1M pH7.6	Sigma	1297640
BSA	Sigma	A7906
Tween 20	Acros	233360010
Citric acid	Sigma	C8532
EDTA pH8	Fluka	03620
Liquid blocker	Daido Sangyo Co.	22309
Hoechst		
Vectashield Mounting medium	Reactolab	H-1000
Incubation chamber	Plastic flat box with wet tissue on the bottom	
Coverslips	Menzel-Glaser	Available in the DBCM stock



Figure 1: Coplin Jar. In the laboratory, we have jars accommodating 8 and 12 slides.

Buffers**20X TBS (1M Tris base, 18% NaCl, pH 7.6)**

Weigh 122 g of Tris and 180 g NaCl dissolve in 800 ml of distilled water. Adjust the pH to 7.6 with HCl 37%. The volume of HCl to add is approximately 65 to 70 ml. Add water to 1000 ml. Store this solution at room temperature. Dilute 1:20 with distilled water before use and adjust pH if necessary.

I) IHC with fluorescence**Buffer 1:** TBS 1x pH 7.6

Dilute TBS 20X, 1:20 with distilled water

Buffer 2: TBS 1x pH 7.6+ Tween 20 0.5%

Dilute TBS 20X, 1:20 with distilled water and add 5 ml of Tween 100% (0.5%).

Buffer 3: TBS 1x pH 7.6 + Tween 20 0.5% + BSA 0.2%

Dilute TBS 20X, 1:20 with distilled water. Add 5 ml of Tween 100% and 2 g of BSA.

Experimental protocol

Slide deparaffinization.

Put the slides on a plate and incubate at 60°C until the paraffin is completely dissolved. Immediately after this (it has to be fast because the paraffin can solidify again), immerse the slides in the first incubation solution described below and then proceed with the subsequent washes.

Incubate sections sequentially in:

- 1°_ xylene 5'
- 2°_ xylene 3'
- 3°_ Ethanol 100% 3'
- 4°_ Ethanol 100% 2'
- 5°_ Ethanol 90%, 2'
- 6°_ Ethanol 75%, 2'
- 7°_ Ethanol 50%, 2'
- 8°_ Wash with water from the sink, distilled water is not necessary.

These solvents are located in a hood besides the radio in Peter Clarke's lab. Turn on the aeration system (top left) of the hood before starting with deparaffinization.

If you have problems of detachment there is an alternative deparaffinization protocol in the annexe.

The slides are now ready for the IHC

Antigen retrieval

The antigen retrieval protocol should be assessed for each antibody. There are cases where no antigen retrieval is needed but this has to be tested for each particular antibody. In the attached table there is a list of already standardised antigen retrieval protocols.

The following two protocols are the most common ones.

Tris-EDTA Buffer (10 mM Tris Base, 1 mM EDTA, 0.01% Tween 20, pH 9)

Tris-base	1.21 g
EDTA	0.37 g
Distilled H ₂ O	1000 ml

Adjust the pH to 9 and then add 0.1 ml of Tween 20. Mix well.

Prepare 1000 ml and put it in a pressure casserole and heat until the second red line is seen on the pressure marker (approximately 10 minutes but it's better to be there before in case there is liquid spilling out the casserole, in this case, remove the recipient from the heating plaque immediately). At this point wait 2 minutes and take the casserole out of the heating plaque. Release the pressure (by pushing down the pressure indicator) and place the casserole in the sink. Pour cold water on the cover without opening it.

Immunohistochemistry (IHC) in fluorescence on paraffin sections

Once the vapour is all out open the casserole and take the slides out. Wash immediately with tap water and begin with the immunohistochemistry staining.

Sodium Citrate Buffer (10 mM Sodium citrate pH 6.0)

Tri-Sodium citrate (dehydrate)	2.94 g
Distilled H ₂ O	1000 ml

Adjust the pH to 6 with HCl and mix well.

This buffer is commonly used and works perfectly well with most antibodies. It gives very nice intense staining with very low background.

This buffer can be used either with the pressure casserole or in the microwaves.

Usually I use it in the microwave. Put the slides into 1000 ml of buffer in a microwave-resistant recipient with a cover. Use the highest power setting until the liquid boils (takes about 7 to 8 minutes).

Once the buffer is boiling, lower the power to the minimum and keep heating for 11 minutes.

Once the procedure is finished, leave the slides to cool down in the same buffer for at least one hour with agitation. To shorten this period of time, ice can be placed into the recipient. For certain antibodies, there is no need to let the buffer get completely cold.

Wash with tap water before starting the immuno-histochemistry procedure.

Immunostaining

Before starting, surround the samples about to be stained with liquid blocker to ensure a minimal area in which the incubations will be done. Air dry the liquid blocker for a few seconds (but do not dry out the sample!). The liquid blocker should be kept at 4°C.

1. Incubate the slides in a Coplin jar with buffer 1 for 5 minutes on a shaker. Repeat this washing step with buffer 2. All the washing steps should be done on the shaker.
2. Blocking of unspecific sites: add 100 µl of blocking solution (buffer 3) onto the section and into the area delimited by the liquid blocker. Incubate the slides in a humid chamber for at least 30 minutes at room temperature. The humid chamber is a plastic box with a wet tissue inside; keep it close to maintain humidity. If desired 15% of serum of the species in which the secondary antibody was made, can be added to the blocking solution (for example, if the secondary antibody is a goat anti-mouse antibody, you have to choose goat serum). Adding serum is not essential but it can be important when doing a double or triple staining.
3. Incubation with the first antibody: Add 100 µl per slide of the primary antibody diluted in buffer 3 according to the datasheet of the given antibody. Incubate in a humid chamber for 1 hour at room temperature. For some antibodies you can increase the signal by incubating the slides over night at 4°C. To avoid evaporation of the liquid you can cover the slide (with the

Immunohistochemistry (IHC) in fluorescence on paraffin sections

antibody solution) with parafilm (just put it over it without pressing). This will also ensure a homogeneous spreading of the liquid.

4. Washings: wash the slides three times in buffer 2 for 5 minutes or two times for 10 minutes.
5. Incubation with secondary antibody: put 100 µl per slide of the secondary antibody diluted in buffer 3. Usually, the dilution is between 1/200 and 1/500 but this should be tested when new antibodies are employed. Incubate the slides in a humid and dark chamber for 1 hour at room temperature. Secondary antibodies are located on the first freezer you find when entering the lab, in the top right drawer.
6. Wash the samples extensively in a dark or covered Coplin Jar. Perform at least 6 washes of 20 minutes each, in buffer 2. An overnight washing at 4°C is recommended but not essential.
7. Nucleus staining: Dilute the Hoechst dye (located in the first fridge you find when entering in the culture room) 1:1000 in buffer 2 and put 100ul per slide. Incubate in a humid and dark chamber for 10 minutes at room temperature (longer incubation time can result in a saturated staining)
8. Mount the slides with Vectashield mounting medium. This is a special medium used to conserve the fluorescence for longer time. Anyway do not wait too much to observe the slides as the quality would not be as good as if you look at them within one week. The volume of Vectashield to be used should be between 5 µl, for small samples, to 20 µl, for big ones. Place a coverslip over it trying to avoid the formation of bubbles
9. Surround the coverslip with nail polish in order to protect the samples from drying out. Keep the slides at 4°C in the dark.

Annexe**Alternative deparaffinization protocol**

Put the slides over a plate at 60°C until the paraffin is completely dissolved. Soon after this, immerse the slides on the first incubation solution described below.

Incubate sections sequentially in:

- 1°_ xylene 5'
- 2°_ xylene 3'
- 3°_ Ethanol 100% 3'
- 4°_ Ethanol 80%, 2'
- 5°_ Put the slides over the plate at 60°C until they dry out completely
- 6°_ Wash with water from the sink, distilled water is not necessary.

Antigen retrieval protocol for some antibodies used in the laboratory

Antibody	Company	Antigen retrieval protocol
Survivin	Cell signalling (2808)	Citrate buffer + microwave

Immunohistochemistry (IHC) in fluorescence on paraffin sections

Cytokeratin 5 (MK5)	Covance (PRB-160P)	Citrate buffer + microwave
Cytokeratin 10 (MK10)	Covance (PRB-159P)	Citrate buffer + microwave
Active caspase-3	Cell signalling (9664)	Citrate buffer + microwave
pAkt (Ser473)	Cell signalling (9271)	Tris-EDTA + pressure
KI-67	Dako (M7249)	Tris-EDTA + pressure

Comments:

There is an alternative staining method that uses the peroxidase enzyme to visualize the stained structures.

This technique is useful if it is important to see the structure of the tissue you are working with.

Author: Nieves Peltzer

Materials and reagents

Materials and reagents	Source/Company	Code
Falcon tubes 15 ml *	Corning	430971
Ethanol	Merck	K38929083
PBS 1x	CHUV	10003240
Propidium iodide	Sigma	P-4170
Trypsin-EDTA solution (1x)	Sigma	T3924
Tri-sodium citrate (dehydrate)	Sigma	C-8532
FCS (fetal calf serum or fetal bovine serum)	GIBCO	10270106
RNase A	Boehringer Mannheim	85340025
Scanning tubes	Beckman Coulter	2523749

*any 15 ml tube can be employed.

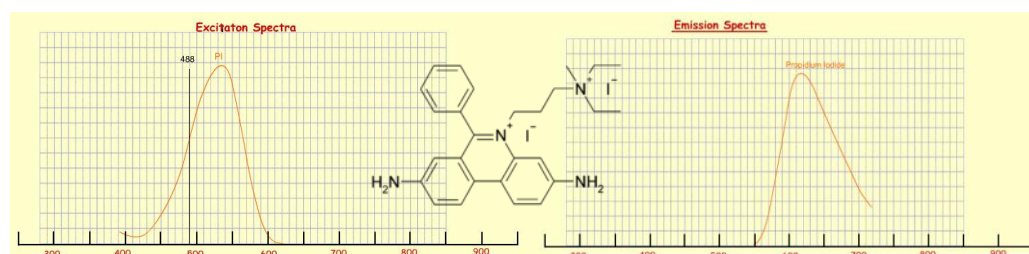


Figure 1: Propidium iodide structure and excitation and emission spectra. Excitation at 488 nm is done with the laser of the Cytometer Beckman Coulter Fc-500 located at the Department of Physiology (2nd floor).

Solutions

Citrate solution (0.038 M) [molecular mass 294.10 Da]

Citrate stock solution 10 mM: dissolve 2.94 g of tri-sodium citrate (dehydrate) and dissolve it in 1000 ml of water. Adjust pH to 7 with HCl.

Citrate 0.038 M: add 380 µl of citrate buffer 1 M in 9.62 ml of distilled water.

Propidium iodide (PI)¹ solution (1 mg/ml) [molecular mass 668.4 Da]

¹ Propidium iodide (or PI) is an intercalating agent and a fluorescent that can be used to stain DNA. When excited by 488 nm of laser light, it can be detected with 562-588 nm band pass filter. Flow cytometry is used to evaluate cell viability or DNA content in cell cycle analysis. It can be used to differentiate necrotic, apoptotic and normal cells.

PI binds to DNA by intercalating between the bases with little or no sequence preference and with a stoichiometry of one dye per 4-5 base pairs of DNA. PI also binds to RNA, necessitating treatment with nucleases to distinguish between RNA and DNA staining. Once the dye is bound to nucleic acids, its fluorescence is enhanced 20- to 30-fold, the fluorescence excitation maximum is shifted ~30-40 nm to the red and the fluorescence emission maximum is shifted ~15 nm to the blue. Although its molar absorptivity (extinction coefficient) is relatively low, PI exhibits a sufficiently large Stokes shift to allow simultaneous detection of nuclear DNA and fluorescein-labeled antibodies, provided the proper optical filters are used. PI is suitable for fluorescence microscopy, confocal laser scanning microscopy, flow cytometry, and fluorometry.

PI is membrane impermeant and generally excluded from viable cells. PI is commonly used for identifying dead cells in a population and as a counterstain in multicolor fluorescent techniques.

[From Wikipedia, the free encyclopedia].

Dissolve 1 mg of PI in 1 ml of citrate buffer 0.038 M.

Store at 4°C protected from light.

Staining buffer

Make a 3 µM solution of PI by diluting 1 mg/ml (1.5 mM) stock solution 1/500 in staining buffer

Tris pH 7.4	100 mM
NaCl	150 mM
CaCl ₂	1 mM
MgCl ₂	0.5 mM
NP-40 (Igepal)	0.1%
RNase A	20 µg/ml

Recipe for 10 ml:

Tris 1 M	1 ml
NaCl 5M	300 µl
CaCl ₂ 1M	10 µl
MgCl ₂ 1M	5 µl
NP-40 10%	100 µl
RNase A 25 mg/ml	8 µl
PI 1 mg/ml	20 µl

Keep this solution at 4°C in the dark. Do not store it for a long time. If it is more than 1 month old, prepare a new one.

Alternatively the buffer can be stored at 4°C for longer periods of time (4-5 months) **without RNase and PI**. Do not forget to add these last two before use!

Experimental protocol

The protocol described here is for solution containing ~500'000 cells/ml.

- 1) Harvest the cells by trypsinization (for 3.5 cm dish):

Put the medium of the cells in which they were cultivated into a tube, wash once with 2 ml of PBS and add this PBS washing volume to the collected medium, trypsinize by adding 100 µl of trypsin and incubating for 1-2 minutes at 37°C. Then flush the cells with the medium and PBS that were previously collected.

- 2) Washing: wash once or twice (if you have few cells wash only once) with cold PBS.

The centrifugation during the washing steps should be 1'200 rpm for 5 minutes (276 g) (Centrifuge SIGMA 3-16PK, rotor 11180, adaptors for 15 ml tubes).

Fixation

Prepare a 15 ml tube with 3 ml of ice-cold ethanol 100%.

3) After the last washing step, discard the supernatant very carefully and resuspend the pellet in 500 µl cold PBS. Mix thoroughly by pipetting up and down. It is very important to obtain a single cell solution because clumps of cells can clog the tubing of the FACS apparatus.

4) Add drop by drop the cells into the ethanol while thoroughly vortexing the tube. Incubate at -20°C for at least 15 minutes. The cells can be stored at this step at -20°C.

Staining

5) Pellet the cells by centrifugation at 1'200 rpm (276 g) (Centrifuge SIGMA 3-16PK, rotor 11180, adaptors for 15 ml tubes) for 5 minutes and wash once with PBS, 1% FCS (serum helps pelleting the cells by preventing their adhesion to the walls of the tubes). Centrifuge 5 minutes at 1'200 rpm (276 g) (Centrifuge SIGMA 3-16PK, rotor 11180, adaptors for 15 ml tubes).

6) Discard the supernatant very carefully and resuspend in 100 µl of cold PBS. Add 1 ml of staining buffer to the cells. Mix thoroughly by pipetting up and down to ensure a single cell suspension.

Transfer the cells in a scanning tube (protect from light) and incubate at room temperature for 15 minutes. The cells are ready to be scanned.

After staining, cells can be stored at 4°C in the dark for a maximum of 4 days.

Flow cytometer parameters

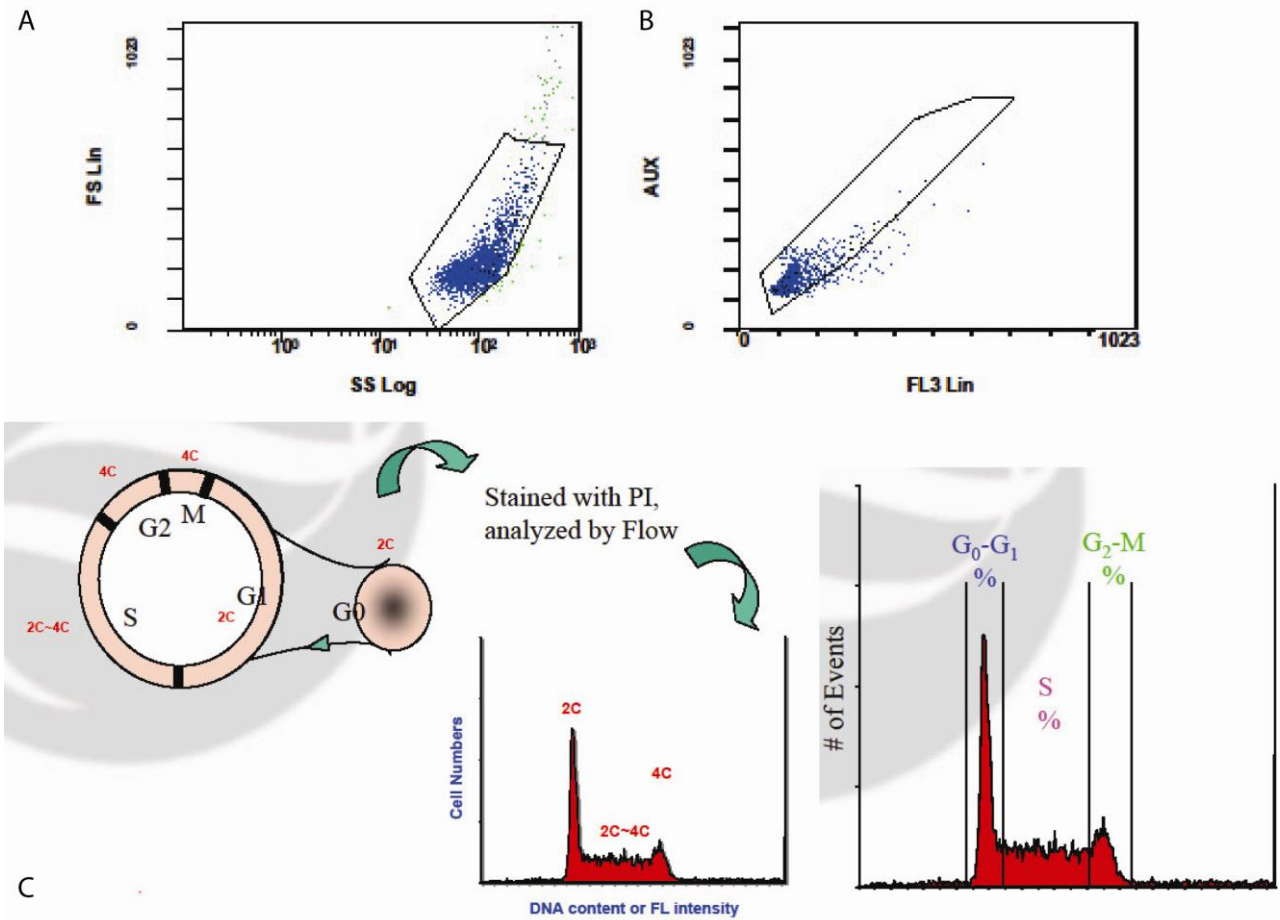
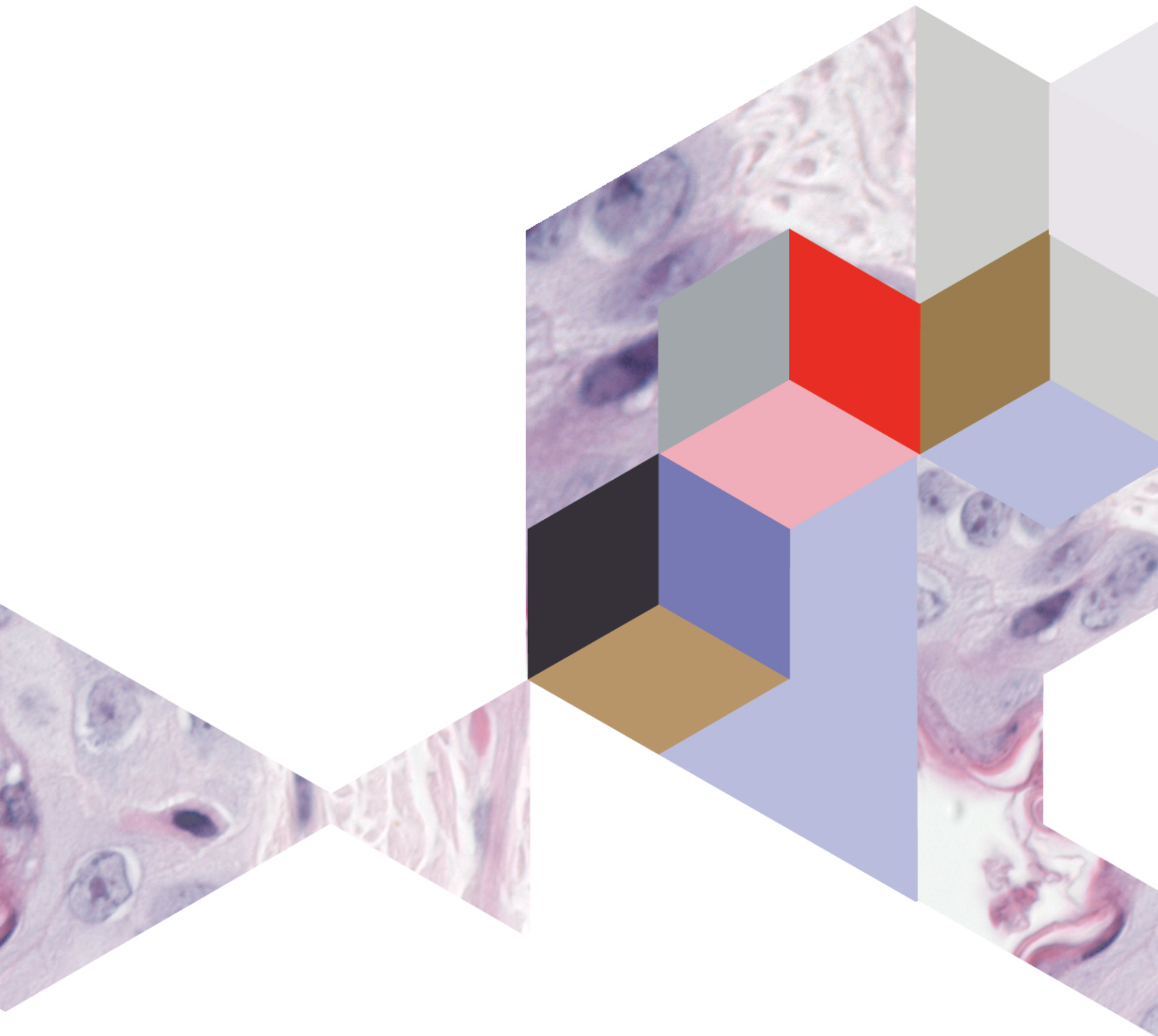


Figure 2: A_ FS vs SS plot: granularity (complexity of the cell) vs size of the cells. These represent the cell population. B_ AUX vs FL3: intensity under fluorescent curve (total fluorescence) vs fluorescence emitted by PI. Cells that are out of the gated region are doublets of cells, ie. not individual cells. C_ DNA staining according to the DNA content and the phase of the cell cycle. The peaks represent different amounts of DNA where G₀-G₁ have 2n, S has 2-4n and G₂ where the cells are about to divide, has 4n.

AKNOWLEDGEMENTS



ACKNOWLEDGEMENTS

I don't want to write a thesis-long text of acknowledgments, so I will keep short and general with some exceptions...

I thank all the people I love and did this work by my side.

I thank all my family for believing in me and for supporting me in this, not always easy, adventure.

I thank all my friends in Argentina, no matter how far distances are... strong bonds will never be broken.

I thank all my friends in Switzerland for making me feel at home.

I thank my sister Laura for making this thesis becoming the "prettiest" thesis ever, and my sister Mercedes for her advises on some topics discussed in this work.

I thank David, because he spent time and loads of energy to help me, because his help, dedication and friendship were and are priceless to me.

I thank Gilles who made my days brighter; I will never stop smiling thinking about you.

I thank Hadi, who made me feel I will never be alone; your kindness calms me and makes me wiser.

You three are special for me.

I thank Jannick, for her friendship and for being such a good person.

I thank all my colleagues, particularly Joël, Natasa, Evrim, Jiang-Yan and Philippe for all the moments shared, for all the discussions and your kindness towards me.

I thank Nick, the "english expert".

I thank all the people that in a way or another "troubleshooted" me. Particularly Julien Puyal, Jean-Christophe Sthele, Gilles Dubuis, Hadi Khalil, David Barras, Evrim Jaccard, Jannick Petremand and Alessandro Annibaldi.

I thank all the people from the DBCM (now DNF): le "coin café", les fêtes de Noël, le secretariat, etc. You people rock! I also thank people from the DP for always smiling back at me.

I thank Christian for mentoring and supporting me. I thank Paul Bigliardi for his precious contribution to this work.

I thank Jean-Pierre Hornung, for accepting being the president of my jury at the very last minute.

I thank Liliane Michalik and Wim Declercq for the valuable questions and discussions.